School of Geography, Archaeology and Environmental Studies

An assessment of the impacts of climate and land use/cover changes on wetland extent within Mzingwane catchment, Zimbabwe.

BY

SETHI SIBANDA (1019068)

Submitted to the Faculty of Science, University of the Witwatersrand, Johannesburg, in partial fulfilment of the requirements for the degree of

Doctor of Philosophy

(Geography and Environmental Science)

Supervisors: Prof. Fethi Ahmed

Prof. Stefan Grab

June 2018

DECLARATION

I declare that this work is my own original work and has not been previously submitted to obtain any academic qualification. Data and information obtained from published and unpublished work of others have been acknowledged in the text and a list of references is herein provided.

Signature: ----------

Date: ----------

DEDICATION

To my late father with love

ACKNOWLEDGEMENTS

I would like to express my sincere gratitude to my supervisors, Prof. Fethi Ahmed and Prof. Stefan Grab for their exceptional academic guidance, encouragement, and support throughout the study. Truly, the experience was academically rewarding. I also appreciate the financial support I received from Prof. Fethi Ahmed, without such support this study was not going to be possible. I also acknowledge various institutions that provided data for the study. I am greatly indebted to my husband and family who have been a pillar of strength throughout the study. Lastly, I would like to extend my gratitude to all my friends and colleagues from Lupane State University whose moral and academic support contributed to the success of this study.

ABSTRACT

Wetlands ecosystems are amongst the most diverse and valuable environments which provide a number of goods and services pertinent to human and natural systems functioning yet they are increasingly threatened by anthropogenic and climatic changes. This thesis, examines the impact of climatic trends and variations, and land use/land (LU/LC) cover changes on wetland extent within Mzingwane catchment, south-western of Zimbabwe. An attempt is made to establish how the two stressors (climate and LU/LC changes) modify areal extents of wetlands over time, grounded on the hypothesis that, climate and LU/LC related changes impact on wetland ecosystems resulting in their degradation, shrinking in size and in some cases overall loss.

To achieve the broader objective of the study, a number of parametric and non-parametric statistical analyses were employed to quantify and ascertain climate variability and change in Mzingwane catchment through the use of historic and current climatic trends in rainfall and temperature (T). Remote sensing data was used for wetland change analysis for the period between 1984 and 2015as well as future land cover predictions based on CA-Markov Chain model. LU/LC changes on nested wetlands were modelled at catchment level. In addition the study simulated future rainfall and extreme events and their implications on wetland dynamics using Regional Climate Models derived from CORDEX data.

Trends in annual T_{max} significantly increased ($p<0.05$) at an average of 0.16 decade^{-1} in 80% of the stations. Results of extreme events indicate a statistically significant increase ($p<0.05$) in the occurrence of extreme dry periods since the 1980s. Rainfall variability results show that contemporary mean annual rainfall has not changed from that measured during the historic period of 1886-1906. However, the number of rainy days (>=1mm) has decreased by

34%, thus suggesting much more concentrated and increased rainfall intensity. A notable shift in both the onset and cessation dates of the rainy season is recorded, particularly during the 21st century, which has resulted in a significant reduction ($p<0.05$) in the length of the rainy season. Land change analysis results show a decline in woodland and wetland cover which could be resulting from both human and natural factors. Major conversions are from wetland cover to crop field, suggesting agricultural encroachment onto wetland areas. Wetland area thus significantly decreased by 60.16% (236, 52 ha) in the last 30 years ($p < 0.05$). CA-Markov model results for the years 2025, 2035 and 2045 predicted an overall increase in the crop field areas at the expense of woodland and wetland areas. LU/LC modelling results suggest that LU/LC changes modify wetland hydrology which consequently influences wetland areal extent. Trend results for projected rainfall suggest a significant decreasing trend in future rainfall (2016-2100) at $p<0.05$. In addition, a general decreasing trend in the number of rainy days is projected for the future climate although the significance and magnitude varied with station location. Regional Climate Models projections suggest an increased occurrence of future extreme events particularly towards the end of this century. The findings are important for developing appropriate sustainable and adaptive strategies given climate changes as well as designing catchment level wetland management approaches aimed at sustaining wetland ecosystems for the current and future generations. Any future efforts towards protection of the remaining wetlands should be combined with developing a sustainable relationship between social and ecological systems which will enable communities to adapt to the effects of changing climates

TABLE OF CONTENTS

LIST OF FIGURES

LIST OF TABLES

LIST OF PLATES

LIST OF ABBREVIATIONS AND ACRONYMS

CORDEX	- Coordinated Regional Climate Downscaling Experiment
CRCN	- Canadian Regional Climate Model
CVA	-Change Vector Analysis
DEM	- Digital Elevation Model
DTR	- Diurnal Rage of temperature
ENSO	- El Niño Southern Oscillation
GCMs	- Global Circulation Models
GDP	-Gross Domestic Product
GHGs	- Greenhouse Gases
GIS	- Geographic Information Systems
IPCC	-Intergovernmental Panel on Climate Change
ITCZ	- Intertropical Convergence Zone
LU/LC	-Land use/land cover
MK	- Mann-Kendall
NOAA	-National Oceanic and Atmospheric Administration
PCA	-Principal Component Analysis
PCI	-Precipitation Concentration Index
PET	- Potential Evapotranspiration
ppm	- parts per million
RCMS	- Regional Climate Models
REMO	- Max Planck Institute Regional Model

RF	-Random Forest
SAR	- Synthetic Aperture Radar
SMHI	- Sveriges Meteorogiska Och Hydrologiska Institute
SPEI	-Standard Precipitation and Evapotranspiration Index
SPI	-Standard Precipitation Index
SST	- Sea-surface Temperature
WMO	-World Meteorological Organisation
DF	-Degrees of freedom
MODIS	-Moderate Resolution Imaging Spectroradiometer
DEM	-Digital Elevation Model
STRM	-Shuttle Radar Topography Mission

CHAPTER 1: GENERAL INTRODUCTION

1.1 Introduction

Wetland ecosystems are the interface between the terrestrial and aquatic ecosystems (Ellery *et al*., 2010) and are globally valuable and fragile diverse environments which are sensitive to any environmental perturbations resulting from both natural and human activities. The Ramsar Convention of 1971 on global wetlands defined wetlands (in Article 1) as

> *'Areas of marsh, fen, peatland or water whether natural or artificial, permanent or temporary with water that is static and flowing, fresh or salty including areas of marine water'* (Kabii, 1996).

Wetland ecosystems provide several functions ranging from flood attenuation, stream flow regulation, sediment trapping, phosphates, and nitrogen removal and toxicant cleansing, carbon storage and the general maintenance of floral and faunal biodiversity (Mitsch and Gossalink, 2000; Millennium Ecological Assessment, 2005; Ellery *et al*., 2010). Wetland ecosystems are thus referred to as the 'kidney' of the Earth (Rundquist *et al*., 2001) because of their important biogeochemical functions. However, despite these aforementioned valuable ecosystem services, wetlands are faced with numerous threats from human activities resulting in their shrinking, modification and overall degradation (Rundquist *et al*., 2001; Schuijt, 2002; Malan and Day, 2005; Mitchell, 2013). Empirical evidence suggests a 60% loss in the global wetland area in the last 100 years (Burkett and Kusler, 2000; Moser, 2010 Junk *et al*., 2013). In Africa, 50% of the wetland areas have been degraded owing to human interference, particularly in countries such as South Africa, Mozambique, Zimbabwe, Malawi and Guinea (Wetland International, 2009). Consequently, wetland loss has increasingly become a major threat to biological diversity emanating from human-environment interactions such as agriculture, urbanisation, damming, road construction, and human settlement, among other activities (Ellery *et al.*, 2016). The situation is further compounded by the increasingly

changing climatic conditions which are likely to alter catchment hydrology, leading to the modification of wetland ecosystems (Finlayson, 2016).

There is a growing consensus that climate change is an additional stressor likely to modify wetland ecosystems, which not only includes the reduction of wetland area, but also changes in structure, vegetation cover, inundation patterns, habitat fragmentation, and reduced water levels (Erwin, 2009; Herrera *et al*., 2012; Lee *et al*., 2015). Literature shows that climate change in Africa is no longer a myth but a proven reality with most countries having experienced changes in both rainfall and temperature patterns (Kruger and Nxumalo, 2017; Kusangaya *et al.*, 2014; Sibanda *et al*., 2017). Such changes are likely to affect abundance, distribution of species and the general functioning of the wetland ecosystems. Annual rainfall is decreasing in central Africa and northern Sahara while southern Africa is projected to experience declining rainfall with increased frequency of extreme events, likely to pose significant disturbances to wetland ecosystems (Barros and Albernaz, 2014).

Zimbabwe is endowed with both perennial and seasonal wetlands (Matiza, 1992).These wetlands are very useful for both natural and human well-being, providing water for domestic and wild animals, especially during the drier seasons (Chikodzi and Mutowo, 2014). Wetlands also supply other materials such as reeds, grass and wood which are used for crafting and carving (Kabii, 1996; Gardner *et al*., 2015). A previous study by Ndhlovu (2009) has shown the impact of human activities on wetland integrity in Zimbabwe and climate variability and change have emerged as a new complex stressor on the already threatened wetland ecosystems. Thus, this thesis examines impacts of climate change and variability on the areal extent of wetlands in Mzingwane catchment of Zimbabwe, the catchment is situated in a semi-arid region which receives erratic rainfall, yet it still consists of perennial and

temporal wetlands. In addition, Mzingwane catchment also supplies neighbouring towns like Gwanda and Bulawayo with water throughout the year. It is acknowledged that human activities are one of the major drivers of wetland degradation; an attempt is made to establish how the two stressors (climate change and land use/land cover change) affect wetlands. The hypothesis is that climate change and variability together with human-induced LU/LC changes have a huge influence on wetland dynamics, which jeopardise wetland integrity. A number of studies have assessed the singular impacts of climate change and land use changes on wetlands globally (Barros and Albernaz, 2014; Fitchett and Grab, 2014; Meng *et al*., 2016).The thesis, builds on the aforementioned studies, albeit focusing on impacts at catchment level which has not been studied in Zimbabwe, in particular, south-western Zimbabwe.

1.2 Background to the study

Global climate change is one of the major contemporary issues of concern and the changes are largely linked to anthropogenic greenhouse gas emission (WMO, 2017). According to the IPCC fourth assessment report (IPCC, 2014), the Earth is expected to warm by between 1.8 - 4°C within the 21st century, which will cause an increase in the melting of ice and sea level rise of between 18 - 59cm. Such warming has promoted increased frequency and duration of extreme weather events such as droughts severe storms and floods (Asadi-Zarch *et al*., 2015). Ecologically, literature reveals that climate change and variations will result in biological diversity loss and subsequent species extinction. Such changes will obviously affect and alter essential life support systems such as biogeographic cycles which will result in compromised wetland ecosystem integrity (Finlayson *et al*., 2013). For instance, an increase in temperature modifies the thermal stratification of wetland water levels (Finlayson *et al*., 2013; Finlayson, 2016). Recurrent extreme events associated with global warming also affect wetland

ecosystems through altered hydrologic patterns during droughts and flooding periods. Other potential impacts of climate change on wetlands include changes in the general ecosystem structure, habitats, ecological function and species composition.

Projections for future climates derived from RCMs indicate a general increase in the global temperature with rainfall varying widely through space and time. Recurrence of extreme events are also worrying, particularly in semi-arid regions not only because of environmental consequences but also because of socio-economic impacts, mainly for developing countries. The probable impacts of climate change in Africa reach far and wide, partly because of its vulnerability and lack of capacity to adapt (WMO, 2017). Changes in wetland water balance under projected climate change could alter wetland area (van der Valk *et al*., 2015). Such changes in wetland area (loss and degradation) emanating from climate variations may also increase flood induced damages, habitat loss and fragmentation, and soil erosion.

Apart from climatic perturbations, human activities also pose threats to the fragile wetland ecosystems through continuous LU/LC changes. Such catchments LU/LC changes pose both direct and indirect impacts on hydrology, which in turn influences wetland ecosystems in various ways. Direct impacts result from activities occurring in the wetland, such as forest removal, cultivation and water harvesting (Russo *et al*., 2016). Indirect impacts entail those activities outside the wetland, but which may eventually disturb the wetland functioning and service provision. These include upland activities that change run-off patterns, influx or reduction of surface run-off, and damming and upslope irrigation activities among other things (Esteves *et al*., 2008). Thus, this study attempts to unravel the extent to which climate and land use/ land cover modify wetlands at a catchment level.

1.3 Problem statement

Wetlands are important biodiversity hotspots in Zimbabwe that provide useful resources to sustain humans and wildlife. They are a source of water for drinking and agriculture, especially during the drier seasons. Wetland vegetation is an integral feature of wetland ecosystem, which constitutes the primary producers for the food chain. It is also a vital habitat for other species like phytoplankton, zooplankton vertebrates, and invertebrates. However, previous studies (Ndhlovu, 2009; Murungweni, 2013; Marambanyika and Beckedahl, 2016) have shown that wetland ecosystems are being degraded by human activities such as agriculture and urbanisation and Mzingwane catchment wetlands are no exception. The situation is further compounded by current climate variability and change, which has seen the catchment experiencing recurrent droughts and increased temperatures (Sibanda *et al*., 2017). Such climatic anomalies will no doubt affect the availability of water and modify wetland ecosystems. Literature shows that more than half of the world's wetlands have been disturbed, transformed and degraded in the last 150 years (Gardner *et al*., 2015).

In response to this problem, the study sought to ascertain climate variability and change in Mzingwane catchment through the use of historic and current climatic trends in rainfall and temperature and modelling impacts of LU/LC changes on nested wetlands as well as through simulating future rainfall and extreme events and their implications on wetland dynamics. It is hoped that the results will help in the crafting of relevant and sustainable policies and strategies for the management of local level wetlands for the benefit of both humans and ecosystems.

1.4 Significance of the study

Wetlands are valuable ecosystems that need to be conserved for sustainability of our global ecosystems. Wetlands play a significant role in the nutrient cycling of carbon and nitrogen

(Mitsch and Gosselink, 2000) and their maintenance of environmental quality through the removal of excess nutrients and toxicants (Richardson, 1994). Monitoring wetlands and detecting changes over time is essential for a better understanding of the impacts of climatic change and long-term sustainability of these fragile environments. Conventional methods of assessing wetland ecosystems are costly and time-consuming (Adam *et al*., 2009; Klemas, 2011; Ozesmi and Bauer, 2014), thus, remote sensing has emerged to be a novel tool for the monitoring and sustainable management of wetland ecosystems (Govender *et al*., 2007). Airborne and satellite multispectral and hyperspectral remote sensing are useful and efficient methods for identifying, classifying and mapping of wetland vegetation species composition (Schmidt and Skidmore, 2003; Akasheh *et al*., 2008 Adam *et al*., 2010). A number of studies have been undertaken to focus on the impact of changing climates on wetlands (Munyati, 2000; Malan and Day, 2005; Rebelo *et al*., 2009; Landmann *et al*., 2010; Ozesmi and Bauer, 2014; Chan and Xu, 2013).

Wetland studies have been carried out in Zimbabwe. Mhlanga *et al*., (2014a) mapped the spatial extent of urban wetlands of Harare using Landsat and SPOT imagery. Murwira *et al*. (2004) used remote sensing to determine the role of riverine wetlands in mitigating flooding in areas downstream of their location Eastern Caprivi wetland in Zambezi catchment. Msipa (2009) and Murungweni (2013) investigated the impact of urbanisation on wetland water quality in Harare while Ndhlovu (2009) assessed the impact of land-use change on wetland health in Intunjambila. Chikodzi and Mutowo (2014) analysed climate change signatures as a means of understanding drying up of Gutu wetlands. Other noted studies by McCartney *et al*. (2013) focused on the hydrologic aspects of wetlands, wetlands and agricultural development (Mharapara, 1998), wetland institutions (Sithole, 1999) and community participation for sustainable utilisation of wetlands in Zvishavane (Marambanyika *et al*., 2016). There is an

evident dearth of published knowledge regarding the combined impacts of changing land use patterns and climate on wetland areal extent. It is hoped that the present study results will also contribute to a better understanding of wetland ecosystem modification and complexities that arise due to the effects of climate variations and change. Such information is imperative for the sustainable management and monitoring of wetland ecosystems. The study hopes to inform policymakers and environmentalists in the design of relevant management strategies under an ever changing global environment.

1.5 Main Aim

This study aims at assessing and predicting combined impacts of land use/cover and climate changes on the areal extent of wetlands in Mzingwane catchment, Zimbabwe.

1.5.1 Specific Objectives

The specific objectives of this study were to;

1. Determine spatio-temporal temperature trends and extreme events in Mzingwane catchment.
2. Investigate long term rainfall trends in Mzingwane catchment for historic (1886-1906) and contemporary periods (1920-2015).
3. Quantify spatio-temporal wetland areal changes in Shashe sub-catchment of Mzingwane catchment.
4. Model the impacts of land use/ cover changes on nested wetlands in Shashe sub-catchment.
5. Simulate future rainfall and extreme events over Mzingwane catchment for 2016-2100.

1.6 Methodological approach

The catchment approach involved the ascertaining of climate variability and change, mapping wetlands and detecting changes over time as well as predicting future wetland area using CA-Markov model. Impacts of catchment LU/LC changes on nested wetlands were modeled based on hydrologic modelling and GIS techniques and multivariate regression analysis determined the most influential land use/land cover on wetland area loss. Finally, RCMs were used to simulate future rainfall and extreme events. Climate assessments were done for the entire Mzingwane catchment for the purposes of using several stations required for statistical reasons while wetland change analysis using Landsat data and LU/LC modelling were done for the Shashe sub-catchment of Mzingwane catchment.

1.7 Structure of the thesis

Each thesis chapter (3-7) has its own aims, results and discussions in a paper format, their combined conclusions answer the broader aim of the study. The thesis has a total of eight substantive chapters including (this) introductory chapter, which outlines the background to the study, rationale and general aim of the study. Chapter 2 explores relevant literature on wetland ecosystems, climate change and LU/LCimpacts on wetland dynamics and future implications of the changes on future wetlands. Chapter 3 investigates spatio-temporal temperature trends and extreme events over the entire Mzingwane catchment. Chapter 4 examines long-term rainfall characteristics in Mzingwane catchment through the analysis of annual and seasonal rainfall trends, the number of rainy days and their trends, rainy season start and end date analysis, as well as the determination of the changes in the length of the rainy season. Extreme rainfall events are established using the Standard Precipitation Index (SPI). Chapter 5 assesses spatio-temporal changes in wetland areal extent using remote sensing techniques. Chapter 6 models the impacts of LU/LC changes on nested wetlands

using a catchment approach. Chapter 7 simulates future changes in rainfall and extreme events and their implications on future wetlands. Finally, chapter 8 synthesises the findings, concludes the thesis and presents recommends for future studies in the area.

CHAPTER 2: GENERAL LITERATURE REVIEW

2.1 Introduction

This chapter reviews theoretical perspectives of key concepts which guide the study, such as wetlands, climate change, and climate variability, land use/land cover changes

2.2 Wetland Ecosystems and their sensitivity to environmental changes

Wetland ecosystems are fragile environments where saturation and water determine the nature of the ecosystem (Cowardin *et al*., 1979). They are also defined as transitional lands between terrestrial and aquatic systems where the water table is always near or at the surface and the surface area is covered in the water (Mitsch and Gosselink, 2007). In Zimbabwe, wetlands are defined by the Environmental Management Act as land that is usually of permanent or seasonal flooding or those areas of subsurface water accumulation through seepage such as vleis or dambos. The sensitivity of wetlands to environmental change may arise from both surface and groundwater fluctuations, urbanisation, agricultural activities and related land reclamation within the catchment (Esteves *et al*., 2008; Mitchell, 2013). Issues of degradation through the incision, drying out of wetland surface water and the introduction of invasive species negatively impact on wetland hydrology and function (Ellery *et al*., 2016).

2.2.1 General importance of wetlands

Wetlands provide a number of ecosystem services which are essential for ecosystem integrity (Mitsch and Gossalink, 2000). These services can be further subdivided into regulatory, supporting, use function and cultural importance (Ellery *et al.*, 2010). Wetland ecosystems contribute and support human survival through the provision of food resources such as fish, water purification, climate regulation, flood control, tourism opportunity and other materials

such as reeds and wood for art and craft (Mitsch and Gosselink, 2000; Schuijt, 2002b). Most rural communities depend on wetlands for livelihood particularly during crop failure and drier seasons, providing productive land for crop production and resources for economic benefits such as fruits, fish, grass, and water.

However, regardless of the aforementioned significance, wetland ecosystems are globally threatened by human activities that degrade their integrity and disturb their functions (International Institute of Sustainable Development, 2012). Human-related threats to wetlands include increased human population pressure which subsequently increases the demand for resources such as water, and land for urbanization (Rebelo *et al*., 2009; Mhlanga *et al*., 2014). Agricultural activities around wetlands have degraded the systems through over discharge, pollution, and the introduction of invasive species (Munyati, 2000; Ndhlovu, 2009; Murungweni, 2013).

2.2.2 Wetland classification

A comprehensive wetland classification system was developed by Cowardin *et al*. (1979). This system recognised two categories of wetlands; coastal and inland wetlands which were further broken down into subsystems. Coastal wetlands develop along the coastlines while inland wetlands are also referred to as fresh water wetlands, and include floodplains, depressions, fens and dambos. Marshes and wet meadows are also very common inland wetlands in Southern Africa and are often dominated by grasses and shrubs (Ollis *et al*., 2015).

In view of the challenges of using USA based wetland classification system, an attempt was made by Dini and Cowan (2001); Ellery (2015); Ollis *et al*. (2015) to modify the Cowardin

system, and came up with a classification approach that suits southern Africa mainly focusing on inland wetlands. The modification by Ellery (2015) is spatially hierarchical in nature, with the first level consisting of marine, estuarine and inland wetlands. Other levels concentrate on inland wetlands using the following criterion; regional setting (level 2), landscape dynamics (level 3), hydro-geomorphic characteristics (level 4), hydrological regimes (level 5) and local biophysical properties (level 6).

2.2.3 Methods of assessing and monitoring wetlands

Traditionally, wetland assessment and monitoring comprised of labour intensive and time consuming field based methods which included the use of quadrats, line transects and field surveys to assess various wetland dynamics such as soil quality, vegetation types, water quality and areal extent. However, such methods have always been difficult, not only because of the time factor but also because of accessibility issues (Adam *et al*., 2009; Klemas, 2011). Thus, the advent of remote sensing technologies in the past five decades or so provided novel techniques for wetland studies. Remote sensing sensors are used to capture data and information about the Earth, necessary for the effective spatio-temporal analysis of Earth resources. Literature shows that in the last 3 to 5 decades remote sensing technology has been widely employed in wetland mapping, change detection, species discrimination, and in assessing changes in biophysical and biochemical parameters of wetland vegetation (Johansen and Phinn, 2006; Rebelo *et al*., 2009; Chan and Xu, 2013; Ghosh *et al*., 2016;). Remote sensing imagery can be obtained from aerial photographs, multispectral optical and microwave, and hyperspectral sensors.

2.3.4 Use of aerial photographs in wetland studies

Aerial photographs were the first remote sensing technique to be used in wetland management during the 1970s (Edwards and Brown, 1960). The photographs offered high spatial resolution, although these lacked spectral accuracy. Based on its efficacy, a number of studies during the 1970s and 80s applied remote sensing data from aerial photos. For instance, Johannessen (1964) used aerial photos of Nehalem Bay to compare wetland marsh boundaries in the United States, while another study by Ibrahim and Hashim (1990) used aerial photographs to identify species of mangrove forest.

Coarse spatial resolution data like Moderate Resolution Imaging Spectroradiometer (MODIS) have also been used in wetland studies (Landmann *et al*., 2010; Ibharim *et al*., 2015; Lee *et al*., 2015). Multispectral airborne and satellite remote sensors provide high spatial resolution data with a reasonable number of spectral bands and as such have been extensively applied in wetland management studies (Dong *et al*., 2014; Quinn and Epshtein, 2014; Bourgeau-Chavez *et al*., 2015; Han *et al*., 2015). More recently, a number of studies employ the efficacy of hyperspectral data from sensors such as Hyperion and Hymap. Such data consist of hundreds of narrow bands and a continuous spectral profile for each pixel, which increases detail in terms of spectral and spatial resolution. Such detail is necessary in the study of submerged wetland vegetation species (Adam *et al*., 2009). Airborne, satellite and handheld sensors have been successfully applied in wetland mapping and species discrimination. For instance, Rosso *et al*. (2005) assessed the capability of hyperspectral data to study the structure of wetlands of San Bay, California and their results indicate that spectral mixture analysis is suitable for mapping marsh wetlands. While a study by Andrew and Ustin (2008) employed Hymap imagery with a 3m spatial resolution to map invasive plant species in Californian wetlands. The potential of high spectral remote sensing data in monitoring and

mapping salt marsh vegetation was assessed by Kumar and Sinha (2014) and most of the species were correctly identified and mapped.

High spatial resolution optical data such as SPOT 5 and 6, RapidEye, WorldView-2 and GeoEye of less than 4 m resolution offer ideal high spatial resolution and more texture information which have greatly improved wetland mapping and monitoring (Davranche *et al*., 2010a, 2010b; Mutanga *et al*., 2012; Adam *et al*., 2014b).

2.3.5 Wetland mapping using remote sensing

During the last 3 decades, wetland mapping has widely applied remote sensing techniques because of its versatility and ability to integrate and analyse data within a GIS environment (Ozesmi and Bauer, 2014). Advancement in Earth observation provides opportunities for better and cheaper methods of mapping complex ecosystems like wetlands through space and time. Thus, a number of studies have mapped wetlands using remote sensing techniques. For instance, Rebelo *et al*. (2009) used remote sensing and GIS data to map and assess changes in wetlands of Srilanka. Mhlanga *et al*. (2014b) also employed Landsat and SPOT imager to map spatial extent of Borrowdale wetlands in Harare. Mwita *et al*. (2013) utilised Landsat imagery to map various types of wetlands in terms of size, use patterns and general spatial distribution using a hybrid classification system. In addition, MODIS data were used to map wide area wetlands in semi-arid Africa (Landmann *et al*., 2010).

Remote sensing is also useful for wetland change detection, mostly because of the availability of archival spatio-temporal data essential for monitoring changes over time. As such, studies by Vanderlinder *et al*. (2014) used remote sensing to assess changes in wetland plant

communities over time in the great salt lake of Utah. Other change detection studies are by Haack (1996); Teferi *et al.* (2010); Chen *et al*. (2014); Han *et al*. (2015); Feng *et al*. (2016b).

The estimation of biophysical and biochemical parameters of wetland vegetation have also applied remote sensing techniques. For example, Ghosh *et al*. (2016) monitored long term biophysical characteristics of tidal wetlands in the northern Gulf of Mexico and used MODIS to map the leaf area index, biomass, chlorophyll content and vegetation fraction while Wang and Liao (2009) estimated wetland vegetation biomass in Poyang ae using Landsat data. In addition, hyperspectral indices were used to estimate standing biomass in papyrus swamps of iSimangaliso wetland park, South Africa by (Adam *et al*., 2010). However, regardless of the vast literature regarding the application of remote sensing in wetland management, Zimbabwe has lagged behind particularly for wetland ecosystems. Thus, this study is hoping to fill this gap of knowledge focusing at micro-level assessments.

2.2.4 Anthropogenic drivers of wetland loss and degradation

The drivers of wetland loss and degradation are both natural and human-induced, creating a very complex mixture of detrimental factors. Anthropogenic causes of wetland loss and degradation include damming, the introduction of invasive species, land reclamation, expansion of agricultural land, urbanisation, mining activities and over-exploitation of resources. For instance, damming improves water availability and supply to local communities but tend to alter natural hydrologic processes. Damming also block the movement of nutrients downstream which often affect deltas (Galatowitsch, 2016).

Expansions of agricultural and urban lands are major drivers of wetland conversion. These result from increased population, which tend to increase demand for land resources for

economic development (Huu Nguyen *et al*., 2016). Agriculture causes downstream sedimentation through increased soil erosion and eutrophication from inorganic fertilisers. Agricultural biocides enter wetlands through overland flow causing negative effects to wetland biota in the form of direct and indirect impacts. Direct impact includes toxicity and compromises species survival while indirect effects comprise reducing primary production, which in turn affects faunal species up the food chain. Crop production also drains wetland water, which compromises wetland water balance with consequential effects on the overall wetland integrity (Borges *et al*., 2018). Agricultural activities in and around wetlands tend to increase wetland vulnerability to the invasion which is transported by runoff events that carry invasive species' seeds into wetlands (Zedler and Kercher, 2004). These, in turn, disturb biochemical cycles and result in loss of wetland services and function.

Urbanisation causes wetland water pollution through petrochemicals, salts and biocides, washed downstream via storm drains (Valtanen *et al*., 2014). Such influx of pollutants from urban environments negatively affects wetland biota and quality of water. Because of this, urbanization has always been linked to wetland biodiversity loss (McKinney, 2008). Timber harvesting of forested wetlands may cause habitat change and fragmentation and subsequently species migration (Sun *et al*., 2001). In addition, over-exploitation of resources necessitated by increased pressure from people seeking livelihood and for food security requirements is another significant impacting factor to wetland loss and degradation (Galatowitsch, 2016). Mining is another impacting factor in water pollution and acidification emanating from acid mine drains.

2.3 Climate Change in Africa

According to the "IPCC - Intergovernmental Panel on Climate Change" (2007), climate change "refers to a change in the state of the climate that can be identified by changes in the mean or the variability of its properties that persists for extended periods". Climate change may also refer to any changes recorded over time due to natural variability and human activity. Rahman (2013) defined climate change as the long-term changes in the statistical distribution of weather patterns over time of between 35-40 years. There is concrete evidence that climate has been changing which includes the current global warming, mainly resulting from the increased concentration of greenhouse gases ("IPCC - Intergovernmental Panel on Climate Change," 2007; Barbee and Heather, 2008). The depletion of ozone layer estimated at 4% per decade is evident enough that climate is changing (Rahman, 2013). There is also tangible evidence displayed by the shrinking of ice sheets, and the rising of sea level of about 17cm (Moser, 2010). In addition, the warming of global oceans is also evident of the changing climate with the top part of 700m of the oceans showing a 0.16 °C higher temperature since 1969 (Fauchereau *et al*., 2003).

A study conducted by Root and Schneider (2002) has shown that the Earth's climate has been changing for the past 100 million years. They noted that earlier changes were naturally induced; for example the Gondwana era. However, recent spasms are largely related to human activities that increase the greenhouse gases. These gases include carbon dioxide, methane and nitrous oxide. Coupled with this is the increase in dust, soot and sulphur dioxide from industries and mining activities that increase the absorption of terrestrial radiation, resulting in warming temperatures (Hulme *et al*., 2001). Studies have shown that surface temperatures of the Earth have increased by an average of 0.6 °C during the last 20th Century. Warming is continuing setting a new temperature record of 1.1 °C higher than the pre-

industrial period and 0.06 °C higher than 2015 record (WMO, 2017). This warming is attributed to an increase in greenhouse gases emission. In this regard, carbon dioxide reached new levels at 400ppm in the atmosphere by the end of 2015. As the warming continues, there is a notable rise in global sea levels of approximately 20cm since the beginning of the 21st century due mostly to thermal expansion of oceans and melting of ice (WMO, 2017). The World Meteorological Organisation Global Atmospheric water programme shows that GHGs reached new levels in 2016 (Table 2.1).

Table 2.1: 2016 levels of GHGs

GHG	Level	% Change from 1750 levels
CO_2	400.00 ± 0.1 parts/million	144
CH_4	1845 ± 2 parts/billion	256
$N2_O$	328.0 ± 0.1parts/billion	121

Source: Wold Meteorological Organisation 2016

There is a noticeable increase in the amount of GHGs in the atmosphere and the NOAA annual GHG Index shows that from 1990-2015, radiative forcing from the GHGs increased by 37% with carbon dioxide accounting for 80% of the increase (Brown and Caldeira, 2017).

In Africa, future climate projections suggest accelerated changes in climatic conditions, which are expected to pose profound environmental impacts. Climate Models project a 1.5°C rise by 2040, which is approximated to cost Africa about 1.7% of its GDP. Thus, as the temperature continues to rise so does the economic cost. For instance, a predicted 4.1°C rise by the end of the century will result in a 10% decline in the continent's GDP (IPCC, 2014). Such changes in climate exert pressure on ecological ecosystems such as wetlands and it

often affects the photosynthesis, respiration, growth, reproduction and general use of water (Finlayson *et al*., 2013; Gates, 1993,). Gates also noted the significant influence of climate variations on the plant physiology.

2.4 Climate change and variability in Zimbabwe

Zimbabwe's rainfall is unimodal and normally begins in October and ends in March, but varies widely through space and time (Therrell *et al*., 2006; Manatsa and Mukwada, 2012). The rainy season is largely dependent on the movement of the Inter-Tropical Convergence Zone (ITCZ) and upper westerly waves from the mid-latitudes, which determine the intensity of the rains during the rainy season (Buckle, 1996). Notably, much of the rainfall variability in Zimbabwe is also associated with El Niño Southern Oscillation (ENSO) phases (Reason *et al*., 2005; Manatsa and Matarira, 2009; Jury, 2013; Mamombe *et al*., 2016). Extreme weather events are occurring more frequent during the 21st century than before (Sibanda *et al*., 2017), thus exposing communities to more food-insecure conditions. Apart from the large-scale atmospheric thermodynamics, rainfall patterns in Zimbabwe are also influenced by micro-level dynamics such as relief, elevation and land cover (Sanchez-Moreno *et al*., 2014).

Investigations on historic and future climatic trends in Zimbabwe have suggested significantly reduced rainfall patterns and increased temperatures which seem to be closely related to climate variability (Sango and Godwell, 2015; Unganai, 1996a). The warming spasm observed in southern Africa has also been statistically proven in Zimbabwe and temperature trends are significantly increasing (Sibanda *et al*., 2017), which is strongly associated with recurrent extreme events. A rainfall reconstruction based on tree rings has indicated a long-term (1800 to 2000) rainfall trend, that past severe droughts correspond to El Niño and with high rainfall variability over time (Therrell *et al*., 2006). Significant changes in

the start and cessation dates of the rain season are detrimental to 'normal' crop production (Mushore *et al*., 2017), as such changes may pose a risk of the occurrence of dry spells within the rain season, and which impacts negatively on crop growth and yields (Moyo *et al*., 2017). Past work has suggested that annual rainfall trends for all of Zimbabwe as being statistically insignificant, but rather that it is the intensity, timing and duration that has shifted (Mazvimavi, 2010; Muchuru *et al*., 2016). However, these findings varied broadly across the entire country; as such more detailed studies are required at sub-catchment level. To this end, the current study aims to assess inter-annual and seasonal rainfall variability and change at the micro-spatial scale (i.e. Mzingwane sub-catchment) and then compare these to those of past studies that have worked at a national scale. It is hoped that such information enables better catchment-scale management for future water needs and wetland sustainability.

2.4 Hydrologic models used for catchment assessment

Rainfall-runoff models can be grouped under two main classes which are the lumped conceptual models and the distributed physically based models. Lumped conceptual models use mathematical descriptions to explain processes such as runoff within a given hydrologic system (Clarke *et al*., 2015). Spatial variations of processes are spatially regionally (Wood, 1995). Whereas physically based models use a number of equations to explain temporal and spatial variations of hydrologic processes.

Hydrologic processes are said to be irregular both in space and time (Pilgrim, 1982). Conceptual models tend to perform better than physically based models. Therefore, this study preferred Pitman rainfall- runoff model for the extrapolating parameters from gauged stations. Pitman has been widely used to analyse monthly hydrology for a number of catchments in southern Africa (Hughes, 1995;Wagener *et al*., 2004; Hughes *et al*., 2006a;

Kapangaziwiri, 2011) and is said to be sensitive to land use changes because it has parameters that control interception (PT), infiltration (AI, ZMIN, ZA VE and ZMAX) and actual evapotranspiration (R and FF) (Hughes, 1997).

Its simplicity provides fewer challenges emanating from parameter uncertainty which normally limits the potential to regionalise the model. This potential to regionalise the model in Zimbabwe was highlighted by Hughes (1997). It is usually quite easier to calibrate and Pitman (1973) provides some guidelines for initial parameter setting.

Like most conceptual models, the Pitman model consists of functions representing important hydrologic processes in a given catchment (Hughes *et al*., 2006b). The Pitman model is a mathematical model that is used to simulate the movement of water through interlinked systems of catchments, river reaches, reservoirs, irrigation areas and wetlands (Pitman, 1973).

Conclusions

Literature has shown the importance of wetland services and goods for both human and natural environments. It has also been widely established that the wetland ecosystems are shrinking in size and in some cases disappearing due to both natural and human causes. Therefore, a number of studies at a global, regional and national scale have been carried out to assess and monitor wetland ecosystems using field based and remotely base techniques. A cursory analysis of the contemporary literature has extensively utilised remote sensing technologies for mapping wetlands, performing change detection, wetland species discrimination and future predictions for sustainable wetland management. Notable drivers of wetland degradation and loss are agricultural activities, urbanisation, damming, over exploitation and population growth. Climate change has emerged as an additional stressor emanating from global warming and related variations in temperature and rainfall patterns as

well as the acceleration of extreme events. Although a several studies have investigated wetlands in relation to changes in land uses and climate, not much has been done in Zimbabwe, specifically in Mzingwane catchment a gap this study intends to bridge.

CHAPTER 3: SPATIO-TEMPORAL TEMPERATURE TRENDS AND EXTREME HYDRO-CLIMATIC EVENTS IN SOUTHERN ZIMBABWE

Abstract

Atmospheric warming and extreme weather events have increasingly become major contemporary issues of global concern, yet relatively few studies have investigated recent decadal-scale climate change and variability in Zimbabwe. This study investigates spatio-temporal temperature (T) and extreme weather events in Mzingwane catchment of southern Zimbabwe for the period 1967-2015. This is achieved by using the Non-parametric Modified Mann-Kendal trend test, while magnitudes of trends are estimated using Sen's slope estimator. Temporal and spatial trends for extreme dryness and wetness are established by using the Standard Precipitation and Evapotranspiration Index (SPEI). The results of annual anomalies show a strong positive anomaly (0.44°C warmer) at all five stations for the summer months, while winter months recorded cool anomaly averaging -0.28°C. Trends in annual T_{max} significantly increased ($p<0.05$) at an average of 0.16 °C decade^{-1} in 4 stations excluding Matopos, which decreased significantly at 0.29°C decade^{-1}. Between 1970 and 2000 the annual average T_{max} was 0.2°C cooler than the historic annual average (1897-1904), with T_{min} recording a negative anomaly of -0.3°C. Results of extreme events indicate a significant increase ($p <0.05$) in the occurrence of extreme dry periods since the 1980s. The findings are important for developing appropriate sustainable and adaptive strategies as climate changes.

Keywords: climate warming, temperature trends, extreme dryness and extreme wetness, SPIE

[1]This chapter is based on: Sibanda S, Grab S.W and Ahmed F (2017). Spatio-temporal temperature trends and extreme hydro-climatic events in southern Zimbabwe. *South African Geographical Journal*, DOI:10.1080/03736245.2017.1397541

3.1 Introduction

Atmospheric warming and extreme weather events have increasingly become major contemporary issues of global concern. Analysis of observed sea and land surface temperatures show that the Earth's mean surface temperature has risen by ~0.3 - 0.6 °C over the last century (Change, 2013; Pachauri *et al*., 2015). Surface air temperatures over Africa have been warming since the 1960's (Lakhraj-Govender et al., 2016; New *et al*., 2006; Osbahr *et al*., 2010; Tadross *et al*., 2005a), with rates ranging between 0.01 °C and 0.17 °C $year^{-1}$ (Dai, 2011). Long-term air temperature trends in southern Africa have increased both in T_{max} and T_{min}, averaging between 0.02 and 0.4 °C per decade (Kruger and Shongwe, 2004a; Kusangaya *et al*., 2014; New *et al*., 2006; Tshiala *et al*., 2011). Such warming is also pertinent to Zimbabwe, where temperature increases of 0.8 °C $decade^{-1}$ have been reported for the eastern regions over the past three decades (Unganai, 1996a; Sanogo *et al*., 2015).

Linked to atmospheric warming is the intensification and recurrence of extreme weather events such as heat waves, droughts and severe storms. Studies regularly advocate an increased occurrence of global extreme weather events (Dai, 2011; Change, 2013; Sheffield *et al*., 2014) with heat-related extremes notably occurring more frequently than cold extremes. In the African context, tropospheric warming has also yielded increased frequency and intensity of extreme weather events such as droughts (Mirza, 2003; Reason and Keibel, 2004; Dai, 2011). In particular, there has been a significant increase in heat extremes over South Africa during the past 60 years, but this has varied regionally in terms of magnitude (Kruger and Sekele, 2013a). For instance, recently homogenized long-term temperature trends for the Western Cape, South Africa, reported a statistically significant increasing temperature trend for the period 1916-2013 (0.13 °C $decade^{-1}$), with the exception of Cape St Blaize, where T_{max} trends insignificantly decreased at -0.03°C $decade^{-1}$ (Lakhraj-Govender *et*

al., 2016). Trends of rapid warming are of particular concern considering that the African continent is vulnerable to changing climates, with its economies heavily reliant on rain-fed agriculture and limited in their adaptive capacity to changing climates (FAO, 2013). Investigations on historic and future climatic trends in Zimbabwe have suggested significantly reduced rainfall patterns and increased temperatures which seem to be closely related to climate variability (Sango and Godwell, 2015; Unganai, 1996a). Based on the Standard Precipitation Index for the period 1901 to 2004, drought occurrence is homogenous over much of Zimbabwe (Manatsa *et al.*, 2010a).

Detailed assessments of sub-regional climate change and variability are still lacking for Zimbabwe and hence the aim of the chapter is to contribute to this knowledge gap. Although, these aforementioned studies focused on large spatial-scale (country-wide) climate trends, there is a necessity to downscale to sub-regional (catchment) scales, especially given that finer spatial scales exhibit unique topography, which influences local weather and long-term climate change in ways that may not necessarily be uniform across larger spatial scales (Diodato, 2005; Bennie *et al*., 2008). The aim of this paper is thus to test temporal and spatial air temperature trends and extreme weather events over the Mzingwane catchment (~63 000km^2) in south-western Zimbabwe using both historic and more contemporary weather records. The catchment is a major water source for the city of Bulawayo and other towns such as Gwanda and Beitbridge. Notwithstanding the semi-arid nature of the catchment, it is endowed with the most extensive alluvial aquifers in the Limpopo basin (Görgens and Boroto, 1997; Moyce *et al.*, 2006) and wetlands which provide water for domestic, commercial irrigation, market gardening and wildlife, particularly during dry seasons (Ndiweni and Gwate, 2014). Such a catchment-based assessment of climate variability is

important for purposes of designing spatially relevant and sustainable adaptive strategies for water resources and disaster risk management.

3.2 Materials and Methods

3.2.1 Study region

Zimbabwe is divided into seven catchment management regions as indicated in Figure 3.1. This paper fuses on the most southerly of these catchment regions, namely the Mzingwane catchment, which is located between 19.8^{o} and 22.4^{o}S and 27.7^{o} and 32.0^{o} E. The catchment includes four sub-catchments (Shashe, Lower Mzingwane, Upper Mzingwane and Mwenezi) covering an area of ~63000 km^{2} (Figure 3.1). The northern part of the catchment is composed of granitic rocks associated with the greenstone belt, which is rich in gold deposits. Granite terrains form large inselbergs (dome-shaped mountain ranges) between which wetlands occur (perennial dams, vleis, swamps or marshes). The Mzingwane catchment hosts five major rivers (Shashe, Umzingwane, Mwenezi, Bubi, and Marico) that feed into the Limpopo River (Görgens and Boroto, 1997).

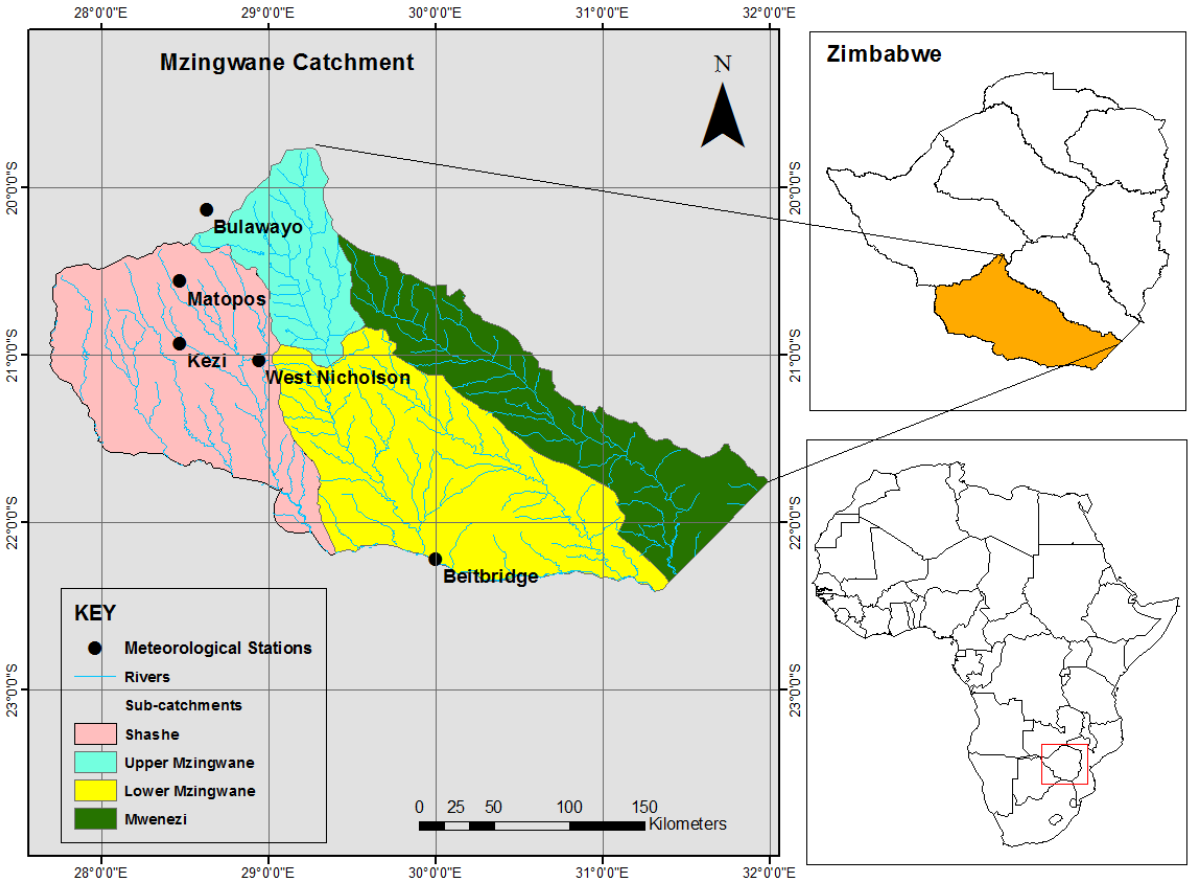

Figure 3.1: Figure 3.1: Mzingwane Catchment showing Shashe, Upper Mzingwane, Lower Mzingwane and Mwenezi sub-catchments

The climate of Mzingwane catchment is semi-arid to arid, but rainfall distribution varies across the catchment, such that the northern regions receive higher mean rainfall (~450 - 600 mm pa) than the southern regions (~200-450 mm pa) (Görgens and Boroto, 1997; Chenje *et al.*, 1998). The wet season typically starts in late October and ends in March, with the highest rainfall occurring between December and February (Unganai and Mason, 2002). Rainfall seasonality is largely influenced by the Inter-Tropical Convergence Zone (ITCZ) which moves southwards during the austral summer, and inter-annually by the El Niño Southern Oscillation (ENSO) which is associated with periods of lower (El Niño) and higher (La Niña) rainfall (Manatsa et al., 2008). The average daily T_{max} for the catchment varies between 27 – 34 °C during summer and 22 – 26 °C in winter (Love *et al.*, 2010), while average T_{min} range

between 18 - 22°C during summer and 5 - 10°C in winter (FAO, 2010). Owing to the relatively low and erratic rainfall, agricultural activities in the catchment are mainly focussed on livestock rearing, as this is the most viable.

3.1.2 Data acquisition and processing

Monthly air temperature data from five meteorological stations (Kezi, West Nicholson, Beitbridge, Matopos, and Bulawayo) in the Mzingwane catchment were used to establish temperature characteristics for the period 1967 - 2015 (Table 3.1). Monthly rainfall data for the same period were used to compute the drought index. Both temperature and rainfall data were obtained from the Zimbabwe Department of Meteorological Services and the National oceanic and Atmospheric Administration (NOAA).

Table 3.1: Monthly air temperature and rainfall data

Station name	Latitude	Longitude	Elevation	Period covered
Bulawayo (Goetz)	-20.13	28.63	1334	1897-1904 1967-2015
Kezi	-20.93	28.47	1000	1967-2015
Matopos	-20.56	28.47	1385	1967-2015
West Nicholson	-21.03	28.94	956	1967-2015
Beitbridge	-22.22	30	486	1967-2015

A primary concern is the limited availability of long-term and good quality weather records for southern Zimbabwe; hence records are spatially limited and confined to only a few reliable stations. Although historic 19th and 20th century data were obtained for Bulawayo, only eight years of temperature data are available for the earliest period (1897-1904), and continuous recording only began in 1967.

Data values were visually inspected to identify outliers and typographic errors on monthly temperature series, while AnClim software was used for automated identification of data errors and outliers at station level (Stepanek *et al*., 2011). Homogeneity testing employed a number of different tests (Alexanderson SNHT, Mann-Whitney Pettit test, and bivariate test and Buish Hands test) because utilising several methods for assessing homogeneity yields more reliable results than a single test (Stepanek *et al*., 2011). The Zimbabwean Meteorological Bureau provided some station metadata (nature of data collection, instrument changes among other things) which helped identify potential change points. Inhomogeneities were adjusted by creating reference series of correlated data from neighbour stations using ProClimDB software (Stepanek *et al*., 2011).

Based on Alexanderson SNHT, the Mann-Whitney Pettit test, Bush Hand test and Bivariate test (Stepanek *et al*., 2011), a number of inhomogeneities were detected. In cases where the detection using various tests was highlighted, adjustments were made using a low-pass filter for adjustment statistics in AnClim software. Methods of observation changed from manual to automatic in the early 1980s and some stations were relocated during the same period. Notably, all identified change points (significant change years) coincided with ENSO events.

3.1.3 Spatial distribution of temperature anomalies

Temperature anomalies were calculated as the difference between observed temperature and the mean reference value for the period 1970-2000, which is the so-called ‘climate normal’ period (Arguez and Vose, 2011). Using anomalies also curtails errors related to station location, elevation effects and missing data (Rapp, 2014).

3.1.4 Trend analysis

A non-parametric Modified Mann-Kendall test (1998) was used to detect seasonal and inter-annual trends in adjusted time series of temperature data and Standard Precipitation and Evapotranspiration Index (SPEI). The null hypothesis states that data are independent and randomly ordered. The test statistic S is computed as:

$$S = \sum_{i=1}^{n-1} \quad \sum_{j=i+1}^{n} sgn(xj - x_{i)} \qquad (1)$$

Where x_j represents the sequential data values, n is the length of the dataset

$$sgn(y) = \begin{Bmatrix} 1 & \dots & if\ (y > 0) \\ 0 & \dots & if\ (y = 0) \\ -1 & \dots & if\ (y < 0) \end{Bmatrix}$$

When the statistic S is approximately normally distributed with the mean

$$E(S) = 0$$

$$V(S) = \frac{n(n-1)(2n+5) - \sum_{i=1}^{m} t_i\,(t_i-1)(2t_i+5)}{18} \qquad (2)$$

Where m is the number of tied groups and t_i is the size of the *ith* tied group. The standard test statistics Z is computed as:

$$Z_{mk} = \begin{Bmatrix} \frac{S-1}{\sqrt{var(S)}} & when & S>0 \\ 0\dots & when & S=0 \\ \frac{S+1}{\sqrt{var(S)}} & when & S<0 \end{Bmatrix} \qquad (3)$$

3.1.5 Seasonal trends in temperature and extreme wet and dry events

Sensitivity to seasonal variations in temperature and extreme wet and dry events are tested using the seasonal Kendall test. This was selected given its sensitivity to seasonal variations in climatic time series data. The null hypothesis states that X is a sample of independent random variables (X_{ij}) and that X_i is a subsample of identical independent random variables.

$$X = (X_1, X_2 \dots X_{12})$$

And $X_i = (X_{i1}, X_{i2} \ldots X_{i12})$

The test statistic S_i is defined as:

$$S_i = \sum_{k=1}^{n_{i-1}} \sum_{j=k+1}^{n_i} sgn(X_{ij} - X_{ik}) \quad (4)$$

3.1.6 Magnitude of trends in temperature and extreme wet and dry events

The magnitudes of trends were estimated using Sen's estimator (1968).The slope T_i was calculated as:

$$T_i = \frac{x_{j-}x_k}{j-k}$$

Where x_j and x_k are data values at time j and k (j>k) respectively. The median of the slope trend is given as the Sen's estimator of the slope computed as:

$$Sen's\ Estimator = \begin{cases} T\left(\frac{N+1}{2}\right) & if\ N\ is\ odd \\ \frac{1}{2}\left(T\frac{N}{2} + T\frac{N+2}{2}\right) & if\ N\ is\ even \end{cases} \quad (5)$$

3.1.7 Standard Precipitation and Evapotranspiration Index (SPEI)

The classification of rainfall extremity was based on the SPEI (McKee *et al*., 1993) as shown in Table 3.2. SPEI was computed in R using station based mean monthly temperature and rainfall data for the period 1967-2015**.** SPEI is a modification of the original Standard Precipitation Index (SPI) by Vicente-Serrano *et al*., (2010). Calculations of the SPEI are based on mean monthly temperature and precipitation data established from 12 month and 1-month timescales. The index is derived from the difference between observed precipitation and potential evapotranspiration (PET) using Thornthwaite (1948) in R to arrive at the monthly index for a given station. Potential Evapotranspiration (PET; after Thornthwaite, 1948) is a monthly estimation based on monthly temperature (T), heat index calculated as the

sum of monthly indices (I) and the coefficient (M) dependent on the heat index. PET is calculated as:

$$PET = 16K(\frac{10T}{I})M \quad (6)$$

Where T=monthly mean temperature

I=Heat index calculated as the sum of monthly indices

M=Coefficient dependent on I

K is a correction coefficient computed from latitude and month

SPEI uses the monthly difference between precipitation and PET and symbolises water balance at different time scales (1month, 6 months and 12 months) as follows:

$$D_i = P_i - PET_i \quad (7)$$

Where D_i=climatic water balance

P_i= Monthly precipitation

PET=Potential Evapotranspiration for a given month

The computed D_i values are summed up at different time scales.

SPEI standardise a variable using a log-logistic distribution function which transforms it to a standard Gaussian variate with a mean of zero and standard deviation of one.

3.1.8 Link between extremes, temperature and ENSO events

To establish the impacts of ENSO on air temperature and extreme events, the NINO 4 SST anomaly index dataset was downloaded from NOAA. To correlate SPEI-1, NINO4 index, T_{max}, T_{min} and T_{mean}, non-parametric Spearman's correlation coefficient was computed using Principal Component Analysis (PCA) in XLSTAT (2016) software.

Table 3.2: Classification of rainfall extremity based on SPEI (McKee *et al*., 1993)

Category	**SPEI value**
2.0+	Extremely wet
1.5 to 1.99	Very wet
1.0 to 1,49	Moderately wet
0 to .99	Near normal
-1.0 to -1.49	Moderately dry
-1.5 to -1.99	Severely dry
-2 and less	Extremely dry

3.2 Results

3.2.1 Annual maximum and minimum air temperature between 1897 and 1904

Monthly historic data were compared to 1970-2000 mean for Bulawayo. The mean T_{max} for the period (1897-1904) is 26.4°C, which is 0.7°C and 1.7°C cooler than the reference average and 2000-2015 average respectively, while historic T_{min} is 0.3°C and 2.1°C cooler (Table 3.3). The highest temperatures recorded were 33.2°C for the period 1897-1904 and 33.2°C for the period 1970-2000.

3.2.2 Spatial distribution of temperature anomaly

Annual temperature anomalies were investigated relative to the 1970-2000 average. These results show a strong positive anomaly averaging 2.4°C warmer for the period 1967 to 2015 at all stations from September to March. A cool anomaly averaging -2.8°C is presented for all winter months (Figure 3.2). The period 1967-2015 experienced approximately 1°C warmer temperatures than the reference average (1970-2000).

Table 3.3: Mean annual air temperatures for Bulawayo (1897-1904)

Year	Mean Tmax	Mean Tmin	Highest Temperature	Lowest temperature
1897	25.7	12.7	30.1	8.7
1898	25.8	12.7	30.1	8.8
1899	26.5	13.1	33	9.7
1900	27.5	12.8	33.2	9.8
1901	26.2	12.9	31.7	8.9
1902	26.3	12.8	31.9	8.3
1903	26.6	12.7	31.9	8.3
1904	25.1	12.1	30.1	7.1
Mean(1897-1904)	**26.4**	**12.8**	**33.2**	**7.1**
Mean(1970-2000)	**27.1**	**13.1**	**32.1**	**12.2**
Mean(2000-2015)	**28.1**	**14.9**	**35.9**	**13.4**

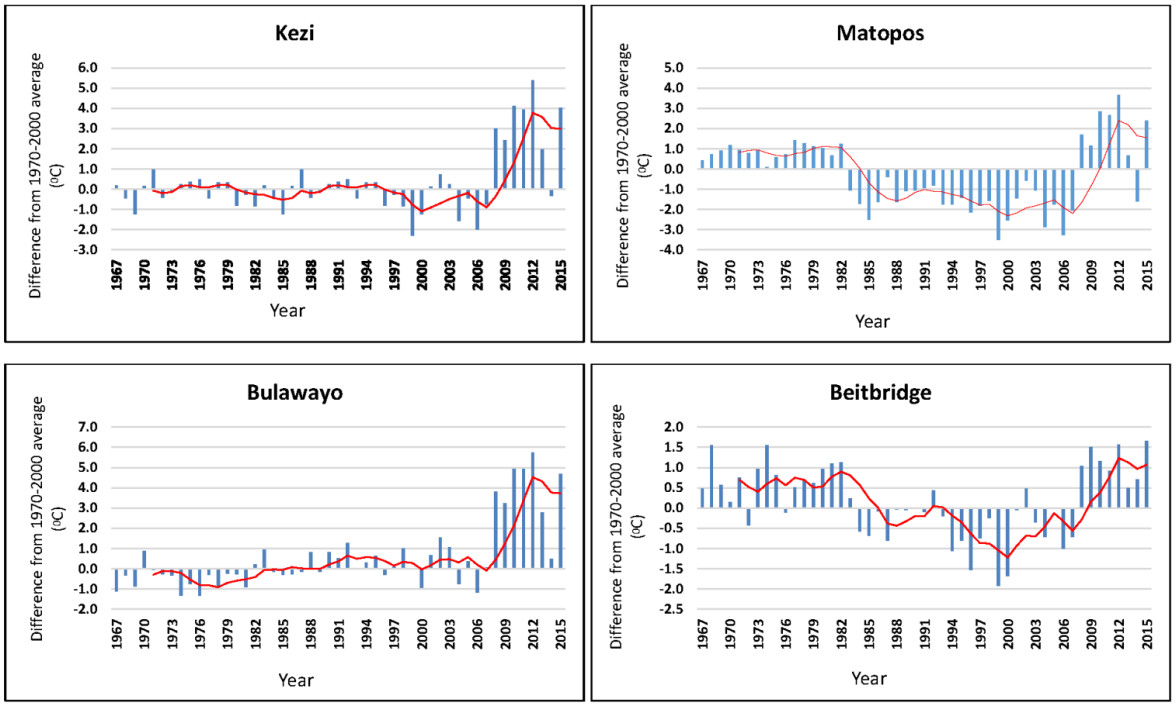

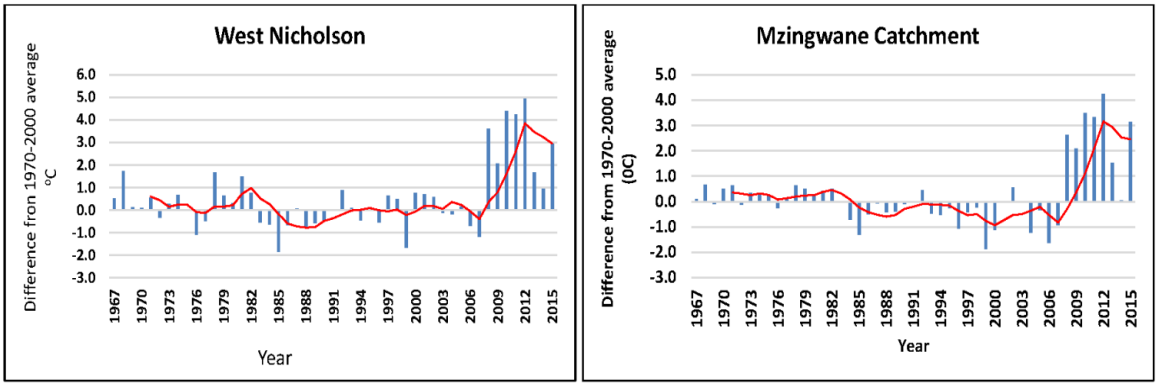

Figure 3.2: Annual air temperature anomaly per station with 5 years moving average for the period 1967-2015

The distribution of T_{mean} and the magnitude of Mann-Kendall trends for the period 1967-2015 is shown in Figure 3.3. Three stations (Bulawayo, West Nicholson, and Beitbridge) show significant warming trends with a Sen's slope of 0.056, 0.032 and 0,045 respectively, while Kezi measured an insignificant increasing trend with a Sen's slope of 0.015. In contrast, Matopos significantly cooled by -0.0059 per year.

3.2.3 Spatio-temporal distribution of seasonal air temperature anomalies

Wet season T_{max} for the period (1897-2015) recorded an average warm anomaly of 0.44°C for all stations when compared to the reference average (1970-2000), with West Nicholson and Matopos measuring highest anomalies of 0.45°C and 0.5°C respectively (Figure 3.5). In contrast, during the wet season, T_{min} varied spatially, with Beitbridge and Kezi recording cool anomalies of -0.25°C and -0.5°C respectively. Matopos and West Nicholson exhibited a positive anomaly of 0.1°C and 0.6°C correspondingly, while Bulawayo measured no change. Overall, wet season T_{min} indicates a negative deviation relative to the 1970 - 2000 average. Dry season T_{max} positively deviated from the reference average for all stations having an average of 0.36°C (Figure 3.3). These results show that winter T_{max} is increasing while Tmin is cooling for Kezi and Beitbridge. T_{min} for Matopos, Bulawayo and West Nicholson were 0.1

to 0.5°C warmer than the 1970 - 2000 average. Our results indicate a T_{max} warming tendency for both wet and dry seasons, while minimum temperatures are cooling at 60% of stations. The catchment wet season T_{max} recorded the highest positive anomaly in 2015 (3.3°C), while that for the dry season was 3.9°C in 2013 (Figure 3.3).

3.2.4 Annual T_{max} and T_{min} trends (1967-2015)

Annual T_{max} trends significantly increased ($p < 0.05$) for Bulawayo (0.24 °C decade^{-1}), Beitbridge (0.25°C decade^{-1}), West Nicholson (0.14°C decade^{-1}) and Kezi (0.13°C decade^{-1}), and average 0.16°C decade^{-1} for the region over the period 1967-2015 (Table 4). In contrast, an insignificant decreasing trend in annual T_{max} (at $p=0.188$) was measured for Matopos (-0.29°C decade^{-1}). Trends in annual T_{min} were insignificant, ranging from -0.05°C decade^{-1} (Beitbridge) to -0.04°C decade (West Nicholson), while Matopos and Kezi had statistically significant decreasing trends (-0.24°C decade^{-1} and -0.13°C decade^{-1} respectively).

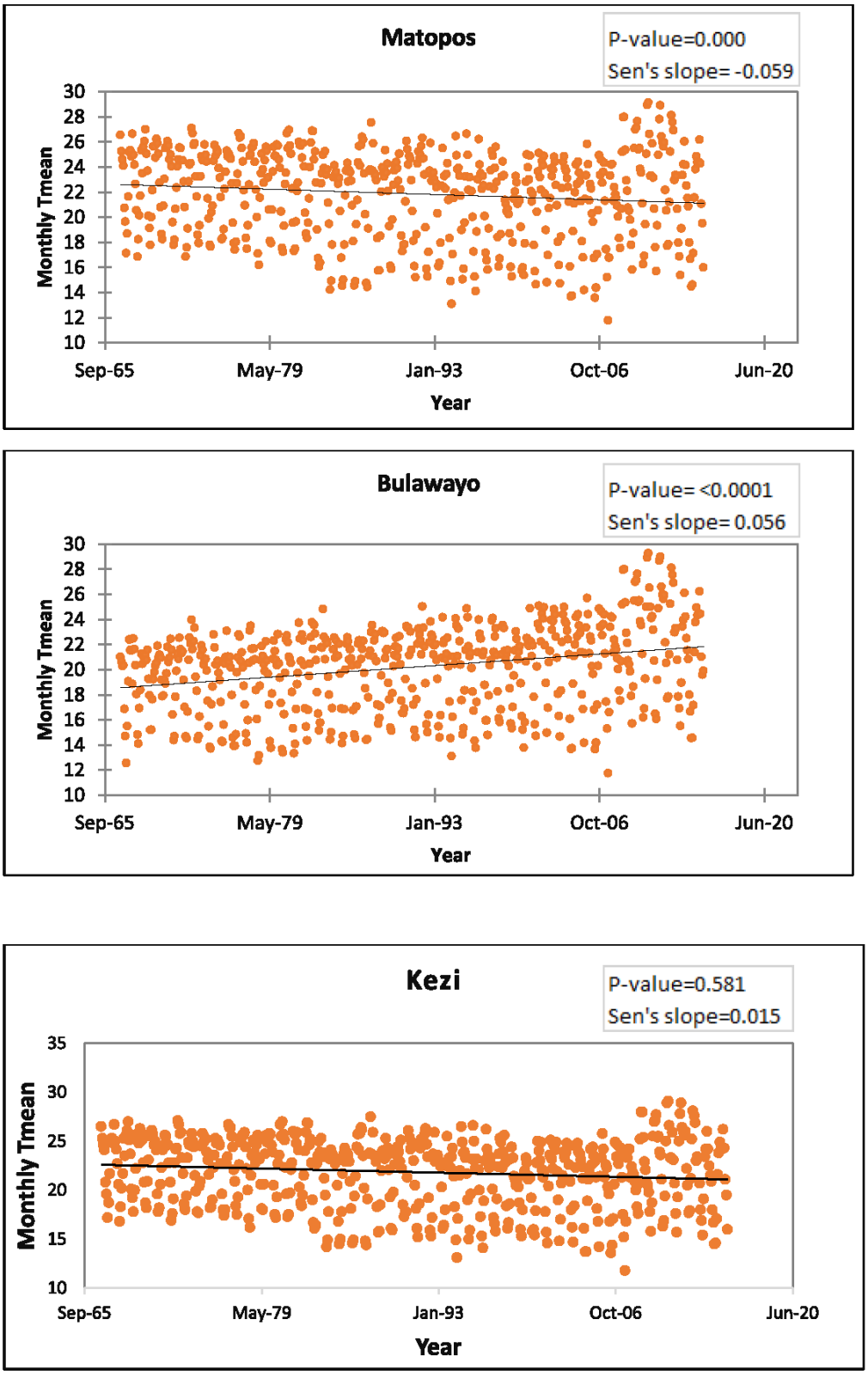

Figure 3.3: Trends in T_{mean} per station (Matopos, Bulawayo, and Kezi) for the period 1967 to 2015

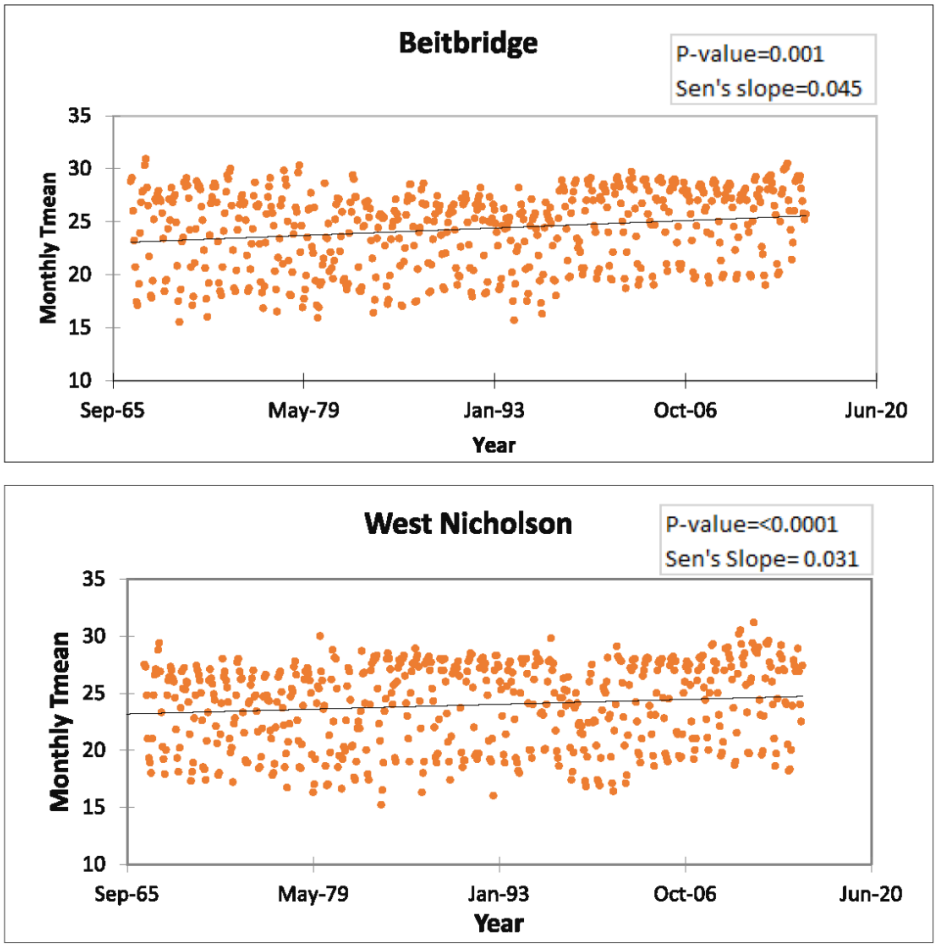

Figure 3.4: Trends in T_{mean} per station (Matopos, Bulawayo, and Kezi) for the period 1967 to 2015

In Bulawayo, T_{min} has significantly increased (0.24°C decade^{-1}) between 1967 and 2015 (Table 3.5). The catchment has experienced increasing Tmax and decreasing T_{min} trends, resulting in the diurnal temperature range (DTR) increasing by 0.03°C Contrary to other stations, Bulawayo has experienced significantly increasing T_{min} values, possibly a consequence, at least in part, to an urban heat Island effect.

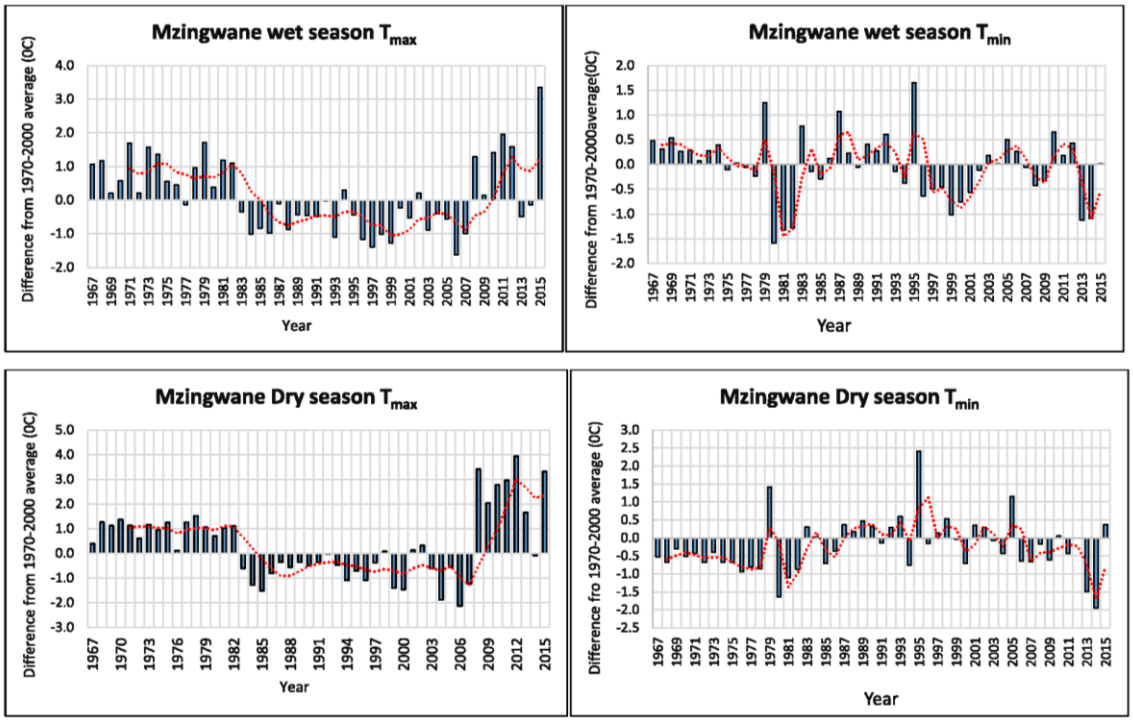

Figure 3.5: Seasonal air temperature anomalies for Mzingwane catchment with a 5-year moving average (1967-2015)

Table 3.4: Tmax annual and seasonal Mann-Kendall trend analysis (1967-2015)

Station T_{max}	**Annual MK**	**Seasonal Kendall**	**Sen' slope**	**Sen' slope**
	P-value	**P- value**	**Per Year**	**Per Decade**
Bulawayo	<0.0001	<0.0001	0.05	0.24
Beitbridge	0.038	0.048	0.053	0.25
West Nicholson	0.051	0.001	0.03	0.14
Kezi	0.0159	0	0.028	0.13
Matopos	0.188	<0.0001	-0.061	-0.29

Table 3.5: Tmin annual and seasonal Mann-Kendall trend analysis (1967-2015)

Station T_{min}	**Annual Mann-Kendall P-value**	**Seasonal Kendall P- value**	**Sen' slope Per Year**	**Sen' slope Per Decade**
Bulawayo	<0.0001	<0.0001	0.050	0.24
Beitbridge	0.385	0.003	-0.011	-0.05
West Nicholson	0.264	0.001	-0.009	-0.04
Kezi	0.003	<0.0001	-0.027	-0.13
Matopos	0.001	<0.001	-0.050	-0.24

3.2.5 Wet and Dry Season air temperature trends

The wet season (October - March) T_{max} trends for Bulawayo, Beitbridge, West Nicholson and Kezi show significant warming trends at an average of 0.33°C decade^{-1}. In contrast, Matopos T_{max} trends significantly decreased by -0.12°C year^{-1} (Table 3.6). These results indicate that the rainy season temperatures are generally increasing except for Matopos. T_{min} trends for the wet season measured statistically significant negative trends for Beitbridge, West Nicholson, Kezi, and Matopos, decreasing at an average of 0.4°C decade^{-1}.

Dry season (April-September) T_{max} trends varied spatially but increased at 60% of stations, with Bulawayo recording a significantly positive trend (0.45°C decade^{-1}), while Beitbridge, West Nicholson, and Kezi warmed at 0.04°C decade^{-1}, 0.08°C decade^{-1} and 0.32°C decade^{-1} respectively. Matopos (-0.50°C decade^{-1}) measured a negative trend for the annual Mann-Kendall test but values were statistically significant for the seasonal Kendall test at $p < 0.05$ (Table 3.7). Dry season T_{min} trends increased significantly for Bulawayo (0.38°C decade^{-1}), while West Nicholson and Beitbridge also recorded positive trends, although statistically insignificant. Northern region stations (Kezi and Matopos) had significantly decreasing T_{min} trends (-0.28°C decade^{-1} and -0.04°C decade^{-1} respectively). Wet season T_{max} trends indicate a warming trend, while that for T_{min} had decreased.

Table 3.6: Wet season air temperature MK trend analysis for 1967 to 2015

Station		Mann Kendall P-value	Seasonal Kendall P- value	Sen' slope Per Year	Sen' slope Per Decade
Bulawayo	Tmax	<0.0001	<0.0001	0.098	0.47
	Tmin	<0.0001	<0.0001	0.032	0.15
Beitbridge	Tmax	0.001	0.019	0.023	0.11
	Tmin	<0.0001	<0.0001	-0.083	-0.63
West Nicholson	Tmax	0.001	<0.0001	0.154	0.7
	Tmin	0.001	<0.0001	-0.059	-0.28
Kezi	Tmax	0.506	0.376	0.009	0.04
	Tmin	0.001	<0.0001	-0.061	-0.29
Matopos	Tmax	0.114	<0.001	-0.122	-0.58
	Tmin	<0.0001	<0.0001	-0.096	-0.46

Table 3.7: Dry season air temperature Mann-Kendall (MK) trend analysis (1967-2015)

Station		Mann Kendall P-value	Seasonal Kendall P- value	Sen' slope Per Year	Sen' slope Per Decade
Bulawayo	T_{max}	<0.0001	<0.0001	0.093	0.45
	T_{min}	0.000	<0.0001	0.08	-0.38
Beitbridge	T_{max}	0.148	<0.0001	0.083	0.04
	T_{min}	0.100	<0.0001	0.087	0.42
West Nicholson	T_{max}	0.692	0.647	0.017	0.08
	T_{min}	0.213	0.581	0.011	0.05
Kezi	T_{max}	0.000	0.000	0.066	0.32
	T_{min}	0.028	<0.001	-0.059	-0.28
Matopos	T_{max}	0.226	<0.0001	-0.105	-0.50
	T_{min}	<0.0001	<0.0001	-0.008	-0.04

3.2.6 Temporal trends in catchment wetness and dryness

Results indicate a significant increase ($p < 0.05$) in the occurrence of extreme dryness during the last three decades (Figure 3.6). The 1-month SPEI identified numerous episodes of extreme dryness and wetness across the entire catchment. The most severe dryness (SPEI $\leq$-1 and $\leq$-1.4) was identified in 1992 and 2012, while the most extreme wetness (events with SPEI greater than 2) was recorded in 1978 and 2000. Flooding conditions (SPEI $\geq$1and

≤1.49) occurred in 1972, 1974-1976, 1981, 1997 and 2000. Findings show an increasing tendency toward severe to extreme dryness in the catchment and these events coincided with El Niño events. Catchment SPEI significantly decreased at -1.05decade^{-1} ($p = 0.001$), which shows that the entire catchment has been tending towards increasingly dry conditions.

3.2.7 Spatial variation of trends in extremely dry and wet events (1967 to 2015)

Station based SPEI-1 trend analysis indicates varied levels of significance for different months. Bulawayo has a significant ($p < 0.05$) drying trend from May to October, from November to March also drying, but insignificantly ($p < 0.05$) (Table 3.8). Kezi records a significant ($p = 0.024$) wetting trend for July, while the period January to June indicates an insignificant ($p < 0.05$) increasing SPEI. Only September recorded a significant ($p = 0.006$) drying trend for Kezi. Beitbridge exhibits a general drying trend throughout the year, with 50% of months recording significant drying trends (Table 3.8). Matopos has become significantly ($p < 0.05$) wetter from April to July, and in December, while September to November has become significantly drier ($p = 0.045$; $p = 0.013$; $p = 0.041$). West Nicholson records drying trends ($p<0.05$) for February and May to November, while December to April shows an insignificant drying trend (Table 3.9).

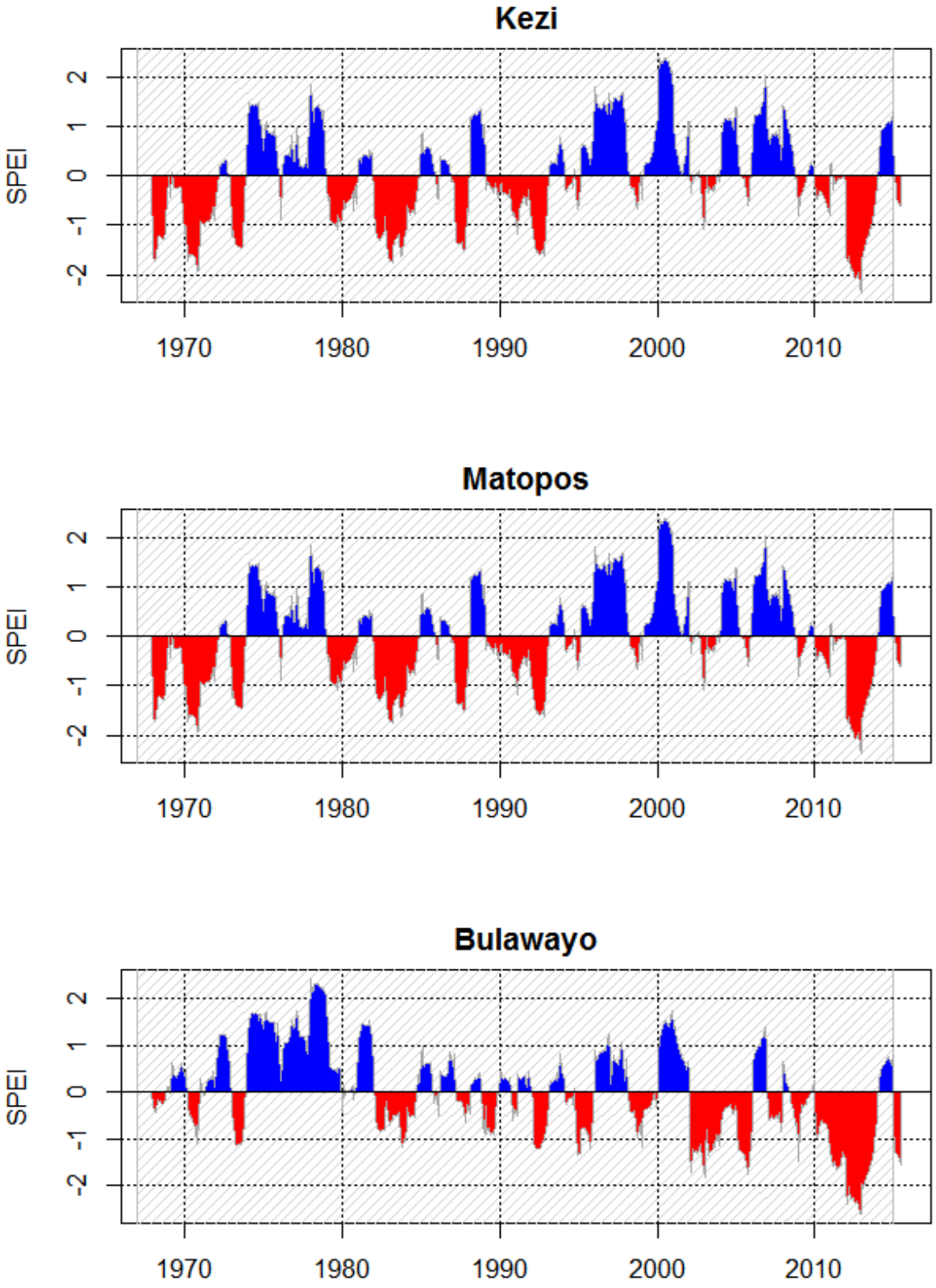

Figure 3.6: Time series of SPEI per station (1967-2015)

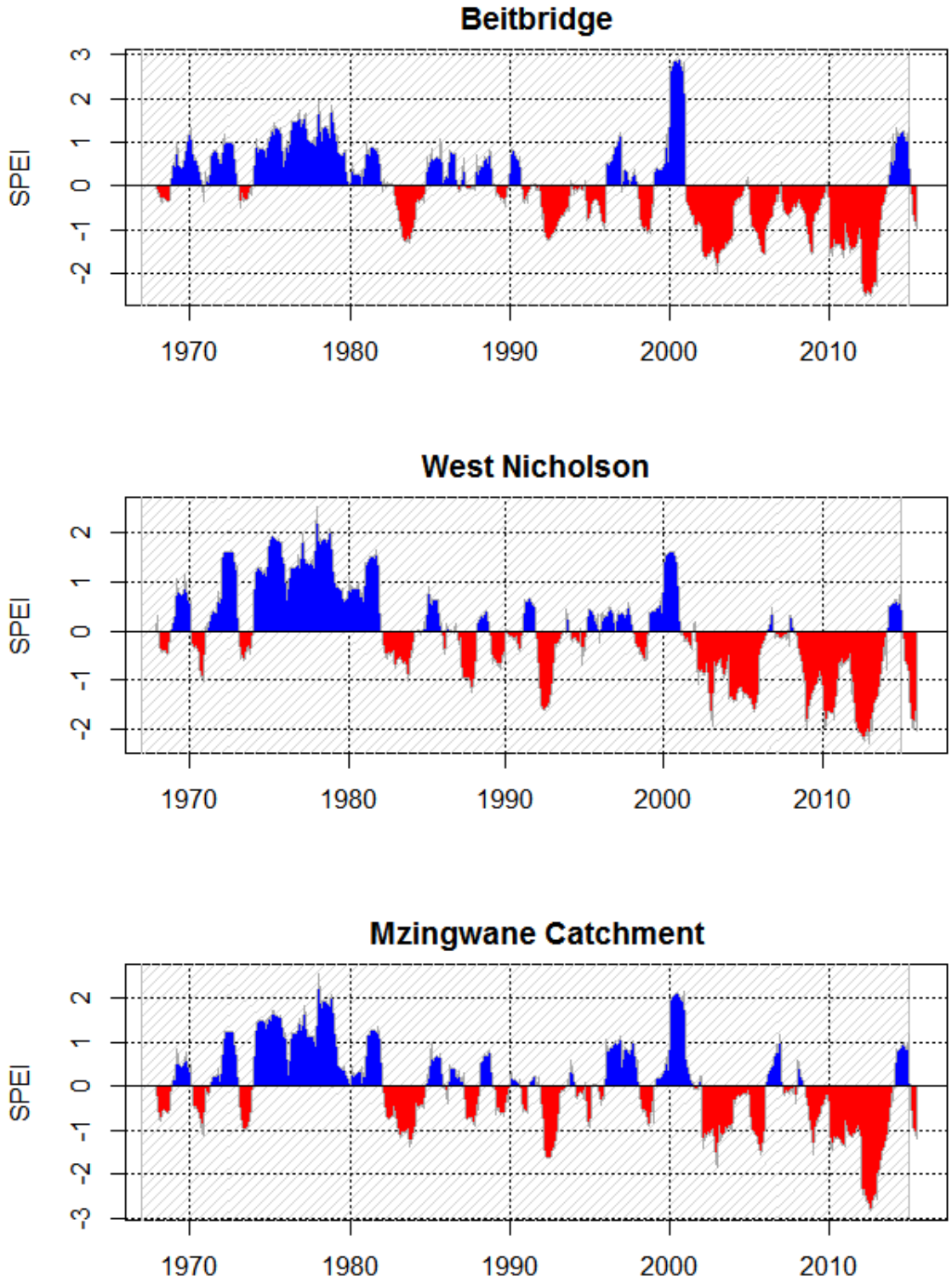

Figure 3.6: Time series of SPEI per station (1967-2015)

Table 3.8: Mann-Kendall trend test for SPEI (1967-2015) per given station

Station		Jan	Feb	March	April	May	June	July	Aug	Sept	Oct	Nov	Dec
Bulawayo	Kendall tau	-0.04	-0.12	-0.05	-0.18	-0.2	-0.2	-0.2	-0.4	-0.2	-0.5	-0.3	-0.03
	P-Value	0.725	0.226	0.589	0.066	**0.04***	**0.012***	**0.039***	**0.000***	**<0.0001***	**<0.0001***	0.006	0.777
Kezi	Kendall tau	0.11	-0.06	0.1	0.02	0.18	0.15	0.23	0.04	-0.28	-0.09	-0.08	0.16
	P-Value	0.291	0.554	0.299	0.844	0.079	0.136	**0.024***	0.73	**0.006***	0.358	0.129	0.281
Beitbridge	Kendall tau	-0.08	-0.19	-0.17	-0.3	-0.28	-0.22	-0.17	-0.36	-0.49	-0.39	-0.22	-0.04
	P-Value	0.137	0.086	0.093	**0.004***	**0.005***	**0.027***	0.093	**0.000***	**<0.001***	**<0.0001***	0.141	0.674
Matopos	Kendall tau	0.12	0.07	0.1	0.11	0.23	0.5	0.38	0.13	-0.2	-0.24	-0.2	0.21
	P-Value	0.232	0.487	0.299	**0.044***	**0.021***	**0.000***	**0.000***	0.19	**0.045***	**0.013***	**0.041***	**0.03***
West Nicholson	Kendall tau	-0.19	-0.22	-0.09	-0.26	-0.33	-0.24	-0.18	-0.44	-0.53	-0.43	-0.25	-0.09
	P-Value	0.061	**0.023***	0.352	0.009	**0.001***	**0.017***	**0.073***	**0.000***	**<0.0001***	**<0.0001***	**0.010***	0.396

3.2.8 Decadal distribution of extreme weather events

The spatial distribution of the number of extremely dry conditions (Figure 3.7 and 3.8) shows that the southern part of the catchment had fewer droughts (0-5monthsdecade^{-1}) during the period 1966-1976 than during the period 2006-2015 (36-55 monthsdecade^{-1}) (Figure 3.7 and 3.8).The northern parts recorded a greater number of drought months during the period 1966-1975 than a most recent decade (2006-2015). The whole catchment received 69 months of moderate to extreme wetness and 46 months moderate to extreme dryness for the first two decades. Decades 1986-1995, 1996-2005 and 2006-2015 experienced a total of 55 months of wetness and 62 months of moderate to extreme dryness (Figure 3.5). Generally, the first two decades (1966-75 and 1976-1985) experienced 4.8% extreme wetness, 13% severe wetness and 21% moderate wetness. In contrast, decades 1996-2005 and 2006-2015 had 6% extreme dryness, 16% severe dryness and 20% moderate dryness (Figure 3.5).

3.2.9 Inter-correlations of Temperature, ENSO, and SPEI

Principal Component Analysis (PCA) was computed to measure the strength of association between climate variables (temperature and rainfall), NINO4 index and SPEI (Figure 3.9).

Findings show a strong positive correlation between T_{max} and T_{min} with NINO4 index (Table 3.10) having loadings of 0.79 and 0.96 respectively. SPEI-1 had a weak negative correlation with T_{max} (-0.172) while T_{min} exhibited a stronger positive correlation with SPEI-1 (0.65 loadings; Table 3.10).

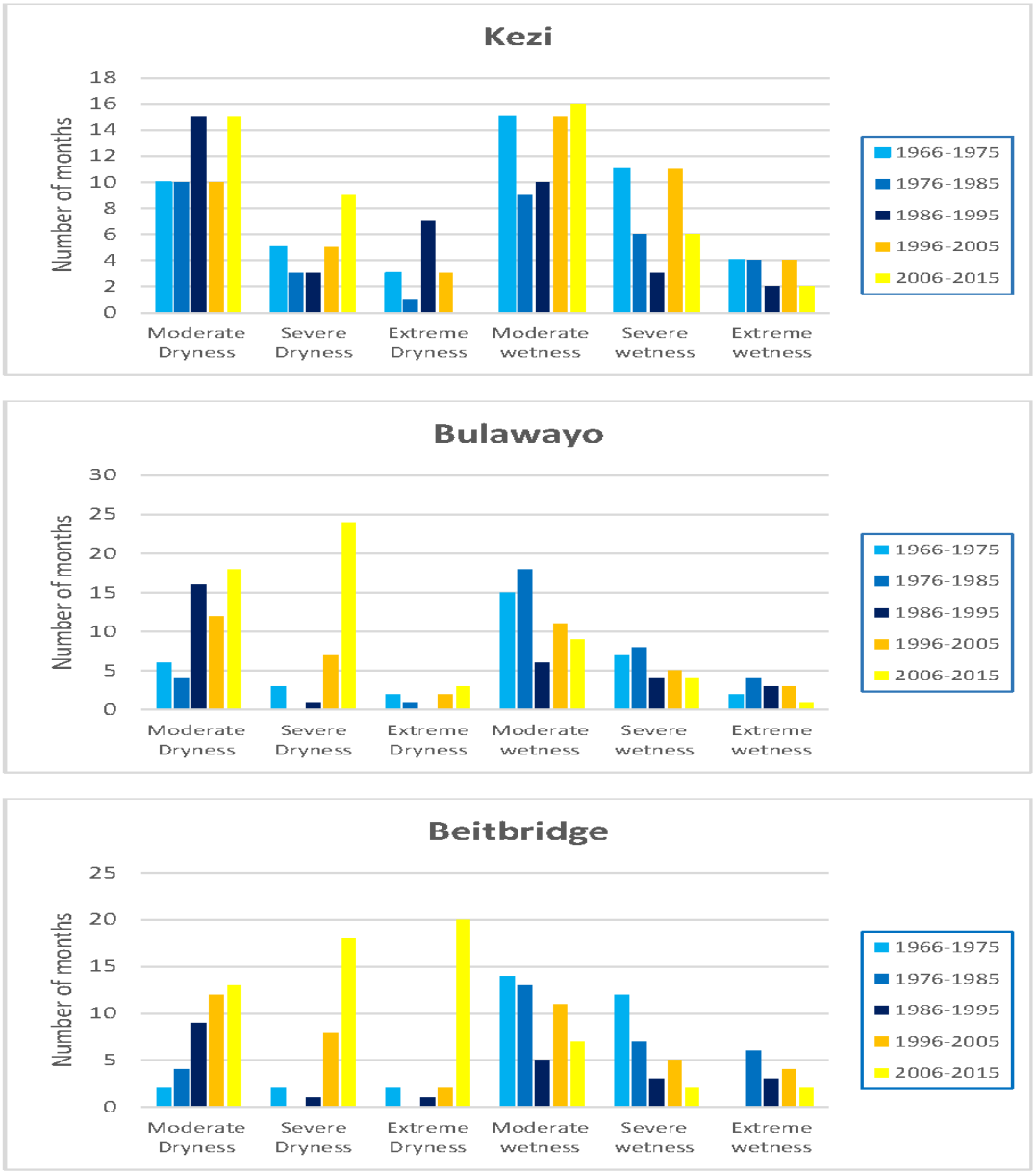

Figure 3.7: Decadal severity of extremes (moderate, severe and extreme dryness and wetness) in Kezi, Bulawayo and Beitbridge for the decades 1966-1975, 1976-1985, 1986-1995, 1996-2005, and 2006-2015

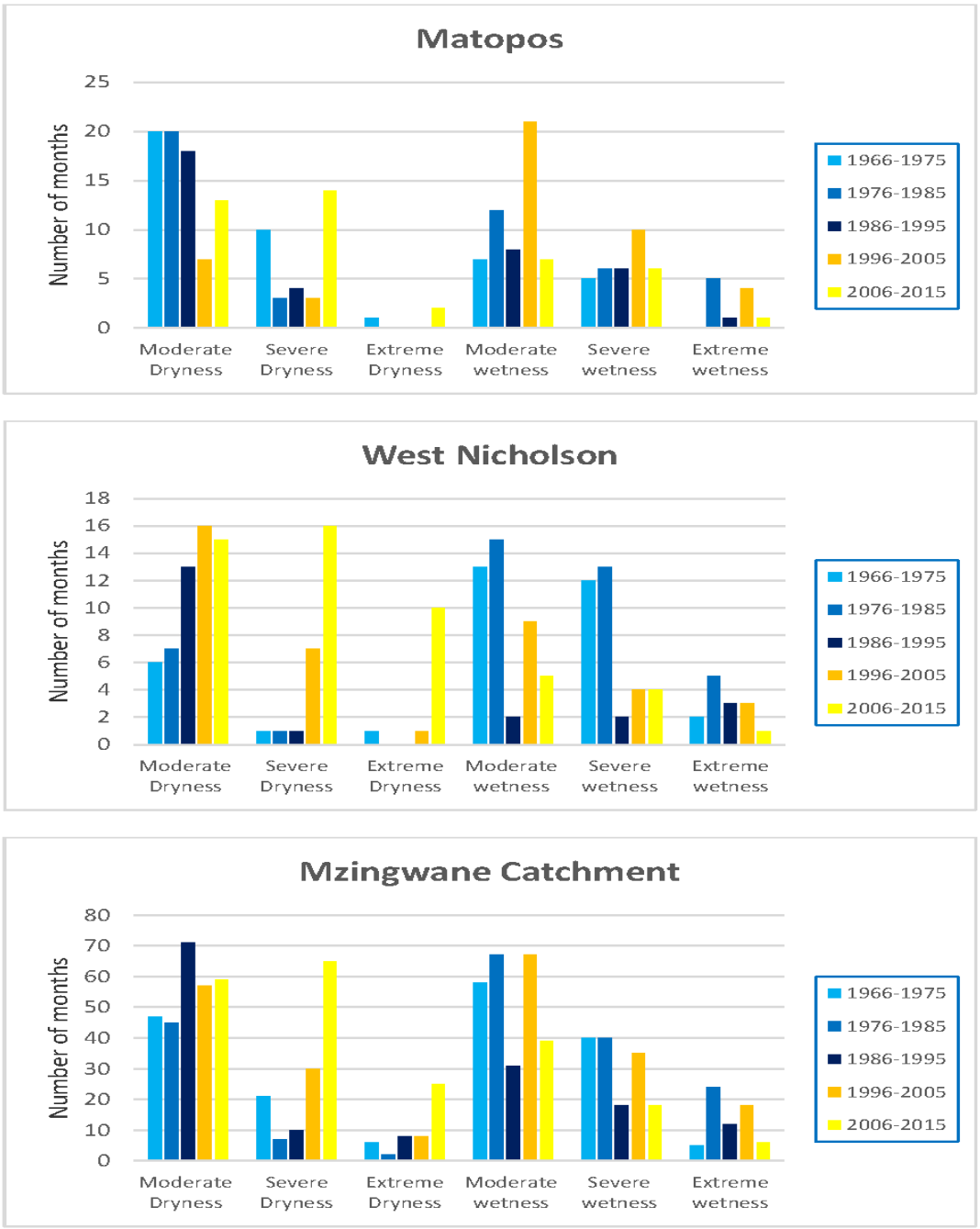

Figure 3.8: Decadal severity of extremes (moderate, severe and extreme dryness and wetness) in Matopos, West Nicholson and Mzingwane catchment for the decades between 1966 and 2015

Table 3.9: PCA loadings for extreme indices (SPEI-1 and NINO4) temperature (T)

	F1	F2	F3	F4	F5
SPEI-1	-0.289	-0.617	-0.342	**0.647**	0.001
NINO4	0.322	0.226	**0.754**	**0.527**	0.003
T_{MAX}	**0.793**	0.359	-0.433	0.201	-0.118
T_{MIN}	**0.959**	-0.180	-0.165	-0.014	0.141
T_{MEAN}	-0.476	**0.761**	-0.336	0.270	0.089

The SPEI-1 and NINO4 Index showed a strong negative correlation of -0.617 loadings (Table 3.9). The Spearman correlation matrix shows that the correlations between variables are weak, as most of them have a coefficient of around 0.1 (Table 10).

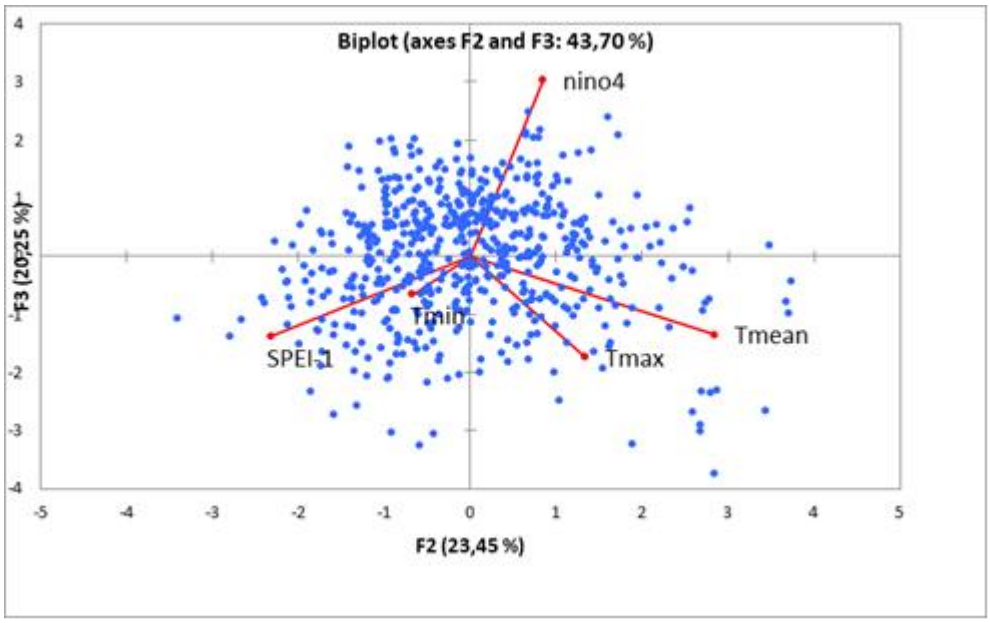

Figure 3.9: PCA variable correlations for extreme indices represented by nino4 and SPEI and temperature (T_{min}, T_{max} and T_{mean})

Table 3.9: Correlation matrix among temperature and extreme indices

Variables	SPEI-1	NINO4	TMAX	TMIN	TMEAN
SPEI-1	**1.000**	**-0.149**	**-0.172**	**-0.119**	-0.042
NINO4	**-0.149**	**1.000**	**0.116**	**0.137**	-0.092
TMAX	**-0.172**	**0.116**	**1.000**	**0.748**	0.084
TMIN	**-0.119**	**0.137**	**0.748**	**1.000**	**-0.530**
TMEAN	-0.042	-0.092	**0.084**	**-0.530**	**1.000**

Values in bold are different from 0 with a significance level alpha = 0.05

3.3 Discussion

3.3.1Temperature trends

This study has presented spatio-temporal trends for air temperature and extreme climatic events in the Mzingwane catchment of south-western Zimbabwe, using both historic and more contemporary instrumental weather records. The period 1967-2015 experienced approximately 1°C warmer conditions than the reference period 1970-2000. Annual T_{max} warmed on average by 0.16°C decade^{-1} and compares favourably with trends for the Limpopo Province of South Africa (0.12°C decade^{-1}), although the magnitude of change varied spatially across these regions (Tshiala *et al*., 2011). Of the 30 catchments studied by Tshiala *et al*. (2011), 13% showed negative trends, while 87% exhibited positive trends in mean annual temperature. The trends for Limpopo Province are important to this study because the Mzingwane catchment forms part of the northern Limpopo basin.

In this study, annual T_{min} decreased for 60 % of the stations with values of -0.04°C to -0.13°C decade^{-1}. These results are contrary to most previous findings in southern and eastern Africa, which have emphasised the general increase in T_{min} (Kruger and Shongwe, 2004; Mengistu *et*

al., 2014; Lakhraj-Govender *et al*., 2016; Kruger and Nxumalo, 2017). Increasing annual T_{min} trends have varied from 0.15°C decade^{-1} in Ethiopia (Mengistu *et al*., 2014) to a mean of 0.14°C decade^{-1} for most of South Africa to 0.12°C for the southwestern Cape region in particular (Lakhraj-Govender *et al*., 2016). A combination of increasing T_{max} and decreasing T_{min} resulted in increasing diurnal temperature range (DTR) by an average of 0.03°C. The results are in agreement with findings by New *et al*. (2006) who reported an increasing diurnal range of temperature for southern Zimbabwe in the period 1961-2000. This pattern could be as a result of differences in topography and localised climate systems (Barry, 1992; Stahl *et al.,* 2006). An increased diurnal temperature range may indicate a changing climate (Karl et al., 1993; Qu *et al*., 2014), but can also result from localised factors such as urbanisation (Wang *et al*., 2012), land use/cover changes (Gallo *et al*., 1999) and changes in cloud cover (Dai *et al*., 1999).

3.3.2 Seasonal air temperature trends

The findings show positive wet season (October-March) T_{max} trends while T_{min} has decreased. A number of studies in South Africa reported warming T_{max} for all seasons, but varying in magnitude (MacKellar *et al*., 2014; Lakhraj-Govender *et al.,* 2016; Kruger and Nxumalo, 2017). However, Kruger and Nxumalo (2017) also highlighted regional disparities in air temperature trends but still noticed largest positive trends in summer (0.018 °C decade^{-1}). In addition, some studies have reported increasing temperatures corresponding with low precipitation (Brunsell *et al*., 2009). Although this relationship is outside the scope of this study, it becomes very pertinent to farmers in the Mzingwane catchment who rely heavily on rain-fed agriculture for their livelihoods. A combination of high temperatures and dry conditions often result in substantial crop failures and livestock diseases/mortality, which

compromise food security. The sub-regional discrepancies concerning T_{min} trends could be a product of sub-regional influences on mesoscale thermodynamics (Mueller *et al*., 2016).

3.3.3 Spatiotemporal trends in extreme events

SPEI has been used in this study to determine extreme wet and dry periods (Figure 4). The study showed that there is a general increase in occurrence and frequency of dry extremes which are strongly linked to ENSO in the last two decades. This result is consistent with global circulation model projections ("IPCC - Intergovernmental Panel on Climate Change," 2007) which emphasise an increase in precipitation extremes under anthropogenic global warming. Similar results were reported by Manatsa *et al*. (2010b), suggesting drying conditions with more frequent intense agricultural droughts in semi-arid Zimbabwe. Current findings have shown that for south-western Zimbabwe, the first two decades (1966-75 and 1976-85) were wetter than the last two decades (1996-2005 and 2006-2015), with the latter period having to experience more extreme dryness (Figure 5). These results are consistent with those from previous southern African work, which have also expressed the tendency toward dryness and a higher frequency of droughts (Jury *et al*., 2007; Sheffield *et al*., 2009; Manatsa *et al*., 2010a; Masih *et al.*, 2014; Spinoni *et al*., 2014).

The results show a strong relationship between ENSO and extreme events, as also previously noted by Mamombe *et al*. (2016). The association between warming temperature and ENSO events is particularly strong in the case of a global and regional scale super ENSO event (Lean and Rind, 2009). More recently, Manatsa and Reason (2017) reported a positive correlation between ENSO and air temperature and explain the significance of large-scale climate systems on local weather. Increased extreme dry conditions have huge repercussions on catchment hydrology, which impact on general water availability. This is of great concern

because the Mzingwane catchment provides water to surrounding urban areas such as Bulawayo. Water shortages have been experienced in the last 10 years in Bulawayo, which has resulted in massive water rationing schemes as supply dams regularly dry up in the Mzingwane catchment.

This and a previous study (Mugandani *et al*., 2012) raise concern regarding recurrent extreme drought conditions in semi-arid regions of Zimbabwe. Such shifts towards drier and warmer conditions are detrimental to not only agriculture but also biodiversity, which may cause species to migrate and/or become regionally extinct (Masters *et al*., 2010). This may also promote the spread of specific invasive species, particularly those which are more adaptive to hot and dry conditions (Masters *et al*., 2010). In addition, fragile ecosystems such as wetlands found in the study region, are likely to be negatively affected by a lowering water table during recurrent extreme dry conditions, and may possibly lead to their complete demise. Further research is required to investigate the relationship between atmospheric warming and precipitation trends at the mesoscale, particularly for the more mountainous regions.

3.4. Conclusions

The study concludes that there has been a significant increase in maximum temperatures at $p<0.005$ for 60% of the Mzingwane catchment while the catchment minimum temperatures show an insignificant decreasing trend, extreme dryness has increased in frequency during the past two decades. Significant drying trends are noted for the summer rainy months, with consequential agricultural drought, while a tendency towards wet months is noted during winter months in mountainous regions. Notably, extreme events are recurring with longer duration during the current decade than the 20^{th} century. There is a strong positive correlation between temperature and the NINO4 index, while SPEI-1 has a weak negative

correlation with T_{max} but is strongly correlated with T_{min}. The SPEI-1 and NINO4 indices significantly correlate, which is confirmed by the correspondence of dry years with ENSO events. The findings are important for developing appropriate sustainable and adaptive strategies at the sub-regional scale, as climate changes.

CHAPTER 4: LONG-TERM RAINFALL CHARACTERISTICS IN THE MZINGWANE CATCHMENT OF SOUTHWESTERN ZIMBABWE

Abstract

Rainfall characteristics during the annual rainy season are explored for the Mzingwane catchment of southwestern Zimbabwe, for both historic period (1886-1906) and more recent times (1950-2015), based on available daily and monthly precipitation series. Annual and seasonal rainfall trends are determined using the Modified Mann-Kendall test, Magnitude of Trends test and Sen's slope estimator. Rainfall variability is quantified using the coefficient of variation (CV), Precipitation Concentration Index (PCI) and Standard Precipitation Index (SPI). Results suggest that contemporary mean annual rainfall may not have changed from that measured during the historic period of 1886-1906. However, the number of rainy days (>=1mm) has decreased by 34%, thus suggesting much more concentrated and increased rainfall intensity. A notable shift in both the onset and cessation dates of the rainy season is recorded, particularly during the 21st century, which has resulted in a significantly reduced ($p<0.05$) in the length of the rainy season. The combination of a reduced number of rainy days (>=1mm) and a shortened rainy season, suggests that long intra-season dry spells have become more common through time and have considerable negative consequences for agriculture and wetland ecosystem in the region. In addition, high spatio-temporal rainfall variability and seasonal PCI values indicate strong seasonality in the rainy season. Based on the SPI results, the El Niño Southern Oscillation (ENSO) strongly influences rainfall variability. The results further suggest high uncertainty in rain season characteristics, which requires effective planning for water needs.

Keywords: rainfall variability, trends, rainy days, rain season length, rainfall indices

[2]This chapter is based on: Sibanda S, Grab S.W and Ahmed F. long-term rainfall characteristics in the Mzingwane catchment of southwestern Zimbabwe. In submission; Theoretical and Applied Climatology Journal.

4.1 Introduction

Climate change is one of the major contemporary concerns of humanity in the 21st century and has not only influenced the quantity of rainfall received, but also other important characteristics, such as rainfall intensity, length of the rain season, rainfall onset and cessation dates, trends and number of rainy days in a given season (Recha *et al*., 2012; Mushore *et al*., 2017; Reason, 2017). Given that much of southern Africa, including the Mzingwane sub-catchment of southwestern Zimbabwe is semi-arid, such changes in rainfall characteristics have significant implications for livelihoods, especially given the widespread subsistence agricultural economy. The situation is further compounded by the fact that most rural communities heavily rely on rain-fed agriculture for their staple food requirements and lack irrigation infrastructure. In addition, most ecosystems in the region (e.g. wetlands) are very sensitive to potential changes in rainfall characteristics and may lead to botanical changes over time or enhanced erosion/degradation.

Zimbabwe's rainfall is unimodal and normally begins in October and ends in March, but varies widely through space and time (Therrell *et al*., 2006; Manatsa and Mukwada, 2012). The rain season is largely dependent on the movement of the Inter-Tropical Convergence Zone (ITCZ) and upper westerly waves from the mid-latitudes, which determine the intensity of the rains during the rainy season (Buckle, 1996). Notably, much of the rainfall variability in Zimbabwe is also associated with El Niño Southern Oscillation (ENSO) phases (Reason *et al*., 2005; Manatsa and Matarira, 2009; Jury, 2013; Mamombe *et al*., 2016). Apart from the large scale atmospheric thermodynamics, rainfall patterns in Zimbabwe are also influenced

by micro-level dynamics such as relief, elevation and land cover (Sanchez-Moreno *et al*., 2014).

Globally, rainfall variability and change has been extensively studied, and downscaled to sub-regions. Several of these studies have noted high spatio-temporal variability in inter and intra rain seasons (e.g. Camberlin *et al*., 2001; Afzal *et al*., 2015; Bisht *et al.*, 2017; Gajbhiye *et al*., 2016; Reason, 2017). Given the predominance of subsistence agriculture which is heavily dependent on rain for its direct moisture supply, there has been much attention on rainfall characteristics (variability, length of the rain season, trends) for many parts of sub-Saharan Africa (e.g. Ngongondo *et al*., 2011; Recha *et al*., 2012; Weldon and Reason, 2014; Nnaji *et al*., 2016; Randriamahefasoa and Reason, 2017). A general outcome from such studies has been the expressed concern over recent trends of increased inter and intra seasonal rainfall variability, and shortening rain seasons. For instance, the number of rainy days in semi-arid Botswana are reported to have decreased on average by -1.38mm $year^{-1}$ between 1975 and 2005, and is also accompanied by increased rainfall variability (Batisani and Yarnal, 2010). In East Africa, rainfall onset dates have varied more strongly than cessation dates due mostly to changes in pressure and sea surface temperatures which modify Indian and Atlantic ocean temperatures. The cooler Indian ocean and the warmer Atlantic ocean are related to high sea level variability, which promotes a conducive environment for enhanced equatorial easterlies and surface divergence over East Africa (Camberlin and Okoola, 2003). Such conditions tend to draw the ITCZ further to the west, resulting in the delayed onset of rains. In part, global warming associated with higher sea surface temperatures and stronger ENSO events has been identified as the primary factor for such African rainfall trends (Mamombe *et al*., 2016).

In the context of Zimbabwe, past investigations on historic and future climate change have indicated a decline in annual rainfall linked to ENSO events (Unganai, 1996b) and the Indian ocean Dipole Zonal mode (Manatsa and Matarira, 2009). A rainfall reconstruction based on tree rings has indicated a long-term (1800 to 2000) rainfall trend, that past severe droughts correspond to El Niño and with high rainfall variability over time (Therrell *et al*., 2006). Significant changes in the start and cessation dates of the rain season are detrimental to 'normal' crop production (Mushore *et al*., 2017), as such changes may pose a risk of the occurrence of dry spells within the rain season, and which impacts negatively on crop growth and yields (Moyo *et al*., 2017). Past work has suggested that annual rainfall trends for all of Zimbabwe as being statistically insignificant, but rather that it is the intensity, timing and duration that has shifted (Mazvimavi, 2010; Muchuru *et al*., 2016). However, these findings varied broadly across the entire country; as such more detailed studies are required at sub-catchment level. To this end, the current study aims to assess inter-annual and seasonal rainfall variability and change at the micro-spatial scale (i.e. Mzingwane sub-catchment) and then compare these to those of past studies that have worked at a national scale. It is hoped that such information enables better catchment-scale management for future water needs and wetland sustainability.

4.2 Methodology

4.2.1 Study area

Zimbabwe has seven catchment management regions as indicated in Figure 4.1. This paper focuses on the most southerly of these catchment regions, namely the Mzingwane catchment, which is located between 19.8^{o} and 22.4^{o}S and 27.7^{o} and 32.0^{o} E. The catchment includes four sub-catchments (Shashe, Lower Mzingwane, Upper Mzingwane and Mwenezi) covering an area of ~63000 km^{2} (Figure 4.1). The northern part of the catchment is composed of

granitic rocks associated with the greenstone belt, which is rich in gold deposits. Granite terrains form large inselbergs (dome-shaped mountain ranges), between which wetlands occur (perennial dams, vleis, swamps or marshes). The Mzingwane catchment hosts five major rivers (Shashe, Umzingwane, Mwenezi, Bubi and Marico) that feed into the Limpopo River (Görgens and Boroto, 1997).

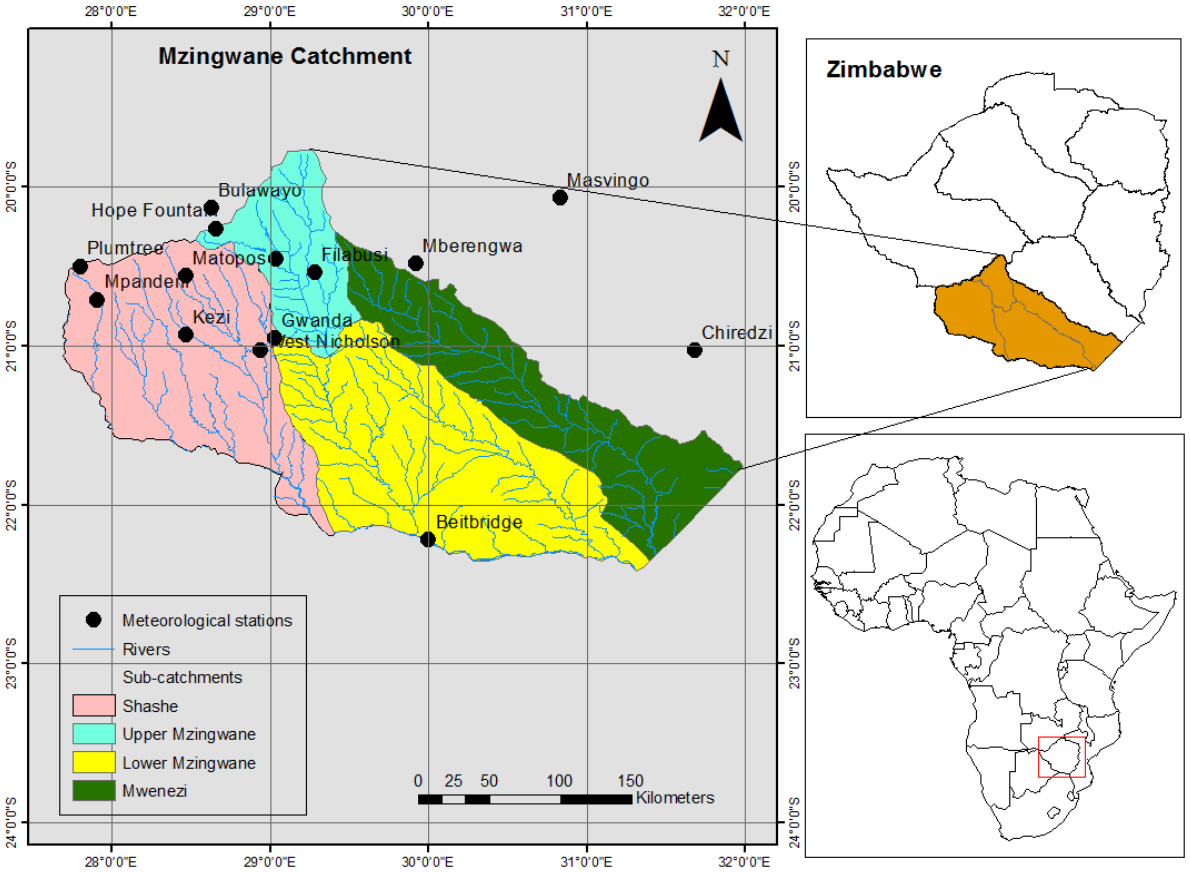

Figure 4.1: Mzingwane Catchment showing Shashe, Upper Mzingwane, Lower Mzingwane and Mwenezi sub-catchments

The climate of Mzingwane catchment is semi-arid to arid, but rainfall distribution varies across the catchment, such that the northern regions receive ~450-600 mm per annum and the southern regions ~200-450 mm pa (Görgens and Boroto, 1997; Chenje *et al.*, 1998). The wet season typically starts in late October and ends in March, with the highest rainfall occurring

between December and February (Unganai and Mason, 2002). Rainfall seasonality is largely influenced by the Inter-Tropical Convergence Zone (ITCZ) which moves southwards during the austral summer, and inter-annually by the El Niño Southern Oscillation (ENSO) which is associated with periods of lower (El Niño) and higher (La Niña) rainfall (Manatsa et al., 2008). The average daily T_{max} for the catchment varies between 27–34°C during summer and 22–26°C in winter (Love *et al*., 2010), while average T_{min} range between 18-22°C during summer and 5-10°C in winter (FAO, 2010; Sibanda et al., 2017). Owing to the relatively low and erratic rainfall, agricultural activities in the catchment mainly involve livestock rearing, as this is the most viable, however crop production is also practised but is concentrated around wetlands and flood plains.

4.2.2 Rainfall Data

Monthly rainfall data for 11 stations (Matopos, Kezi, Bulawayo, Gwanda, Filabusi, West Nicholson, Beitbridge, Mwenezi, Plumtree, Masvingo and Mberengwa) were acquired from the Department of Meteorological Services in Zimbabwe. Although there is some variation in the lengths of station data sets, most cover ca. 65 years (Table 4.2). In addition, daily rainfall data are available for 8 stations (Bulawayo, Matopos, Mbalabala, Plumtree, Chiredzi, Hope Fountain, Mpandeni and Gwanda) (Table 4.1).

Prior to trend analysis, quality control measures were undertaken which involved careful visual inspection of the data to identify missing values, outliers and typographic errors in the data series. Having inspected the data, homogeneity testing was computed based on the Standard Normal Homogeneity test (SNHT), Pettit's test and the Buishand's Range test (BR) at 5% significant level for individual stations using SNHT library of R statistical packages

version 3.3.3 (R Development Core Team, 2016). Homogeneity testing was for the purposes of identifying significant change points in the time series data, which normally emanate from changes in station location, or instrumentation, such as moving from manual to automated instruments. For the change to be considered significant, change detection was required by more than one test.

Table 4.1: Daily rainfall data location, elevation and period covered

Station	Latitude	Longitude	Elevation	Start Year	End Year
Bulawayo	-20.13	28.63	1334	1930	2015
				1896	1906
Filabusi	-20.54	29.28	1108	1920	2013
Matopos	-20.56	28.47	1385	1930	2015
Mbalabala	-20.45	29.04	1093	1930	2015
Plumtree	-20.50	27.80	1363	1963	2014
Chiredzi	-21.03	31.68	396	1965	2014
Hope Fountain	-20.26	28.66	1446	1886	1906
Mpandeni	-20.70	27.91	1204	1896	1906
Gwanda	-20.95	29.03	999	1899	1906

Table 4.2: Monthly rainfall data location, elevation and period covered for 11 stations within Mzingwane catchment

Station	Latitude	Longitude	Elevation	Start Year	End Year
Bulawayo	-20.13	28.63	1334	1950	2015
Gwanda	-20.95	29.03	999	1950	2015
Beitbridge	-22.22	30.00	486	1950	2015
Filabusi	-20.54	29.28	1108	1950	2015
Kezi	-20.93	28.47	1000	1951	2015
Matopos	-20.56	28.47	1385	1950	2015
West Nicholson	-21.03	28.94	956	1950	2015
Chiredzi	-21.03	31.68	396	1965	2013
Mberengwa	-20.48	29.92	1035	1950	2015
Plumtree	-20.50	27.80	1363	1950	2015
Masvingo	-20.07	30.83	1076	1950	2015

4.2.3 Trend detection

The Mann-Kendall trend test is a widely used statistical analysis tool for hydro-meteorological data because it is appropriate for non-normal data associated with climatic parameters. Its primary advantage is in its independence of the data and tolerance to outliers (Hamed and Rao, 1998). The Modified Mann-Kendall test was applied to monthly rainfall data for detecting statistically significant trends in rainfall series. The standard test statistic Z is computed as;

$$Z_{MK}=\begin{cases}\frac{S-1}{\sqrt{Var(S)}} & when \quad S>0\\ 0\ldots & when \quad S=0\\ \frac{S+1}{\sqrt{Var(S)}} & when \quad S<0\end{cases}$$

Where,

$$S=\sum_{i=1}^{n-1}\sum_{j=i+1}^{n} sgn(x_{j-}\, x_i)$$

Sen's Slope Estimator Test (1968) was used to determine the magnitude of the trends. The slope T_i was calculated as;

$$Sen's\ Estimator=\begin{cases}T\left(\frac{N+1}{2}\right) & if\ N\ is\ odd\\ \frac{1}{2}\left(T\frac{N}{2}+T\frac{N+2}{2}\right) & if\ N\ is\ even\end{cases}$$

4.2.4 Rain season characteristics

To quantify the quality of the rain season, the number of rainy days, frequency, and trends in rainy days were established. Seasonal rainfall onset and termination dates, as well as the length of the rain season, were computed to determine variations in the rain season quality. The study applied the threshold procedure to define a rainy day based on the method by Marteau *et al*. (2011), as shown in Table 4.3. Dry days were taken to be days with less than 1mm of rain.

Table 4.3: Rain day classification criteria by Marteau *et al*. (2011

Day	Rainfall threshold
Rainy	>=1mm
Heavy rain	>=10 < 20mm
Very Heavy rain	>=20 < 30mm
Extremely heavy rain	>=30 mm

The definition for the start of the rainy season varies widely depending on the climatic and geographic location to which it is applied. However, there seems to be some consensus that the first rains need not necessarily be the start of the rain season (Mazandarani *et al*., 2013). This study defines the start of the rainy season as a date when rainfall accumulation in 1 or 2 days is 20mm within 3 dekads, but not followed by a period of more than 10 consecutive dry days in the next 3 dekads (Edoga, 2007). Determining the cessation of the rainy season is even more complex given the semi-arid nature of the sub-catchment. Mazandarani *et al*. (2013) define the end of the rainy season as the last date of precipitation in March of less than 10mm, and followed by no fewer than 20 dry days. Here we adopt the proposal by Tadross *et al.* (2005) that the end of the rainy season is defined as 3 dekads with less than 20mm of rain followed by 2 dekads of dry days. The length of the rain season is thus determined by such start and end dates (Moyo *et al*., 2017; Mupangwa *et al*., 2011).

4.2.5 Rainfall variability

Several indices are computed to measure rainfall variability through space and time using R statistical packages version 3.3.2. The Coefficient of Variance (CV) was computed based on monthly data. This is a measure of how an individual datum varies around the mean value. It explains the deviation of the data series from its central tendency as a ratio of standard deviation to the mean. It is mathematically calculated as follows;

$$CV = \frac{S_x}{\bar{x}} * 100 \quad (1)$$

Where S_x = standard deviation

$\bar{x}$= mean

A greater CV is an indicator of large spatial variability in rainfall. Previous studies by Recha *et al*. (2012) and Bari *et al*. (2017) also expressed that a CV >30% of rainfall data indicate great variability in quantity and distribution of precipitation.

The Standard Precipitation Index (SPI) by McKee *et al*. (1993) is a normalised index which is based on the likely occurrence of the observed rainfall data. Negative values of the index show rainfall deficit while positive values denote rainfall surplus. The values around zero indicate close to normal rainfall (Table 4.4).

Table 4.4: Classification of rainfall extremity based on SPEI (McKee *et al*., 1993)

Category	**SPEI value**
2.0+	Extremely wet
1.5 to 1.99	Very wet
1.0 to 1,49	Moderately wet
0 to .99	Near normal
-1.0 to -1.49	Moderately dry
-1.5 to -1.99	Severely dry
-2 and less	Extremely dry

The Precipitation Concentration Index (PCI), originally introduced by Oliver (1980), but later modified by Nsubuga *et al*. (2014), is calculated as follows;

$$PCI = 100 * \sum_{i=1}^{12} P_i^2 \quad (2)$$

Where P_i= rainfall amount of the ith month calculated for each station per year. PCI values below 10 indicate uniform rainfall distribution per year, while values of 11-20 disclose a seasonal rainfall distribution. Values above 20 depict substantial rainfall variability (Nel, 2009; Ngongondo *et al*., 2011).

4.3 Results and Discussion

4.3.1 Data quality control

Based on the Pettit's, SNHT and Buishand's tests, none of the stations had a significant change point, suggesting that the rainfall series were fairly homogenous (Table 4.5). Although the SNHT test detected a change point for Bulawayo in February 1950 and Mberengwa in March 2013 and West Nicholson in February (Buishand's test), these were not considered significant as they were not detected by the other two tests (Stepanek *et al*., 2011).

Table 4.5: Homogeneity using the Pettit's, SNHT and Buishand's tests

	Pettit's test		**SNHT test**		**Buishand's test**	
Station	**K**	**P-value**	**T_0**	**P-value**	**Q**	**P-value**
Bulawayo	11618	0.71	13.012	**0.046***	26.695	0.304
Gwanda	16617	0.125	3.605	0.750	18.459	0.748
Beitbridge	10657	0.872	4.426	0.571	15.483	0.893
Filabusi	9521	0.777	3.452	0.782	21.356	0.59
Kezi	13925	0.314	4.594	0.586	19.915	0.655
Chiredzi	9701	0.226	2.476	0.893	14.737	0.813
Mberengwa	13252	0.322	19.525	**0.018***	22.031	0.512
Plumtree	8562	0.716	4.686	0.571	17.209	0.800

4.3.2 Time series decomposition

The rainfall series were decomposed in R using packages "timeSeries" and "TTR" (Figure 4.2). Time series decomposition employed an addictive model approach embedded in R software to assess the rate of change through decomposing time series into three main components- namely trend, seasonal and random components (Figure 4.2). The series shows that there is a regular seasonality in rainfall pattern in a given year. Overall, the time series plots indicate slightly, but not statistically significantly at $p < 0.05$, decreasing rainfall trends at most stations, averaging -0.0085mm/year.

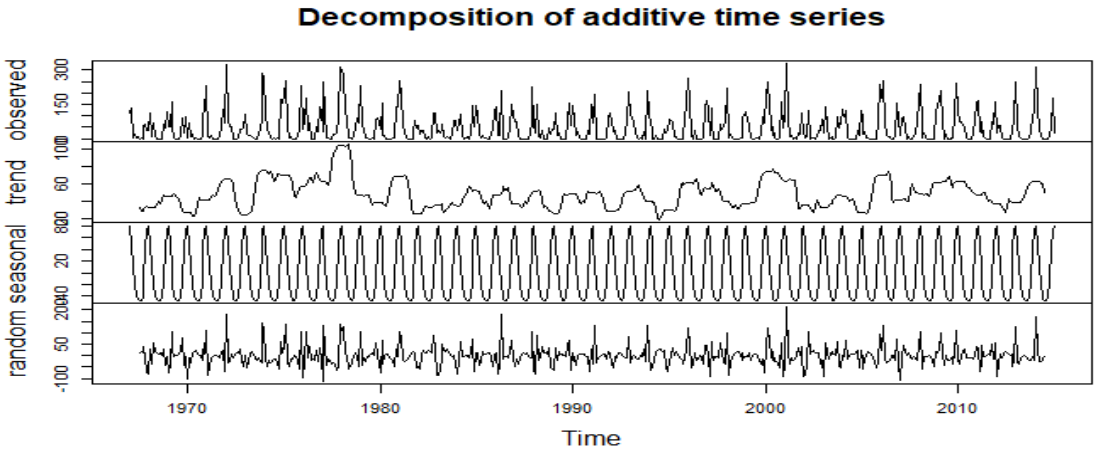

(a)

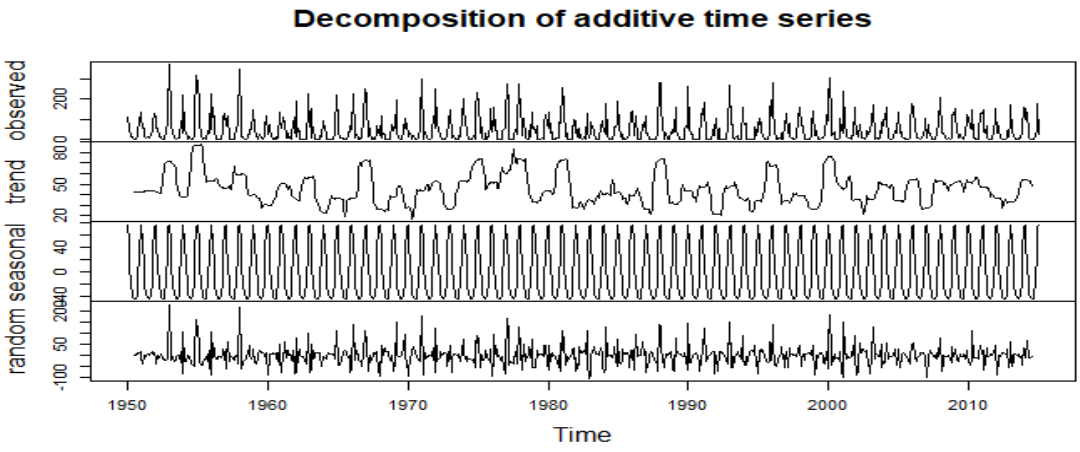

(b)

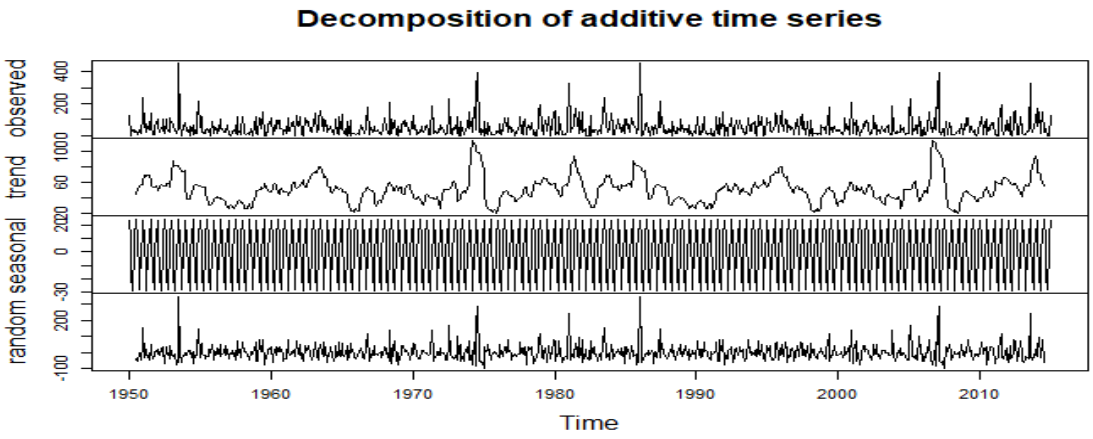
Decomposition of additive time series
observed
trend
random
seasonal
Time
1950
1960
1970
1980
1990
2000
2010

(c)

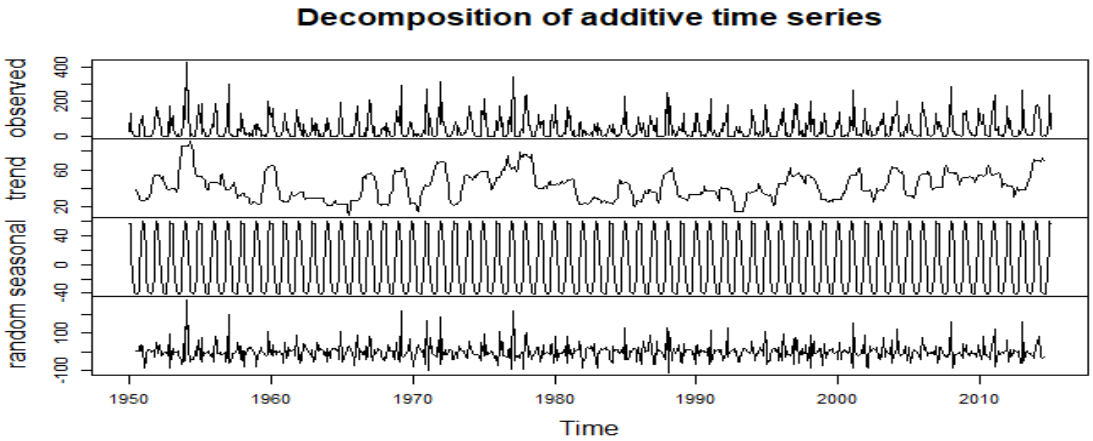
Decomposition of additive time series
observed
trend
random
seasonal
Time
1950
1960
1970
1980
1990
2000
2010

(d)

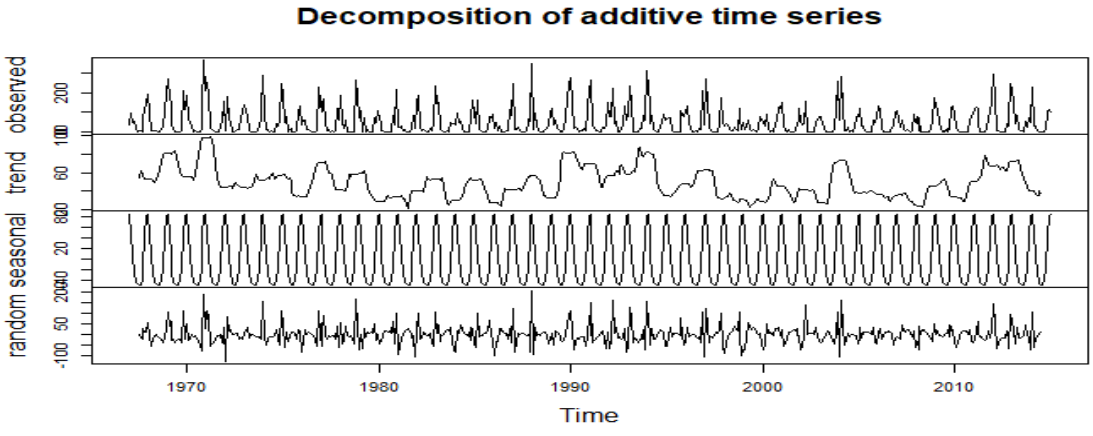
Decomposition of additive time series
observed
trend
random
seasonal
Time
1970
1980
1990
2000
2010

(e)

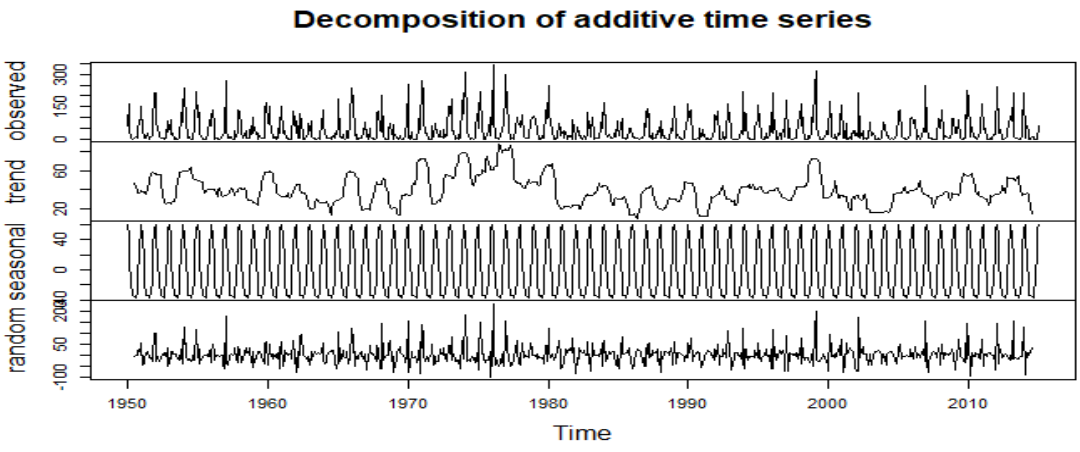

(f)

Figure 4.2: Monthly rainfall timeseries decomposition for: (a) Bulawayo, (b) Filabusi, (c) Beitbridge, (d) Gwanda, (e) Matopos and (f) Kezi for 1950-2015

4.3.3 Annual rainfall trends

Insignificant decreasing annual rainfall trends are measured for Bulawayo (-0.908mm year^{-1}), Filabusi (-0.085mm year^{-1}), Kezi (-2.056mm year^{-1}), Matopos (-0.969mm year^{-1}), West Nicholson (-0.091mm year^{-1}), Masvingo (-2.319mm year^{-1}) and Chiredzi (-1.333mm year^{-1}) (Table 4.5). In contrast, insignificant increasing trends are recorded for Gwanda (0.124mm year^{-1}), Mberengwa (0.014mm year^{-1}) and Plumtree (0.063mm year^{-1}), while at Beitbridge no trend is measured between 1950 and 2015 (Table 4.6). The results indicate that the catchment experienced statistically insignificant decreasing trends across 65% of the stations (Figure 4.3). These findings are similar to those of Mazvimavi (2010), who noted insignificantly decreasing annual rainfall trends across 40 Zimbabwean stations between 1892 and 2000. Similarly, Muchuru *et al*. (2016) reported a comparable rainfall trend for Kariba catchment area of the Zambezi river basin, in which 11 of the 13 stations (the exception being Mhondoro) exhibited insignificant trends. These findings confirm that rainfall quantity over the past 65 years has not significantly changed despite global climate warming. Nonetheless, although not statistically significant, there is a noticeable reduction in rainfall amount,

consistent with climate change projections that anticipate a general decline in precipitation within the tropics (Change, 2013).

Table 4.6: Annual MK trend test at 5% significance level

Station	Kendall's Tau	P-value	Sen's slope
Bulawayo	-0.14	0.097	-0.908
Filabusi	-0.083	0.327	-0.085
Gwanda	0.094	0.265	0.124
Kezi	-0.029	0.738	-2.056
Matopos	-0.107	0.205	-0.969
West Nicholson	-0.086	0.316	-0.091
Masvingo	-0.155	0.071	-2.319
Chiredzi	-0.045	0.654	-1.333
Mberengwa	0.014	0.871	0.188
Plumtree	0.063	0.473	1.313
Beitbridge	0.000	1.000*	0.000

** no trend*

4.3.4 Seasonal rainfall trends

Rainfall trends during the rainy season (October-March) show a significant downward trend for Bulawayo (-1.81mm year^{-1}; p=0.054) and Masvingo (-3.144mm year^{-1}; p=0.022) (Table 4.7). Insignificant negative trends are recorded for Gwanda (-0.900mm year^{-1}; p=0.314), Kezi (-0.854 mm year^{-1}; p=0.591), Matopos (-1.526 mm year^{-1}; p=0.20), West Nicholson (-1.350 mm year^{-1}; p=0.22) and Chiredzi (-0.737; p=0.75) stations. In contrast, Filabusi (0.721 mm year^{-1}; p=0.47), Mberengwa (0.342mm year^{-1}; p=0.72), Plumtree (0.104 mm year^{-1}; p=0.901), and Beitbridge (0.203 mm year^{-1}; p=0.86) measured insignificantly increasing rainfall trends at p<0.05 (Table 4.8). Broadly across the catchment, the rain season has experienced a slight decline in rainfall across 64% of stations, while marginally increasing at the remaining stations. Such trends have hydrologic implications on wetland ecosystems.

Dry season (April to September) rainfall trends insignificantly increased for the majority (73%) of stations at an average of 0.267 mm year $^{-1}$(Table 8), while Filabusi (-0.017 mm year $^{-1}$; p=0.956), Chiredzi (-0.432 mm year $^{-1}$; p=0.546) and Beitbridge (-0.104 mm year $^{-1}$; p=0.698) recorded statistically insignificant negative trends (Table 4.8). Such an increase in trends of rainfall during the dry season may be signifying a shift in season, meaning that the rain season onset is delaying and stretching into the drier months, particularly April and early May. Inter-annual variability of seasonal rains has largely been attributed to El Niño Southern Oscillation (ENSO) events (Mamombe *et al*., 2016a) which normally induce inter-season dry spells resulting in widespread crop failure and food insecurity, particularly over semi-arid regions.

Table 4.7: Rainy season MK trend test at 5% significance level for 1950-2015

Station	**Kendall's Tau**	**P-value**	**Sen's slope**
Bulawayo	-0.15	**0.054***	-1.812
Filabusi	0.063	0.465	0.721
Gwanda	-0.085	0.314	-0.900
Kezi	-0.046	0.591	-0.854
Matopos	-0.108	0.201	-1.526
West Nicholson	-0.104	0.221	-1.350
Masvingo	-0.197	**0.022***	-3.144
Chiredzi	-0.032	0.751	-0.737
Mberengwa	0.031	0.719	0.342
Plumtree	0.011	0.901	0.104
Beitbridge	0.015	0.864	0.203

** significant at p < 0.05*

4.8: Dry season MK trend test at 5% significance level

Station	Kendall's Tau	P-value	Sen's slope
Bulawayo	0.02	0.816	0.068
Filabusi	-0.005	0.956	-0.017
Gwanda	0.13	0.128	0.633
Kezi	0.003	0.973	0.012
Matopos	0.033	0.698	0.147
West Nicholson	0.047	0.583	0.208
Masvingo	0.051	0.555	0.378
Chiredzi	-0.06	0.546	-0.432
Mberengwa	0.021	0.889	0.041
Plumtree	0.114	0.190	0.646
Beitbridge	-0.033	0.698	-0.104

4.3.5 Historic rainfall (1886-1906)

Historic catchment rainfall between 1886 and 1906 is presented in Figure 4.3 for Bulawayo, Hope fountain, Mpandeni and Gwanda (values obtained from Wallace, 1907). Interestingly, the mean annual rainfall recorded for Bulawayo between 1896 and 1906 (538.27mm) is identical to that during more recent times (1930 to 2015), for which the mean is 538.4mm. The longest and oldest rainfall record is for Hope fountain (1886 to 1906) which recorded a mean annual rainfall of 730.5mm.

Historic daily rainfall data are only available for Bulawayo and the results show that most years started the rainy season during the first dekad and third dekad of October and ended in the second and third dekad of March, except for the 1900/01 season which ended during the first dekad of April (Table 4.9). The mean duration of the rainy season was 156 days with a mean number of 74 rainy days >2.5mm, which is ca 34% more than that for the 1950-2015 period (mean = 46 rainy days). Historic data for the period 1896-1906, indicate that the rainy season lasted on average 161 days, while that for the period 1950-2015 averaged 144 days

and that for the most recent 10 years (2005-2015) averaged 112 days. These results tentatively indicate that the rainy season length has significantly reduced by 30% in the last 10 years and 13% (1950-2015) in comparison to the historic period (1896-1906).

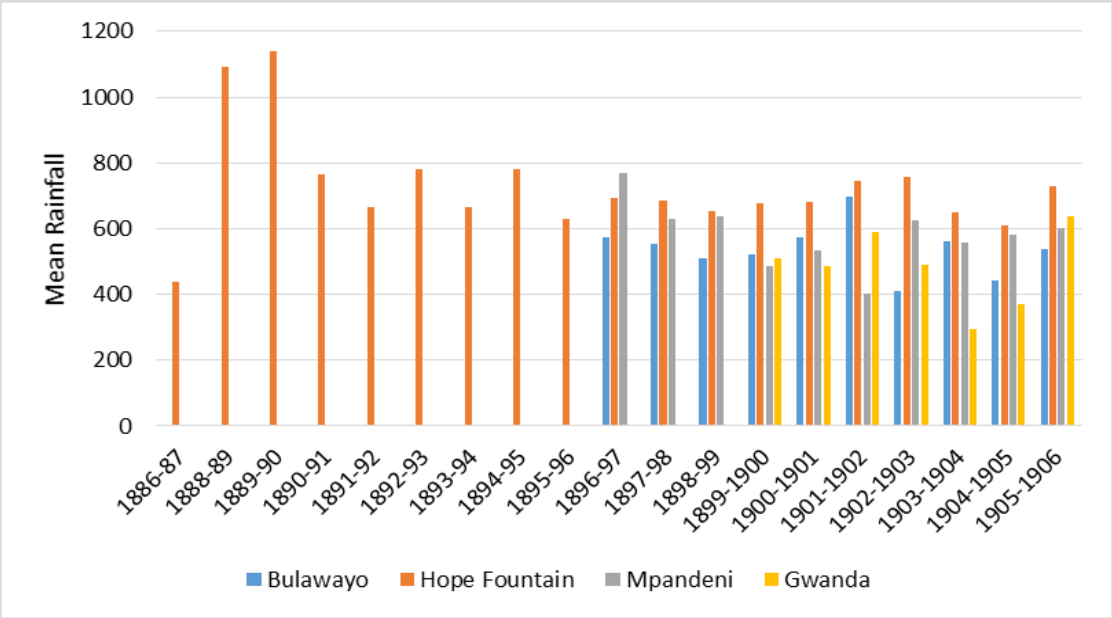

Figure 4.3: Historic mean annual rainfall (mm) per station for the period between 1886 and 1906

4.3.6 Variation in number of rainy days

Bulawayo recorded the highest (49) average number of rainy days (≥1mm) per rain season between 1930 and 2015, while the lowest number is for Matopos (44 days) (Table 4.10). Heavy rainy days (10-30mm) average 10 to 15 days across the catchment, while very heavy rainy days typically occur on 3-5 occasions during the rainy season (Figures 4.4, 4.5; Table 4.10). The Mann-Kendall trend results for the number of rainy days provide varied results. Bulawayo, Mbalabala and Plumtree measured insignificant decreasing trends (0.009 days decade $^{-1}$, 0.004 days decade $^{-1}$ and 0.013 days decade $^{-1}$ respectively) in the number of rainy

days ≥ 1mm while Matopos significantly decreased (0.02 days decade $^{-1}$; p=0.003) (Table 12). In contrast, the number of rainy days at Filabusi has increased, albeit statistically insignificant (0.009 days decade $^{-1}$).

Table 4.9: Duration of the rainy season for Bulawayo (1896-1906)

Season	Started	Ended	Duration (Days)	Rainy Days
1896-97	21-Oct	23-Mar	153	76
1897-98	26-Oct	30-Mar	155	67
1898-99	23-Oct	28-Apr	188	82
1899-1900	05-Nov	18-Mar	133	80
1900-1901	30-Oct	07-Apr	159	81
1901-1902	30-Oct	21-Mar	142	84
1902-1903	04-Oct	21-Mar	168	59
1903-1904	10- Oct	20-Mar	161	81
1904-1905	14-Oct	07-Mar	144	59
1905-1906	09-Oct	14-Mar	156	73
Mean			**156**	**74**

Trends are similar for heavy rainy days, with that for Matopos still significantly decreasing (-0.01 days decade $^{-1}$; p=0.0000) (Table 4.11). Very heavy rainy days have increased insignificantly (0.0001 days decade $^{-1}$; p = 0.455) at Plumtree, while both Bulawayo and Filabusi measured zero trends (p=0.587 and p=0.15 respectively) at p<0.05 (Table 4.11). Generally, the results indicate that the number of rainy days is decreasing in the catchment (Figure 4.4 & 4.5), which has important implications for soil and catchment hydrology, and consequently the duration of water availability to communities, wetlands and for agricultural production. The results are not dissimilar to those from neighbouring semi-arid Botswana where the number of rainy days has declined by an average of -1.31 days year $^{-1}$ between 1975 and 2005 (Batisani and Yarnal, 2010). Similar findings were also noted in Rwanda by

Muhire and Ahmed (2015) indicating a significant decrease in the number of rainy days over eastern and central plateau.

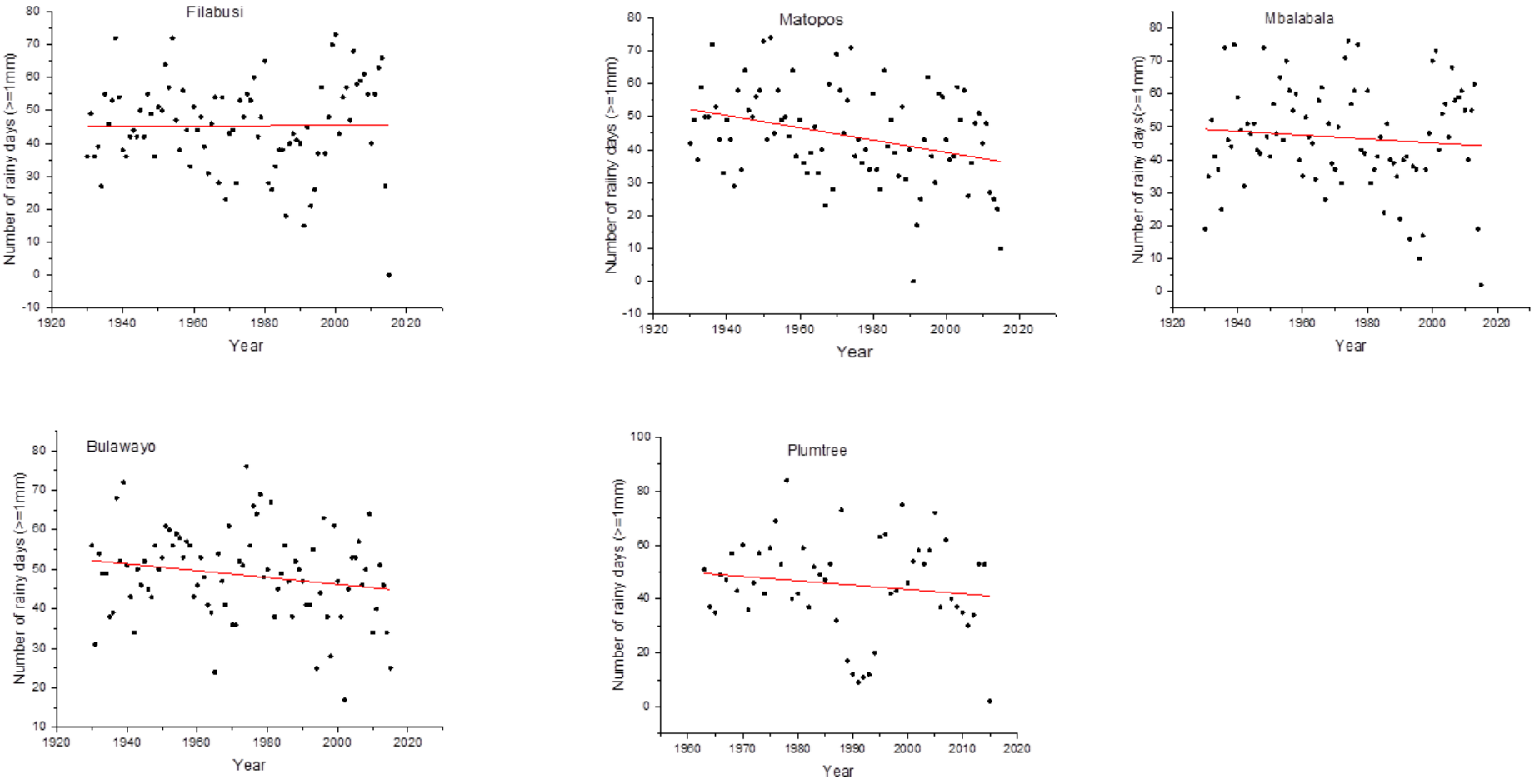

Figure 4.4: Number of rainy days of greater than 1mm day-1per station from 1960 to 2015 in Plumtree and 1920 to 2015 for Filabusi, Matopos, Mbalabala, and Bulawayo

Table 4.10: Number of rainy days per given class

Station	Number of rainy days (>1mm)		Number of heavy rainy(>=10>30)		Number of very heavy rainy days (>=30)	
	65 years	Mean/season	65 years	Mean/season	65 years	Mean/season
Bulawayo	4187	49	822	10	359	4
Filabusi	4277	45	1322	14	266	3
Matopos	3811	44	1197	14	384	5
Plumtree	2399	45	821	15	235	4
Mbalabala	4047	47	1323	15	407	4

4.3.7 Onset and cessation of the rainy season

Bulawayo rains are starting between the second and third dekad of October and second dekad of November, with cessation dates estimated on average in late March and the first dekad of April (Figure 4.6). The length of the rainy season in Bulawayo, ranged between 90 days (2006/07 season) and 208 days (1999/2000 season) (Figure 4.7a). The longest rainy seasons coincided with La Niña events while the shortest seasons were associated with El Niño years. At Filabusi, onset dates were within the second and third dekad of October and the third dekad of November. Some exceptions are noted in the years 1935, 1974, 1992 and 1994, when onset dates occurred within the second and third dekad of December and were severe drought years associated with El Niño events (Figure 4.6). The length of the rainy season in Filabusi ranged from 94 days (1994/95 season) to 185 days (1955/56 season) (Figure 4.7c). At Matopos, the rain season starts within the second dekad of October and the second dekad of November, while cessation dates varied from the third dekad of February to first dekad of April (Figure 4.6). The length of the rainy season for Matopos ranged from 61 days (2011/2012 season) to 201 days (1976/77 season) (Figure 4.7b). Mbalabala and Plumtree

have similar onset dates estimated in the second and third dekad of October and the third dekad of November, while cessation dates fell between the third dekad of February and third dekad of April (Figure 4.6).

Table 4.11: Mann-Kendall trend test for rainy days at 5% level of significance

Station	>=1mm rainy day		>=10>30mm heavy rainy day		>=30 mm very heavy rainy days	
	Kendall tau	**P-value**	**Kendall tau**	**P-value**	**Kendall tau**	**P-value**
Bulawayo	-0.124	0.096	-0.069	0.363	-0.042	0.587
Filabusi	0.099	0.158	0.089	0.211	-0.107	0.15
Matopos	-0.222	**0.003***	-0.278	**0.000***	-0.159	**0.041***
Mbalabala	-0.034	0.652	-0.056	0.456	-0.159	**0.038***
Plumtree	-0.076	0.433	-0.024	0.811	0.075	0.455

**Significant at 5% significant level*

The Mann-Kendall trend test for the length of the rainy season for all stations significantly decreased at $p<0.05$, implying that the catchment is experiencing shorter rainy seasons than before. However, a combination of reduced rainy days and shortened rainy seasons suggests a drier season of short duration which is detrimental to crop growth and water availability for livestock and general ecosystem functioning. Such short, dry rainy seasons has caused widespread crop failures in southern Africa, particularly semi-arid regions such as the Mzingwane catchment. Previous studies have also raised concern for such long intra-season dry spells in parts of southern Africa (e.g. Cook *et al*., 2004; Usman and Reason, 2004). The inter-seasonal dry spells seem linked to the northward shift and the weakening of the ITCZ over southern Africa (Cook *et al*., 2004). It has been established that the dry spells frequency

over southern Africa is often highest during the ENSO events, associated with the shift in the location of tropical temperate trough systems central to rain production (Usman and Reason, 2004). Similarly, the results of this study also noted that about half of the rainy season experiences dry spells.

The Zimbabwean results indicate a major shift in the rainy season onset dates from October (1999 to 2015) to late November and in some instances even into the third dekad of December (2012 to 2015). These results are consistent with the IPCC climate change projections for southern Africa, which postulate a decline in rainfall and a decrease in the number of rainy days.

4.3.8 Rainfall variability

Different indices are used to assess rainfall variability in the Mzingwane catchment. The Coefficient of Variation (CV) was computed using monthly rainfall data per station and the results for all the stations are higher than 30% (Table 4.13), suggesting large temporal and spatial variation in rainfall amount and distribution. A number of previous studies have reported similar high variability during the rainy season in southern Africa (e.g. Cook *et al*., 2004; Reason *et al*., 2005; Reason and Jagadheesha, 2005; Tadross *et al*., 2009; Batisani and Yarnal, 2010; Muchuru *et al*., 2016).

The Precipitation Concentration Index (PCI) is a powerful indicator of the temporal distribution of precipitation over time, which is applied to the Mzingwane catchment. The summer PCI for all stations ranged between 10 and 15 (mean = 10), indicating strong seasonality in rainfall distribution (Figure 4.8). During autumn, the PCI ranged between 13 and 18, with a mean value of 15.5 while during spring it ranged from 13 to 19, again

indicating strong rainfall seasonality. In winter the PCI varied widely with some years having values of over 25, suggesting substantial variability and that rainfall is largely concentrated during a few months of the year (Figure 4.8). The seasons with the highest rainfall had the lowest PCI values and these results correspond to those by Ngongondo *et al.* (2011) and Nsubuga *et al.* (2014) who reported that stations with highest mean rainfall have the lowest PCI values, while high PCI values indicated higher variability in rainfall. The PCI trends for Filabusi (0.0227), Bulawayo (0.005), Gwanda (0.010) and Plumtree (0.017) show an overall positive trend, while that for Matopos decreased at a magnitude of -0.017 for the full time series. Such predominantly increasing trends in PCI indicate a more concentrated rainfall.

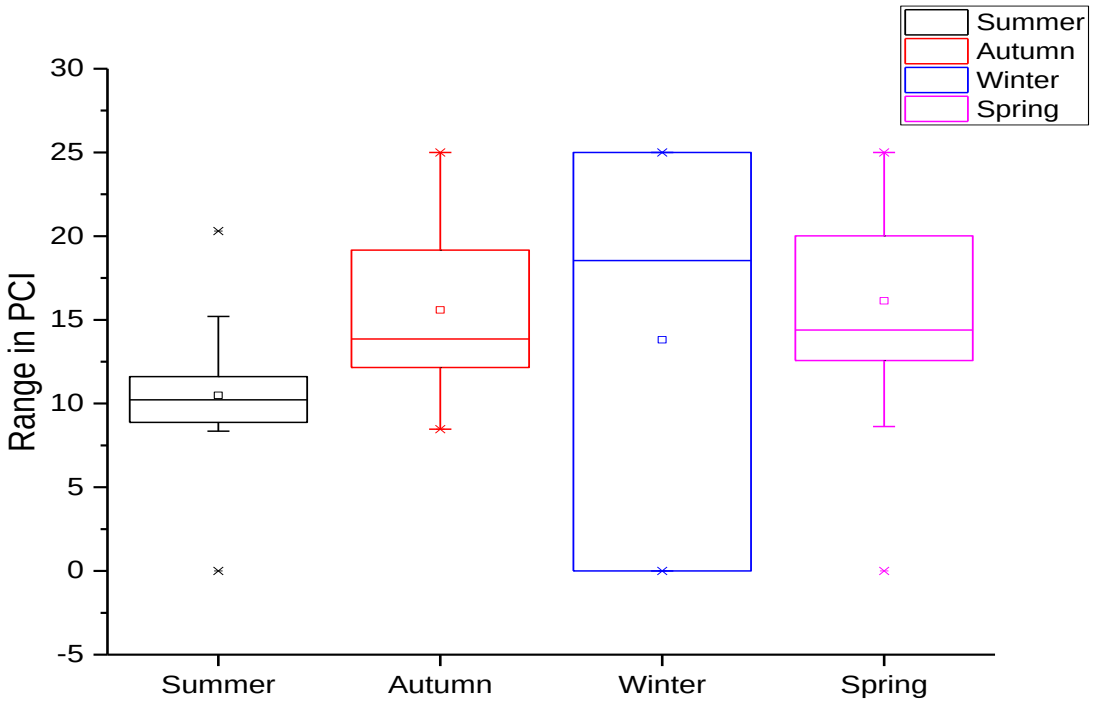

Figure 4.5: Seasonal Precipitation concentration Index for Mzingwane for 1950-2015

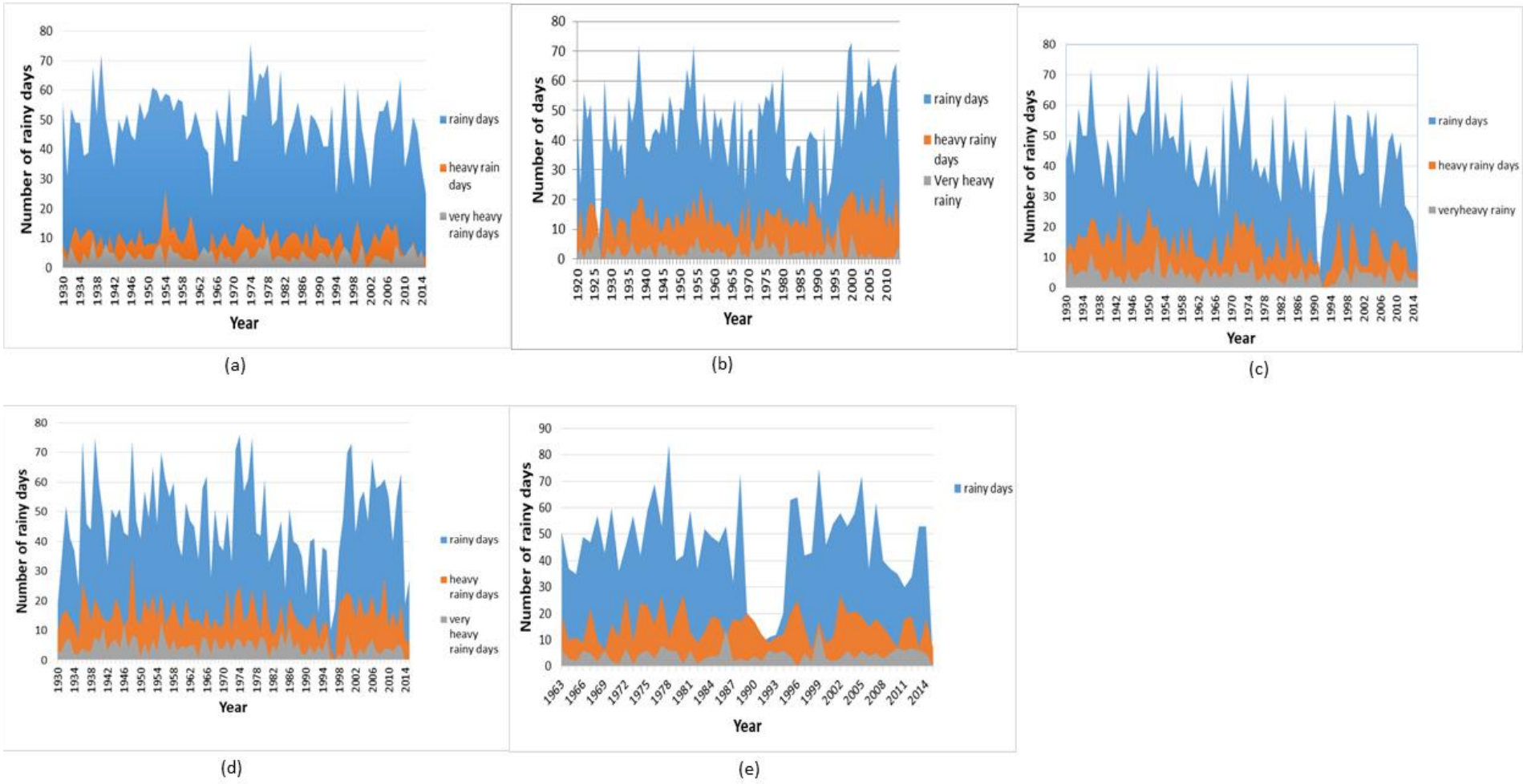

Figure 4.6: Time series of a number of rainy days in a given class for which rainy (≥ 1mm day^{-1}), heavy rainy (≥10>30 day^{-1}) and (≥30mm day^{-1} : (a) Bulawayo, (b) Filabusi, (c) Matopos, (d) Mbalabala and (e) Plumtree

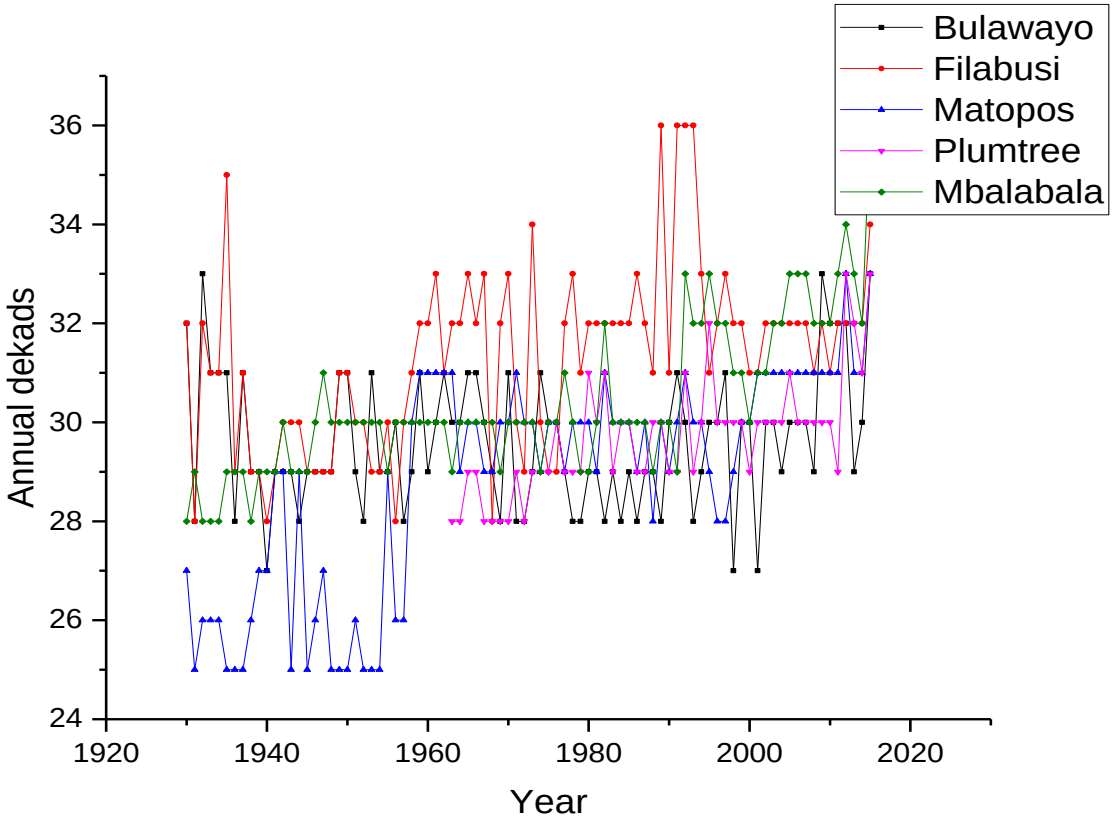

Figure 4.7: Estimated onset dates per station from dekad 24 to dekad 36 for the period between 1930 and 2015 for Bulawayo, Filabusi, Matopos and Mbalabala while Plumtree was analysed from 1960 to 2015.

4.3.9 Rainfall anomalies based on the SPI

The 1-month SPI is used to analyse monthly rainfall anomalies and results indicate that the Bulawayo rainy seasons are moderately wet, with occasional years of very wet conditions in 1952, 1978, 2000, 2008 and 2014, which coincided with the ENSO La Niña phase. Dry season months (May to September) recorded moderate dryness with some years experiencing near normal conditions (Figure 4.10a). At Filabusi, the rainy season was predominantly within moderate wetness, but some years recording very wet to extremely wet conditions (1954, 1958, 1967, 1972, 1981, 1996 and 2000) (Figure 4.10b).

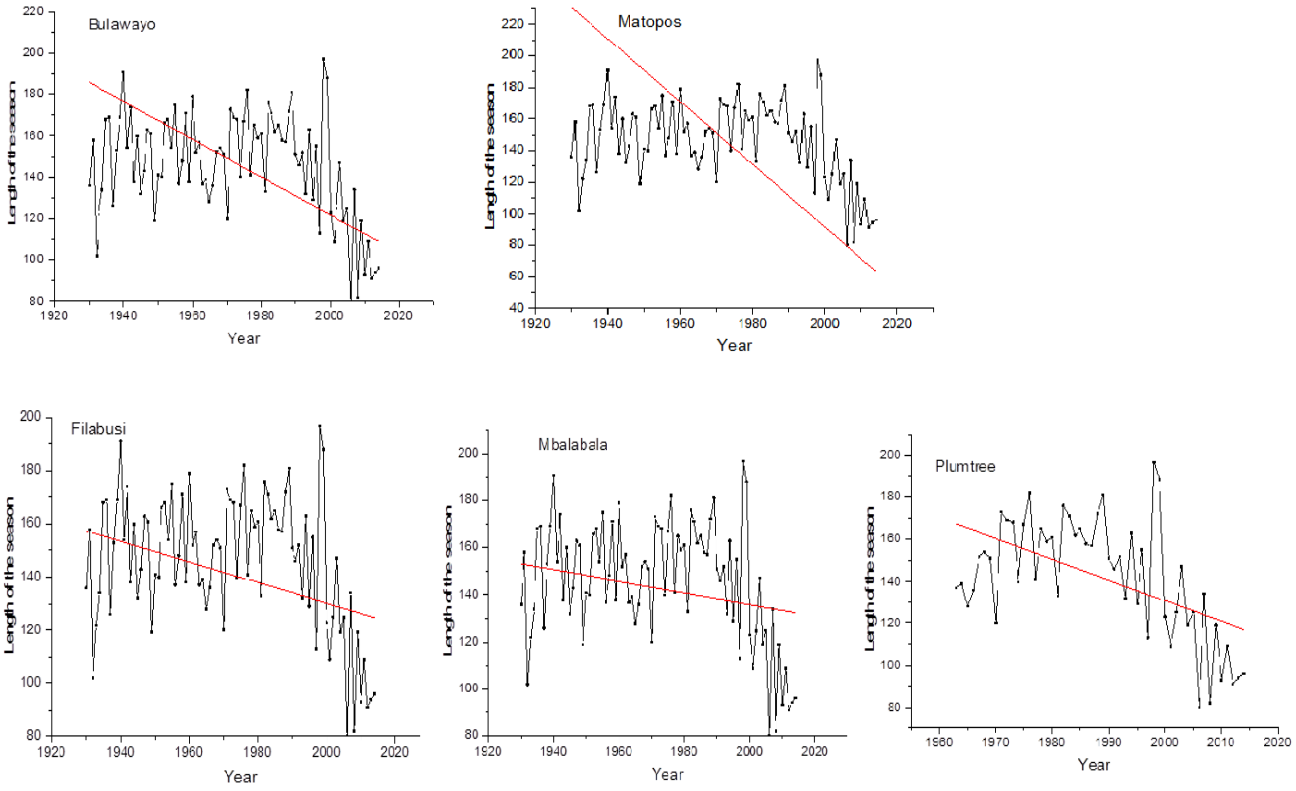

Figure 4.8: Length of the rainy season per given station for the period between 1930 and 2015 for Bulawayo, Filabusi, Matopos and Mbalabala while Plumtree was analysed from 1960 to 2015.

Table 4.12: Rainy season coefficient of variation (CV)

Station	Rainy season rainfall amount (mm)	CV
Bulawayo	538.40	0.83
Filabusi	493.39	0.86
Gwanda	458.08	0.89
Kezi	468.07	0.89
Matopos	533.90	0.81
West Nicholson	421.59	0.94
Masvingo	525.50	0.96
Chiredzi	548.33	0.97
Mberengwa	300.70	0.93
Plumtree	469.80	0.97
Beitbridge	500.71	1.00

Gwanda measured moderately to very wet conditions during the rainy season months (October-March), and dry months being near normal (Figure 4.10i). Beitbridge recorded wet conditions for the rainy months while the dry season ranged from moderately to severely dry. Plumtree rainfall anomalies were unusual, with the rainy months recording SPI values of -1 to -1.49 (moderate dryness), while the dry months measured moderate to very wet conditions (Figure 4.10f). Kezi displays similar trends to Bulawayo (Figure 4.10c).The 1-month SPI for West Nicholson indicates that the rainy season months received moderate to normal wetness and isolated very wet conditions, notably in 1952, 1958, 1967, 1972, 1978, 2000 and 2014. In contrast, the dry season months became very dry with most years recording SPI values of between -1 and -2 (Figure 4.10d). Chiredzi measured normal rainfall for all rainy season months in the series, while the dry months had moderate to very wet conditions (Figure 4.10h). In Masvingo, the SPI values indicate normal to moderate wetness for the wet season, with isolated very wet conditions for January and February in the years 1954, 1964, 1978, 1996 and year 2000. The dry months recorded moderate to very dry conditions for the entire

series (Figure 4.10g). The results confirm that rainfall anomalies are closely associated with ENSO phases, with dry conditions (drought) coinciding with El Niño events and wet conditions with La Niña. Strong relationships between rainfall and ENSO indices have also been identified for historical times in Zimbabwe, before the 20th century (Therrell *et al*., 2006).

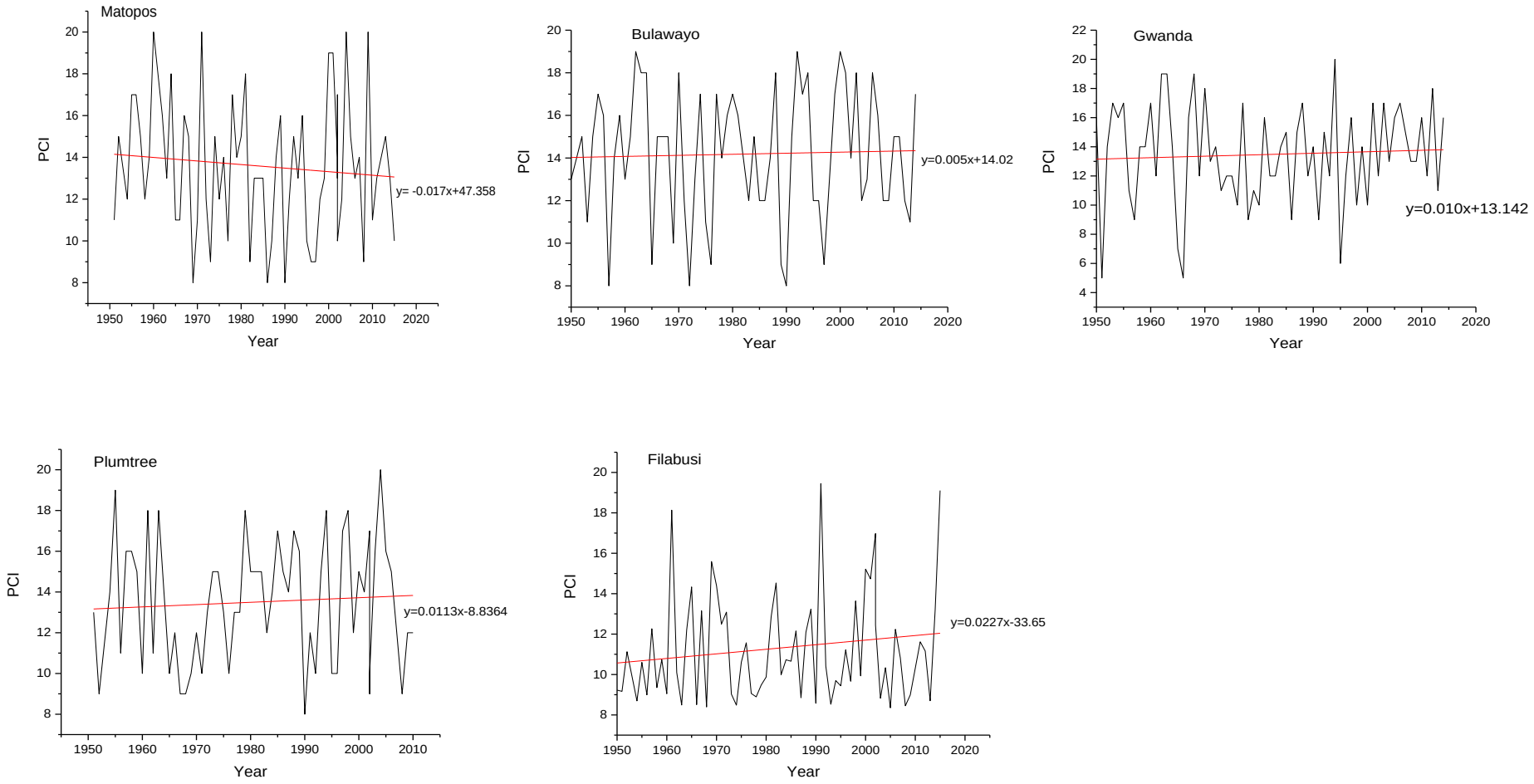

Figure 4.9: Station based PCI time series from the period 1950 to 2015.

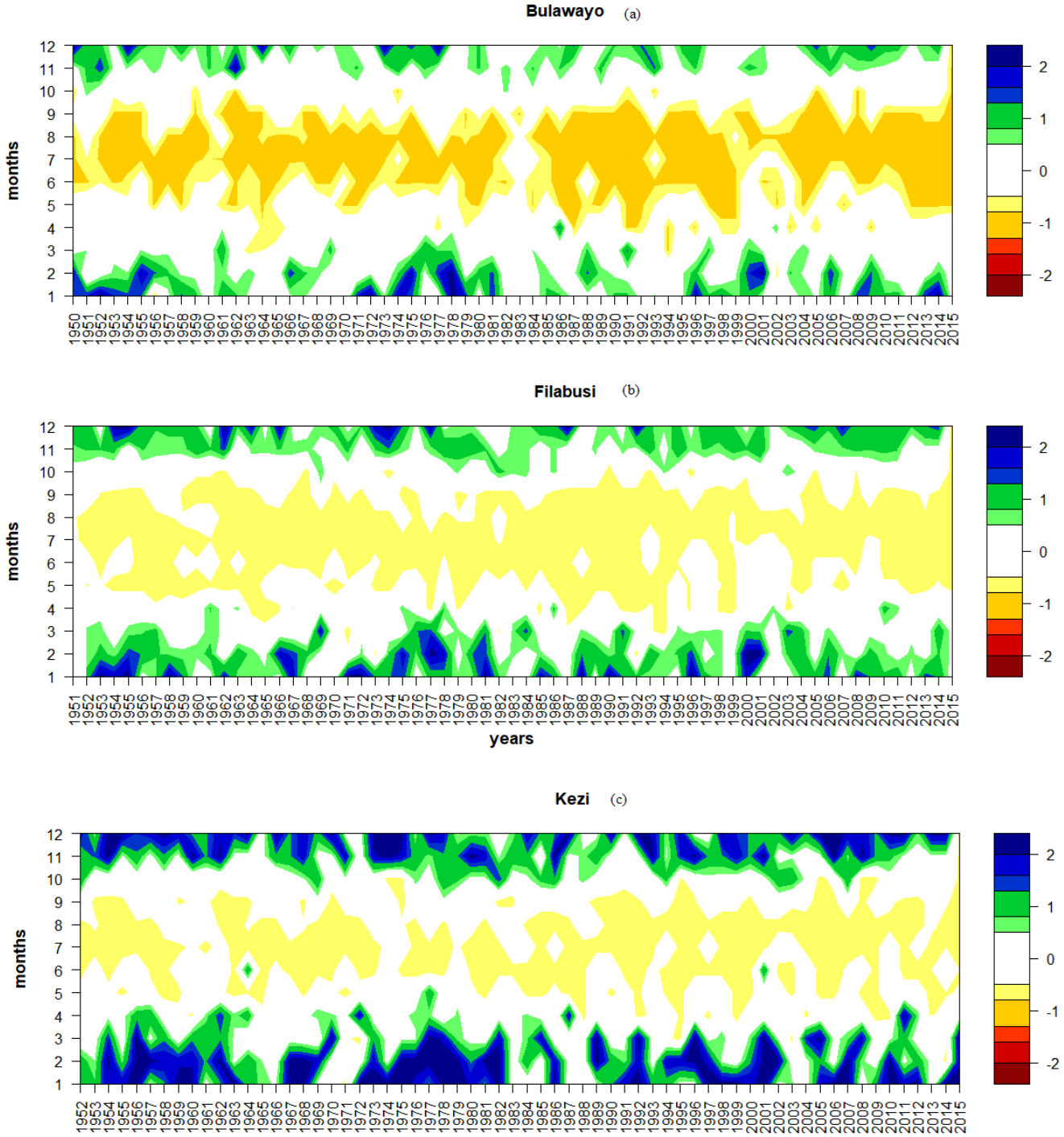

Figure 4.10: SPI-3months per station: Bulawayo (a), Filabusi (b), Kezi (c), West Nicholson (d), Beitbridge (e), Plumtree (f), Masvingo (g), Chiredzi (h), and Gwanda (i).

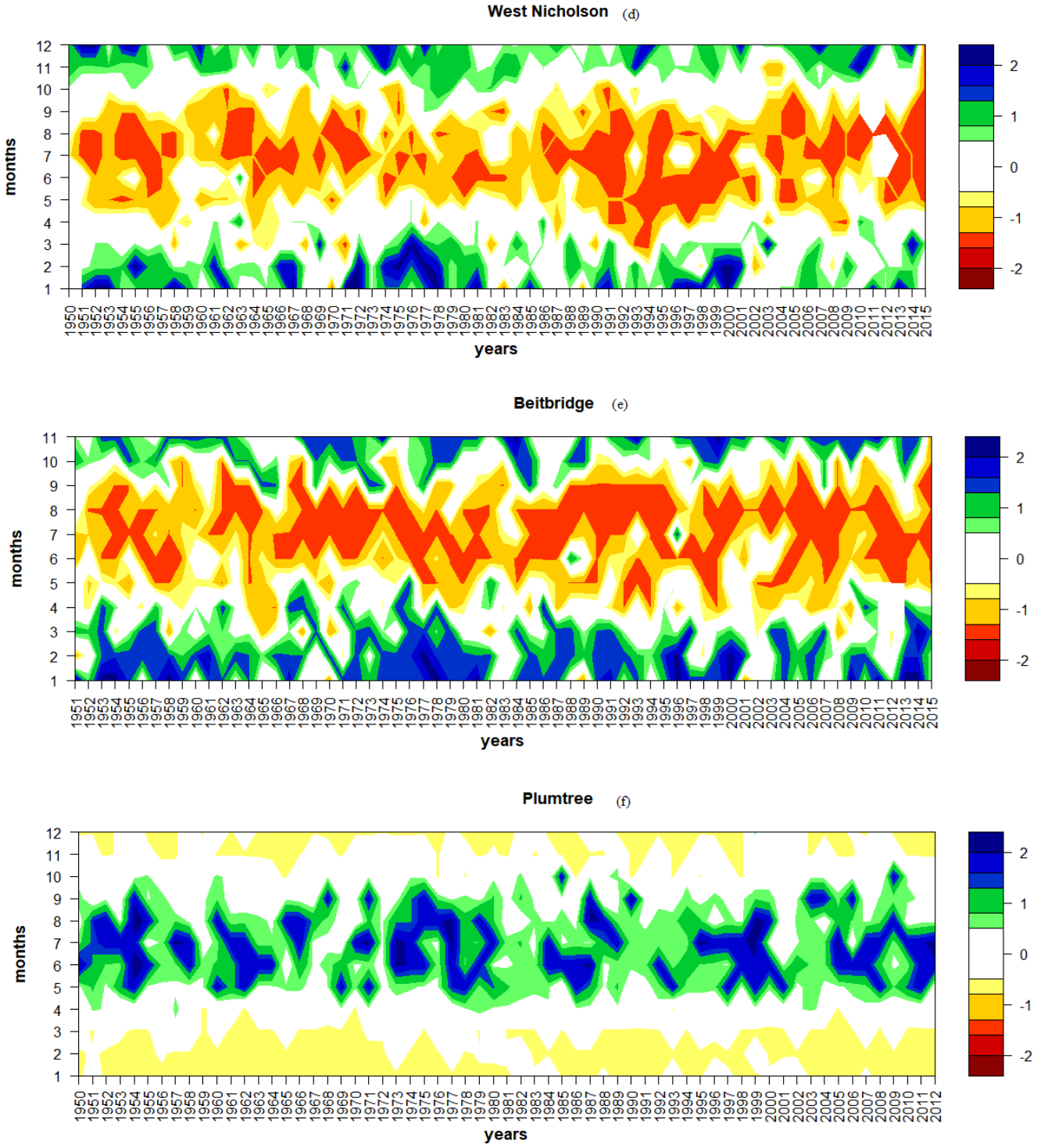

Figure 4.10: (Continued)

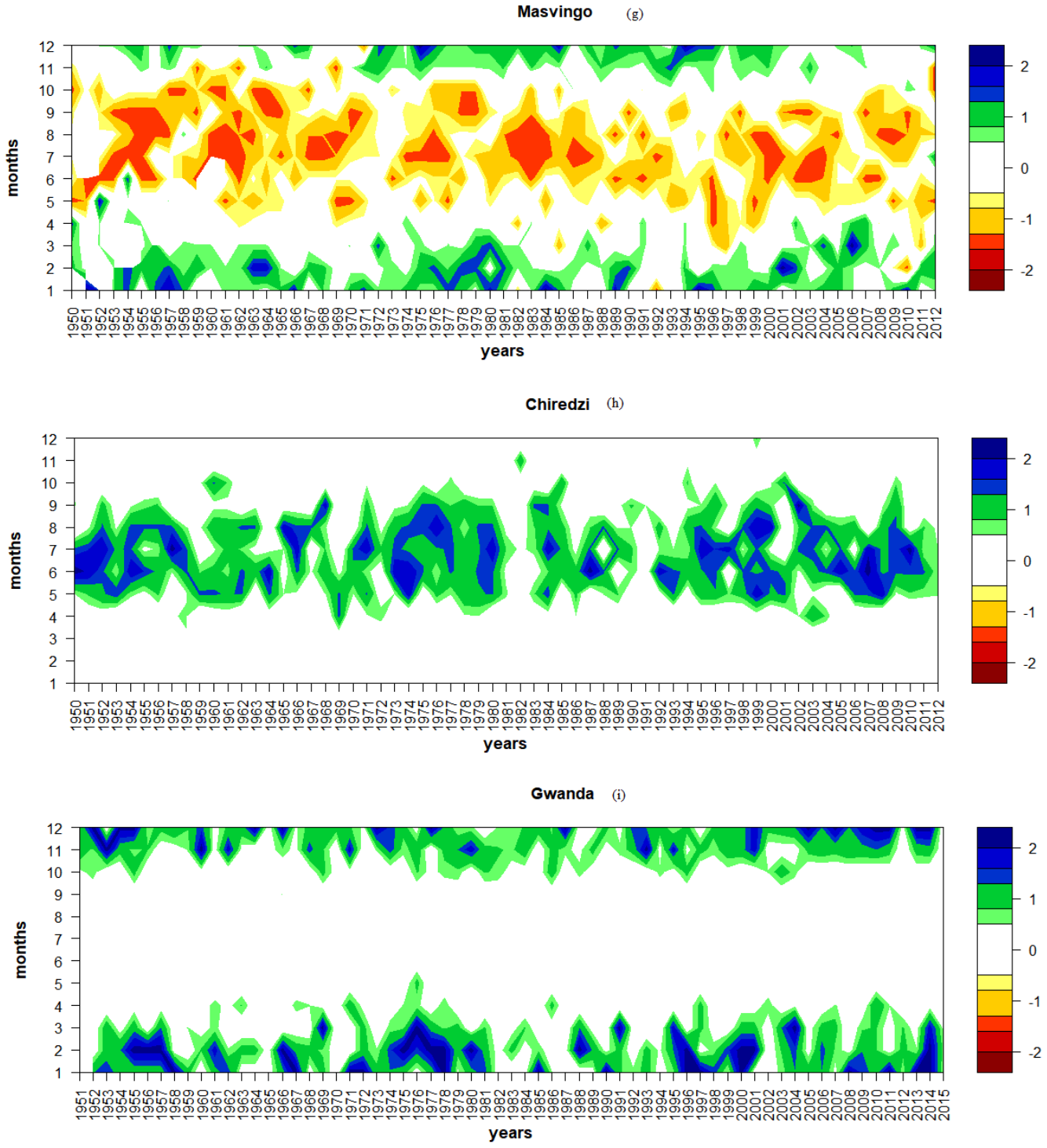

Figure 4.10: (Continued)

4.4 Conclusions

The study quantified rainfall variability and changes in rain season characteristics in Mzingwane catchment. The results of the study show that mean annual rainfall has not changed from historic (1896-1906) to more recent times (1950-2015), but the number of rainy days (>=1mm) has decreased by almost 34%. In addition, the duration of the rain season has shortened, with longer intra-season dry spells which are detrimental to crop growth. The period of 1950 to 2015 experienced a decrease in the number of rainy days, which could be attributed to global warming and related to climate variation. Onset and cessation results indicate a shift in season onset from first and second dekad of October to the third dekad of November, and in some cases encroaches into the second dekad of December. Cessation dates have shifted into the second dekad of April. Thus, a combination of a reduced number of rainy days and shortened rainy season has substantial hydrologic implications for most natural ecosystems such as wetlands. The results based on variability indices indicate strong rainfall variability both in space and time. The seasonal PCI indicates seasonality for summer and autumn seasons while winter rainfall substantially varied. Based on the SPI results, it is apparent that ENSO events play a profound role in spatio-temporal rainfall variability. Notably, extreme events seem to be occurring more frequently in the current century than during the 20^{th} century. Generally, the results for rain season characteristics show that this season is no longer reliable as a rainfall (water) producer, and as such poses high uncertainties to farmers which could be addressed through the provision of timely seasonal weather forecasts, which would then enable more effective planning and the organization of supplementary water supply through irrigation systems.

CHAPTER 5: QUANTIFYING SPATIO-TEMPORAL CHANGES OF NESTED WETLANDS IN THE SHASHE SUB-CATCHMENT, ZIMBABWE

Abstract

Wetlands are diverse and fragile ecosystems which are susceptible to anthropogenic and natural perturbations. Globally, wetlands provide several ecosystem goods and services, yet they are increasingly faced with numerous threats from human activities leading to their modification and loss. This chapter aims to assess changes in wetland spatial distribution and areal extent in the Shashe sub-catchment, Zimbabwe, over time. This was achieved through using archival Landsat imagery and Random Forest Image Classification Algorithm using R software. This chapter compares advanced machine learning random forest classifier with traditional supervised Maximum Likelihood algorithm. The results for land change analysis show a decline in woodland and wetland cover, which may be due to both human and natural factors. Major conversions are from wetland cover to crop fields, suggesting agricultural encroachment onto wetland areas. Wetland area thus significantly decreased by 6% (236.52 ha) in the last 30 years ($p<0.05$). CA-Markov model results for the years 2025, 2035 and 2045 predicted an overall increase in crop fields at the expense of woodland and wetland areas. In particular, the total area of wetlands is expected to shrink by 46% by the year 2045 (72.67 hectares). Quantifying such wetland changes over time is important, not only for pure-scientific purposes, but also for appropriately developing locally relevant and sustainable management strategies.

Key words: Wetland area, change detection, future prediction, random forest, land change analysis

[3]This chapter is based on: Sibanda S, Grab S.W and Ahmed F. (*In Preparation*). Quantifying spatio-temporal changes of nested wetlands in the Shashe sub-catchment, Zimbabwe.

5.1 Introduction

Wetlands are diverse and fragile ecosystems susceptible to anthropogenic and natural perturbations (Mitsch and Gosselink, 2000). Globally, wetlands account for about 6.2% of the Earth's land (Ellery *et al*., 2010) and contain 12 % of the global carbon pool (Ferrati and Canziani, 2005). They are also recognised as important ecosystems supporting endemic and rare species of flora and fauna. Africa is endowed with wetlands of great importance which are amongst the most diverse in the world (Kabii, 1996), hosting some 2000 fish species, aquatic mammals such as dolphins, insects, reptiles and amphibians (Kabii, 1996). Wetlands provide essential ecosystem functions that range from flood attenuation, stream flow regulation, sediment trapping, phosphates and nitrogen removal, toxicant cleansing as well as carbon storage (Mitsch and Gossalink 2000; Ellery *et al*., 2010). Economically, wetlands offer food in the form of fish, water, natural gas, lumber and forest resources, tourism and raw materials for art and craft (Chaikumbung *et al*., 2016).

Despite these vital services and products, wetlands are faced with numerous threats from human activities, resulting in their shrinking, modification and overall degradation (Schuijt, 2002; Jogo and Hassan, 2010). Empirical evidence suggests a 60% loss in the global wetland area in the last 100 years (Burkett and Kusler, 2000; Junk *et al*., 2013). In Africa, 50% of wetland areas have been degraded owing to human interference, particularly in countries such as South Africa, Mozambique, Zimbabwe, Malawi and Guinea (Wetland International, 2009). Consequently, wetland loss has increasingly become a major threat to biological diversity emanating from human–environment interactions such as agriculture, urbanisation, damming, road construction, and human settlement, among other activities (Ellery *et al*., 2016). The situation is further compounded by accelerating changing climatic conditions which are likely to alter catchment hydrology, leading to the modification of wetland ecosystems (Finlayson,

2016). There is a growing consensus that climate change is an additional stressor, likely to modify wetland ecosystems, which not only includes the reduction of wetland area, but also changes in structure, vegetation cover, inundation patterns, habitat fragmentation, and reduced water levels (Erwin, 2009; Lee *et al*., 2015a).

In part as a consequence to wetland losses, African greenhouse gas emissions are said to be increasing due to reduced carbon sinks on the continent. Emissions from African wetlands are reported d to have increased by 20% since 1990, amounting to 47-57 million tonnes of carbon dioxide per year (Wetland international, 2009). In Sub-Saharan Africa (excluding South Africa), greenhouse gas emissions resulting from the loss of organic wetland soils are equal to 25% of the fossil fuel emissions in the region (Wetland International, 2009). Under these circumstances, sustainable protection and management will require effective monitoring of wetland changes over time to ensure continued ecosystem provision. Remote sensing technology offers ideal repetitive and spatially explicit data, which is cost effective in mapping and monitoring inaccessible wetland ecosystems (Adam *et al*., 2009; Ozesmi and Bauer, 2014).

Based on its versatility, a number of global studies have employed the efficacy of remote sensing in wetland mapping, monitoring and change detection (Davranche *et al*., 2010a; Szantoi *et al*., 2013; Chen *et al*., 2014; Singh *et al*., 2014; Vanderlinder *et al*., 2014; Dronova *et al*., 2015; Han *et al*., 2015; Lee *et al*., 2015; Feng *et al*., 2016b; Li *et al*., 2016; Liu *et al*., 2016; Haque and Basak, 2017). Small wetlands in Kenya and Tanzania were also mapped using remote sensing by (Mwita *et al*., 2013). Remote sensing based wetland inventory mapping and change analysis were applied by Rebelo *et al.*, (2009). Employing 250 m resolution MODIS time series data, Landmann *et al.* (2010) achieved high accuracy mapping

of wetlands in West Africa. Some studies have used remote sensing techniques to detect and evaluate changes in wetland features over time (Haack, 1996; Kashaigili *et al.*, 2006; Munyati, 2000; Tolessa *et al.*, 2017).

In the context of Zimbabwe, wetland ecosystems are a critical source of water for both domestic and wild animals, particularly during the dry season (Chikodzi and Mutowo, 2014). Communities harvest raw materials such as reeds, grass and wood for crafting and carving (Ndhlovu, 2009). Some of the wetlands are also culturally preserved as sacred places of worship.

Previous wetland studies in Zimbabwe include a study by Marambanyika *et al.* (2016) who assessed wetland utilisation patterns in semi-arid communal areas of Zimbabwe and noted an increase in the cultivation and general dependency on wetland ecosystems. While public perceptions regarding vulnerability of wetlands to climate change were studied by (Ndiweni and Gwate, 2014). The role of wetlands in flood mitigation was confirmed by (Murwira *et al.*, 2004) and they noted a significant role played by wetlands in regulating river flow within the Zambezi catchment.

Relatively few studies have attempted to apply remote sensing technology to wetland management in Zimbabwe. Landsat and SPOT imagery was used by (Mhlanga *et al*., 2014a) to map the spatial extent of Harare wetlands and observed a shrinking pattern over years due to urbanisation. In an earlier study, (Msipa, 2009) analysed the impact of land use/ cover changes on urban wetland in Harare and reported an increase in settlement and agriculture activities which contributed to urban wetland size shrinkage. A similar study was carried out by Ndhlovu (2009) at Intunjambila wetland and recorded a decline in wetland health owing to

human interference. Although wetlands have previously been mapped using remote sensing in Zimbabwe, such work has not yet attempted to establish wetland changes over time and future LU/LC prediction, using such technology – a research gap the study aims to address. The chapter compares the performance of advanced machine learning random forest classifier with that of the traditional maximum likelihood for mapping LU/LC change in a wetland ecosystem. Therefore, the aim of the chapter was to use historic and current Landsat data to establish changes in wetland area over time and to correlate changes in wetland size to population and climate trends in Shashe sub-catchment. Wetland change detection was done only for Shashe sub-catchment instead of the whole Mzingwane catchment mainly because wetlands are mostly located along the mountainous region of Shashe sub-catchment. It is also within the scope of the study to predict future LU/LC based on past changes. Such analysis may provide valuable information for future wetland utilisation and management.

5.2 Methodology

5.2.1 Study area

The Shashe sub-catchment is one of four sub-catchments of the Mzingwane catchment and extends from 27^{o} to 29^{o}E and 20^{o} to 22^{o}S. It has a surface area of 18991km^{2}. The mean annual rainfall ranges between 450mm and 600mm per annum and the rain season begins in October and ends in April (Mugandani *et al*., 2012). Soils in the Shashe sub-catchment are generally shallow sandy loam soils which are derived from gneiss and kaolinitic sands and granitic rocks, as well as some isolated moderate clay patches formed from greenstone belts (Ashton *et al*., 2001).The southern part consists of Limpopo belt gneisses while the far south is composed of Karoo basalts. Land uses to the north of the sub-catchment are mainly commercial, private and resettled farmlands focusing on irrigated crop production and commercial livestock rearing, while the southern part consists of communal settlements and

agriculture limited to small livestock production. The Shashe sub-catchment is rich in both wild flora and fauna, specifically in the more protected Matopos National park which covers an area of about 44 500 hectares.

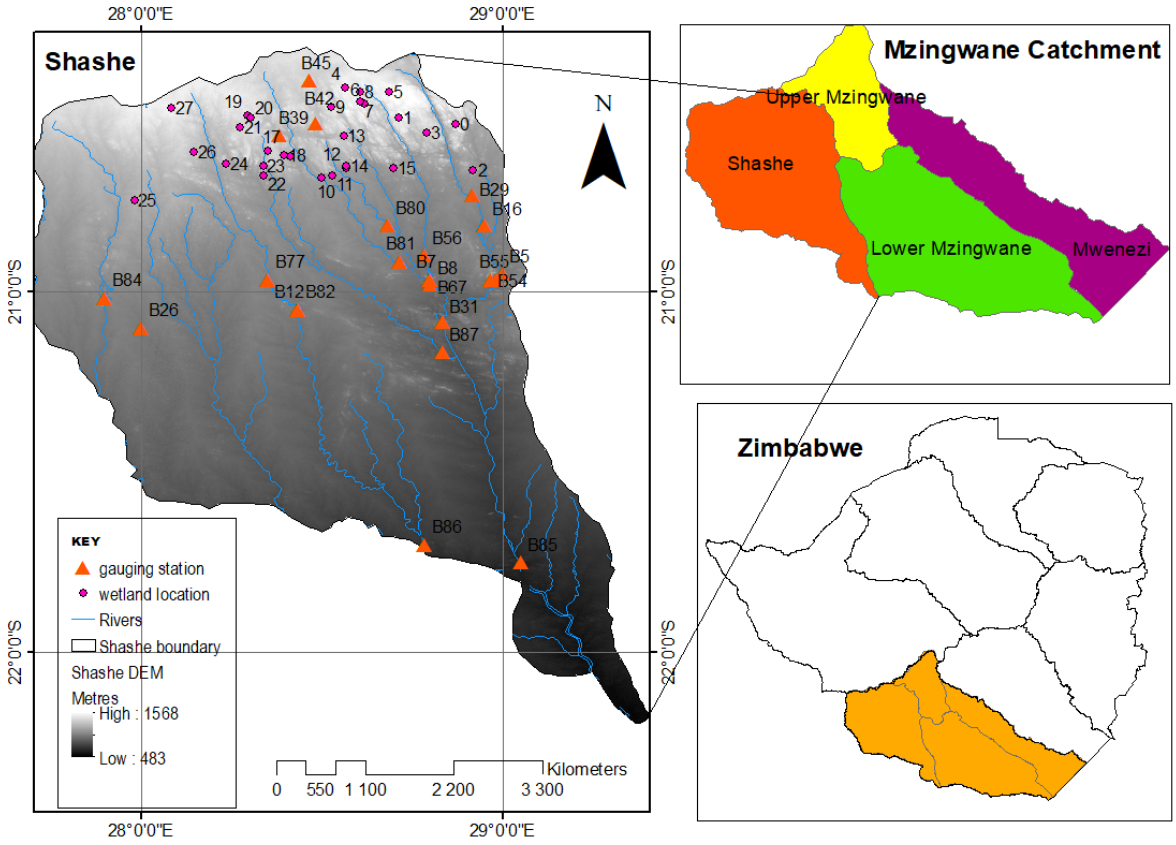

Figure 5.1: Shashe sub-catchment with gauging stations and wetland location

5.2.2 Remote sensed data

Three scenes (170/75; 171/74 and 171/75) for June Landsat TM and OLI imagery were obtained from the USGS website (Table 5.1) and were partially pre-processed, as such there was no need for image registration. 30m Digital Elevation Model (DEM) data from Shuttle Radar Topography Mission (SRTM) were sourced to aid classification, particularly because wetlands are usually located in low lying areas; therefore, a slope gradient image was created

from the DEM data. Ancillary data consist of soil maps, hydrologic maps, topographic maps and land use maps. All data were projected to the UTM zone 35S Datum WGS84, in meters.

Table 5.1: Attributes of remote sensing imagery used in this study

Year	Date	Sensor type	Spatial resolution (M)
1984	29/06/1984	MSS	60
1995	21/06/1995	TM	30
2005	07/06/2005	TM	30
2015	19/06/2015	OLI	30

5.2.3 Image pre-processing

Landsat time series data for 1984, 1995, 2005 and 2015 were radiometrically corrected in ENVI 5.3 software (E*xelis* Visual Information Solutions, 2016). All images were calibrated using the Dark pixel subtraction algorithm (Hadjimitsis *et al*. 2010) for atmospheric correction. This was followed by the conversion of Digital Numbers (DN) to at-satellite reflectance using a radiometric calibration module in ENVI 5.3. Atmospheric correction employed the Fast-Line-of-sight Atmospheric Analysis of Spectral Hyper-cubes (FLAASH) model as was applied by Feng *et al*. (2016b). Because the Shashe sub-catchment is located in a mountainous region, the topographic correction was inevitable as all images were co-registered to each other using an error of less than 1 pixel. Mosaicking of the three scenes was then done after pre-processing using seamless Mosaic module in ENVI. To correct sensor differences, Landsat MSS and TM were resampled to Landsat 8 (OLI) 30m resolution using the nearest neighbour resampling methods, as was applied by Han *et al*., (2015).

A total of 617polygon training sites were randomly collected from the field (300) and from google earth (317) using a stratified random sampling methodology which aided the separation of wetland cover types and non-wetland surfaces. Land cover class types were assigned in the field with other detailed class characteristics and aerial photographs were used aid the classification.

5.2.4 Image classification

Landsat images were analysed using supervised Random Forest (RF) algorithm embedded within the **RStoolbox** package in R program. Random Forest is a non-parametric machine learning algorithm which uses an ensemble of decision trees, randomly sampled subsets of the training data. Studies have shown that combinations of randomised multiple trees tend to improve classification accuracy (Jhonnerie *et al.*, 2015). Random classification is based on *ntree and mtry* parameters which require optimisation for the best and accurate classification results. In this regard, prior to the classification process, the grid-search approach in caret, gbm and **randomForest** packages were used to tune random forest parameters in R software based on stochastic gradient boosting. There are two commonly used ensemble methods for random forest classifier, the boosting and bagging (Breiman, 1996). This study applied the superclass function embedded in the RStoolbox which ensured non-overlap between training and validation data, for the purposes of avoiding bias performance estimates. The training data were split through the trainPartition function which divides training data into training polygons and validation polygons which are extracted from the image using the PredValue function. Random forest classifiers have been scientifically proven to outperform single algorithms and are robust against overfitting and can handle high dimensional data with great accuracy (Breiman, 2001). Tree based learning algorithms also provide predictive models with high accuracy (Nan Liu and Wang, 2010).

Maximum likelihood classifier is a parametric classification algorithm, which is widely used for LU/LC classification. It is based on a principle that the cells in each class sample of multidimensional space are normally distributed and also based on the Baye's theorem for decision making (Foody *et al*., 1992). Maximum likelihood decision rule is based on probability, the probability of a pixel belonging to a defined class is calculated and the pixel is assigned the class with the highest probability.

Post classification is an essential process for refining the classified image and reduces errors that may arise from similarities in spectral responses of certain classes. In this regard, majority filter analysis was employed for further refinement of the classification and used 90 by 90 pixel size as the minimum mapping unit which is equivalent to a hectare.

5.2.5 Wetland change analysis

Changes in wetland over time were analysed through Change Vector Analysis (CVA). To achieve this, classified land cover maps were masked in R to show wetland cover only, and subsequently vectorised for change analysis. Vector maps were then used to compute changes in areal extent over time.

5.2.6 Classification accuracy assessment

Accuracy assessment employed both qualitative and quantitative approaches. A confusion matrix proposed by Congalton, (1991) was used as a quantitative approach. A total of 150 ground truthing training sites were obtained from the field in 2015 using a hand held Geographic Positioning System (GPS) for the validation of the 2015 imagery. For historic images for the years 1984, 1995 and 2005, accuracy assessment used historic land use maps for the corresponding years and was further aided by aerial photographs for 1975 and 1995,

as well as prior knowledge of the area. The confusion matrix was used to calculate Kappa coefficient.

5.2.7 Future prediction of LU/LC changes using CA-Markov chain model

Having classified LULC for the years 1984, 1995, 2005 and 2015, post classification land cover transitions and future predictions were analysed using coupled Cellular Automata-Markov model within TerrSet/IDRISI Geospatial Monitoring and Modelling software, version 18.3 (Clark Labs, 2017). The Markov model considers the past land use/covers to predict how each LU/LC will change in future. It produces transition probability matrix, which shows the probability of each LU/LC to change to any other cover type given and is obtained by cross tabulation of the earlier and later LU/LC maps. A transition area map is also produced, and it contains the number of pixels that are likely to change to another class during the prediction period. Markov chain is acknowledged for its ability to quantify the states of conversion over time; however, it is unable to show the spatial distribution of the changes. Thus, CA provided the spatial distribution and spatial transitions for the projected LULCs (Subedi *et al.*, 2013). The change analysis module in Land Use Change Modeler module in IDRISI, allowed for the production of gains, losses, net change and transitions, both in graphs and maps for the earlier and latter maps, while the change abstraction tools were used to uncover complex trends in the transitions. This was followed by modelling the potential to change using past changes to develop a mathematical model and a GIS data layer of transition potential (Sang *et al.*, 2011). Each transition was modelled through the Multi-layer Perceptron neural network which produced a potential map for each transition. The CA-Markov model was then used to model LULC changes based on 1984 and 2015. This coupled model provided a robust combination of spatio-temporal dynamic modelling and prediction which usually results in good simulations of LULC (Yang *et al.*, 2014). The generated

transition maps were then used to predict LULC for 2025, 2035 and 2050 based on the main transitions between 1984 and 2015 LULC. The 2015 LULC map was used as a base map for validation and the Kappa statistic was applied in the evaluation of the accuracy of the forecasted 2015 LULC map in comparison to the actual 2015 LULC map. A comparison of the random forest classified 2015 and projected 2015 LU/LC map were used to validate the model (Figure 5.13) employing the VALIDATE function in IDRISI Andes software. Kappa statistics (k) for similarity analysis was used to evaluate the agreement between the classified 2015 LULC map and the simulated 2015 map.

5.2.8 Factors influencing wetland area change

Multi linear regression model in R software version 3.3.3 was used to establish a relationship between wetland area and explanatory variables such as rainfall, temperature trends obtained from chapter 3 and 4 were used while population data for the periods 1984, 1995, 2005 and 2015 were sourced from Zimbabwe Statistics Office.

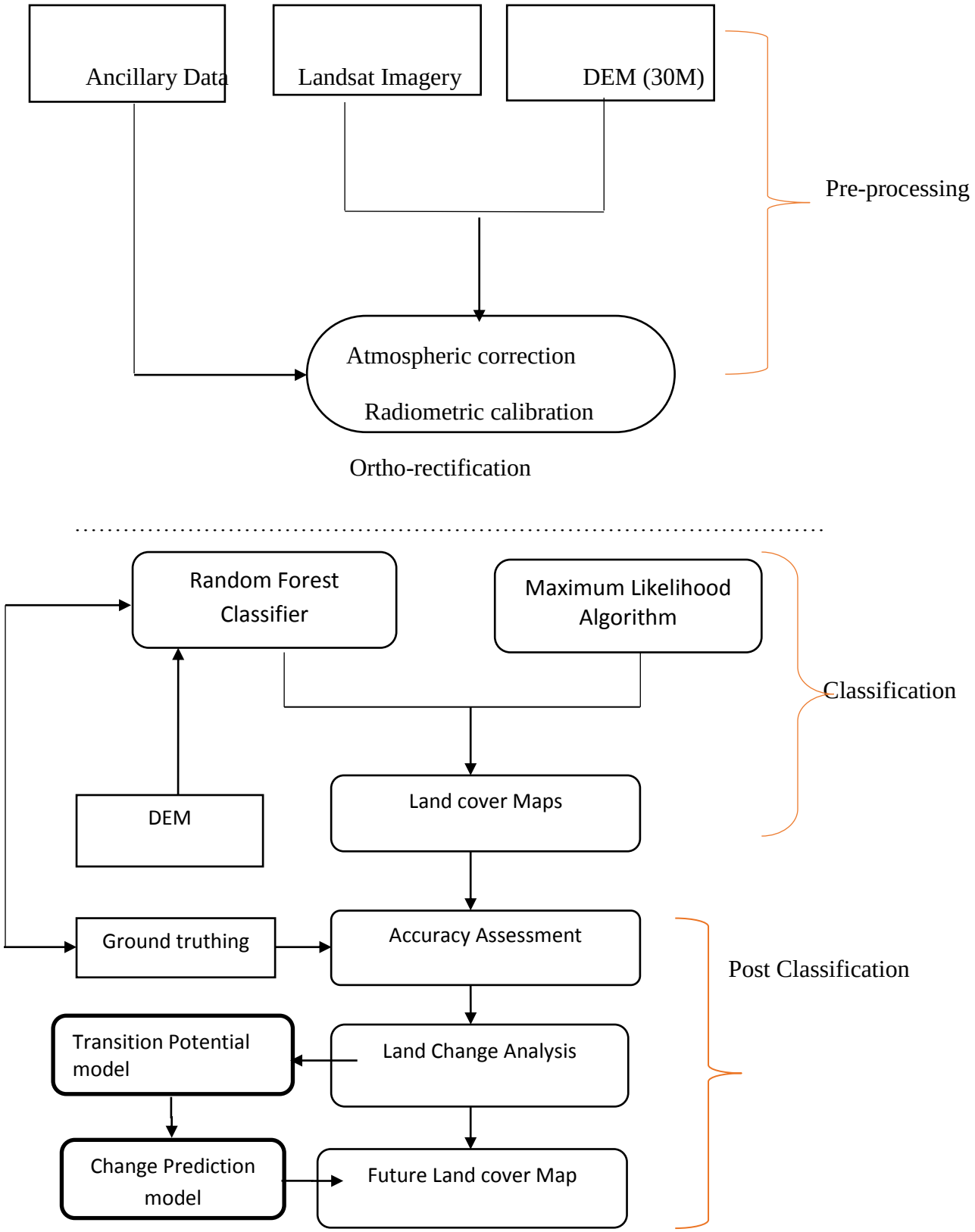

Figure 5.2: Workflow of the image analysis process starting with pre-processing, classification, post classification and future land cover prediction

5.3 Results and Discussion

5.3.1 Parameter optimisation

Ntree and tree depth were tested from 50-1500 at combinations of depth (1, 5 and 9) and (1, 2 3) using the boosting approach. RF tuning at tree depth 1, 3 and 9 produced an overall accuracy of 84.6% (Figure 5.3a. As the number of trees increased, the rate of accuracy decreased. At depth 1 the maximum accuracy was around 80.5% from 50 trees. When the number of trees increased to 1500 at the same depth, accuracy dropped to 77.2% and this pattern was noted for all depths (Figure 5.3a). Meanwhile, a combination of 1, 2, 3 depths using the boosting approach produced much higher results with an average accuracy of 95% and a Kappa coefficient of 0.94 (Figure 5.3b). The highest accuracy of 95% and Kappa (0.94) was obtained from 150 trees at a depth value of 1 (Table 5.2), while the lowest accuracy of 77% was produced from 1500 trees. The best parameters *(mtry*=1 and *ntree*=150) were used for supervised image classification using RF algorithm in "RStoolbox package" embedded in R software.

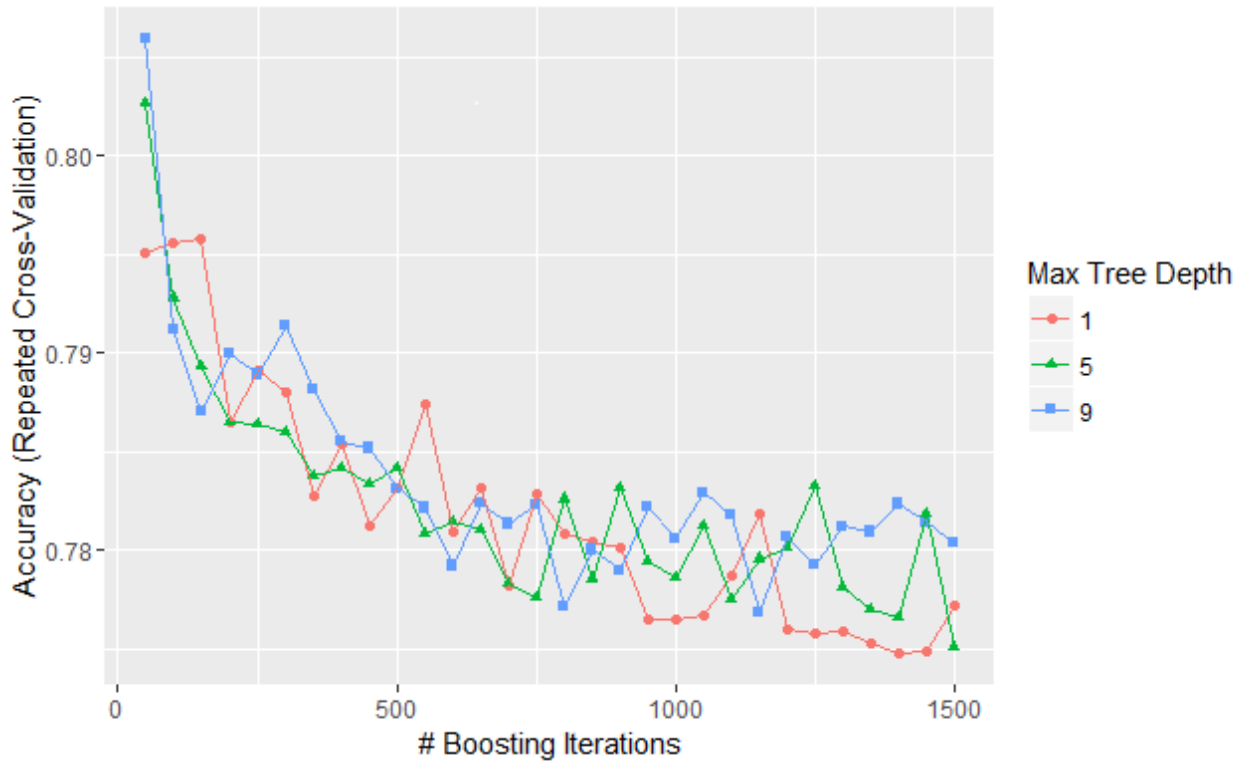

Figure 5.3a: RF parameter optimisation using boosting approach

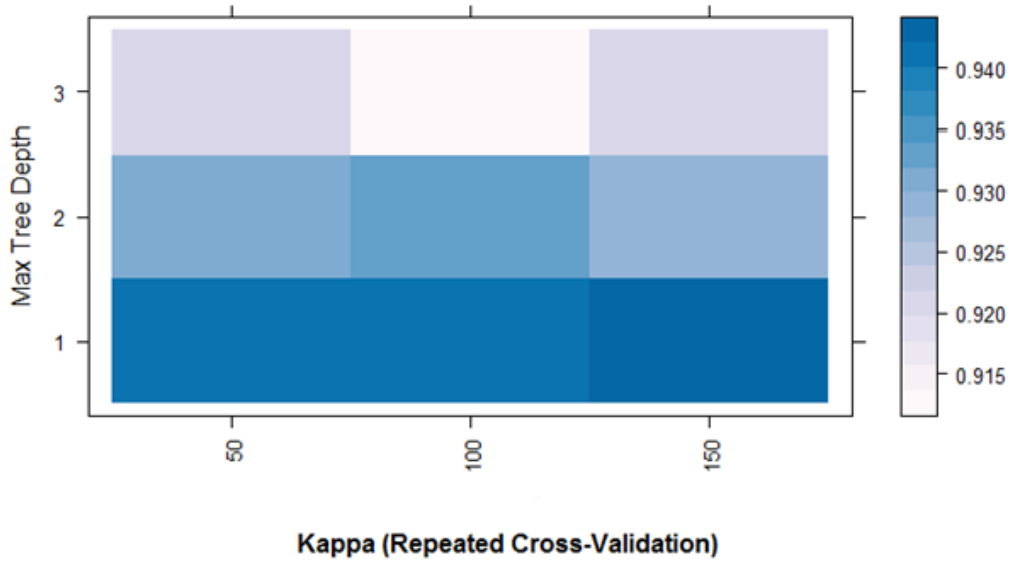

Figure 5.3b: Classification accuracy assessment using the Kappa coefficient at low depth of 1, 2 and 3.

Table 5.2: Classification accuracy optimisation at depths 1, 2 and 3

Interaction depth	n.trees	Accuracy	Kappa
1	50	0.93	0.91
1	100	0.95	0.92
1	150	0.95	0.94
2	50	0.93	0.92
2	100	0.94	0.93
2	150	**0.95**	**0.94**
3	50	0.93	0.92
3	100	0.92	0.91
3	150	0.93	0.91

These results confirm the importance of parameter optimisation and the general influence of *ntree* and *mtry* changes on the overall accuracy. They are in agreement with previous studies (Adam *et al.*, 2014a; Grimm *et al.*, 2008) which reported that the default *mtry* produce the best results.

5.3.2 Classification accuracy

Accuracy assessment for random forest classifier for the years 1984, 1995, 2005 and 2015 were relatively higher than those for maximum likelihood (Table 5.3). The average accuracy for RF is 85.7% and 78.7% for maximum likelihood algorithm. Random forest outperformed maximum likelihood classification by 7.05% accuracy. Minor grassland cover was misclassified as crop field because most of the crop field had been left fallow for more than five years owing to recurrent droughts, hence successive grass species have emerged within crop fields. Visual analysis of the land cover maps was done to evaluate whether the classification was consistent with prior knowledge of the area and the results from random forest classifier were satisfactory.

Table 5.3: Accuracy and Kappa coefficient computed from Random Forest (RF) and Maximum Likelihood (ML)

Year	**RF**		**ML**	
	Overall Accuracy (%)	**Kappa**	**Overall Accuracy (%)**	**Kappa**
1984	84.3	0.81	78	0.76
1995	84.2	0.82	79.2	0.77
2005	90.0	0.89	79.7	0.77
2015	85.3	0.83	78	0.76

5.3.3 Classification results

Figure 5.4 shows land use/cover classification maps. The Shashe sub-catchment was classified into eight major land classes: water, rock outcrop, mountain vegetation, wetland, bare crop field, riverine vegetation, woodland and grassland. Figure 5.5 displays land change modeler results in terms of losses and gains. The net change results (Figure 5.6) show that grassland, woodland, mountain vegetation and wetland covers were reduced in size during 1984-2015, losing by -4%, -5.2%,-2% and -6% change respectively. Meanwhile, riverine vegetation, crop field and rock outcrop gained by about 0.5%, 4% and 10.2% respectively. Transition results indicate a considerable change from woodland to crop fields for agricultural production. Similar findings were echoed by (Mwita *et al*., 2013) who also observed a significant increase in cropping area due to population demand for land and food.

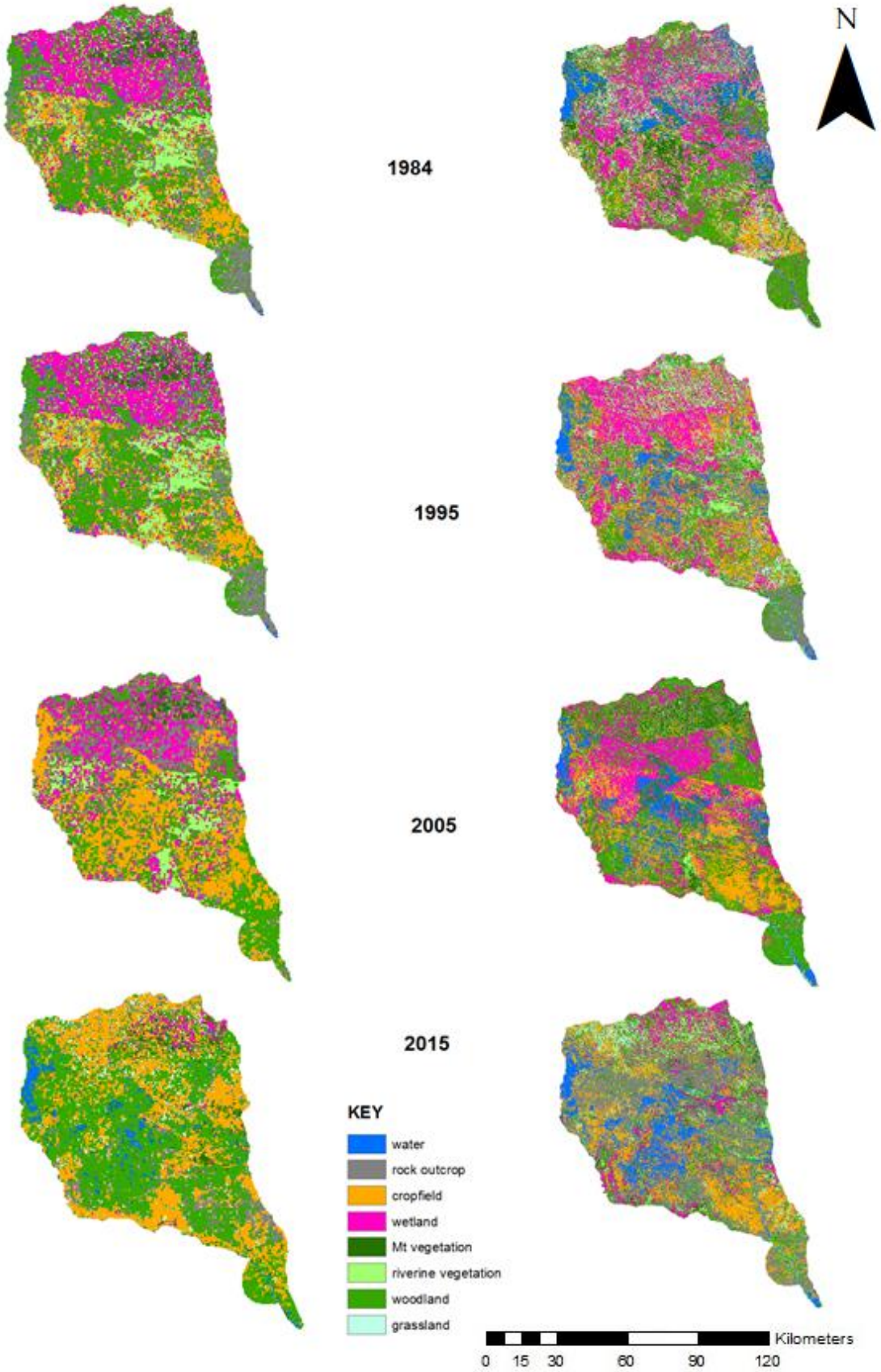

Random forest algorithm **Maximum Likelihood**

Figure 5.4: Comparison of LU/LC maps produced using random forest and Maximum likelihood classification algorithms

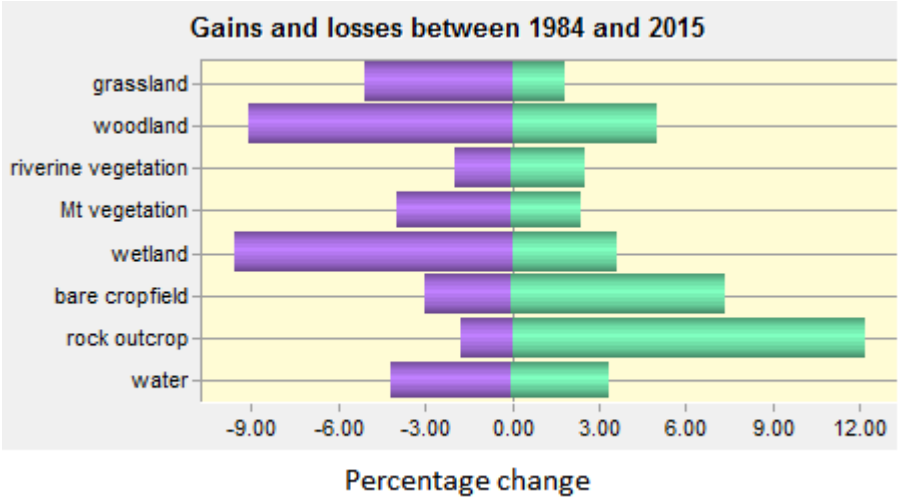

Figure 5.5: LU/LC percentage gains and losses by individual land cover classchanges

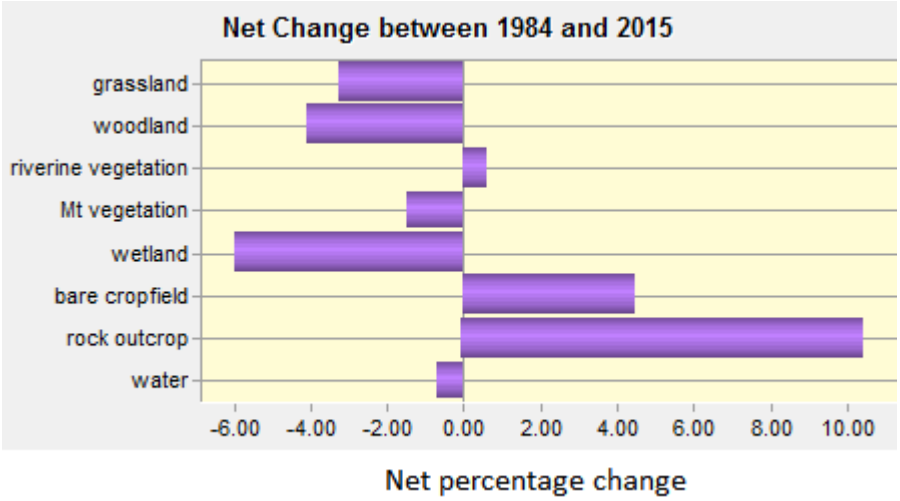

Figure 5.6: Net percentage change among land cover classes for the period between 1984 and 2015. Positive change means a percentage gain while negative means a percentage loss

5.3.4 Wetland area change between 1984 and 2015

Figure 5.8 displays spatial distribution of wetland cover over time. The results show a decline in wetland areal extent between 1984 and 2015 by 237.12 hectares. The wetland areal extent for the years 1984, 1995, 2005 and 2015 is 393.12, 397.80, 272.25 and 156 hectares respectively. The period between 1984 and 1995 saw an increase of 4.68 hectares (ha) in wetland area (Table 5.4). A dramatic wetland area decline was noted between 1995 and 2005, losing about 125.55 ha. This could be attributed to documented El Niño Southern Oscillation droughts of 1995, 1998, 2002 and 2005 (Sithole and Murewi, 2009). The results show a further decline in wetland area between 2005 and 2015 (by 115.65 ha), probably because of the intense El Niño droughts experienced in the catchment for five consecutive years (Sango and Godwell, 2015). From the wetland vector maps (Figure 5.8), there is a statistically significant decline in wetland area over the past 31 years at $p<0.05$ (Figure 5.10). Land change analysis reveals that changes in the crop field and rock out crop and soil exposure contributed more to changes in wetland area owing to the influence of human activities and climate variations (Figure 5.9).

Table 5.4: Wetland area coverage between 1984 and 2015

Year	Wetland area(ha)	Change in area (ha)
1984	393.12	
1995	397.8	4.68
2005	272.25	-125.55
2015	156.6	-236.52
2025	133.11	-23.49
2035	129.12	-3.99
2045	83.93	-45.19

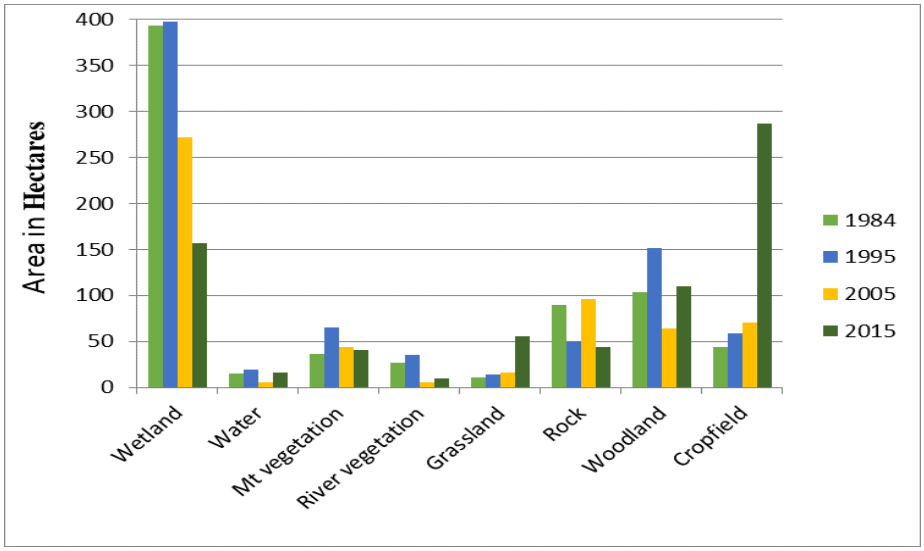

Figure 5.7: Changes in areal coverage of the different land covers

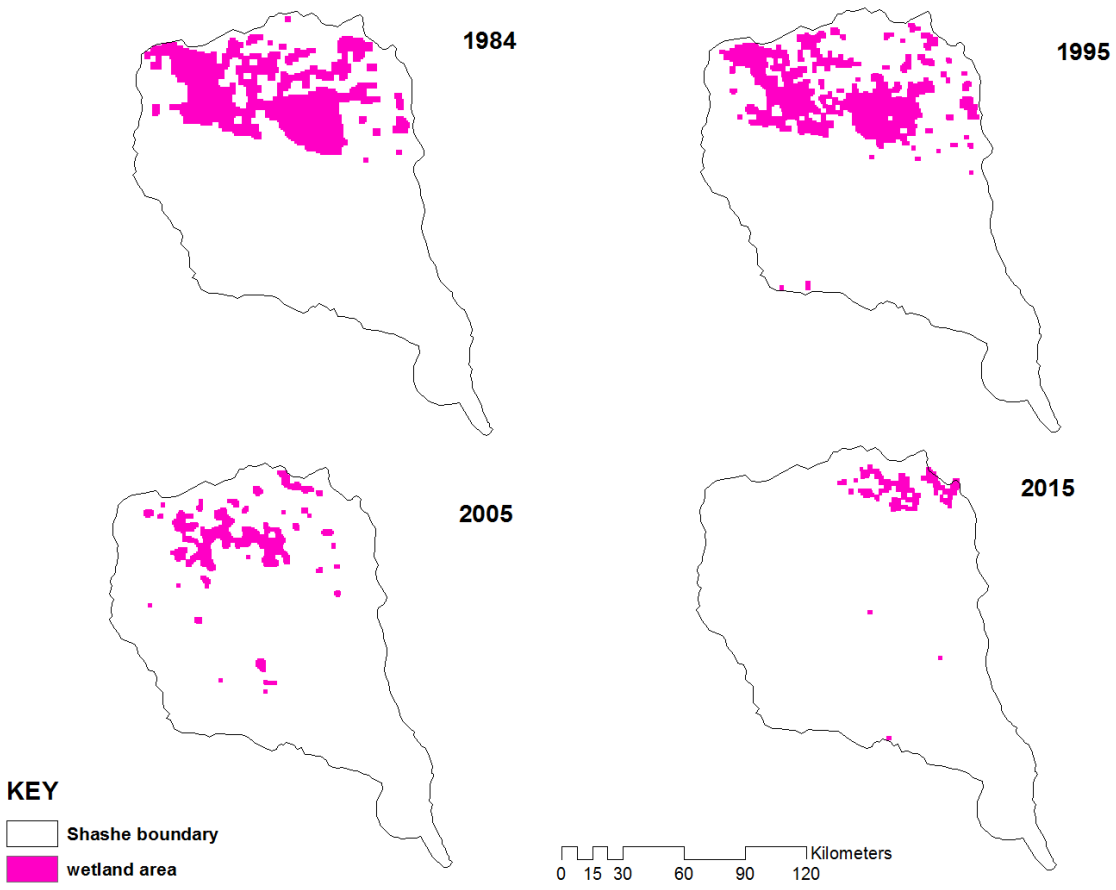

Figure 5.8: Spatial distribution of wetlands for the years 1984, 1995, 2005, and 2015

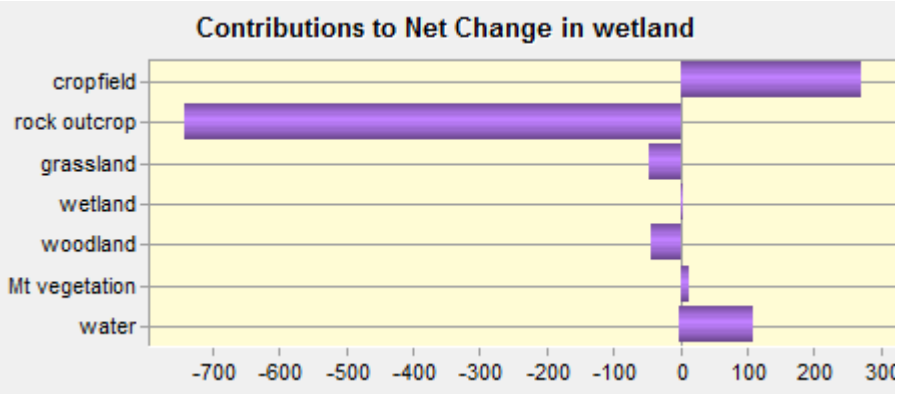

Figure 5.9: Contributions to wetland changes by other LU/LCs for the period between 1984 and 2015

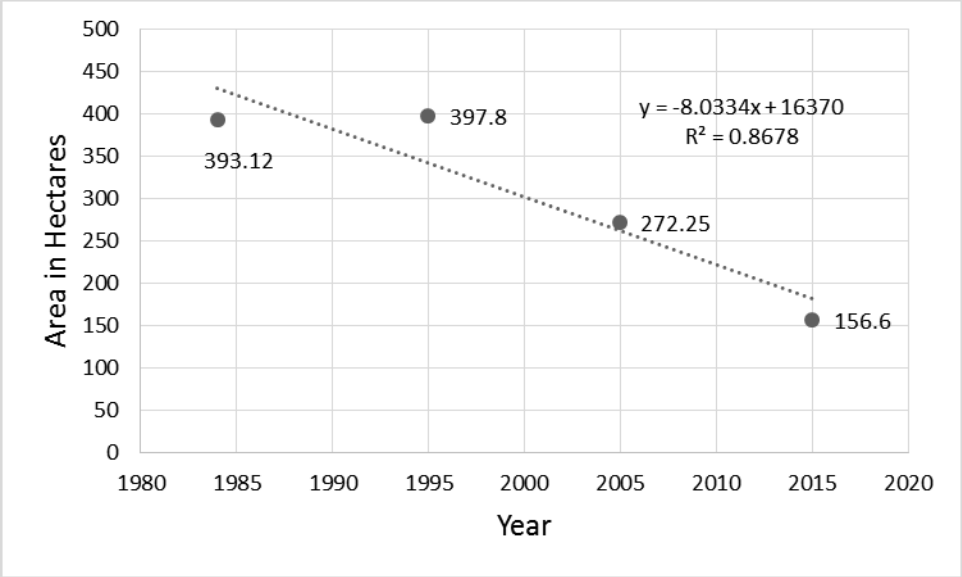

Figure 5.10: Wetland area coverage in hectares for the years 1984, 1995, 2005, and 2015

5.3.5 Modelling land use/ land cover changes

The transition matrix (Table 5.5) and change transition map (Figure 5.11) were generated and used as inputs for future modelling of the LULC changes for the years 2025, 2035 and 2045. The Markov chain modelling was aided by influential variables such as rainfall for 1984 and 2015, Digital Elevation Model (DEM), elevation and population growth. Trends in the chosen variables are used by the model to predict future changes. From the transition

probability maps, major changes involved the transformation of woodland and wetland to cropfield, which suggest agricultural disturbance and were considered for the prediction of future changes (Figure 5.11).

5.3.6 Future land use/ cover change prediction results

Figure 5.12 shows the predicted land use/ land cover changes for the next 30 years. From the three predictions, it is apparent that recent past and present trends in LU/LC changes are likely to continue into the future (2045). The 2025 model predictions show that wetland and woodland land types will decrease by 15% and 11% respectively. Conversely, an increase is observed for crop fields (7%) and mountain vegetation (6%). However, water, riverine vegetation, and grassland land types remained unchanged (Table 5.6). LULC predictions for 2035 projected an increase in the cropfield land type (36%) and grassland (2%) while a decrease is expected for mountain vegetation (-12%), wetland (-3%) and woodland (-47%). Water, rock outcrop and riverine areal coverage will remain unchanged. The 2045 predictions suggest that water, rock outcrop and riverine vegetation continue unchanged while woodland is projected to gain 23% of the land area and mountain vegetation to increase by 15%. Unlike the 2035 prediction period, cropfield coverage is expected to experience -17% decrease in the land area, wetland land type will continue to decrease (-35%). Overall, the LU/LC prediction results suggest that crop fields will continue to expand in future while woodland and wetland areas shrink.

Table 5.5: Transition probability matrix for 2025 to 2045

	water	cropfield	Mt vegetation	wetland	riverine vegetation	rock outcrop	woodland	grassland
water	**0.48**	0.25	0.24	0.02	0.02	0.00	0.00	0.00
cropfield	0.03	0.43	0.09	0.05	0.01	0.11	0.23	0.04
Mt vegetation	0.08	0.19	0.51	0.04	0.02	0.00	0.11	0.04
wetland	0.00	0.28	0.05	0.19	0.14	0.11	0.17	0.06
riverine	0.55	0.29	0.05	0.02	0.07	0.02	0.00	0.00
rock	0.07	0.26	0.00	0.05	0.19	0.33	0.09	0.00
woodland	0.00	0.17	0.20	0.16	0.02	0.06	0.30	0.08
grassland	0.08	0.34	0.28	0.08	0.04	0.00	0.11	0.08

Table 5.6: Predicted LU/LC change for the years 2025, 2035, and 2045

	Percentage Change		
LULC type	**2025**	**2035**	**2045**
water	0	0	0
cropfield	7	36	-17
Mt vegetation	6	-12	15
wetland	-15	-3	35
riverine vegetation	0	0	0
rock outcrop	0	0	0
woodland	-11	-47	23
grassland	0	3	12

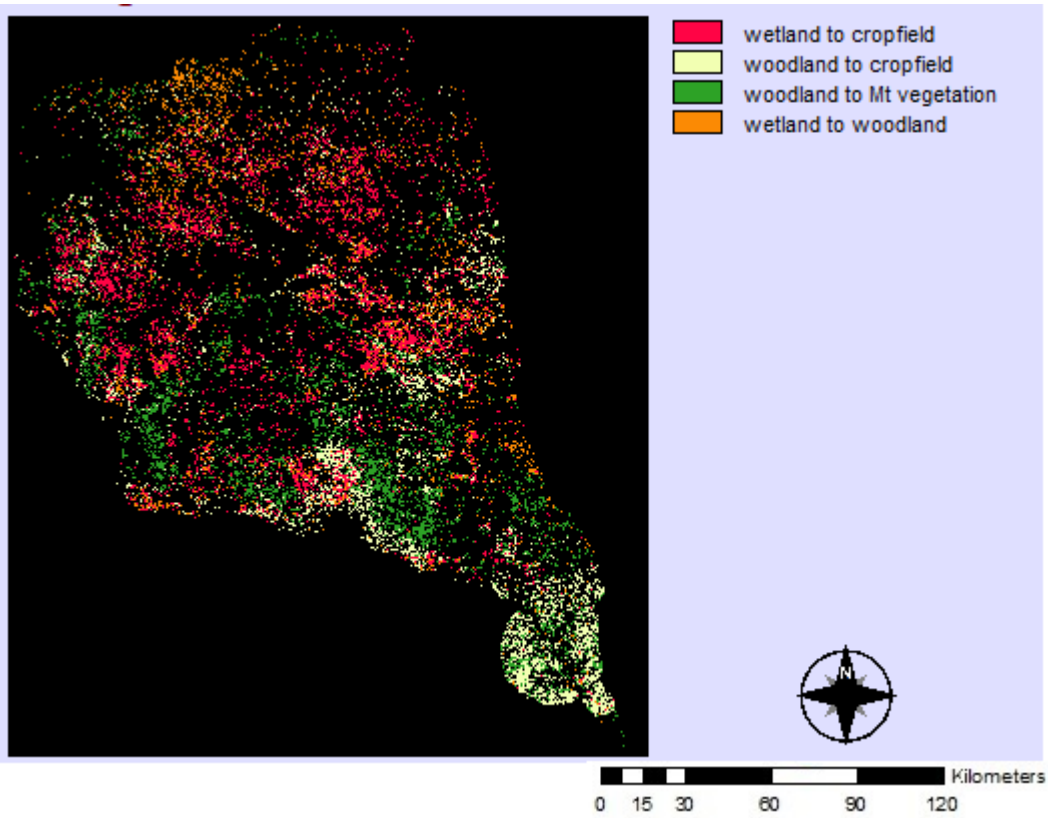

Figure 5.11: Potential changes in land cover between 1984 and 2015

5.3.7 Validation of the model results

A comparison of the random forest classified 2015 and projected 2015 LU/LC map were used to validate the model (Figure 5.13) employing the VALIDATE function in IDRISI Andes software. Kappa statistics (k) for similarity analysis was used to evaluate the agreement between the classified 2015 LULC map and the simulated 2015 map. Following k statistics were obtained; $k_{standard}$ =84.12%, k_{no}=87.72% and $k_{locality}$=85.30. k_{no} is used to evaluate the overall accuracy of the model while $k_{locality}$ indicates the model's ability to identify correct locations. The $k_{standard}$ statistic combines location error and quantification error (Hagen, 2002). These results indicate that the coupled CA-Markov model was able to simulate well future LULC changes within the sub-catchment.

5.3.8 Future wetland area change

CA-Markov model predictions suggest a decrease in wetland area of 23.49 hectares (ha) by 2025, resulting in a total area of 133.11ha, down from 156.6 in 2015 (Figure . In 2035, wetland area is expected to continue decreasing, this time with a very low percentage of 3%, amounting to a total area of 129.2 ha by 2035. The 2045 simulation results demonstrate a further shrink in wetland area by a substantial percentage (35%), leaving the total wetland area at 83.92 ha. Statistical analysis of wetland loss shows that by 2045, the sub-catchment will have lost a total of 309.2 ha, which is equivalent to 79%. Such substantial wetland area loss has adverse implications on socio-economic and natural environments (e.g. wetlands).

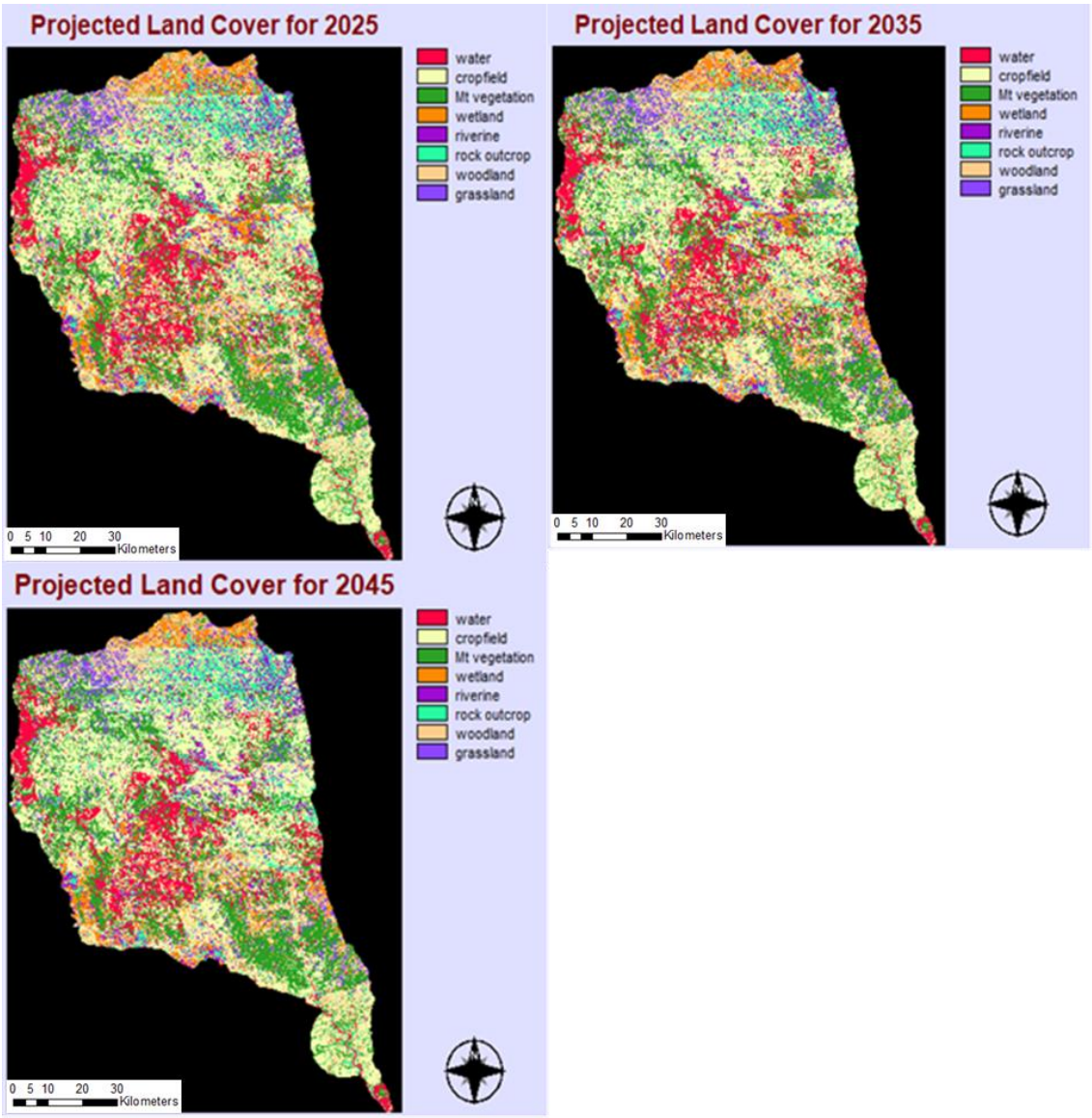

Figure 5.12: Predicted LU/LC for the period 2025, 2035 and 2045

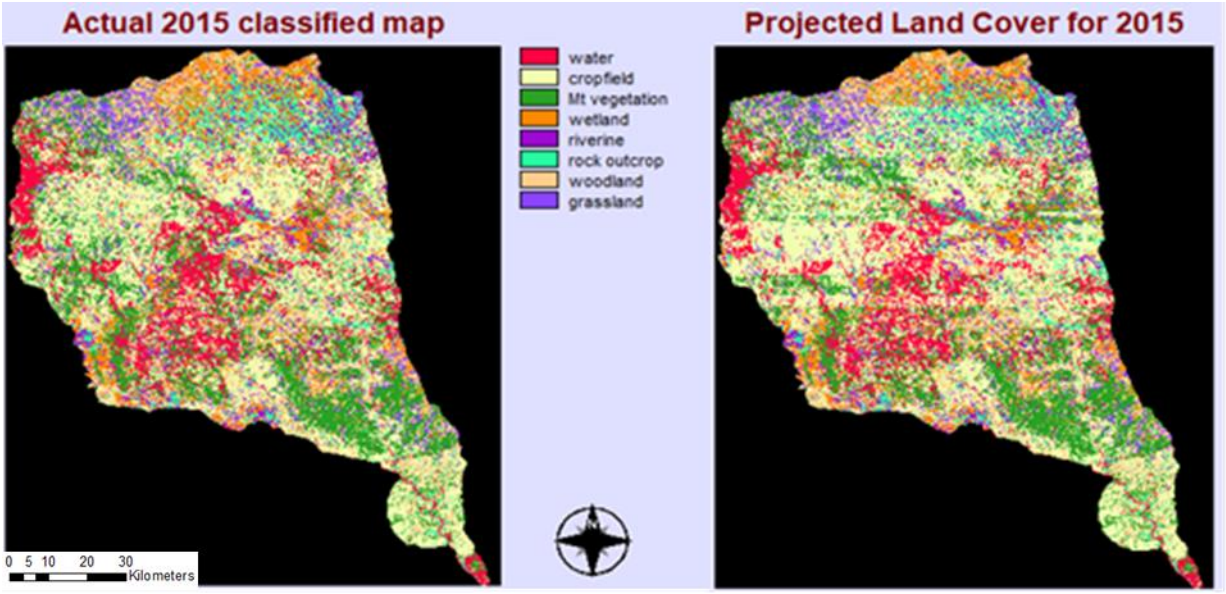

Figure 5.13: A comparison of the classified and projected 2015 LU/LC maps

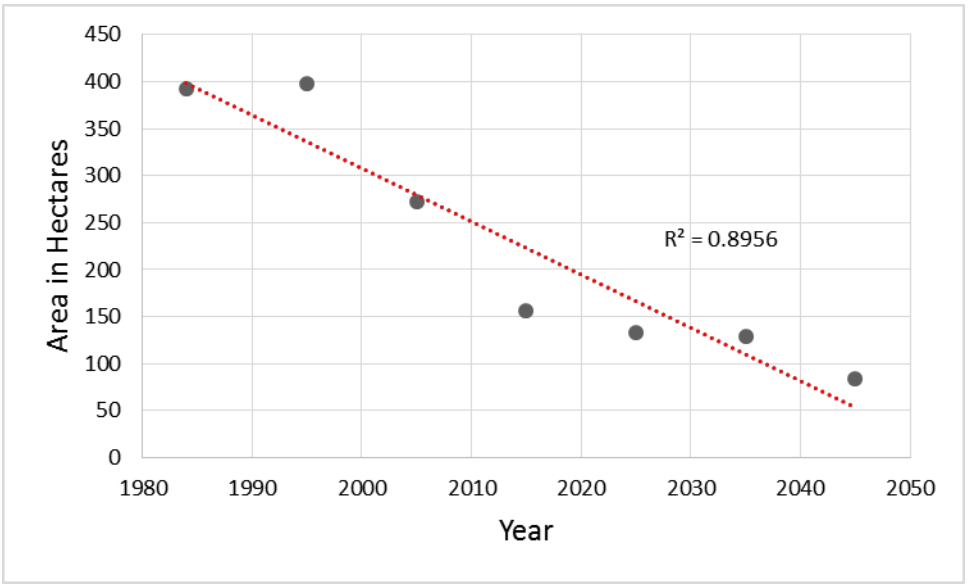

Figure 5.14: Historic, current and future wetland area changes

5.4 Factors influencing wetland area change

Population is one of the variables that influence wetland area. Table 5.7 shows that population had a strong negative correlation with wetland area. This means that the size of wetland reduced as the population increased. Mean temperature also strongly correlated with

wetland area (R^2=-0.92) while rainfall measured a strong positive correlation with wetland area (Figure 5.14).

Table 5.7: Variable changes over time

Year	Population	Wetland Area(ha)	Tmean	Total Annual Rainfall
1984	177,795	393.12	22.2	473.4
1995	209,170	397.8	22.5	545.2
2005	232,929	272.3	22.8	481.5
2015	245,188	156.6	25.4	161.3

5.5 Discussion

5.5.1Trends in LULC

The Shashe LULC trends showed that the area experienced notable transitions in three decades under study. Major land covers such as woodland, grassland, mountain vegetation and wetland shrunk in size during 1984-2015 periods. This could be attributed to an increase in population in the sub-catchment where population for 1984 was 177,795 and 245,188 for 2015, amounting to an increase of 67393 (ZIMSTAT, 2016). Such an increase in the number of people could have instigated high demand for land resources resulting in unprecedented deforestation which reduced woodland and grassland cover (Ibarrola-Rivas *et al*., 2017). Another possible explanation could be the intensification and extensification of agriculture; this is much so because communities in Shashe sub-catchment rely on agriculture for livelihood hence the crop field cover gained 10.2% at the expense of other land covers such as wetland. Similar results were reported by Scharsich *et al*. (2017) who observed increase in common agricultural lands owing to a fast track land reform programme of the year 2000 in Matobo district.

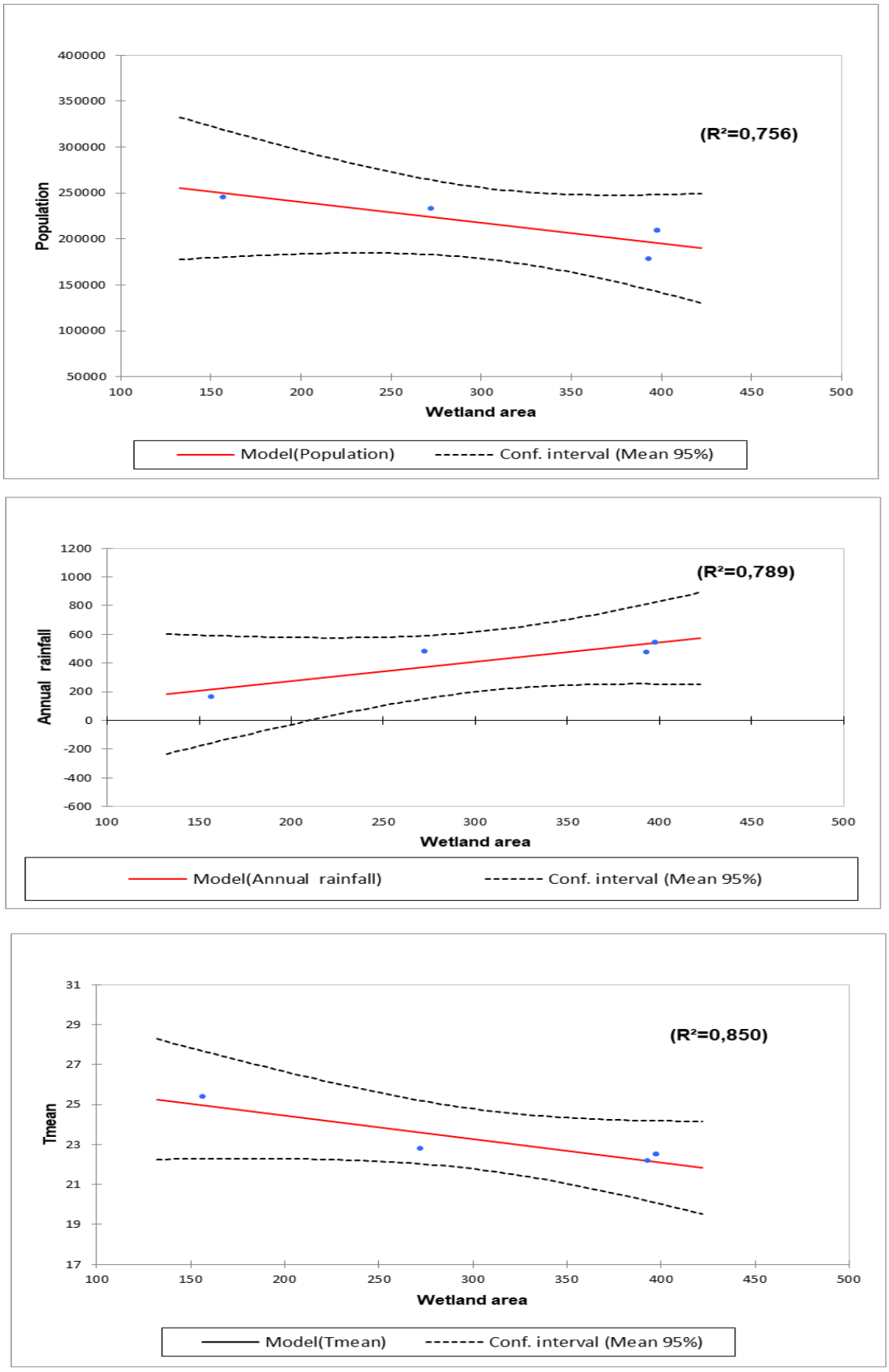

Figure 5.14: Regression analysis results for factors influencing wetland change

The results showed that the wetland area significantly decreased at $p < 0.05$, although the period between 1984 -1995 recorded an increase of about 4.68 hectares, which could be attributed to good rainfall during that period. However, there are several drivers that could be used to explain or account for wetland loss and these can be grouped under climatic, demographic, economic and technological and political factors. Overall percentage drop in wetland area between 1984 and 2015 amount to 60.16% which is quite a substantial loss.

Climate patterns could have contributed to wetland loss, not only through influencing water levels and fluctuations in the water table, but also through increasing water harvesting demand for both animals and human use during drought periods (Feng *et al*., 2012, 2016b). The Shashe sub-catchment has been experiencing a warming trend with a decreasing rainfall trend (Sibanda *et al*., 2017) (Table 5.5). Regressing wetland area and rainfall showed a significant correlation at $p < 0.005$ (Table 5.6). In this regard, variations in rainfall patterns coupled with prolonged El Niño Southern Oscillation related droughts could have jeopardised wetlands and made them more vulnerable to LULC changes. Naturally, wetland area will diminish during low rainfall periods, partly because of reduced runoff, and also due to the fact that wetlands remain the only source of water, and thus threatened with over harvesting/ water extraction. If such climate extremes recur more frequently, wetland ecosystems may eventually disappear (Change, 2013). Furthermore, climate variations will not only modify the wetland hydrology but may influence floral and faunal species. As observed by Ricaurte *et al*. (2017); Rodríguez *et al*. (2017), variations in climate variables have a propensity of shifting the distribution and abundance of wetland organisms.

Economically, wetland area loss may arise from damming, diversions and irrigation activities (Verhoeven *et al*., 2006). In Zimbabwe for instance, a number of dams and irrigation systems

were constructed after independence under the community empowerment programme. This means that during low rainfall, and no flooding years, the dams capture most of the water leading to the shrinking of wetlands. In the context of Matobo district, people have always relied on these wetlands for both material and spiritual gains. People harvest goods and plant vegetables in and around the wetlands throughout the year to supply neighbouring towns like Bulawayo. As the economic meltdown intensifies in Zimbabwe, market gardening remains one of the available livelihood options for the unemployed, which further exacerbate pressure on wetlands. The preference to cultivate near and in the wetland is necessitated by the need for fertile soils and adequate soil moisture during dry periods. However, such activities do not only disturb the watershed, but also modify wetland vegetation and structure and in some instances can lead to the total disappearance of the wetland (Wagner *et al*., 2013). Such agricultural encroachment on wetlands result in wetland fragmentation which undoubtedly compromises overall wetland integrity (Madebwe and Madebwe, 2005; Marambanyika *et al*., 2016).

Population dynamics coupled with policies of land tenure are also important drivers of wetland change, as the population increases so do the demand for natural resources such as water and land (Madebwe and Madebwe, 2005). For example, following fast track land reform of the year 2000, the population of Shashe increased by approximately 38%, which subsequently increased the demand for land. The regression model for wetland area and population proved this true by having a coefficient of determination of 0.756 (Figure 5.10).

5.5.2 Implications of future land use/ land cover changes on wetlands

The study depicts the utility of remote sensing in monitoring wetland area under climatic change. It was from classified Landsat imagery that change analysis over time was performed

for 1984-2015. The CA-Markov model successfully predicted future LU/LC with overall Kappa coefficient of 87%.

The shrinking of wetland area reported in this study is of great environmental concern and partly, and more attributed to increases in population, continuous LU/LC changes and climate change and variations. Population growth increases the demand for productive land resources forcing communities to encroach into wetland area during dry periods in search of water for crop production. Wetland areal extent is a function of catchment hydrology, which is usually influenced by LU/LC in the catchment. Future loss of the wetland area could result in the modification of wetland ecosystem structure and habitats, which will subsequently affect species distribution and diversity in a number of ways such as reproduction and food chain (Lamsal *et al*., 2017). In addition, wetland loss increases the amount of carbon dioxide lost into the atmosphere as studies show that wetlands are a significant carbon sink with the amount of carbon stored equivalent to that of the atmosphere (Ricaurte *et al*., 2017). Similarly, the loss of future wetlands will increase methane gas emission as most of it is trapped in wetlands which will increase greenhouse gases in the atmosphere and subsequently increase global warming.

5.6 Conclusions

The chapter results confirm the need for RF parameter optimisation for accurate classification results. The results for land change analysis show a decline in woodland and wetland cover, which could be attributed to both human and climatic influences. Major conversions were from wetland cover to crop field, suggesting agricultural encroachment on wetland area which results in lowering the water table and consequently reduced wetland area. Wetland area decreased by 60.16% in the last 30 years, which amounts to 115.6 hectares loss. Future

LULC prediction suggests a decrease in wetland area by about 53% by 2045 which is equivalent to 72.68 hectares. Therefore, the study concludes that the total wetland area in Shashe sub-catchment is decreasing due to cumulative anthropogenic and natural impacts. Quantifying wetland changes over time provides scientific bases for wetland protection, thus, further research is required to determine the significance of various factors for the purposes of designing locally relevant, sustainable monitoring and conservation strategies.

CHAPTER 6: MODELLING THE IMPACTS OF LAND USE/ LAND COVER CHANGES ON NESTED WETLAND CATCHMENTS IN THE SHASHE SUB-CATCHMENT, SOUTHWESTERN ZIMBABWE.

Abstract

Catchment LU/LC changes pose direct and indirect impacts on wetland hydrology, which in turn influences wetland ecosystems in various ways. This chapter describes a method for modelling impacts of LU/LC at wetland catchment level. The Pitman hydrologic model together with catchment delineation using Arc-Hydro extension for ArcGIS (v. 10.3) was used to model the impact of LU/LC changes for 25 wetlands in Shashe sub-catchment. The results show that LU/LC changes modify wetland hydrology, which consequently influences wetland areal extent evident by a significant decrease in a total wetland area between 1984 and 2015. This corresponded to a similar decrease in catchment runoff for the same period. Cropfield cover, which represents crop production, is one of the decisive variables in wetland extent, even though other factors such as climate variability, runoff and population growth have some influence. Thus, there is an urgent need to design catchment level strategies for the sustainability of wetland services.

Key words: wetland catchments, land use/land cover, catchment hydrology, hydrologic modelling

[4]This chapter is based on: Sibanda S, Grab S.W and Ahmed F. (*In Preparation*). Modelling the impacts of land use/ land cover changes on nested wetland catchments in the Shashe sub-catchment, southwestern Zimbabwe.

6.1 Introduction

Catchment land use/land cover (LU/LC) has become a popular research interest in global hydrological studies, partly because catchments are so hydrologically defined, hence any changes in LU/LC in a given catchment will undoubtedly impact on wetland dynamics (Poff *et al*., 1997; Hayashi *et al*., 2016; Wu and Lane, 2017). The accelerated rate of population growth and increased demand for productive agricultural land, coupled with increasingly varying weather and climate patterns, have accounted for considerable changes in LU/LC in many catchments of the World (Cuo *et al.*, 2013; Lee *et al.*, 2015b; McCauley *et al*., 2015). Such catchment LU/LC changes pose both direct and indirect impacts on hydrology, which in turn influences wetland ecosystems in various ways. Direct impacts result from activities occurring in the wetland, such as forest removal, cultivation and water harvesting (Russo *et al*., 2016). Indirect impacts entail those activities outside the wetland, but which may eventually disturb the wetland functioning and service provision. These include upland activities that change run-off patterns, influx or reduction of surface run-off, and damming and upslope irrigation activities among other things (Esteves *et al*., 2008).

It has been observed that wetland ecosystem and catchment hydrology play a complementary role in a given catchment. Wetland ecosystem regulates water balance, retains flood waters for use during drier periods, slowly recharges ground water and provides fresh water for various uses (Moore and Garratt, 2006), while catchment hydrology provides water for the survival of the wetland ecosystem. Therefore, studies of factors influencing wetland catchments and hydrology are invaluable for the sustainability of fragile wetland ecosystems. Hydrologic models have been widely applied to study the influence of climate factors on wetland hydrology (Lee *et al*., 2015b; Martin *et al*., 2017). These models range from simple

regression models to more complex distributed mathematical models such as SWAT, MIKE-SHE, SCS-CN, which have been implemented to simulate both climatic and LU/LC impacts at catchment level.

Previous studies have noted detrimental effects of LU/LC changes on catchment hydrology, manifested through the modification of ground water levels, surface flows and general catchment hydrology, which subsequently modify wetland ecology. Changes in LU/LC can also increase the number of nutrients, degradation and contamination of waters through biochemical pollution (Mander *et al*., 2000; Ramachandra *et al*., 2013). There is documented global evidence of the hydrologic impacts of LU/LC at catchment level. A study by Esteve *et al*. (2008) noted hydrologic modification of Marmenor wetlands in south-eastern Spain owing to the intensification of agriculture and tourism activities. Run-off patterns are said to be vulnerable to LU/LC changes and this was revealed by McCauley *et al*. (2015), who reported wetland drainage as being the most significant factor controlling wetland hydrology. LU/LC transformations also lead to a decline in total wetland area (Guofu and Shengyan, 2004) and alter their physical, biological and chemical integrity which is essential for the survival of wetland species (Ramachandra *et al*., 2013). Thus, as a consequence of LU/LC transformations, key wetland vegetation species are reported to have disappeared (Houlahan *et al*., 2006; De Cauwer and Reheul, 2009). Hydrologic modelling of LU/LC changes has shown that wetland water levels are significantly modified in various ways under human intervention (Voldseth *et al*., 2007). A study by Camacho *et al*. (2016) also highlighted LU/LC changes as the most influential driver responsible for 40% of wetland loss, either directly or indirectly.

A number of studies in sub Saharan Africa have investigated the impacts of LULC changes on wetland ecosystems at catchment level. For instance, the study by Walters *et al*. (2006) reported the influence of land tenure systems on the structure and composition of wetlands in the southern Drakensburg of South Africa, while a large decline in wildlife numbers has been reported from Kimana wetland in Kenya due to human interference (Nyamasyo and Kihima, 2014). It has also been established that increases in degraded areas and agricultural activities resulting from LU/LC changes, have a tendency to enhance annual and seasonal stream flow and sediment yield (Welde and Gebremariam, 2017). Apart from human induced LU/LC changes, natural factors also impact on wetland ecosystems in various ways; for example sea level rise has a potential not only to increase the wetland acreage by periodically flooding gentle terrain, but also through a general increase in surface run-off and water depth within a wetland ecosystem (Glick *et al*., 2013). Wetland hydrology is significantly affected by climate variability (Voldseth *et al*., 2007), with greatest impacts on those in tropical, semi-arid and arid regions (House *et al*., 2016). In addition, studies have shown that changing climates increase the risk of flooding and soil erosion (Field, 1995; Cuo *et al*., 2013). Associated with climate change, are the recurrences of weather extremes which have been reported to disturb the overall integrity of wetland ecosystems (Lee *et al*., 2015b). For instance, the projected frequency of droughts affects wetland ecology and habitats, which may eventually lead to loss of wetland floral and faunal species (Rashford *et al*., 2016). Thus, LU/LC changes are primary human-induced transformations that disturb wetland ecosystem services and large-scale biodiversity loss (Voldseth *et al*., 2007; Cousins *et al*., 2015).

There has been an absence of work in Zimbabwe attempting to model the effects of catchment LU/LC changes on wetland dynamics. This chapter aims to address this research gap by investigating temporal variations in wetland areal extent in response to LU/LC

changes in southwestern Zimbabwe which utilised classified images from chapter 5 (Figure 5.4). A further aim is to quantify and model the impacts of LU/LC on nested wetlands in the Shashe sub-catchment, which is made possible through combining GIS and remote sensing with hydrologic modelling. In this case, the Pitman model is used to quantify wetland sub-catchments hydrologic responses to different LU/LC dynamics.

6.2 Methodology

6.2.1 Data

Spatial data include Shashe LU/LC maps from 1984, 1995, 2005 and 2015, which were classified from Landsat imagery using procedures employed in chapter 5. A soil map of Zimbabwe and 30m resolution Digital Elevation Model were downloaded from STRM for catchment delineation. Meteorological data include daily rainfall records from four stations in the sub-catchment. These rainfall records cover 31 years (1984-2015) and were provided by the Department of Meteorology, Zimbabwe. Hydrological data from three gauging stations (Maleme, Mpopoma and Ove) were obtained from the Zimbabwe Water Authority (ZINWA), and cover the same period as the meteorological data.

6.2.2 Study Area

The Shashe sub-catchment is one of the four sub-catchments of the Mzingwane catchment (Figure 6.1) and extends from 27^{o} to 29^{o}E and 20^{o} to 22^{o}S, covering an area of 18 991km^{2}. The mean annual rainfall ranges between 450mm and 600mm, with the rain season beginning in October and ending in April (Mugandani *et al*., 2012). Soils are generally shallow sandy loam soils which are derived from gneiss and kaolinitic sands and granitic rocks, as well as some isolated moderate clay patches formed from greenstone belts (Ashton *et al*., 2001). The southern part of the catchment consists of Limpopo belt gneisses, while the far south is

composed of Karoo basalts. Land use to the north of the sub-catchment is mainly commercial, private and resettled farmlands focusing on irrigated crop production and commercial livestock rearing, while the southern part consists of communal settlements and agriculture limited to small livestock production. The Shashe sub-catchment is rich in both wild flora and fauna, specifically in the more protected Matopos National park which covers an area of about 44 500 hectares.

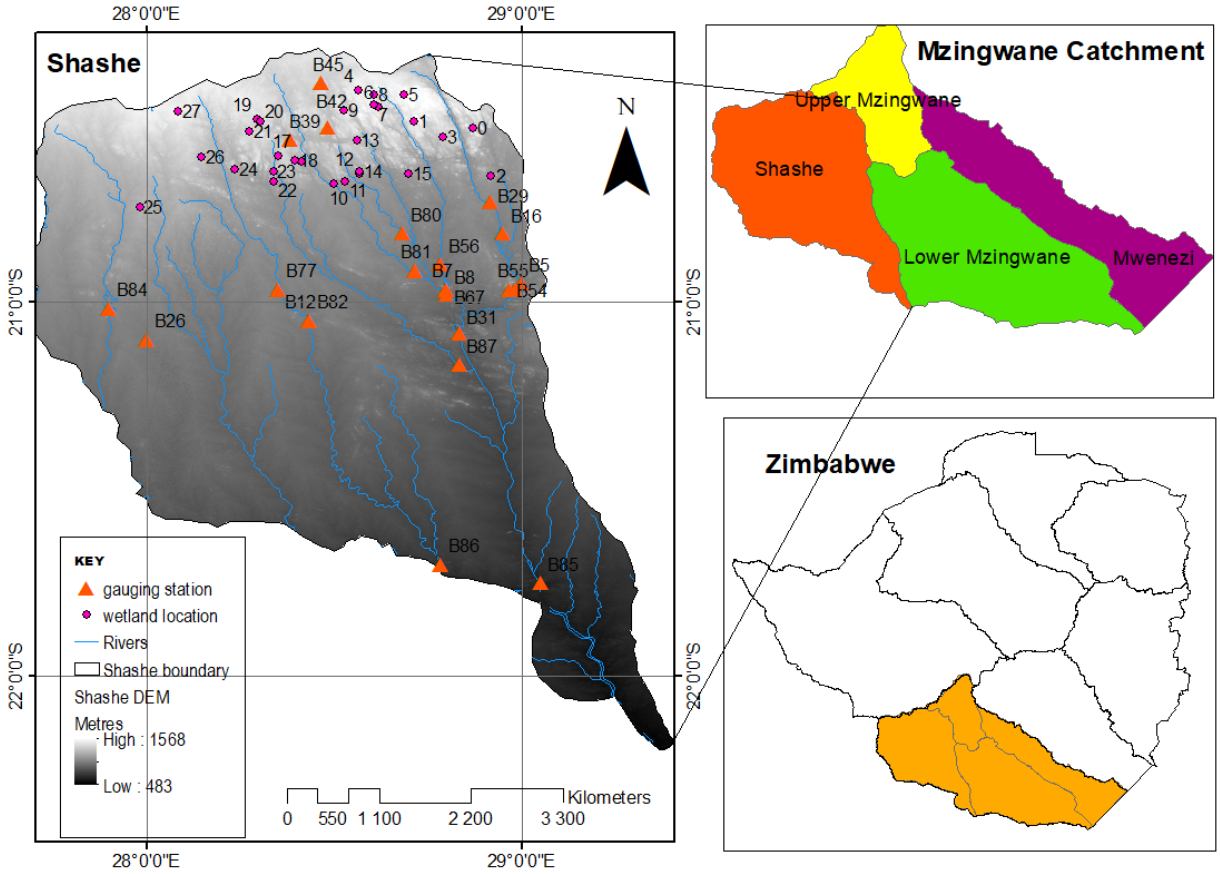

Figure 6.1: Shashe sub-catchment with gauging stations and wetland locations

6.2.3 Methods

A catchment approach is employed to model the impacts of catchment LU/LCchanges on nested wetlands in the Shashe sub-catchment. This method was chosen due to its strength in identifying and attributing major influential LU/LC to a given wetland catchment which is

distinct from other catchments (McCauley and Anteau, 2014). The approach is shown in Figure 6.2.

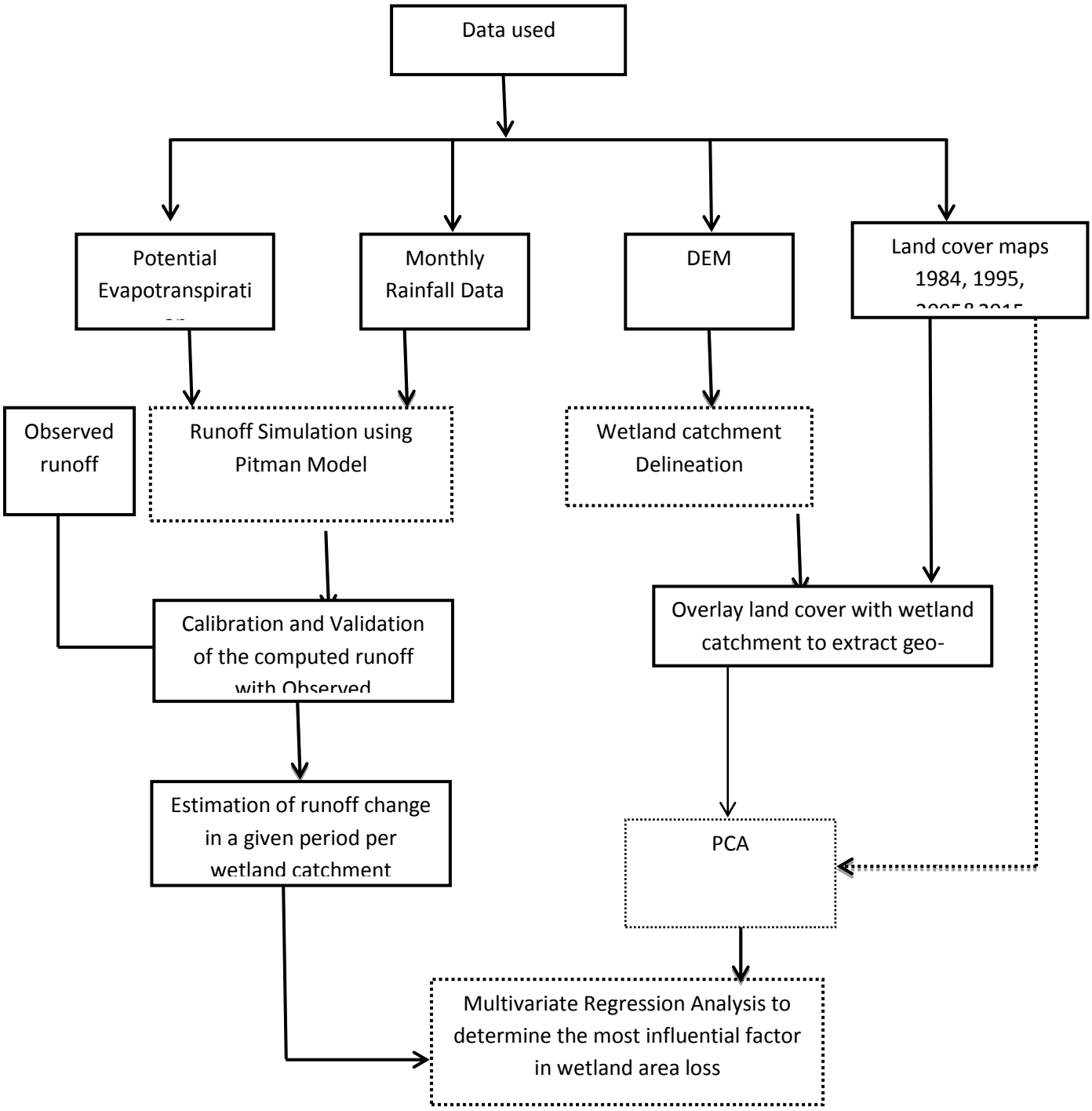

Figure 6.2: Workflow diagram to quantify the impacts of LU/LC changes on wetland area

6.2.4 Delineation of wetland catchments

A wetland catchment is defined as an area in which surface water drains into a given wetland, which may include other wetlands resulting in a nested concept. Catchments for 25 wetlands were delineated and these vary between 1.5 to 55 hectares in size. Delineation of wetland catchments helps establish the landscape that directly influences a given wetland. Following a procedure of catchment generation as suggested by McCauley and Anteau (2014), the boundaries of the wetland catchments were delineated using Arc-Hydro extension for ArcGIS v. 10.3 (ESRI, 2016), together with a 30m STRM Digital Elevation Model (DEM). This procedure involves modelling water bodies and flow direction which are created from the DEM for the purpose of establishing discrete boundaries of the area draining into each wetland. A number of hydrologic terrain attributes were derived from the DEM, which include flow path, flow direction, flow length, flow accumulation and catchment boundaries. Flow direction is important for computing flow accumulation, and for the purpose of this study, the Eight Direction Flow Model in Arc-Hydro software was utilized. Flow accumulation helped to locate interfluves (ridgelines) and delineate the catchment boundary.

Each wetland was selected and the watershed command used in ArcGIS to identify catchments for individual wetlands. The wetland exit points were used as pour points for the delineation of the wetland catchment. Individual catchments were then merged using ArcGIS Model Builder, thereby creating discrete and nested wetland catchments. Nesting was only done to those overlapping catchments.

6.2.5 Estimating runoff per wetland catchment

Surface run-off per given wetland catchment was simulated for the years 1984, 1995, 2005 and 2015 using the Pitman monthly rainfall-runoff Model for ungauged locations. Like most

conceptual models, the Pitman model consists of functions representing important hydrologic processes in a given catchment (Hughes *et a*l., 2006b). The Pitman model is a mathematical model that is used to simulate the movement of water through interlinked systems of catchments, river reaches, reservoirs, irrigation areas and wetlands (Pitman, 1973) (Figure 6.3). WRSM2000 software was used to simulate runoff per wetland catchment based on runoff, reservoir and channel modules linked by routes, which are lines through which water flows. WRSM2000/Pitman has been widely used to analyse monthly hydrology for a number of catchments in southern Africa (Wagener *et al*., 2004; Hughes *et al*., 2006a; Kapangaziwiri, 2011) and is said to be sensitive to land use changes because it has parameters that control interception (PT), infiltration (AI, ZMIN, ZA VE and ZMAX) and actual evapotranspiration (R and FF) (Hughes, 1997). Inputs to the model were monthly precipitation and mean monthly potential evapotranspiration and wetland catchment boundaries (Table 6.1). The interception function is controlled by interception parameters (PIV and PIF) for open and afforested conditions (Table 6.1). Runoff data for Maleme and Mpopoma gauging stations were used to calibrate the Pitman model in order to generate runoff for all ungauged wetland catchments. This means that calibrated model parameters from Maleme and Mpopoma River catchments were used to generate flows for ungauged wetland catchments. The validation was based on a comparison of observed and simulated runoff using regression analysis. Runoff trend analysis was also computed to determine changes over time, with values then correlated with rainfall and wetland cover change.

LU/LC maps classified from Landsat images were overlayed for each period on delineated wetland catchments to determine individual and nested wetland catchment LU/LC. Extracted percentage and area of each LU/LC together with the simulated runoff and rainfall were used

to compute multivariate analysis, regressed to establish the most influential variable in wetland areal change.

Table 6.1: Pitman model parameters (Hughes *et al*., 2006a)

Parameter	Units	Description
PIV, PIF	mm	Interception storage parameters for natural grassland and forest cover
AL	%	Impervious part of the sub-catchment
Z		Three parameters defining the asymmetric triangular frequency distribution of catchment absorption rates:
ZMIN	mm month^{-1}	Minimum
ZAVE	mm month^{-1}	Average
ZMAX	mm month^{-1}	Maximum moisture storage capacity
ST	mm	Maximum moisture storage capacity
FT	mm month^{-1}	Runoff from moisture storage at full capacity (ST)
FF		Ratio of forest/grassland potential evapotranspiration
R		Evaporation-moisture storage relationship parameter
POW		Power of the (runoff-soil moisture) curve

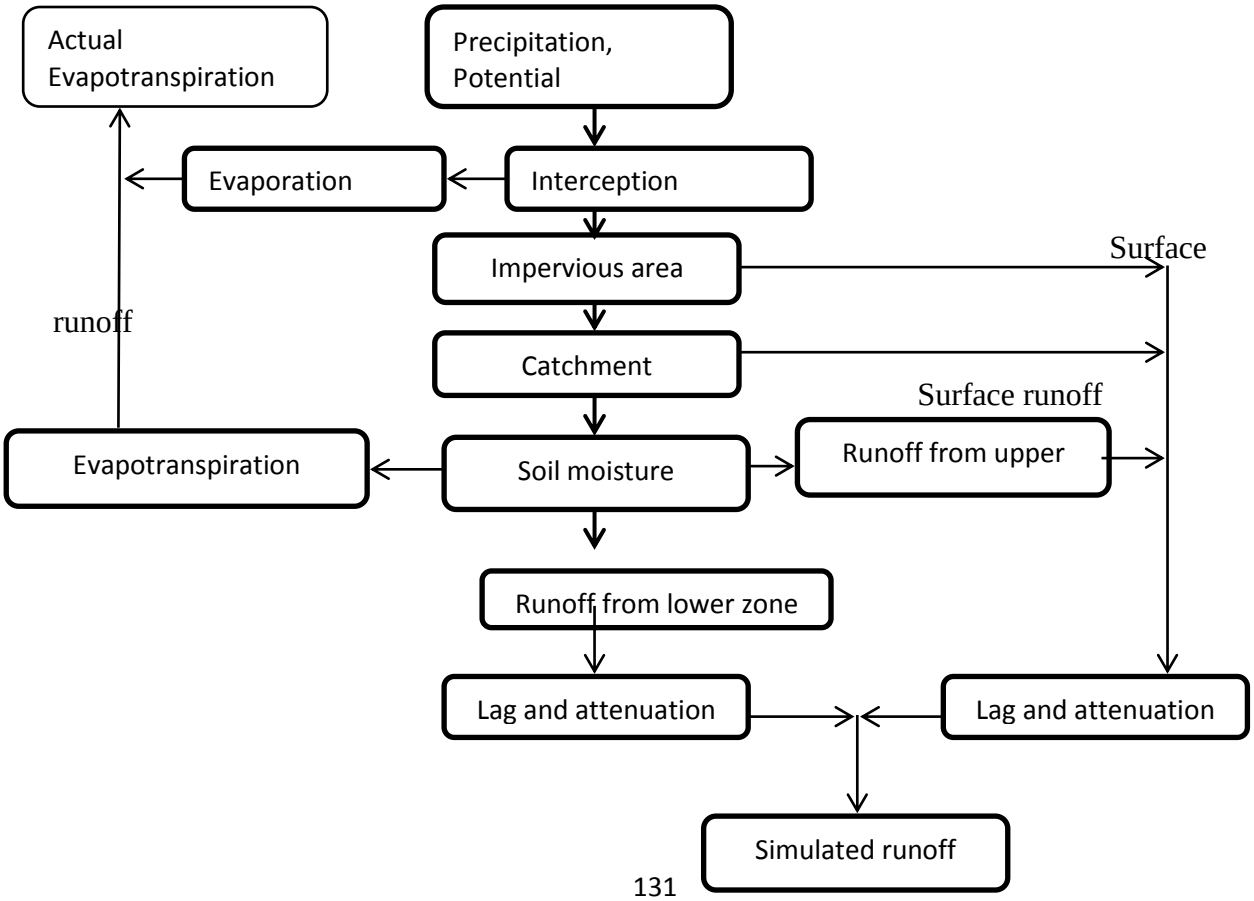

Figure 6.3: Flow diagram for runoff simulation

Multiple regression model procedures were used for the purposes of obtaining a parsimonious model with the most significant variables and the best statistical performance. Prior to multiple regression modelling, correlation analysis was applied and tested for multicollinearity of variables, which used the Variable Inflation Factor (VIF) to decide whether the variables are collinear. Where the VIF1 signified no correlation between independent variables, a VIF value of less than 5 meant that variables were not correlated significantly enough to affect the regression model, while VIF values of > 5 were not considered fit for the multiple regression analysis, signifying high multicollinearity.

6.3 Results

6.3.1 Delineation of wetland catchments

A total of 11 individual and nested catchments were delineated (Table 6.2) using Arc-Hydro extension for ArcGIS version 10.3 (Figure 6.4). Only catchments from permanent and semi-permanent wetlands were modelled using a 30m DEM.

Table 6.2: Delineated wetland catchments from nested wetlands

wetland catchment	Nested wetlands
1	0, 2
2	3
3	1,5,6,7,8
4	9,13,15
5	4,12,14
6	10,11
7	16,18
8	19,20
9	17,21,22,23
10	24,26,27
11	25

6.3.2 Geospatial statistics for individual LULC per given catchment

Time series of areal coverage according to each land cover type indicates that 1984 has the highest wetland area (393.12 ha), followed by 1995 (397.8 ha), 2005 (272.25 ha) and 2015 (156.6 ha), demonstrating a dramatic decline through time (Figure 6.5). Crop fields had increased significantly by 2015 (from 21.85ha in 1984 to over 283.25 ha in 2015), likely due to accelerating population growth and the associated greater demand for agricultural land (Berakhi *et al*., 2015). In part, this may be the result of the Fast Track Land Reform programme which was introduced in 2000 and apparently led to an approximately 38% increase in the population (ZIMSTAT, 2016).

In 1984 wetland cover dominated and covered some 44% of the area while crop fields only constituted about 4% of land cover (Figure 6.6a). In 1995 wetland cover remained the highest cover type (38%), followed by woodlands (26%) and crop fields (6%) (Figure 6.6b). By 2005 wetland areas had been reduced to 25% (a 13% drop) while woodlands had decreased to only 11%. In contrast, crop fields had increased to 9% of total cover by 2005 (Figure 6.6c). In 2015, wetland area covered only 12% and by then crop fields had increased most dramatically to 47% of the total areal cover, other covers constituted the following percentages; water (10%), grassland (8%), riverine (5%), mountain vegetation (6), rock out crop (9) and water (3).

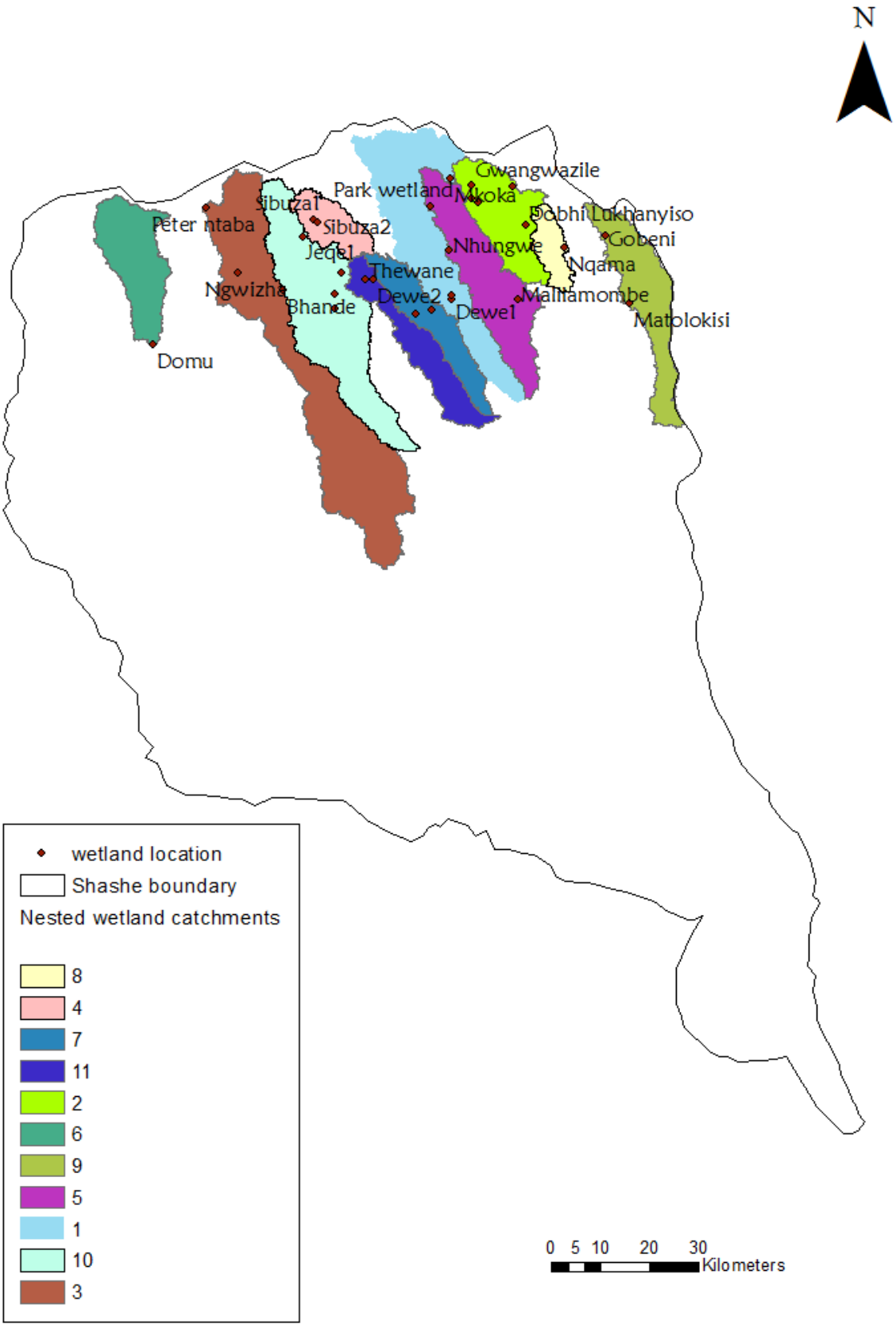

Figure 6.4: Spatial distribution of wetland catchments delineated from combining of wetlands that share catchments forming what are called nested catchments

These results are consistent with results by Mwita (2013) who also reported a 35% increase in cropland cover in Kenya and Tanzania at the expense of wetland area. The results are also similar to those from east African region in Kagera river basin, which too observed the substantial expansion of agricultural land at the expense of wetland areas (Berakhi *et al*., 2015). The trend across much of East and southern Africa is one of rapid population growth which increases the demand for natural resources and crop land (i.e. food), hence the recent decadal changes in LU/LC changes (Ibarrola-Rivas *et al*., 2017). Changing climate could also account for some of the observed LU/LC changes through modifying catchment hydrology as well as increasing wetland water harvesting during recurrent drier periods (Feng et al., 2012, 2016a). Incidentally, the Shashe community relies on market gardening near and within the wetland for their livelihoods throughout the year, and hence water extraction would have increased with time. The situation has been further exacerbated by the economic meltdown in Zimbabwe which saw the rate of employment rising beyond 85% in 2016, and as such, unemployed youths now engage on market gardening within the wetlands as a form of self-employment.

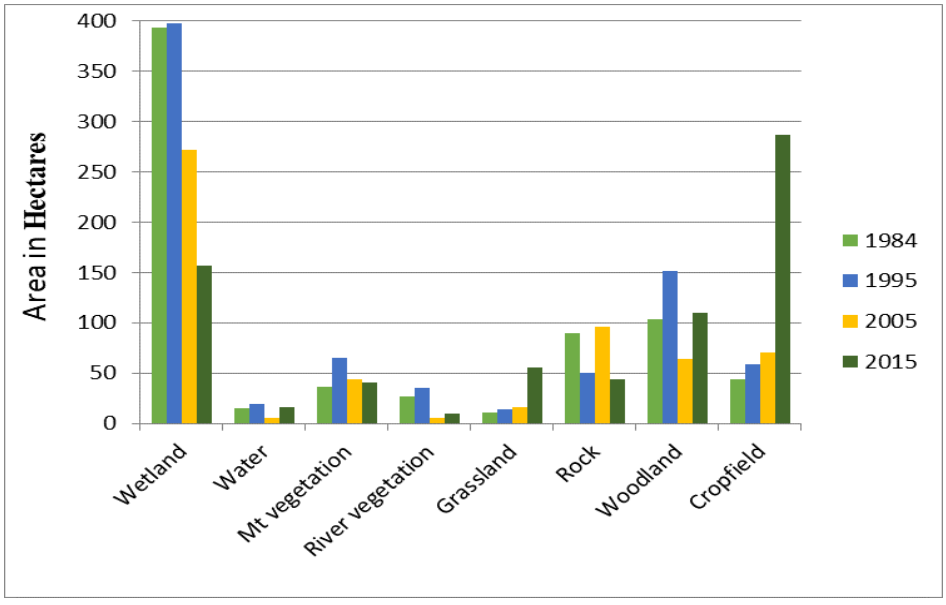

Figure 6.5: Land use / cover for the Shashe sub-catchment (1984, 1995, 2005 and 2015)

The general absence of reliable and recent LU/LC data at catchment level is a major challenge for sustainable wetland management because such information is essential for monitoring trends in LU/LC and ultimately for safeguarding the regions' natural resources. The Zimbabwean government has put in place policies in line with the Ramsar convention to curb wetland loss and promote their sustainability, as well as to ensure that set regulations are adhered to, through the Environmental Management Agency (EMA). The effectiveness of these strategies is heavily marred by recurrent extreme weather conditions making the wetlands the only available source of water for domestic and agricultural use.

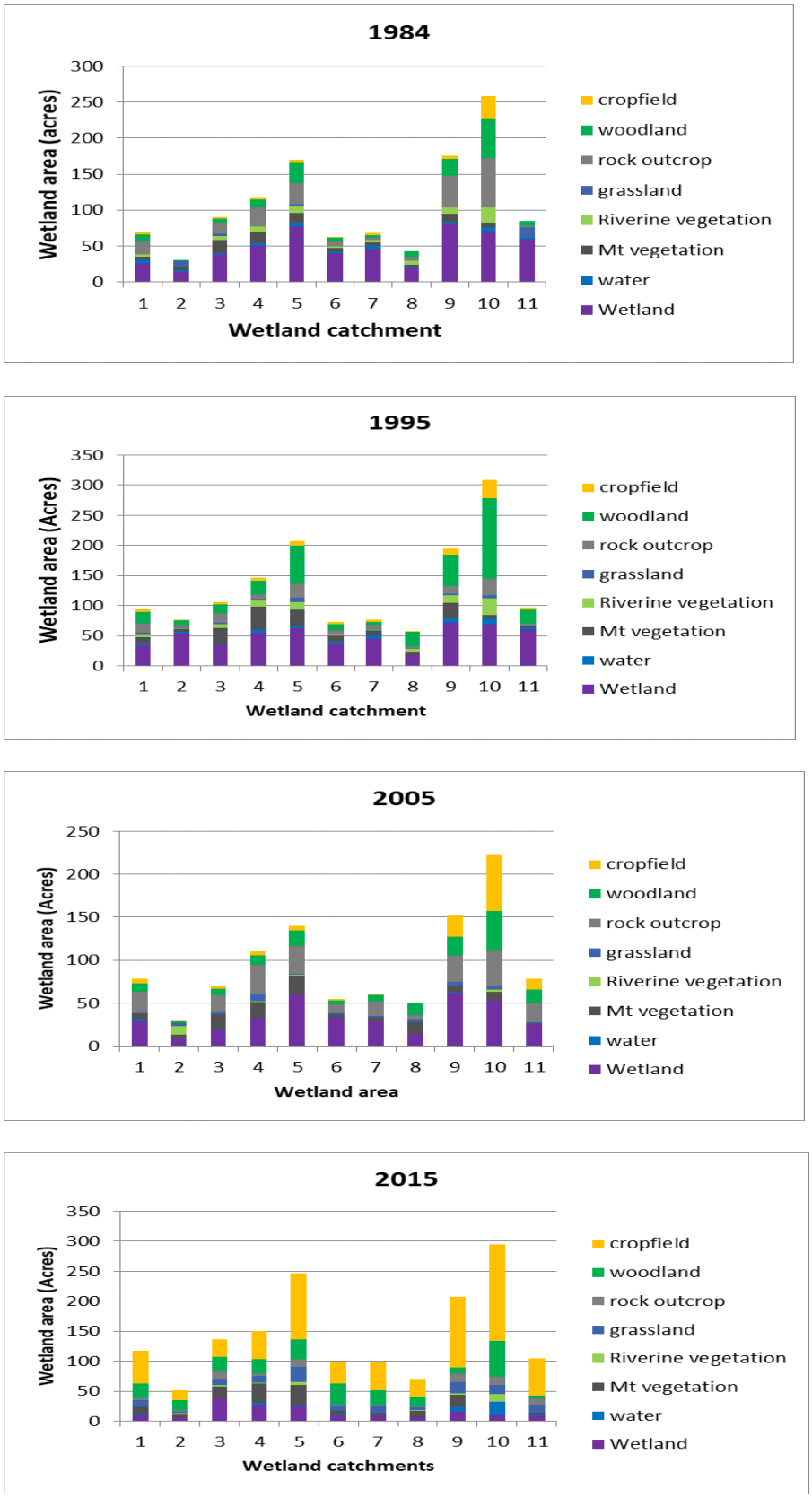

Figure 6.6: Spatio-temporal variation in land use/cover area per wetland catchment (1984, 1995, 2005 and 2015)

6.3.3 Comparison of observed and simulated runoff time series

The comparison between observed and simulated runoff data is shown in Figures 6.7 and 6.8. Validation using the linear regression model was very good with an R^2 value of 0.90 and the model parameters were then used to compute runoff for the ungauged wetland catchments (Figure 6.7). Generally, the high flows and low flows were estimated fairly well (Figure 6.7), although there were a few cases of under estimation, such as in 1992 and 2000, while over estimation was recorded for the years 1975, 1995 and 1996. These discrepancies may emanate from landscape uncertainties which could not be accounted for during the simulation process. The highest runoff is measured for wetland catchment WC2 followed by WC9, while WC1 recorded close to zero million cubic metres runoff for all periods (Figures 6.9 and 6.10). This might be attributed to catchment size differences (Pilgrim *et al*., 1982). Studies have shown the influence of catchment size on runoff, where it is argued that larger catchments tend to yield higher runoff compared to smaller catchments because of differences in their hydrologic responses (Pilgrim *et al*., 1982). For the periods studied, 1995 recorded the highest river flow (4401.5 Mm^3), followed by 2005 (3974.9 Mm^3). In contrast, 2015 recorded the lowest flows (3327.5 Mm^3), probably attributed partly to the dry period during the year 2015. Similarly, a study in Lake Urmia basin of Iran, also reported a significant decline in runoff with time owing to changes and variations in rainfall patterns (Sanikhani *et al*., 2017).

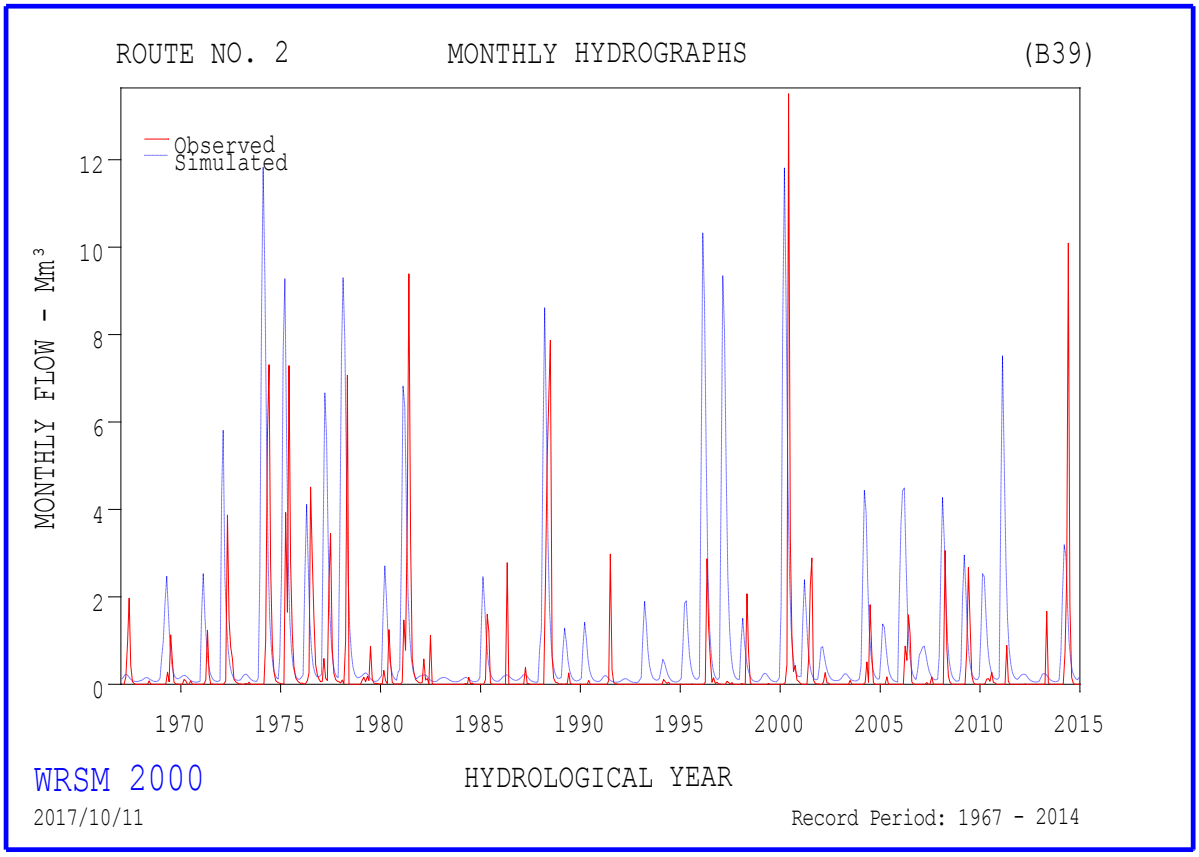

Figure 6.7: Observed versus simulated runoff for Maleme gauging station (B39) for the period 1967 to 2015

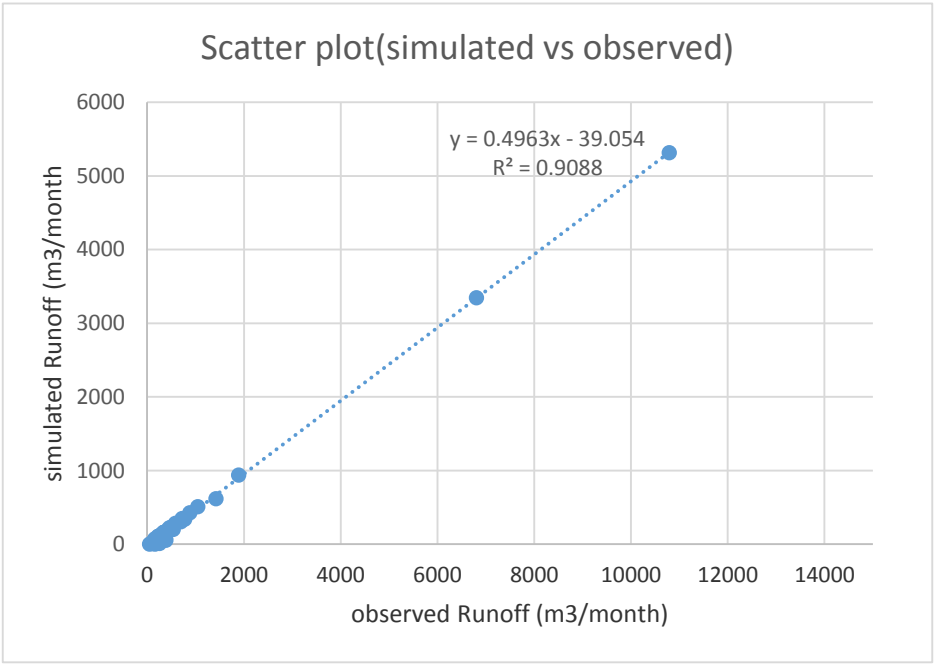

Figure 6.8: Scatter plot of simulated and observed runoff for Mpopoma (B39) gauging station

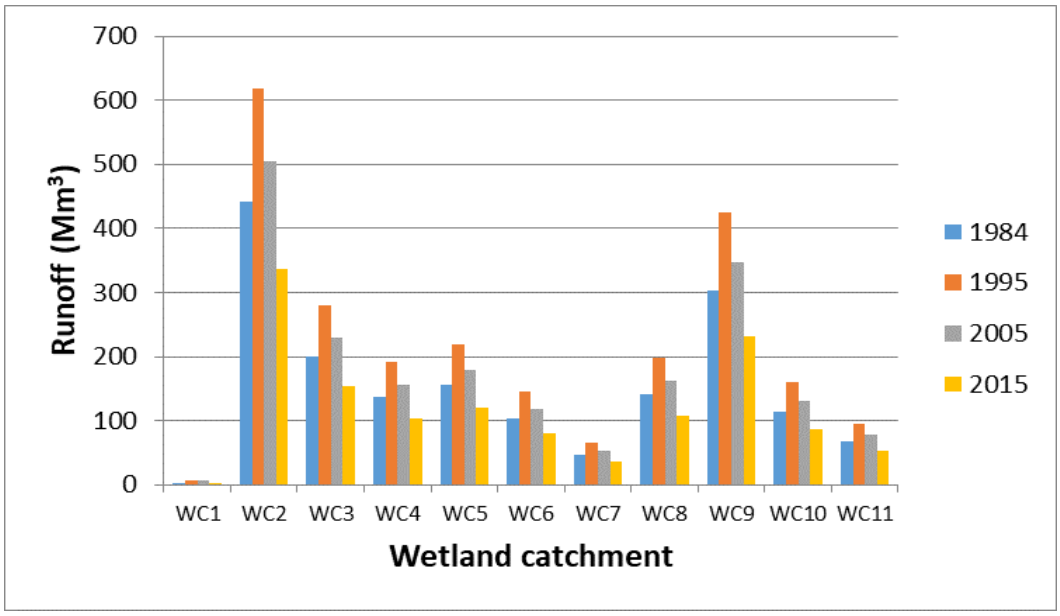

Figure 6.9: A comparison of runoff per wetland catchment for the periods 1984, 1995, 2005, and 2015

Results in Figure 6.10 show that wetland catchment 2 and 9 recorded the highest runoff of 617.77Mm^3 and 425.04Mm^3 respectively for the period 1967 to 2015. The result shows that the bigger the catchment size the lower the rate of runoff (Figure 6.11).

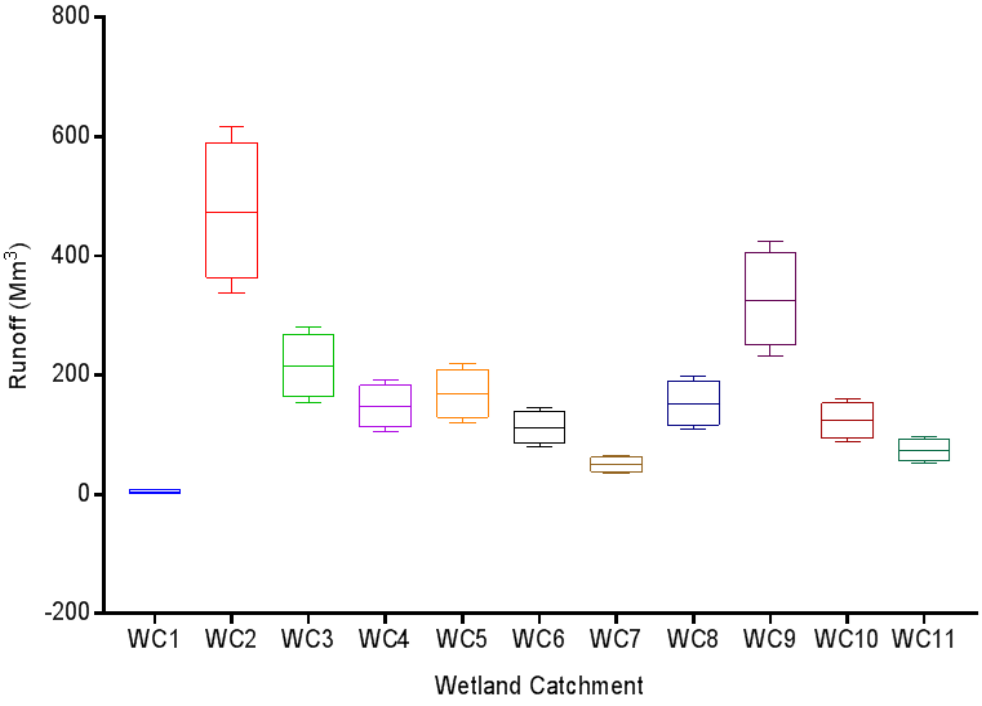

Figure 6.10: Variation in runoff per given catchment for the period 1967-2015.

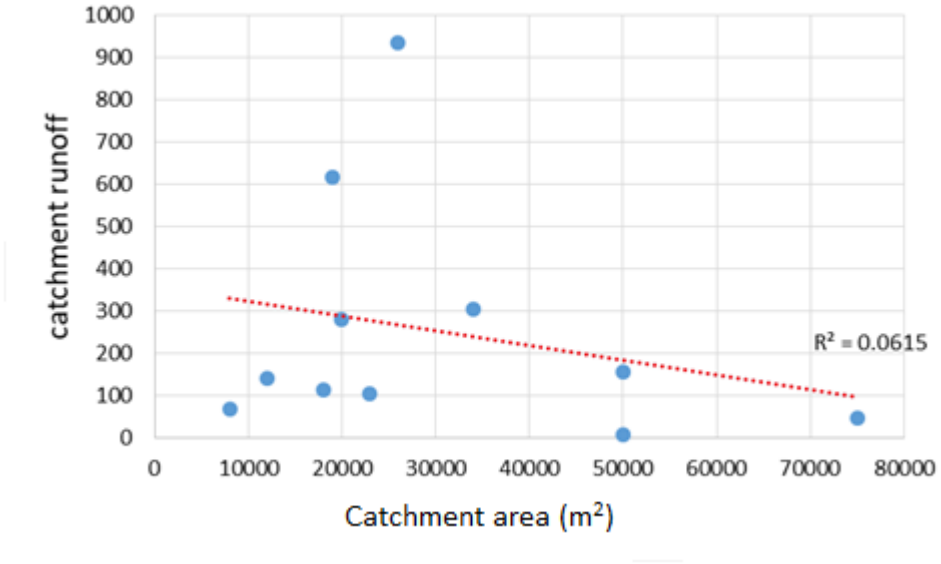

Figure 6.11: Regresion of wetland catchment runoff and catchment area in square meters (m^2)

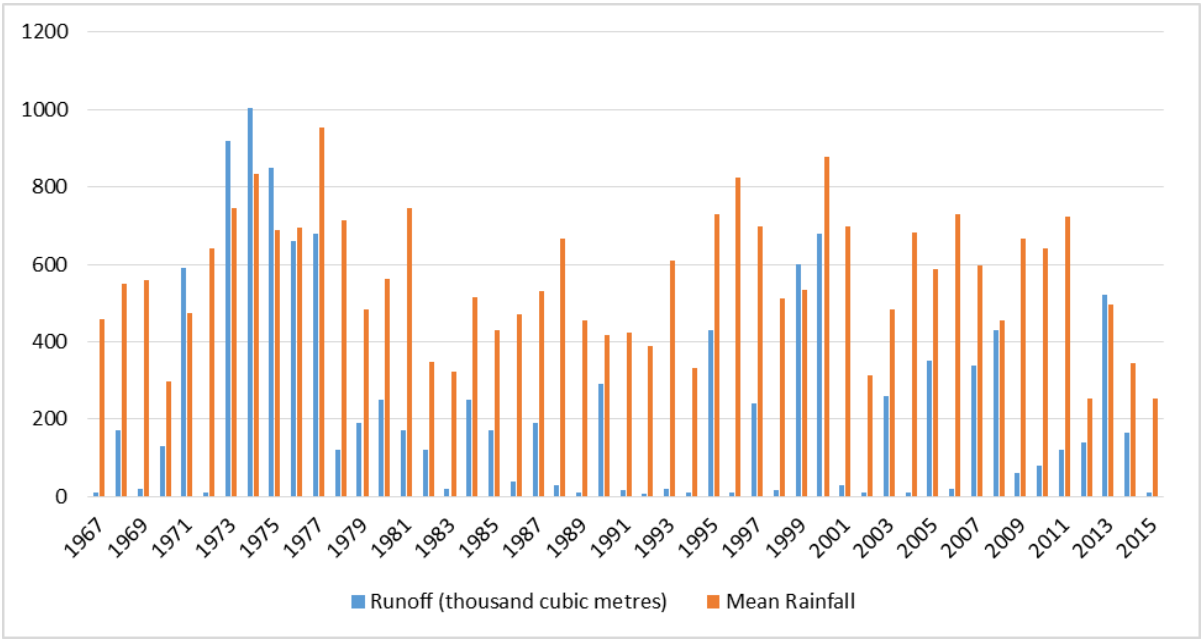

Figure 6.12: Annual runoff and mean rainfall for Maleme gauging station

Drought years (low rainfall mean) 1972, 1982, 1992, 1994, 2002, 2012, 2014 and 2015 recorded low runoff while high rainfall years measured higher runoff totals (Figure 6.12). The results confirm the contribution of rainfall amount on catchment runoff.

6.3.4 Variables impacting wetland aerial changes

Multiple regression was computed for the purposes of identifying the most influential variables in wetland loss at wetland catchment level. Specifically, backward variable elimination procedure was employed. This method starts with all the predictors and applies a step wise elimination based on the smallest F-statistic to remove the variable from the model until the remaining variables' removal makes no difference. In this case, the model began with 8 variables and remained with 5 significant ones which recorded an R^2 of 0.65, meaning that 65% of wetland change may be explained by 4 independent variables, riverine vegetation, grassland, wood land and crop field (Table 6.3 and Figure 6.13). However, the F-statistic computed by ANOVA shows that the model was significant at $p < 0.05$ (Table 6.4). From the model, it is clear that based on the Type 111 sum of square, crop field land cover is the most influential factor contributing to changes in wetland extent (Table 6.5).

Table 6.3: Multiple regression results

Regression Statistics	
Multiple R	0.807920782
R Square	0.65273599
Adjusted R Square	0.607043358
Standard Error	14.2934447
Observations	44

	Coefficients	Standard Error	t Stat	P-value	Lower 95%	Upper 95%	Lower 95.0%	Upper 95.0%
Intercept	0.443197656	0.122071	3.630668	0.000708	0.197482	0.688913	0.197482	0.688913
Observed	1.382265157	0.19727	7.006986	8.89E-09	0.985182	1.779348	0.985182	1.779348

Table 6.4: Analysis of variance (wetland)

Source	DF	Sum of squares	Mean squares	F	Pr > F
Model	5	12398.32	2479.664	9.463	< **0.0001**
Error	38	9957.862	262.049		
Corrected Total	43	22356.18			

Computed against model Y=Mean(Y)

Table 6.5: Type III Sum of Squares analysis (Wetland):

Source	DF	Sum of squares	Mean squares	F	Pr > F
Riverine vegetation	1	309.651	309.651	1.182	0.284
Grassland	1	45.542	45.542	0.174	0.679
Woodland	1	234.336	234.336	0.894	0.35
Cropfield	1	1902.569	1902.569	7.26	**0.01**

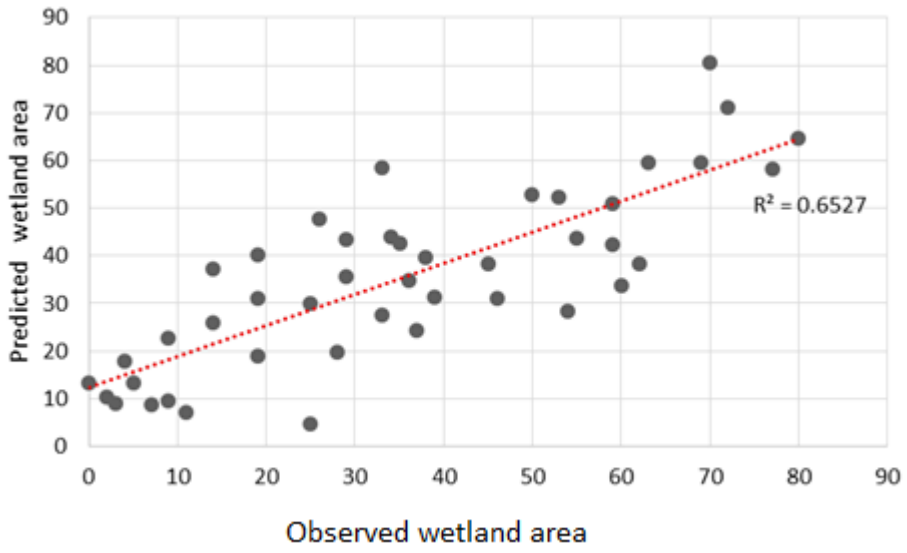

Figure 6.13: Predicted versus observed wetland area

These results substantiate the belief that agriculture is one of the major human factors that impact on wetlands (Sica *et al*., 2016). Studies by Madebwe and Madebwe (2005) also

observed similar trends in Shurungwi, Zimbabwe, and reported declining wetland areas due to agricultural encroachment. Sub-regionally, the trends may differ somewhat as Al-Hamdan *et al*. (2017) report net forest and crop expansion for eastern and southern Africa. Malawi recorded net deforestation and crop production, but wetland decline.

Runoff correlated well with rainfall and wetland area giving a coefficient of 0.932, which shows that it is an important variable in wetland hydrological change (Table 6.7 and 6.8).

Table 6.7: Correlation for rainfall, wetland area and runoff

	Rainfall (mm)	Wetland area(ha)	Runoff (Mm^3)
Rainfall (mm)	1	**0.878**	**0.956**
Wetland area (ha)	**0.878**	1	**0.774**
Runoff (Mm3)	**0.956**	**0.774**	1

Table 6.8: Regression between mean monthly runoff and mean monthly rainfall

Regression of variable Runoff (Mm^3) and rainfall	
Observations	4
Sum of weights	4
DF	1
R^2	**0.932**
Adjusted R^2	0.797

6.4 Conclusions

This chapter describes a method for modelling impacts of LU/LC at wetland catchment level, and the study found that understanding individual wetland disturbances at catchment level

provides a better understanding of direct human impacts on wetland ecosystems (McCartney *et al*., 2013). Such LU/LC impacts will also be influenced by other catchment characteristics such as the catchment size and amount of rainfall. The multiple regression model identified major LU/LC factors influencing wetland area in the Shashe sub-catchment. However, from the results it is clear that LU/LC changes could not wholly explain the variation in wetland area over time. It is concluded that:

- LU/LC changes in wetland catchments modify hydrology and influence wetland areal extent.
- Crop field cover, which represents crop production, is one of the decisive variables in wetland extent, even though other factors such as climate variability, runoff and population growth have some influence.
- Total wetland area significantly decreased between 1984 and 2015, and a similar trend was also observed for runoff.
- The application of the Pitman model allowed for accurate runoff simulation.
- Multiple regression analysis showed that four variables (riverine vegetation, woodland, crop field and grassland) account for 65% of the observed wetland areal changes, with crop fields making the most significant contribution ($p<0.05$).

Although wetlands contribute to household food and livelihood security in the short term, long-term sustainability under such utilization is very questionable. Thus, there is a need to design catchment level strategies for the sustainability of wetland services.

CHAPTER 7: AN EVALUATION OF THE CORDEX REGIONAL CLIMATE MODELS IN SIMULATING FUTURE RAINFALL AND EXTREME EVENTS OVER MZINGWANE CATCHMENT, ZIMBABWE.

Abstract

The study evaluated CORDEX-RCMs' ability to project future rainfall and extreme events in the Mzingwane catchment using an ensemble average of three RCMs (RCA4, REMO2009 AND CRCM5). Model validation employed the statistical mean and Pearson correlation while trends in projected rainfall and number of rainy days were computed using the Mann-Kendall trend test and the magnitudes of trends were determined by the Sen's slope estimator. Temporal and spatial distribution of future extreme dryness and wetness were established by using the Standard Precipitation Index (SPI). The results show that RCMs adequately represented annual and inter-annual rainfall variability and the ensemble average outperformed individual models. Trend results for projected rainfall suggest a significant decreasing trend in future rainfall (2016-2100) for all stations at $p<0.05$. In addition, a general decreasing trend in the number of rainy days is projected for future climate, although the significance and magnitude varied with station location. Model results suggest an increased occurrence of future extreme events, particularly towards the end of the century. The findings are important for developing proactive sustainable strategies for future climate change adaption and mitigation.

Key words: CORDEX, Regional Climate Models, future rainfall, projected extremes, rainy days

[5]This chapter is based on: Sibanda S, Grab S.W and Ahmed F. (In submission). An evaluation of the CORDEX regional climate models in simulating future rainfall and extreme events over Mzingwane catchment, Zimbabwe. Theoretical and Applied Climatology Journal.

7.1 Introduction

Anthropogenic global climate change is no longer a myth but a proven reality in Africa (Change, 2013). Evidence of changing climates has been witnessed and experienced by Africa as a whole, and include, variations in temperature and rainfall, as well as the recurrence of extreme weather events (Hulme *et al*., 2001; Kruger and Shongwe, 2004; Reason *et al*., 2005; Kruger and Sekele, 2013; Kruger and Nxumalo, 2017; Sibanda *et al*., 2017). The World Meteorological Organisation (WMO, 2017) reported continuing global warming which has set a new temperature record of 1.1°C increase above the pre-industrial period which is 0.06°C higher than the 2015 record. This global warming is largely attributed to anthropogenic greenhouse gas emissions (GHGS), chiefly being carbon dioxide whose levels had reached 400.00 ppm in the atmosphere by 2015 (WMO, 2017). The sea levels have risen by 20mm since the start of the twenty first century due to the looming global warming spasm.

A cursory review of the climate change projection literature in Africa and southern Africa in particular suggests accelerated current and future changes in climatic conditions under the 'business as usual' scenario (Carson *et al*., 2016; Hansen *et al.*, 2016). Such changes are projected to continue into the end of the century and IPCC (2014) the fifth report suggests that Africa will be the most vulnerable to these future changes in climatic conditions which are expected to cause detrimental socio-economic consequences. For instance, it is predicted that a 4.1°C rise in temperature by the end of the century will result in 10% loss of the African GDP (WMO, 2017). Thus, there is a pressing need to simulate future climatic conditions as a way of minimising uncertainties and to proactively develop sustainable adaptive and mitigative strategies for the future. Although developed countries have committed to reducing GHGs emission by at least 15% by 2020, warming is set to continue,

which will see temperatures rising by close to 4°C by 2060. Such warming is and will be detrimental to natural ecosystems functioning particularly to the fragile wetland ecosystems which are heavily dependent on rain water for their survival. For instance, wetland hydrology is strongly influenced by changes in the amount of rainfall and runoff; therefore, any alterations of the normal climatic patterns are likely to affect wetland ecosystems. A projected decline in rainfall may also result in the decrease of the wetland area which may subsequently cause a decline in endemic floral and faunal species (Barros and Albernaz, 2014). In addition, an increase in rainfall would also affect and disturb wetland ecosystems through the elimination of species with low tolerance levels.

Linked to global warming is the recurrence of extreme droughts, notably in southern and eastern Africa where several millions of people have been faced with extreme food insecurity during the last two decades (Bremner, 2017; WMO, 2017). Previous studies have shown that droughts disturb wetland ecosystems resulting in the drying of the wetland (Burkett and Kusler, 2000).

A number of studies have simulated future climatic conditions based on Global Circulation Models (GCMs) and these GCMs are extensively used in the assessment of past and future climatic conditions based on different scenarios of concentrations (Nikulin *et al.*, 2012). However, their direct application in impact studies is limited by their coarse spatial resolutions (100-300km) which provides inadequate information at regional and local scales (Ramirez-Villegas and Jarvis, 2010). Downscaling of the GCMs is thus used to obtain data required for regional and local level variability and change. Downscaling can either be empirical (statistical), which relates large scale circulation models to a local variable of interest. The relationships are used to estimate local level values by means of Regional

Climate Models (RCMs) (Ramirez-Villegas and Jarvis, 2010). These RCMs are run at between 10 to 50km horizontal resolutions over a specified area for example Regional model (REMO).

CORDEX-AFRICA is a collaborative project aimed at generating high resolution climate simulations for Africa, funded by the World Climate Research Program (WCRP), providing regional data for all continents, Africa included. It is with this focus that CORDEX-AFRICA has provided huge sums of data for use in climatic studies in Africa, which has been utilised by a number of studies. For instance, Nikulin *et al.* (2012) were amongst the first to employ CORDEX data in southern Africa. They analysed the ability of 10 RCMs to simulate precipitation over Africa. They found that the present set of CORDEX AFRICA RCMs provided meaningful information on climate projections over Africa. Akinsanola *et al*. (2015) used CORDEX RCMs to simulate rainfall patterns in the West African summer monsoon. Their results showed that RCMs in the CORDEX framework simulated the main features of the rainfall climatology well. Similarities between GCM and RCM temperatures were reported by Dosio and Panitz (2016). Shongwe *et al*. (2015) evaluated the ability of CORDEX RCMs to simulate monthly rainfall variation over southern Africa. They noticed that the RCMs adequately revealed precipitation probability density function although a few showed bias towards excessive light rainfall events.

A study by Pinto *et al*. (2016) examined extreme events in the CORDEX data models and showed that simulations are able to capture observed climatology of spatial and temporal extreme precipitation. Kalognomou *et al*. (2013) analysed 10 RCMs and simulated precipitation over southern Africa within CORDEX framework and observed that all spatio-temporal characteristics of the rainfall patterns were reasonably well captured by all RCMs,

although individual models presented biases in the wet and dry conditions for some regions. A strong link between projected SPEI and ENSO over southern Africa was confirmed by Meque and Abiodun (2015). Recently, Mutayoba and Kashaigili (2017) evaluated the performance of CORDEX downscaling RCMs to simulate rainfall patterns for Mbarali catchment in Tanzania; their results indicated that RCMs from CORDEX reproduce rainfall characteristics better and reproduced inter-annual variability of rainfall fairly well. Although some work has utilised CORDEX-AFRICA data in Africa and some parts of southern Africa, there is no published study that has attempted to employ the same data in Zimbabwe. Thus, this chapter seeks to analyse and evaluate the ability of CORDEX RCMs to simulate future rainfall trends, extreme events and their probable implications on future wetlands over Mzingwane catchment. This work is premised on the understanding that future climatic conditions are critical for the sustainable conservation and management of future ecosystems like wetlands, and is paramount in the development of future adaptive and mitigative strategies towards climate change consequences.

7.2 Methodology

7.2.1 Study area

Zimbabwe has seven catchment management regions as indicated in Figure 7.1. This chapter focuses on the most southerly of these catchment regions, namely the Mzingwane catchment, which is located between 19.8^{o} and 22.4^{o}S and 27.7^{o} and 32.0^{o} E. The catchment includes four sub-catchments (Shashe, Lower Mzingwane, Upper Mzingwane and Mwenezi) covering an area of ~63000 km^2 (Figure 7.1). The northern part of the catchment is composed of granitic rocks associated with the greenstone belt, which is rich in gold deposits. Granite terrains form large inselbergs (dome-shaped mountain ranges), between which wetlands occur (perennial dams, vleis, swamps or marshes). The Mzingwane catchment hosts five

major rivers (Shashe, Umzingwane, Mwenezi, Bubi and Marico) that feed into the Limpopo River (Görgens and Boroto, 1997).

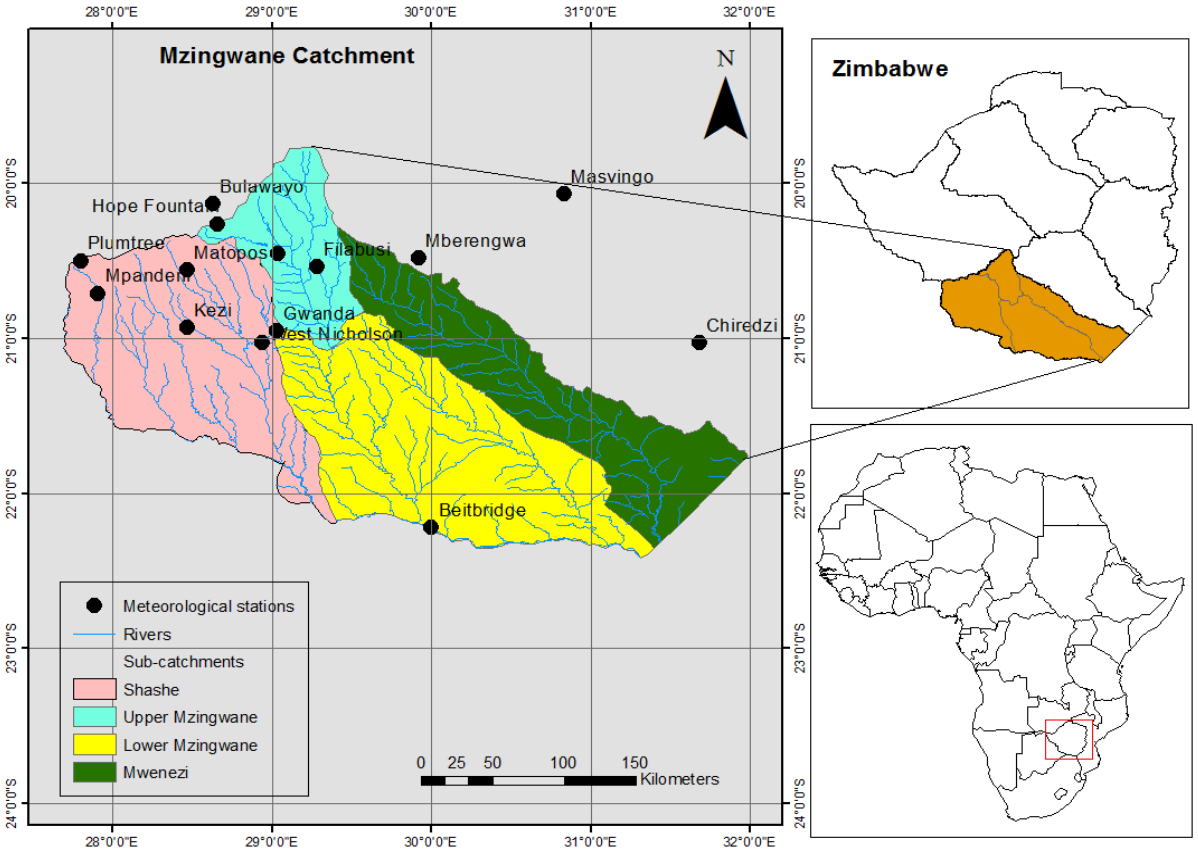

Figure 7.1: Mzingwane catchment showing four sub-catchments (Shashe, Upper Mzingwane, Lower Mzingwane and Mwenezi)

The climate of Mzingwane catchment is semi-arid to arid, but rainfall distribution varies across the catchment, such that the northern regions receive higher mean rainfall (~450 - 600 mm pa) than the southern regions (~200-450 mm pa) (Görgens and Boroto, 1997; Chenje *et al.*, 1998). The wet season typically starts in late October and ends in March, with the highest rainfall occurring between December and February (Unganai and Mason, 2002). Rainfall seasonality is largely influenced by the Inter-Tropical Convergence Zone (ITCZ) which moves southwards during the austral summer, and inter-annually by the El Niño Southern

Oscillation (ENSO) which is associated with periods of lower (El Niño) and higher (La Niña) rainfall (Manatsa *et al*., 2008). The average daily T_{max} for the catchment varies between 27 – 34 °C during summer and 22 – 26 °C in winter (Love *et al*., 2010), while average T_{min} range between 18 - 22°C during summer and 5 - 10°C in winter (FAO, 2010). Owing to the relatively low and erratic rainfall, agricultural activities in the catchment mainly involve livestock rearing, as this is the most viable.

7.2.2 Data and Methods

Monthly and daily rainfall data for the period 1950 to 2100 simulated by three regional climate models in the Coordinated Regional Climate Downscaling Experiment (CORDEX) database are used. The data are set to 0.44º by 0.44º spatial resolution, equivalent to 50km by 50km and are quality controlled by the CORDEX-AFICA and may be used based on terms of use provided by http://wcrp-cordex.ipsl.jussieu.fr/. An advanced quality checker was developed by CORDEX using DKRZ (Hamburg), which targeted missing values, time steps, errors in units, suspicious values and many other aspects. The Regional Climate Models (RCMs) included the Max Planck Institute Regional model (REMO), the Sveriges Meteorogiska Och Hydrologiska institute (SMHI), Rossby Centre Regional Atmospheric Climate Model, version 4 (RCA4), and the Canadian Regional Climate Model, version 5 (CRCM5) (Table 7.1). The observed monthly and daily rainfall and temperature data for the period between 1950 and 2015 were used to validate CORDEX RCMs datasets and this employed Root mean Square error (RMSE) and Pearson correlation. To test the model's ability to simulate present and future extremes and rainfall trends, linear regression was computed for the observed and projected future data.

Table 7.1: CORDEX RCMs data used

Domain	Regional Climate Model	Driving Global Climate Model
AFR-44	RCA4	ICHEC-EC-EARTH
AFR-44	REMO2009	ICHEC-EC-EARTH
AFR-44	CRCM5	MPI-M-MPI-ESM-LR

Trend analysis of the projected (2016-2100) monthly rainfall data were computed using Mann-Kendall (MK) trend test while the Sen's slope estimator was used to estimate the gradient of the trends for the remaining part of the century. The Sen's slope estimator is more robust than the least squares because it takes into account the outliers and the extreme values into consideration, typical of the climate data (Hamed and Rao, 1998). The number of rainy days for the same period was also calculated and their trends computed again based on MK trend test. A detailed description of mathematical formula for MK test and Sen's slope estimator is shown below:

$$Z_{MK}=\begin{cases}\frac{S-1}{\sqrt{Var(S)}} & when \quad S>0\\ 0\ldots & when \quad S=0\\ \frac{S+1}{\sqrt{Var(S)}} & when \quad S<0\end{cases}$$

Where,

$$S=\sum_{i=1}^{n-1}\sum_{j=i+1}^{n} sgn(x_{j-}\, x_i)$$

Sen's Slope Estimator Test (1968) was used to determine the magnitude of the trends. The slope T_i was calculated as;

$$Sen's\ Estimator=\begin{cases}T\left(\frac{N+1}{2}\right) & if\ N\ is\ odd\\ \frac{1}{2}\left(T\frac{N}{2}+T\frac{N+2}{2}\right) & if\ N\ is\ even\end{cases}$$

The study computed the Standard Precipitation Index (SPI) based on the projected rainfall to identify future extremes. SPI compares the total precipitation received at a given location with the long-term rainfall distribution for the same period of time at that location. It can be computed on 1, 3, 6 and 12 month time scales. Table 7.2 shows drought categories as defined by McKee et al. (1993).

Table 7.2: Extreme rainfall categories as defined by McKee *et al*. (1993)

Category	**SPEI value**
2.0+	Extremely wet
1.5 to 1.99	Very wet
1.0 to 1,49	Moderately wet
0 to .99	Near normal
-1.0 to -1.49	Moderately dry
-1.5 to -1.99	Severely dry
-2 and less	Extremely dry

7.3 Results and Discussion

7.3.1 Validation of simulated data

Simulated mean monthly rainfall data for 1950-2015 were evaluated against observed data for the same period. The results indicate a very strong correlation for the ensemble average, obtaining a correlation coefficient of 0.975 (Figure 2) which is a clear indication that CORDEX RCMs can adequately represent rainfall characteristics.

7.3.2 Simulation of rainfall

All RCMs adequately simulated the mean annual cycles and the spatial variations, albeit individual models showed varying biases in different stations. Figure 3 shows how RCMs managed to simulate the annual cycle of rainfall pattern of Mzingwane catchment.

REMO2009 performed much better followed by AQAM-CRCM5, while SMHI-RCA4 over estimates the amount of rainfall. The ensemble average outperformed individual models due mostly as a result of the removal of oppositely signed biases across the models. The correlation between individual RCM and observed rainfall data indicate that AQAM-CRCM5 represented the annual cycle much better than the two RCMs because the model employed the Kain-Fritsch scheme which is believed to exhibit a much better representation (Nikulin *et al*., 2012). Previous studies in southern Africa have shown that CORDEX RCMs are able to sufficiently capture the main characteristics of precipitation within the region (Nikulin *et al*, 2012; Shongwe *et al*., 2015; Luhunga *et al*., 2016; Mutayoba and Kashaigili, 2017). All the models were also able to represent the inter-annual variability of rainfall (Figure 4) with the ensemble performing well. UQAM-CRCM5 presented accurate annual averages while SMHI-RCA4 over estimates the annual averages for the catchment, with some years reaching an average of 1200mm per year.

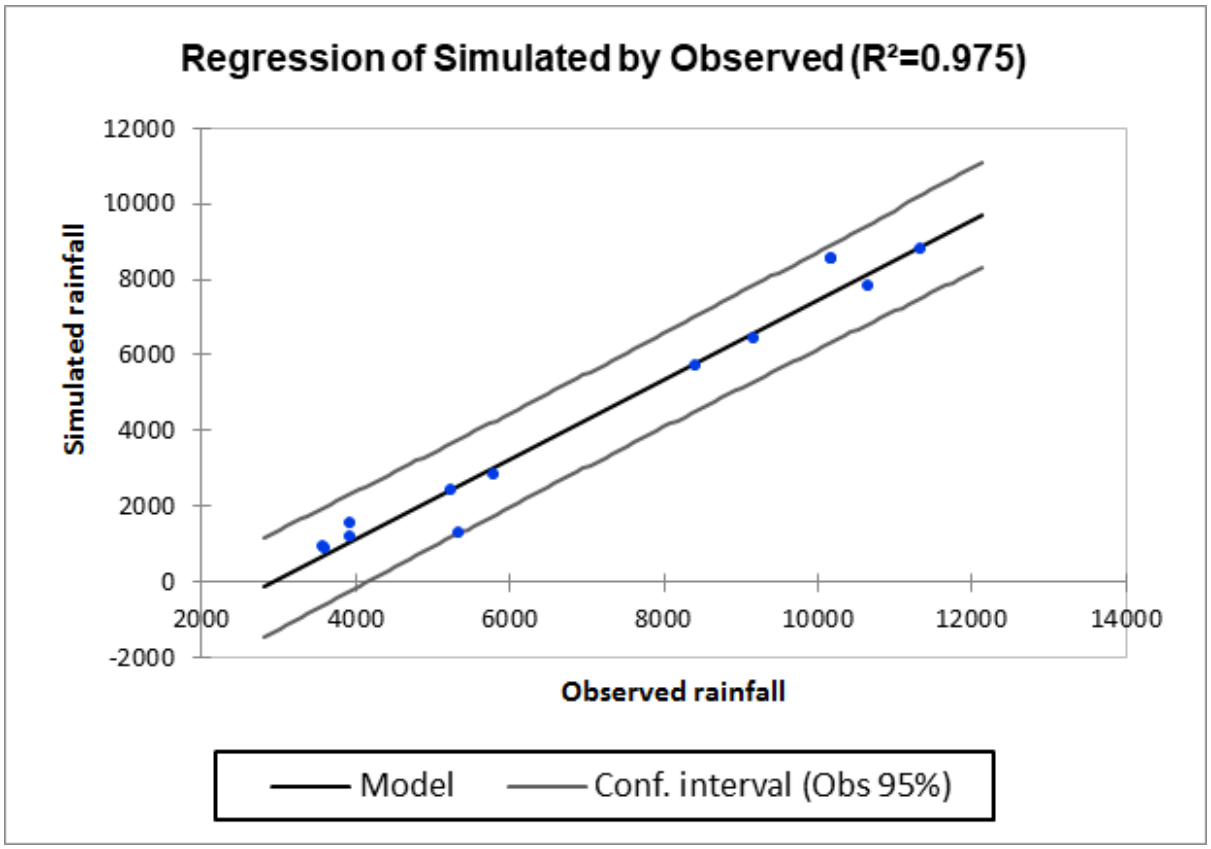

Figure 7.2: Correlation between observed and simulated mean monthly rainfall for Mzingwane catchment computed for the period 1950 to 2015.

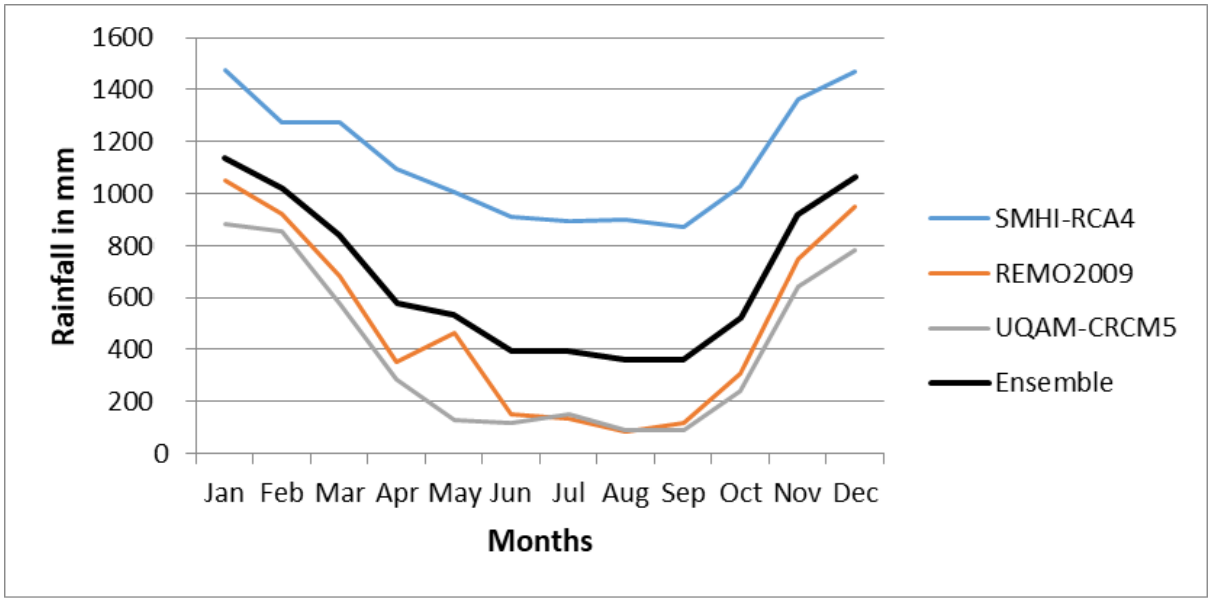

Figure 7.3: Average annual cycle for rainfall over Mzingwane catchment

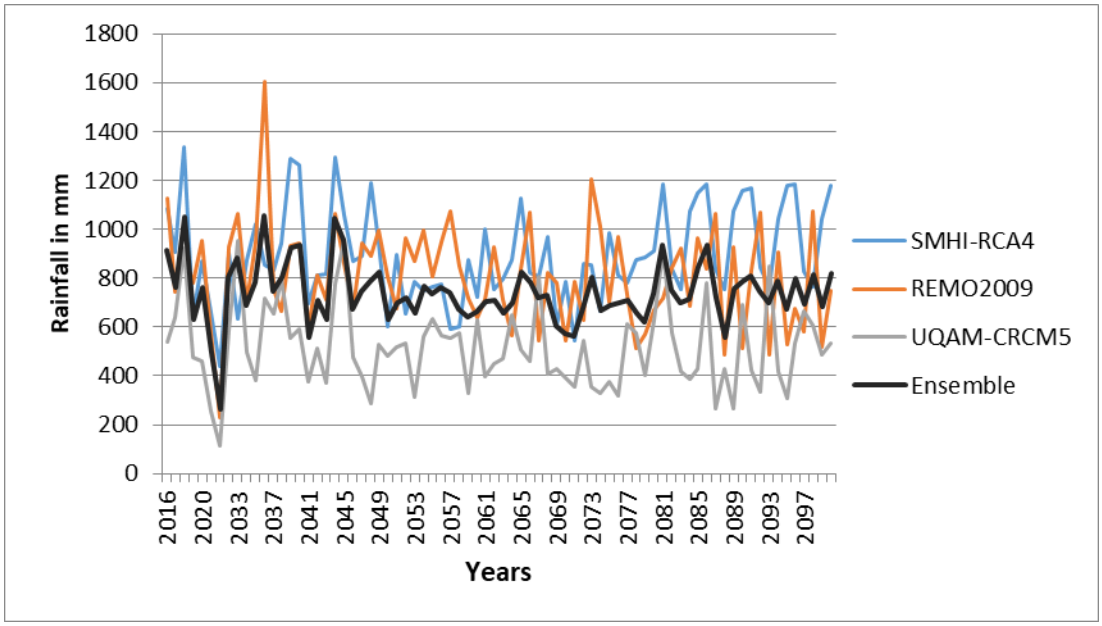

Figure 7.4: Annual average RCMs and the ensemble average for Mzingwane catchment

7.3.3 Trends in projected future rainfall (2016-2100)

An ensemble of the three RCMs (RCA4, REMO2009 and CRCM5) was used to compute trends for future rainfall (2016-2100). The simulated trend results indicate a significant spatial decrease in rainfall for all the stations at $p < 0.05$ (Table 7.3). Rainfall amount is projected to decrease significantly over the catchment during the mid and end of the century, with a high likelihood of variability in space and time. The magnitude of change is apparently high for all stations, with Sen's slope ranging between 1.4 and 5 for the period under study (Table 7.3). A decrease in rainfall was also projected by "IPCC - Intergovernmental Panel on Climate Change" (2007) for some areas in tropical regions.

7.3.4 Quantifying projected rainy days

The projected number of rainy days for the period 2016-2100 significantly decreased for Gwanda, Matopos and Beitbridge at a magnitude of -0.292, -0.18 and -0.121mm respectively for the entire period of study (Table 7.4). Other stations, such as Bulawayo (-0.109 year^{-1}),

Kezi (-0.143 year^{-1}), Filabusi (-0.158 year^{-1}), Plumtree (-0.0085 year^{-1}) and West Nicholson (-0.118 year^{-1}) exhibit a downward trend, albeit statistically insignificant. The projected number of rainy days accurately represents the spatial climatology of the stations.

Table 7.3: Mann-Kendall (MK) trend test for daily rainfall

Station	**Kendall's tau**	**P-value**	**Sen's slope**	
			In 84 years	**Per decade**
Bulawayo	-0.04	<0.0001	3.6	0.4
Gwanda	-0.03	<0.001	5.0	0.6
Kezi	-0.04	<0.0001	1.4	0.2
Matopos	-0.03	<0.0001	4.2	0.5
Filabusi	-0.12	<0.0001	5.0	0.6
Beitbridge	-0.04	<0.0001	4.5	0.5
Plumtree	-0.04	<0.0001	2.8	0.3
West Nicholson	-0.03	<0.0001	3.3	0.4

For instance, Beitbridge and Plumtree are the driest in the region and RCMs projected similar trends. On the contrary, there is a noticeable bias towards wetter conditions in West Nicholson, Filabusi and Gwanda. Overall, an ensemble of RCMs projected a general decrease in the number of rainy days for the future. However, a cursory temporary assessment of the results indicates that, although the number of rainy days is reduced, more extreme wetness and dryness are expected through space and time (Figure 7.4). These results conform to findings by Pohl *et al*. (2017) who also noted a decrease in the number of rainy days with more extreme rainfall by the end of the 21st century in southern Africa.

The foregoing observation is likely to modify the quality of the rainy season as a result of enhanced episodes of droughts and floods to the detriment of a number of bio-geographic cycles and wetland ecosystems in particular. For instance, literature shows that extreme rainfall affects wetlands in various ways; drought lowers water table through reduced ground water recharge, modifies runoff patterns, and affect the general wetland catchment hydrology

which in turn, may reduce wetland area and consequently force wetland floral and faunal species to migrate and in extreme cases be driven to extinction. In addition, flooding conditions also affect those endemic plant species with low tolerance levels (Pecl *et al*., 2017).

7.3.5 Projected future precipitation extremes

The ensemble of RCM (RCA4, REMO2009 AND CRCM5) projected rainfall for the mid (2016-2069) and end of the century (2070-2100) were used to compute a Standard Precipitation Index on a 3-month scale for the identification of probable future years likely to experience extreme precipitation events. Figure 5 represents a projected temporary time series of extreme events in Mzingwane catchment for the mid-century (Figure 7.5a) and end of the century (Figure 7.5b). Projections for the mid-century suggest less extreme dryness for the decade 2020-2030 than the extreme wet conditions, meaning that the decade is likely to experience more flooding conditions. Severe dryness (SPI $\leq$-1$\leq$-1.49) are projected to occur during following years; 2032, 2040, 2042, 2044, 2048, 2050, 2056, 2062, 2065 and 2068 (Figure 7.5a). While the probable years for extreme dryness (SPI $\leq$2) include 2038, 2034, 2054 and 2066. Notably, the last decade of the mid-century has more extreme dryness with only one extreme wet condition, suggesting recurrent droughts with great implications on food security, water availability and general ecosystem function, particularly the fragile wetland ecosystems.

Table 7.4: Mann-Kendall (MK) trends in number of projected rainy days

Station	Mean annual No. of rainy days	Kendall's tau	P-value	Sen's slope
Bulawayo	79	-0.083	0.266	-0.109
Gwanda	83	-0.282	**0.000***	-0.292
Kezi	73	-0.133	0.074	-0.143
Matopos	73	-0.158	**0.034***	-0.18
Filabusi	95	-0.130	0.081	-0.158
Beitbridge	53	-0.155	**0.038***	-0.121
Plumtree	57	-0.116	0.121	-0.085
West Nicholson	83	-0.111	0.135	-0.118

***significant at $p<0.05$*

Model projections for the future extreme wetness indicate only three years of moderate wet conditions (2033,2035 and 2061) shown in Figure 5a, but suggest more years of very wet conditions which include; 2030, 2034, 2041, 2046, 2048, 2051, 2051 and 2068. In addition, extreme wetness is projected for 2018, 2023, 2024, 2028, 2047 and 2058 (Figure 7.5a).

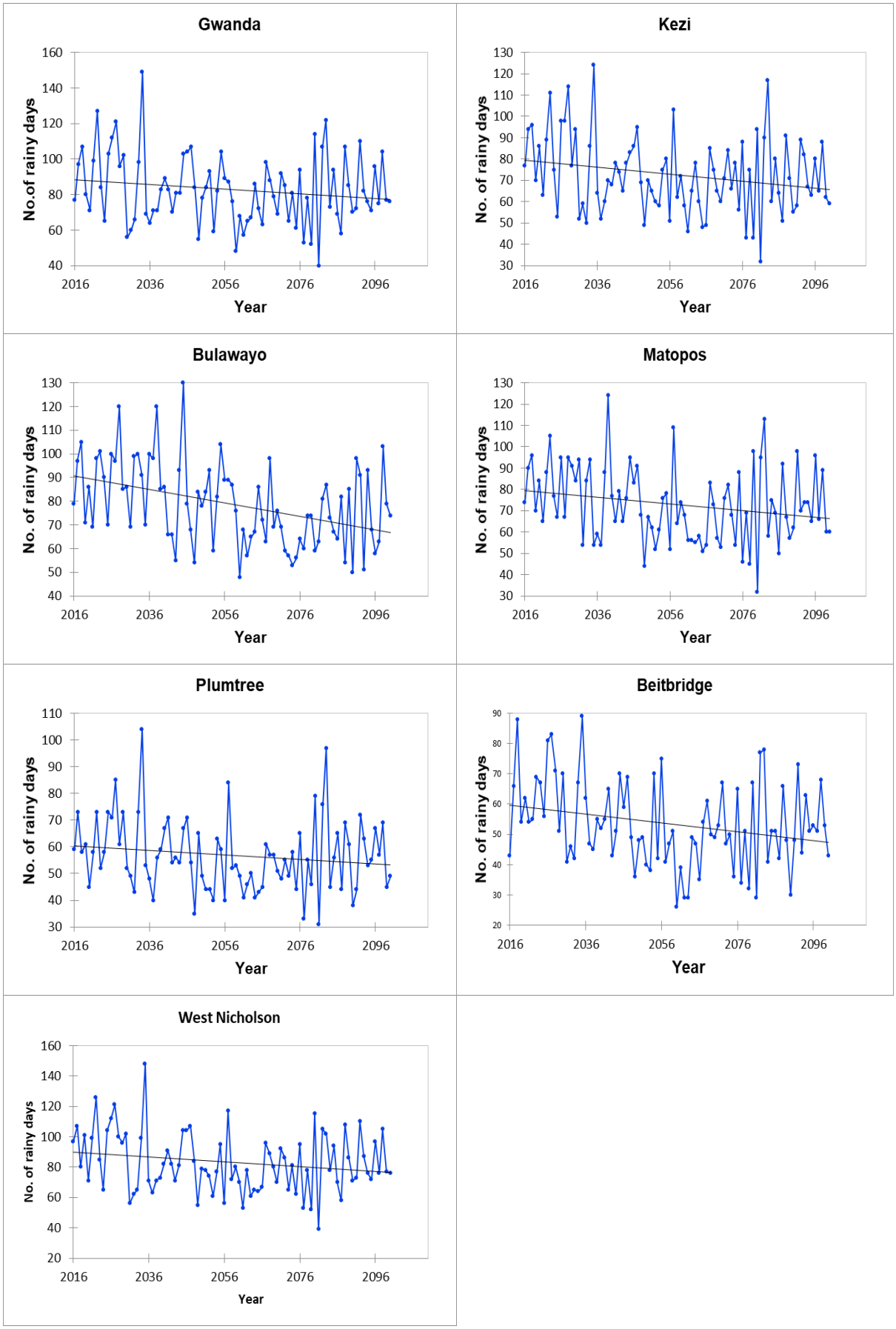

Figure 7.5: Projected number of rainy days for the period 2016-2100 per station

Generally, model projections suggest more extreme wetness conditions with high flooding risks and related consequences. These results suggest a high risk of flooding within the catchment, particularly during the mid-century period except the period 2060-2070 which is expected to experience recurrent droughts.

Projected extreme events for the end of the century (2070-2100) are shown in Figure 5b. Results show that only 2073 and 2098 are likely to experience moderate dryness while severe droughts are expected in 2071, 2078, 2079, 2080, 2081, 2085, 2088, 2091, 2092 and 2096 and seem to be having 2 years duration pattern during the end of century period. Only one extreme dry condition was identified in 2077. On the other hand, moderate extreme wet conditions (SPI $\geq 1.0 \leq 1.49$) are projected for 2073, 2074, 2083, 2084, 2088, 2089 and 2094. Very wet conditions are likely to be experienced in 2076, 2094, 2095, 2097 and 2098, while extreme wetness is projected for 2072, 2082 and 2093 with a noticeable 10 year cycle (Figure 7.5b). Such extreme wetness conditions will certainly pose flooding risks and disaster in the catchment, causing substantial threats to the environment and socio-economic well-being of the society in and around the catchment. The foregoing results are consistent with global circulation model results (IPCC, 2007) which projected an increase in precipitation extremes under global warming. Similar findings were reported by Pinto *et al*. (2016), who also noted a decrease in annual precipitation accompanied by an increase in the occurrence of projected extreme precipitation events over southern Africa. Extreme dry conditions (droughts) have huge implications on water availability in the catchment. In addition, if such extreme events recur, wetland ecosystems are likely to suffer not only from hydrologic modifications, but also from over harvesting by communities during dry periods leading to their shrinking and in some instances disappearance.

(a)

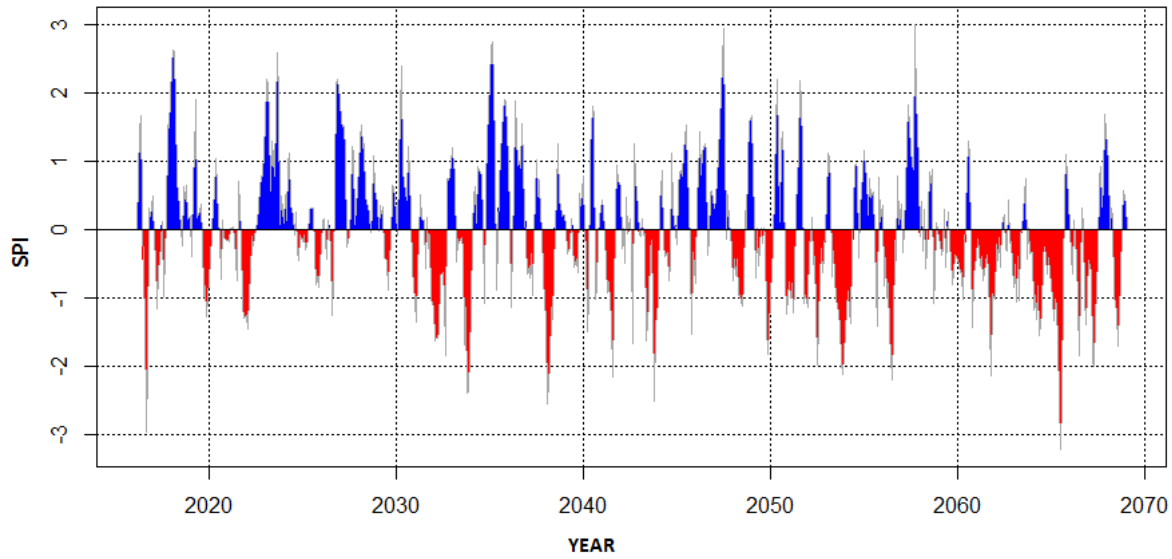

(b)

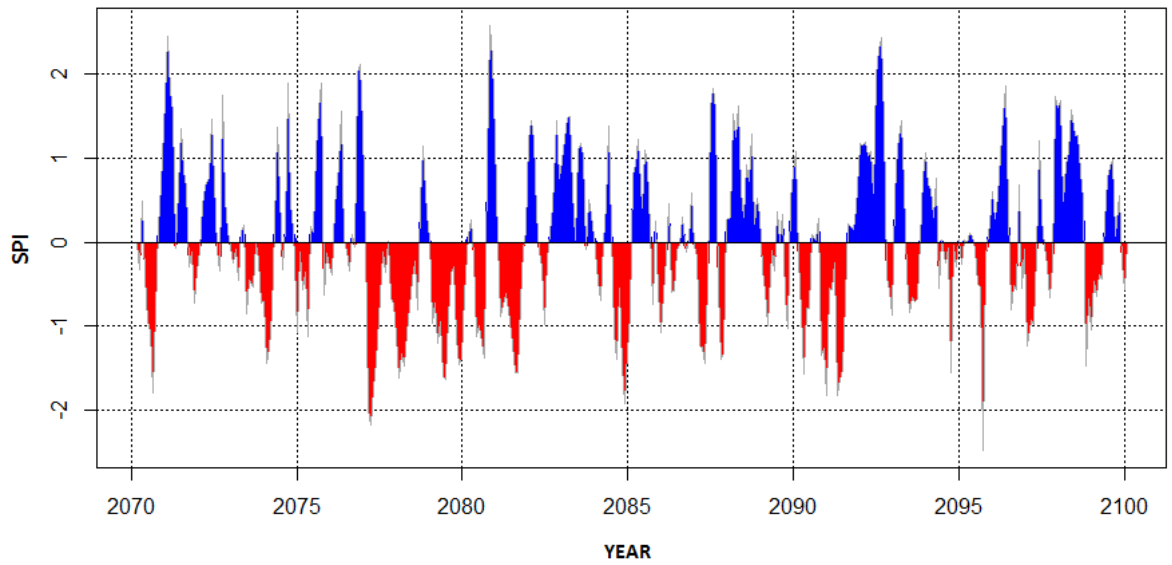

Figure 7.6: Projected extreme precipitation (a) for the mid-century 2016-2069 (b) end of century period 2070-2100

7.4 Implications of future rainfall on wetlands

Wetlands are highly susceptible to climate changes and variations and are likely to be affected by the changes in hydrologic regimes at catchment level, changes in precipitation patterns, increase in temperature and recurrent extreme weather events (Burkett and Kusler,

2000). Model projections suggest a decrease in precipitation and number of rainy days, with an increase in extreme events. Such changes will influence wetlands in various ways, such as the modification of the structure, pattern and general function of wetland ecosystems resulting from modified hydrology and biochemical cycles. A decrease in rainfall, coupled with increased evaporation related to high temperatures, will also reduce soil water and increase soil salinity which might subsequently reduce primary productivity and species diversity (Carrington *et al*., 2001; Lamsal *et al*., 2017). The projected future climate is likely to influence wetland area due to changes in hydrologic regimes. Figure 6 shows the relationship between wetland area and total rainfall and reveals that wetland area tends to increase with an increase in rainfall while the reverse is true, as the rainfall decreases, the wetland area shrinks in size. Such a trend has significant implications on the future of wetlands. Habitats will be modified, affecting species survival and reproduction which could either force species to migrate or be naturally eliminated if they fail to adapt (Barros and Albernaz, 2014).

Reduced rainfall and frequent dry extremes could result in low water levels which may also contribute to reduced wetland area. Projected future climates are likely to affect communities depending on the wetland ecosystem for water and economic livelihoods. It is noteworthy that future climate change impacts on wetlands will be exacerbated by anthropogenic land use/ land cover changes in wetland catchments. Therefore, sustainable future wetland conservation will require appropriate management of anthropogenic modifications so as to minimise climate change impacts.

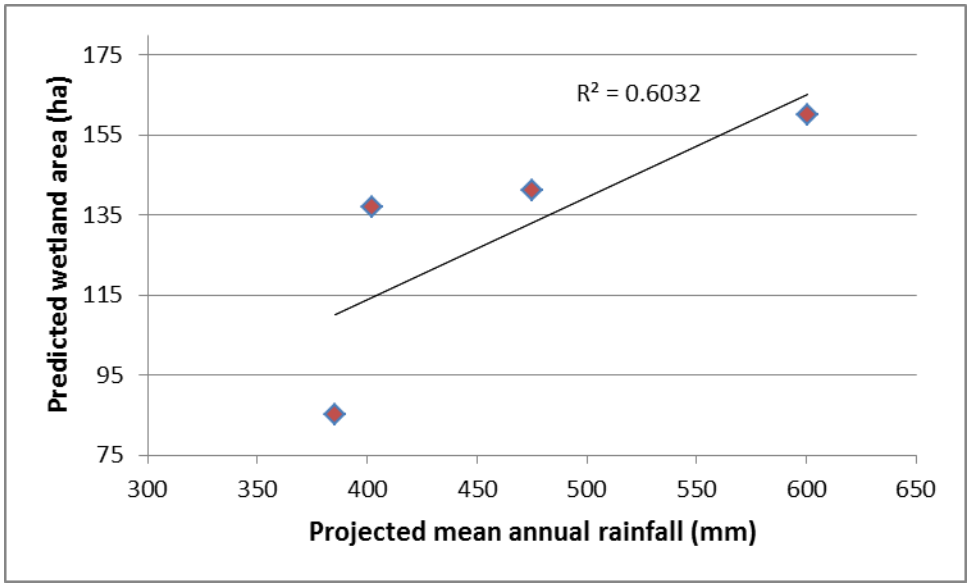

Figure 7.7: Correlation between predicted wetland area and projected rainfall for the periods 2015, 2025, 2035, and 2045 which gave four data points.

7.5 Conclusions

The study evaluated the ability of CORDEX RCMs to simulate future rainfall trends and extreme events for the period 2016-2100. RCMs sufficiently captured annual rainfall cycles and spatial distribution and all models managed to represent inter-annual rainfall variability and the ensemble of RCMs outperformed individual models. The results indicate a significant decrease in future rainfall for all stations at $p < 0.05$. A general decreasing trend in the number of rainy days is projected for the remainder of the century, although the magnitude of trend varied with locations. In addition, extreme events are expected to increase in occurrence in future, particularly towards the end of the century. Such continued climatic changes are a huge threat to wetland species survival and general natural systems functioning. The findings are imperative for future conservation and proactive development of sustainable adaptive and mitigative strategies essential for the protection of wetlands.

CHAPTER 8: SYNTHESIS, CONCLUSIONS AND RECOMMENDATIONS

8.1 Synthesis and general conclusions

This final chapter presents an overview of the key findings and conclusions of the thesis as well as recommendations for future studies. Literature shows that wetlands are diverse and useful ecosystems to both humans and natural systems, yet they are seriously threatened by human related activities and natural perturbations, which compromise their integrity and service provision. This study thus aimed to assess and predict the impacts of land use/cover and climate changes on the areal extent of wetlands, premised on the accelerated global wetland degradation and loss. Chapter two of the study reviewed relevant literature which helped reveal the gap of knowledge of concern. To achieve the broader aim and the specific objectives of the study, the third chapter of the study investigated spatio-temporal temperature and extreme weather events in the entire Mzingwane catchment for the period 1967 to 2015, using observed monthly temperature data. This was followed by chapter four which gave an in-depth analysis of the long-term rainfall characteristics (such as rainfall intensity, length of the rain season, rainfall onset and cessation dates, trends and number of rainy days in a given season) for the Mzingwane catchment of south-western Zimbabwe, for both historic period (1886-1906) and more recent times (1950-2015), based on available daily and monthly precipitation series. Having analysed climatic trends, the spatio-temporal changes in wetland distribution and areal extent over time were quantified using remote sensing techniques for 1984 to 2045 in chapter five and were correlated with climatic trends obtained from the third and fourth chapter. Chapter six of the thesis modelled the impacts of LU/LC changes on nested wetlands based on hydrologic modelling and GIS approach based on the wetland classification results obtained in chapter five. The last substantive chapter 7,

evaluated rainfall and extreme events based on projections from CORDEX-AFRICA data. This methodology helped to accomplish the aim and the objectives of the study.

The study concludes that there has been a significant increase in maximum temperatures at $p<0.005$ for 60% of the Mzingwane catchment, while the catchment minimum temperatures show an insignificant decreasing trend, extreme dryness has increased in frequency during the past two decades. Significant drying trends were noted for the summer rainy months, with consequential agricultural drought, while a tendency towards wet months was noted during winter months in mountainous regions. Notably, extreme events are recurring with longer duration during the current decade than the 20^{th} century. There is apparently a strong positive correlation between temperature and the NINO4 index, while SPEI-1 has a weak negative correlation with T_{max} but is strongly correlated with T_{min}. The SPEI-1 and NINO4 indices significantly correlate, which is confirmed by the correspondence of dry years with ENSO events. With regards to rainfall variation, the study concludes that the mean annual rainfall has not changed from historic (1896-1906) to contemporary times (1950-2015), but the number of rainy days (>=1mm) has decreased by almost 34%. The duration of the rain season has shortened, with longer intra-season dry spells which are detrimental to crop growth. There is a notable decrease in the number of rainy days for the period 1950-2015, which might be, in part, attributed to global warming and related climate variation. Results indicate a shift in the onset and cessation dates for rainy season. Onset date has moved from first and second dekad of October to the third dekad of November and in some cases encroaching into the second dekad of December. Cessation dates have shifted into the second dekad of April. Thus, a combination of a reduced number of rainy days and shortened rainy season has huge hydrologic implications for most natural ecosystems like wetlands. The results based on variability indices indicate strong rainfall variability, both in space and time. Seasonal PCI

indicated seasonality for summer and autumn seasons while winter rainfall substantially varied. Based on the SPI results, it is apparent that ENSO events play a profound role in spatio-temporal rainfall variability. Notably, extreme events seem to be occurring more frequent in the current century than during the 20th century. Generally, the results for rainy season characteristics show that the rain season is no longer reliable and as such poses high uncertainties to farmers which could be addressed through the provision of timely weather forecasts for effective planning and supplementary water through irrigation systems.

The study employed remote sensing packages in R program to map and detect changes in wetland and land use/cover in the Shashe sub-catchment and results confirm the need for RF parameter optimisation for accurate classification results. The results for land change analysis show a decline in woodland and wetland cover, which could be attributed to both human and climatic influences. Major conversions were from wetland cover to crop field, suggesting agricultural encroachment on wetland area which results in lowering the water table and consequently reduced wetland area. Wetland area is reported to have decreased by 6% in the last 30 years, which amounts to 115.6 hectares loss. Future LULC prediction suggests a decrease in wetland area by about 53% by 2045, which is equivalent to 72.68 hectares. Therefore, the study concludes that the total wetland area in Shashe sub-catchment is decreasing due to cumulative anthropogenic and natural impacts.

In terms of projecting future climatic conditions, Regional Climate Models from CORDEX-AFRICA data were examined. It was found that RCMs sufficiently captured annual rainfall cycles and spatial distribution and all models managed to represent inter-annual rainfall variability and the ensemble of RCMs outperformed individual models. The results indicated a significant decrease in future rainfall for all stations at $p < 0.05$, coupled with a general

decreasing trend in the number of rainy days, projected for the remainder of the century, although the magnitude of trend varied with locations. In addition, extreme events are expected to increase in occurrence in future, particularly at the end of the century. Such continued climatic changes are a huge threat to wetland species survival and general natural systems functioning. This highlights the need to develop relevant sustainable adaptive and mitigative strategies for the future.

In summary, temperatures are on a warming trend in Mzingwane catchment while extreme events are recurring more frequently during the 21st century. Contemporary mean annual rainfall has not changed from that during the historic period 1886-1906. However, the number of rainy days has decreased by 34%, suggesting a more concentrated and intense rainfall. The onset and cessation dates of the rainy season have shifted during the 21st century, resulting in a reduced length of the rainy season. Rainfall variability is strongly linked to ENSO phases. Wetlands in the Shashe sub-catchment have significantly decreased areal extents in the last 30 years (1984-2015) and are predicted to continue shrinking up to 2045. LU/LC changes modify wetland hydrology which consequently influences wetland area. Downscaled RCM projections suggest a decreasing trend in both future rainfall and number of rainy days, while future extremes are expected to increase in occurrence, although the severity will vary in space and time. Therefore, further work should be done on the impacts of climate and anthropogenic changes on other wetland dynamics such as wetland vegetation, water levels, wetland pollution and invasive species.

The study was buttressed by the combination of two major wetland stressors; climate and land use/land cover. The catchment approach was most appropriate for catchment level modelling while the prediction of both future climates and land cover provided a strong

foundation for the development of future proactive adaptation and mitigation strategies. However, the study was limited by inadequate spatial distribution of meteorological station particularly for temperature; the study relied on only four complete station data. The other limitation was low spatial and spectral resolutions for Landsat imagery of which better results could be obtained with high spatial and spectral resolution imagery.

8.2 Recommendations

Based on the foregoing conclusions, there is a pressing need to develop holistic catchment level strategies to address long- and short-term impacts of climate variations and land use changes on wetland ecosystems. Such measures will go a long way in curbing further wetland degradation and loss under the global environmental change spasm. The study thus recommends the following pre-emptive strategies;

- Adoption of community-based wetland management systems to promote proprietorship and encourage sustainable utilisation. This community-based approach may entail community level adaptation planning, utilisation of traditional skills, knowledge and practices to sustainable wetland management.
- To scale up wetland rehabilitation and conservation efforts with tighter regulations on wetland resource use.
- Enactment of wetland and land use policies that will foster sustainable utilisation and reduce destructive human activities in and around the wetlands.
- Improving rain water harvesting and storage facilities for the storage of erratic and intense rain water for use during the drier period so as to reduce pressure on wetlands which will help communities to adapt to changes in climate.

- There is also a need to design overreaching climate change policies and programmes focusing on poverty alleviation and sustainable development, which will promote general socio-economic development and in turn, reduce pressure on fragile wetlands.
- Any future efforts towards protection of the remaining wetlands should be combined with developing a sustainable relationship between social and ecological systems which will enable communities to adapt to the effects of changing climates.

REFERENCES

Adam, E., Mutanga, O., Abdel-Rahman, E.M., Ismail, R., 2014a. Estimating standing biomass in papyrus (*Cyperus papyrus* L.) swamp: exploratory of *in situ* hyperspectral indices and random forest regression. Int. J. Remote Sens. 35, 693–714. https://doi.org/10.1080/01431161.2013.870676

Adam, E., Mutanga, O., Odindi, J., Abdel-Rahman, E.M., 2014b. Land-use/cover classification in a heterogeneous coastal landscape using RapidEye imagery: evaluating the performance of random forest and support vector machines classifiers. Int. J. Remote Sens. 35, 3440–3458. https://doi.org/10.1080/01431161.2014.903435

Adam, E., Mutanga, O., Rugege, D., 2010. Multispectral and hyperspectral remote sensing for identification and mapping of wetland vegetation: a review. Wetl. Ecol. Manag. 18, 281–296. https://doi.org/10.1007/s11273-009-9169-z

Adam, E., Mutanga, O., Rugege, D., 2009. Multispectral and hyperspectral remote sensing for identification and mapping of wetland vegetation: a review. Wetl. Ecol. Manag. 18, 281–296. https://doi.org/10.1007/s11273-009-9169-z

Afzal, M., Gagnon, A.S., Mansell, M.G., 2015. Changes in the variability and periodicity of precipitation in Scotland. Theor. Appl. Climatol. 119, 135–159. https://doi.org/10.1007/s00704-014-1094-2

Akasheh, O.Z., Neale, C.M.U., Jayanthi, H., 2008. Detailed mapping of riparian vegetation in the middle Rio Grande River using high resolution multi-spectral airborne remote sensing. J. Arid Environ. 72, 1734–1744. https://doi.org/10.1016/j.jaridenv.2008.03.014

Akinsanola, K., Ogunjobi, I., Ajayi, V.., 2015. Assessing capabilities of Three Regional Climate Models over CORDEX AFRICA in simulating West African Summer

Monsoon Precipitation. Advances in Meteorology, Volume 2015, Article ID 935431, http://dx.doi.org/10.1155/2015/935431

Al-Hamdan, M.Z., Oduor, P., Flores, A.I., Kotikot, S.M., Mugo, R., Ababu, J., Farah, H., 2017. Evaluating land cover changes in Eastern and Southern Africa from 2000 to 2010 using validated Landsat and MODIS data. Int. J. Appl. Earth Obs. Geoinformation 62, 8–26. https://doi.org/10.1016/j.jag.2017.04.007

Andrew, M.E., Ustin, S.L., 2008. The role of environmental context in mapping invasive plants with hyperspectral image data. Remote Sens. Environ. 112, 4301–4317. https://doi.org/10.1016/j.rse.2008.07.016

Arguez, A., Vose, R.S., 2011. The Definition of the Standard WMO Climate Normal: The Key to Deriving Alternative Climate Normals. Bull. Am. Meteorol. Soc. 92, 699–704. https://doi.org/10.1175/2010BAMS2955.1

Asadi Zarch, M.A., Sivakumar, B., Sharma, A., 2015. Droughts in a warming climate: A global assessment of Standardized precipitation index (SPI) and Reconnaissance drought index (RDI). J. Hydrol. 526, 183–195. https://doi.org/10.1016/j.jhydrol.2014.09.071

Ashton, P.J., Love, D., Mahachi, H., Dirks, P., 2001. An overview of the impact of mining and mineral processing operations on water resources and water quality in the Zambezi, Limpopo and Olifants Catchments in Southern Africa. Contract Rep. Min. Miner. Sustain. Dev. South. Afr. Proj. CSIR-Environ. Pretoria Geol. Dep. Univ. Zimb.-Harare Rep. No ENV-PC 42.

Barbee, R.W., Heather, A., 2008. Natural climate variability and global warming: Holocene perspective. Blackwell Publishing Ltd, United Kingdom.

Bari, S.H., Hussain, M.M., Husna, N.-E.-A., 2017. Rainfall variability and seasonality in northern Bangladesh. Theor. Appl. Climatol. 129, 995–1001. https://doi.org/10.1007/s00704-016-1823-9

Barros, D., Albernaz, A., 2014. Possible impacts of climate change on wetlands and its biota in the Brazilian Amazon. Braz. J. Biol. 74, 810–820. https://doi.org/10.1590/1519-6984.04013

Barry, R., 1992. Mountain weather and Climate, Second. ed. Routledge, USA.

Batisani, N., Yarnal, B., 2010. Rainfall variability and trends in semi-arid Botswana: Implications for climate change adaptation policy. Appl. Geogr. 30, 483–489. https://doi.org/10.1016/j.apgeog.2009.10.007

Beguería, S., Vicente-Serrano, S.M., Reig, F., Latorre, B., 2014. Standardized precipitation evapotranspiration index (SPEI) revisited: parameter fitting, evapotranspiration models, tools, datasets and drought monitoring. Int. J. Climatol. 34, 3001–3023. https://doi.org/10.1002/joc.3887

Bennie, J., Huntley, B., Wiltshire, A., Hill, M.O., Baxter, R., 2008. Slope, aspect and climate: Spatially explicit and implicit models of topographic microclimate in chalk grassland. Ecol. Model. 216, 47–59. https://doi.org/10.1016/j.ecolmodel.2008.04.010

Berakhi, R.O., Oyana, T.J., Adu-Prah, S., 2015. Land use and land cover change and its implications in Kagera river basin, East Africa. Afr. Geogr. Rev. 34, 209–231. https://doi.org/10.1080/19376812.2014.912140

Bisht, D.S., Chatterjee, C., Raghuwanshi, N.S., Sridhar, V., 2017. Spatio-temporal trends of rainfall across Indian river basins. Theor. Appl. Climatol. https://doi.org/10.1007/s00704-017-2095-8

Borges, A.V., Darchambeau, F., Lambert, T., Bouillon, S., Morana, C., Brouyère, S., Hakoun, V., Jurado, A., Tseng, H.-C., Descy, J.-P., Roland, F.A.E., 2018. Effects of

agricultural land use on fluvial carbon dioxide, methane and nitrous oxide concentrations in a large European river, the Meuse (Belgium). Sci. Total Environ. 610–611, 342–355. https://doi.org/10.1016/j.scitotenv.2017.08.047

Bourgeau-Chavez, L., Endres, S., Battaglia, M., Miller, M., Banda, E., Laubach, Z., Higman, P., Chow-Fraser, P., Marcaccio, J., 2015. Development of a Bi-National Great Lakes Coastal Wetland and Land Use Map Using Three-Season PALSAR and Landsat Imagery. Remote Sens. 7, 8655–8682. https://doi.org/10.3390/rs70708655

Breiman, L., 2001. Random forests. Mach. Learn. 45, 5–32.

Breiman, L., 1996. Bagging predictors. Mach. Learn. 24, 123–140.

Bremner, J., 2017. Population, food security and climate change, in: Africa's Population; In Search of a Demographic Dividend.

Brown, P.T., Caldeira, K., 2017. Greater future global warming inferred from Earth's recent energy budget. Nature 552, 45.

Brunsell, N.A., Jones, A.R., Jackson, T.L., Feddema, J.J., 2009. Seasonal trends in air temperature and precipitation in IPCC AR4 GCM output for Kansas, USA: evaluation and implications. Int. J. Climatol. 30, 1178–1193. https://doi.org/10.1002/joc.1958

Buckle, C., 1996. Weather and Climate in Africa. Longman, Harlow.

Burkett, V., Kusler, J., 2000. Climate change: Potential impacts and interactions in wetlands of the United States. Wiley Online Library.

Camacho, V.V., Ruiz-Luna, A., Berlanga-Robles, A.C., 2016. Effects of Land Use Changes on Ecosystem Services Value Provided By Coastal Wetlands: Recent and Future Landscape Scenarios. J Coast Zone Manag 19, 418.

Camberlin, P., Janicot, S., Poccard, I., 2001. Seasonality and atmospheric dynamics of the teleconnection between African rainfall and tropical sea-surface temperature: Atlantic vs. ENSO. Int. J. Climatol. 21, 973–1005. https://doi.org/10.1002/joc.673

Camberlin, P., Okoola, R.E., 2003. The onset and cessation of the “long rains” in eastern Africa and their interannual variability. Theor. Appl. Climatol. 75, 43–54.

Carrington, D.P., Gallimore, R.G., Kutzbach, J.E., 2001. Climate sensitivity to wetlands and wetland vegetation in mid-Holocene North Africa. Clim. Dyn. 17, 151–157.

Carson, M., Köhl, A., Stammer, D., A. Slangen, A.B., Katsman, C.A., W. van de Wal, R.S., Church, J., White, N., 2016. Coastal sea level changes, observed and projected during the 20th and 21st century. Clim. Change 134, 269–281. https://doi.org/10.1007/s10584-015-1520-1

Chaikumbung, M., Doucouliagos, H., Scarborough, H., 2016. The economic value of wetlands in developing countries: A meta-regression analysis. Ecol. Econ. 124, 164–174. https://doi.org/10.1016/j.ecolecon.2016.01.022

Chan, K.K.Y., Xu, B., 2013. Perspective on remote sensing change detection of Poyang Lake wetland. Ann. GIS 19, 231–243. https://doi.org/10.1080/19475683.2013.843589

Change, I.C., 2013. The Physical Science Basis. Working Group I Contribution to the Fifth Assessment Report of the Intergovernmental Panel on Climate Change. Camb. U. K. N. Y. USA.

Chen, L., Jin, Z., Michishita, R., Cai, J., Yue, T., Chen, B., Xu, B., 2014. Dynamic monitoring of wetland cover changes using time-series remote sensing imagery. Ecol. Inform. 24, 17–26. https://doi.org/10.1016/j.ecoinf.2014.06.007

Chenje, M., Sola, L., Palencny, D. (Eds.), 1998. The state of Zimbabwe’s Environment. Ministry of Mines, Environment and Tourism, Harare.

Chikodzi, D., Mutowo, G., 2014. Analysis of climate change signatures on micro-catchments as a means of understanding drying up of wetlands: The Case of Mutubuki Wetland. Ethiop. J. Environ. Stud. Manag. 7, 821. https://doi.org/10.4314/ejesm.v7i2.2S

Clark Labs, 2017. TerrSet Geospatial Monitoring and Modelling software. Clark University.

Clark, M.P., Nijssen, B., Lundquist, J.D., Kavetski, D., Rupp, D.E., Woods, R.A., Freer, J.E., Gutmann, E.D., Wood, A.W., Brekke, L.D. and Arnold, J.R., 2015. A unified approach for process-based hydrologic modeling: 1. Modeling concept. *Water Resources Research*, *51*(4), pp.2498-2514.

Congalton, R., 1991. A review of assessing accuracy of classification of Remote sensing data. Remote Sensing of Environment 37, 35–46.

Cook, C., Reason, C.J., Hewitson, B.C., 2004. Wet and dry spells within particularly wet and dry summers in the South African summer rainfall region. Clim. Res. 26, 17–31.

Cousins, S.A.O., Auffret, A.G., Lindgren, J., Tränk, L., 2015. Regional-scale land-cover change during the 20th century and its consequences for biodiversity. AMBIO 44, 17–27. https://doi.org/10.1007/s13280-014-0585-9

Cowardin, L.M., Carter, V., Golet, F.C., LaRoe, E.T., 1979. Classification of wetlands and deepwater habitats of the United States. US Department of the Interior, US Fish and Wildlife Service.

Cuo, L., Zhang, Y., Gao, Y., Hao, Z., Cairang, L., 2013. The impacts of climate change and land cover/use transition on the hydrology in the upper Yellow River Basin, China. J. Hydrol. 502, 37–52. https://doi.org/10.1016/j.jhydrol.2013.08.003

Dai, A., 2011. Characteristics and trends in various forms of the Palmer Drought Severity Index during 1900–2008. J. Geophys. Res. 116. https://doi.org/10.1029/2010JD015541

Dai, A., Trenberth, K.E., Karl, T.R., 1999. Effects of clouds, soil moisture, precipitation, and water vapor on diurnal temperature range. J. Clim. 12, 2451–2473.

Davranche, A., Lefebvre, G., Poulin, B., 2010a. Wetland monitoring using classification trees and SPOT-5 seasonal time series. Remote Sens. Environ. 114, 552–562. https://doi.org/10.1016/j.rse.2009.10.009

Davranche, A., Lefebvre, G., Poulin, B., 2010b. Wetland monitoring using classification trees and SPOT-5 seasonal time series. Remote Sens. Environ. 114, 552–562. https://doi.org/10.1016/j.rse.2009.10.009

De Cauwer, B., Reheul, D., 2009. Impact of land use on vegetation composition, diversity and potentially invasive, nitrophilous clonal species in a wetland region in Flanders. Agron. Sustain. Dev. 29, 277–285. https://doi.org/10.1051/agro:2008049

Dini, J.A., Cowan, G.I., 2001. Proposed classification system for the South African National Wetland Inventory,p.73. Diodato, N., 2005. The influence of topographic co-variables on the spatial variability of precipitation over small regions of complex terrain. Int. J. Climatol. 25, 351–363. https://doi.org/10.1002/joc.1131

Dong, Z., Wang, Z., Liu, D., Song, K., Li, L., Jia, M., Ding, Z., 2014. Mapping Wetland Areas Using Landsat-Derived NDVI and LSWI: A Case Study of West Songnen Plain, Northeast China. J. Indian Soc. Remote Sens. 42, 569–576. https://doi.org/10.1007/s12524-013-0357-1

Dosio, A., Panitz, H.-J., 2016. Climate change projections for CORDEX-Africa with COSMO-CLM regional climate model and differences with the driving global climate models. Clim. Dyn. 46, 1599–1625. https://doi.org/10.1007/s00382-015-2664-4

Dronova, I., Gong, P., Wang, L., Zhong, L., 2015. Mapping dynamic cover types in a large seasonally flooded wetland using extended principal component analysis and object-based classification. Remote Sens. Environ. 158, 193–206. https://doi.org/10.1016/j.rse.2014.10.027

Edoga, R.N., 2007. Determination of length of growing season in Samaru using different potential evapotranspiration models. AU JT 11, 28–35.

Edwards, R.W., Brown, M.W., 1960. An Aerial Photographic Method for Studying the Distribution of Aquatic Macrophytes in Shallow Waters. J. Ecol. 48, 161. https://doi.org/10.2307/2257314

Ellery, F., 2015. Classification System for Wetlands and Other Aquatic Ecosystems in South Africa. Afr. J. Range Forage Sci. 32, 290–291. https://doi.org/10.2989/10220119.2015.1025843

Ellery, W., Grenfell M., Jaganath C., Kotze M. H., 2010. A method for assessing cumulative impacts on wetlands function at the catchment o Landscape scale. WRC.

Ellery, W., Grenfell, S., Grenfell, M., Powell, R., Kotze, D., Marren, P., Knight, J., 2016. Wetlands in southern Africa: a geomorphic threshold perspective, in: Quaternary Environmental Change in Southern Africa: Physical and Human Dimensions. Cambridge, United Kingdom: Cambridge University Press, pp. 188–202.

Erwin, K.L., 2009. Wetlands and global climate change: the role of wetland restoration in a changing world. Wetl. Ecol. Manag. 17, 71–84. https://doi.org/10.1007/s11273-008-9119-1

Esteves, F.A., Caliman, A., Santangelo, J.M., Guariento, R.D., Farjalla, V.F., Bozelli, R.L., 2008. Neotropical coastal lagoons: an appraisal of their biodiversity, functioning, threats and conservation management. Braz. J. Biol. 68, 967–981.

FAO (Ed.), 2013. The multiple dimensions of food security, the state of food insecurity in the world. FAO, Rome.

FAO, 2010. Global Forest Resources Assessment 2010. Rome.

Fauchereau, N., Trzaska, S., Rouault, M., Richard, Y., 2003. Rainfall variability and changes in southern Africa during the 20th century in the global warming context. Nat. Hazards 29, 139–154.

Feng, L., Han, X., Hu, C., Chen, X., 2016a. Four decades of wetland changes of the largest freshwater lake in China: Possible linkage to the Three Gorges Dam? Remote Sens. Environ. 176, 43–55. https://doi.org/10.1016/j.rse.2016.01.011

Feng, L., Han, X., Hu, C., Chen, X., 2016b. Four decades of wetland changes of the largest freshwater lake in China: Possible linkage to the Three Gorges Dam? Remote Sens. Environ. 176, 43–55. https://doi.org/10.1016/j.rse.2016.01.011

Feng, L., Hu, C., Chen, X., Cai, X., Tian, L., Gan, W., 2012. Assessment of inundation changes of Poyang Lake using MODIS observations between 2000 and 2010. Remote Sens. Environ. 121, 80–92. https://doi.org/10.1016/j.rse.2012.01.014

Ferrati, R., Canziani, G.A., 2005. An analysis of water level dynamics in Esteros del Ibera wetland. Ecol. Model. 186, 17–27. https://doi.org/10.1016/j.ecolmodel.2005.01.019

Field, C.D., 1995. Impact of expected climate change on mangroves. Hydrobiologia 295, 75–81.

Finlayson, C.M., 2016. Climate Change and Wetlands, in: Finlayson, C.M., Everard, M., Irvine, K., McInnes, R.J., Middleton, B.A., van Dam, A.A., Davidson, N.C. (Eds.), The Wetland Book: I: Structure and Function, Management and Methods. Springer Netherlands, Dordrecht, pp. 1–12.

Finlayson, C.M., Davis, J.A., Gell, P.A., Kingsford, R.T., Parton, K.A., 2013. The status of wetlands and the predicted effects of global climate change: the situation in Australia. Aquat. Sci. 75, 73–93. https://doi.org/10.1007/s00027-011-0232-5

Fitchett, J.M., Grab, S.W., 2014. A 66-year tropical cyclone record for south-east Africa: temporal trends in a global context. Int. J. Climatol. 34, 3604–3615. https://doi.org/10.1002/joc.3932

Foody, G.M., Campbell, N.A., Trodd, N.M. and Wood, T.F., 1992. Derivation and applications of probabilistic measures of class membership from the maximum-

likelihood classification. *Photogrammetric engineering and remote sensing*, *58*(9), pp.1335-1341.

Gajbhiye, S., Meshram, C., Mirabbasi, R., Sharma, S.K., 2016. Trend analysis of rainfall time series for Sindh river basin in India. Theor. Appl. Climatol. 125, 593–608. https://doi.org/10.1007/s00704-015-1529-4

Galatowitsch, S.M., 2016. Natural and Anthropogenic Drivers of Wetland Change, in: Finlayson, C.M., Milton, G.R., Prentice, R.C., Davidson, N.C. (Eds.), The Wetland Book: II: Distribution, Description and Conservation. Springer Netherlands, Dordrecht, pp. 1–10. https://doi.org/10.1007/978-94-007-6173-5_217-1

Gallo, K.P., Owen, T.W., Easterling, D.R., Jamason, P.F., 1999. Temperature trends of the US historical climatology network based on satellite-designated land use/land cover. J. Clim. 12, 1344–1348.

Gardner, R.C., Barchiesi, S., Beltrame, C., Finlayson, C.M., Galewski, T., Harrison, I., Paganini, M., Perennou, C., Pritchard, D., Rosenqvist, A., others, 2015. State of the World's Wetlands and Their Services to People: A Compilation of Recent Analyses.

Ghosh, S., Mishra, D.R., Gitelson, A.A., 2016. Long-term monitoring of biophysical characteristics of tidal wetlands in the northern Gulf of Mexico — A methodological approach using MODIS. Remote Sens. Environ. 173, 39–58. https://doi.org/10.1016/j.rse.2015.11.015

Glick, P., Clough, J., Polaczyk, A., Couvillion, B., Nunley, B., 2013. Potential Effects of Sea-Level Rise on Coastal Wetlands in Southeastern Louisiana. J. Coast. Res. 63, 211–233. https://doi.org/10.2112/SI63-0017.1

Görgens, A.H.M., Boroto, R.A., 1997. Limpopo River: flow balance anomalies, surprises and implications for integrated water resources management. Proc. 8th South Afr. Natl. Hydrol. Symp.

Govender, M., Chetty, K., Bulcock, H., 2007. A review of hyperspectral remote sensing and its application in vegetation and water resource studies. Water Sa 33, 145–151.

Grimm, R., Behrens, T., Märker, M., Elsenbeer, H., 2008. Soil organic carbon concentrations and stocks on Barro Colorado Island — Digital soil mapping using Random Forests analysis. Geoderma 146, 102–113. https://doi.org/10.1016/j.geoderma.2008.05.008

Guofu, L., Shengyan, D., 2004. Impacts of human activity and natural change on the wetland landscape pattern along the Yellow River in Henan Province. J. Geogr. Sci. 14, 339–348.

Haack, B., 1996. Monitoring wetland changes with remote sensing: an East African example. Environ. Manage. 20, 411–419.

Hagen, A., 2002. Multi-method assessment of map similarity, in: Proceedings of the Fifth AGILE Conference on Geographic Information Science, Palma, Spain. Association of Geographic Information Laboratories Europe, pp. 171–182.

Hamed, K.H., Rao, A.R., 1998. A modified Mann-Kendall trend test for autocorrelated data. J. Hydrol. 204, 182–196.

Han, X., Chen, X., Feng, L., 2015. Four decades of winter wetland changes in Poyang Lake based on Landsat observations between 1973 and 2013. Remote Sens. Environ. 156, 426–437. https://doi.org/10.1016/j.rse.2014.10.003

Hansen, J., Sato, M., Hearty, P., Ruedy, R., Kelley, M., Masson-Delmotte, V., Russell, G., Tselioudis, G., Cao, J., Rignot, E., Velicogna, I., Tormey, B., Donovan, B., Kandiano, E., von Schuckmann, K., Kharecha, P., Legrande, A.N., Bauer, M., Lo, K.-W., 2016. Ice melt, sea level rise and superstorms: evidence from paleoclimate data, climate modeling, and modern observations that 2 °C global warming could be dangerous. Atmospheric Chem. Phys. 16, 3761–3812. https://doi.org/10.5194/acp-16-3761-2016

Haque, M.I., Basak, R., 2017. Land cover change detection using GIS and remote sensing techniques: A spatio-temporal study on Tanguar Haor, Sunamganj, Bangladesh. Egypt. J. Remote Sens. Space Sci. https://doi.org/10.1016/j.ejrs.2016.12.003

Hayashi, M., van der Kamp, G., Rosenberry, D.O., 2016. Hydrology of Prairie Wetlands: Understanding the Integrated Surface-Water and Groundwater Processes. Wetlands 36, 237–254. https://doi.org/10.1007/s13157-016-0797-9

Herrera, S., Gutiérrez, J.M., Ancell, R., Pons, M.R., Frías, M.D., Fernández, J., 2012. Development and analysis of a 50-year high-resolution daily gridded precipitation dataset over Spain (Spain02). Int. J. Climatol. 32, 74–85. https://doi.org/10.1002/joc.2256

Houlahan, J.E., Keddy, P.A., Makkay, K., Findlay, C.S., 2006. The effects of adjacent land use on wetland species richness and community composition. Wetlands 26, 79–96.

House, A.R., Thompson, J.R., Acreman, M.C., 2016. Projecting impacts of climate change on hydrological conditions and biotic responses in a chalk valley riparian wetland. J. Hydrol. 534, 178–192. https://doi.org/10.1016/j.jhydrol.2016.01.004

Hughes, D.A., Andersson, L., Wilk, J., Savenije, H.H.G., 2006a. Regional calibration of the Pitman model for the Okavango River. J. Hydrol. 331, 30–42. https://doi.org/10.1016/j.jhydrol.2006.04.047

Hughes, D.A., Demuth, S., Gustard, A., Planos, E., Seatena, F., Servat, E., 2006b. An evaluation of the potential use of satellite rainfall data for input to water resource estimation models in southern Africa. IAHS Publ. 308, 75.

Hulme, M., Doherty, R., Ngara, T., New, M., Lister, D., 2001. African climate change: 1900-2100. Clim. Res. 17, 145–168.

Huu Nguyen, H., Dargusch, P., Moss, P., Tran, D.B., 2016. A review of the drivers of 200 years of wetland degradation in the Mekong Delta of Vietnam. Reg. Environ. Change 16, 2303–2315. https://doi.org/10.1007/s10113-016-0941-3

Ibarrola-Rivas, M.J., Granados-Ramírez, R., Nonhebel, S., 2017. Is the available cropland and water enough for food demand? A global perspective of the Land-Water-Food Nexus. Adv. Water Resour. https://doi.org/10.1016/j.advwatres.2017.09.018

Ibharim, N.A., Mustapha, M.A., Lihan, T., Mazlan, A.G., 2015. Mapping mangrove changes in the Matang Mangrove Forest using multi temporal satellite imageries. Ocean Coast. Manag. 114, 64–76. https://doi.org/10.1016/j.ocecoaman.2015.06.005

Ibrahim, S., Hashim, I., 1990. Classification of mangrove forest by using 1:40 000-scale aerial photographs. For. Ecol. Manag. 33–34, 583–592. https://doi.org/10.1016/0378-1127(90)90220-6

International Institute of Sustainable Development, 2012. Summary of the 11th Conference of the parties to the Ramsar Convention on wetlands. Earth Negotiations 17.

IPCC, 2014. Climate change 2014: Impacts, Adaptation and Vulnerability. Part B:Regional Aspects. Cambridge University Press, USA.

IPCC - Intergovernmental Panel on Climate Change [WWW Document], 2007. URL https://www.ipcc.ch/publications_and_data/publications_ipcc_fourth_assessment_report_synthesis_report.htm (accessed 7.18.16).

Jhonnerie, R., Siregar, V.P., Nababan, B., Prasetyo, L.B., Wouthuyzen, S., 2015. Mangrove coverage change detection using Landsat imageries based on hybrid classification in Lembung river, Bengkalis Island, Riau province. J. Ilmu Dan Teknol. Kelaut. Trop. 6.

Jogo, W., Hassan, R., 2010. Balancing the use of wetlands for economic well-being and ecological security: The case of the Limpopo wetland in southern Africa. Ecol. Econ. 69, 1569–1579. https://doi.org/10.1016/j.ecolecon.2010.02.021

Johannessen, C.L., 1964. Marshes prograding in Oregon: aerial photographs. Science 1575–1578.

Johansen, K., Phinn, S., 2006. Mapping Structural Parameters and Species Composition of Riparian Vegetation Using IKONOS and Landsat ETM+ Data in Australian Tropical Savannahs. Photogramm. Eng. Remote Sens. 72, 71–80. https://doi.org/10.14358/PERS.72.1.71

Joshua, N.N., Onalenna, G., 2014. Public perceptions of climate variability risks on wetland management: A case of ward 15 of Matobo North District, Zimbabwe. Asian J. Soc. Sci. Humanit. Vol 3, 1.

Junk, W.J., An, S., Finlayson, C.M., Gopal, B., Květ, J., Mitchell, S.A., Mitsch, W.J., Robarts, R.D., 2013. Current state of knowledge regarding the world's wetlands and their future under global climate change: a synthesis. Aquat. Sci. 75, 151–167. https://doi.org/10.1007/s00027-012-0278-z

Jury, M., 2013. Climate trends in Southern Africa. S Afr. J Sci. 109.

Jury, M., Rautenbach, H., Tadross, M., Philipp, A., 2007. Evaluating spatial scales of climate variability in sub-Saharan Africa. Theor. Appl. Climatol. 88, 169–177. https://doi.org/10.1007/s00704-006-0251-7

Kabii, T., 1996. An overview of African wetlands.

Kalognomou, E.-A., Lennard, C., Shongwe, M., Pinto, I., Favre, A., Kent, M., Hewitson, B., Dosio, A., Nikulin, G., Panitz, H.-J., Büchner, M., 2013. A Diagnostic Evaluation of Precipitation in CORDEX Models over Southern Africa. J. Clim. 26, 9477–9506. https://doi.org/10.1175/JCLI-D-12-00703.1

Kapangaziwiri, E., 2011. Regional application of the Pitman monthly rainfall-runoff model in southern Africa incorporating uncertainty. Rhodes University.

Karl, T.R., Jones, P.D., Knight, R.W., Kukla, G., Plummer, N., Razuvayev, V., Gallo, K.P., Lindseay, J., Charlson, R.J., Peterson, T.C., 1993. Asymmetric trends of daily maximum and minimum temperature. Pap. Nat. Resour. 185.

Kashaigili, J.J., Mbilinyi, B.P., Mccartney, M., Mwanuzi, F.L., 2006. Dynamics of Usangu plains wetlands: Use of remote sensing and GIS as management decision tools. Phys. Chem. Earth Parts ABC 31, 967–975. https://doi.org/10.1016/j.pce.2006.08.007

Klemas, V., 2011. Remote Sensing of Wetlands: Case Studies Comparing Practical Techniques. J. Coast. Res. 418–427. https://doi.org/10.2112/JCOASTRES-D-10-00174.1

Kruger, A.C., Nxumalo, M., 2017. Surface temperature trends from homogenized time series in South Africa: 1931-2015: TEMPERATURE TRENDS IN SOUTH AFRICA: 1931-2015. Int. J. Climatol. 37, 2364–2377. https://doi.org/10.1002/joc.4851

Kruger, A.C., Sekele, S.S., 2013a. Trends in extreme temperature indices in South Africa: 1962-2009. Int. J. Climatol. 33, 661–676. https://doi.org/10.1002/joc.3455

Kruger, A.C., Sekele, S.S., 2013b. Trends in extreme temperature indices in South Africa: 1962-2009. Int. J. Climatol. 33, 661–676. https://doi.org/10.1002/joc.3455

Kruger, A.C., Shongwe, S., 2004a. Temperature trends in South Africa: 1960–2003. Int. J. Climatol. 24, 1929–1945.

Kruger, A.C., Shongwe, S., 2004b. Temperature trends in South Africa: 1960–2003. Int. J. Climatol. 24, 1929–1945.

Kumar, L., Sinha, P., 2014. Mapping salt-marsh land-cover vegetation using high-spatial and hyperspectral satellite data to assist wetland inventory. GIScience Remote Sens. 51, 483–497. https://doi.org/10.1080/15481603.2014.947838

Kusangaya, S., Warburton, M.L., Archer van Garderen, E., Jewitt, G.P.W., 2014. Impacts of climate change on water resources in southern Africa: A review. Phys. Chem. Earth Parts ABC 67–69, 47–54. https://doi.org/10.1016/j.pce.2013.09.014

Lakhraj-Govender, R., Grab, S., Ndebele, N.E., 2016. A homogenized long-term temperature record for the Western Cape Province in South Africa: 1916-2013: LONG-TERM TEMPERATURE RECORD FOR THE WESTERN CAPE IN SOUTH AFRICA. Int. J. Climatol. https://doi.org/10.1002/joc.4849

Lamsal, P., Kumar, L., Atreya, K., Pant, K.P., 2017. Vulnerability and impacts of climate change on forest and freshwater wetland ecosystems in Nepal: A review. Ambio 46, 915–930. https://doi.org/10.1007/s13280-017-0923-9

Landmann, T., Schramm, M., Colditz, R.R., Dietz, A., Dech, S., 2010. Wide Area Wetland Mapping in Semi-Arid Africa Using 250-Meter MODIS Metrics and Topographic Variables. Remote Sens. 2, 1751–1766. https://doi.org/10.3390/rs2071751

Lean, J.L., Rind, D.H., 2009. How will Earth's surface temperature change in future decades?: SURFACE TEMPERATURE FORECASTS. Geophys. Res. Lett. 36, n/a-n/a. https://doi.org/10.1029/2009GL038932

Lee, H., Yuan, T., Jung, H.C., Beighley, E., 2015. Mapping wetland water depths over the central Congo Basin using PALSAR ScanSAR, Envisat altimetry, and MODIS VCF data. Remote Sens. Environ. 159, 70–79. https://doi.org/10.1016/j.rse.2014.11.030

Lee, S.-Y., Ryan, M.E., Hamlet, A.F., Palen, W.J., Lawler, J.J., Halabisky, M., 2015a. Projecting the Hydrologic Impacts of Climate Change on Montane Wetlands. PLOS ONE 10, e0136385. https://doi.org/10.1371/journal.pone.0136385

Lee, S.-Y., Ryan, M.E., Hamlet, A.F., Palen, W.J., Lawler, J.J., Halabisky, M., 2015b. Projecting the Hydrologic Impacts of Climate Change on Montane Wetlands. PLOS ONE 10, e0136385. https://doi.org/10.1371/journal.pone.0136385

Li, X., Xue, Z., Gao, J., 2016. Dynamic Changes of Plateau Wetlands in Madou County, the Yellow River Source Zone of China: 1990–2013. Wetlands 1–12. https://doi.org/10.1007/s13157-016-0739-6

Liu, J., Feng, Q., Gong, J., Zhou, J., Li, Y., 2016. Land-cover classification of the Yellow River Delta wetland based on multiple end-member spectral mixture analysis and a Random Forest classifier. Int. J. Remote Sens. 37, 1845–1867. https://doi.org/10.1080/01431161.2016.1165888

Love, D., Uhlenbrook, S., Twomlow, S., Zaag, P. van der, 2010. Changing hydroclimatic and discharge patterns in the northern Limpopo Basin, Zimbabwe. Water SA 36, 335–350.

Luhunga, P., Botai, J., Kahimba, F., 2016. Evaluation of the performance of CORDEX regional climate models in simulating present climate conditions of Tanzania. J. South. Hemisphere Earth Syst. Sci. 66, 32–54. https://doi.org/10.22499/3.6601.005

MacKellar, N., New, M., Jack, C., 2014. Observed and modelled trends in rainfall and temperature for South Africa: 1960-2010. South Afr. J. Sci. 110, 1–13.

Madebwe, V., Madebwe, C., 2005. An exploratory analysis of the social, economic and environmental impacts on wetlands: The Case of Shurugwi District, Midlands Province, Zimbabwe. J. Appl. Sci. Res. 1, 228–233.

Malan, H.L., Day, J., 2005. Wetland water quality and ecological Reserve. A report to Water Research Commission (WRC).

Mamombe, V., Kim, W., Choi, Y.-S., 2016a. Rainfall variability over Zimbabwe and its relation to large-scale atmosphere-ocean processes: RAINFALL VARIABILITY OVER ZIMBABWE. Int. J. Climatol. https://doi.org/10.1002/joc.4752

Mamombe, V., Kim, W., Choi, Y.-S., 2016b. Rainfall variability over Zimbabwe and its relation to large-scale atmosphere-ocean processes: RAINFALL VARIABILITY OVER ZIMBABWE. Int. J. Climatol. https://doi.org/10.1002/joc.4752

Manatsa, D., Chingombe, W., Matarira, C.H., 2008. The impact of the positive Indian Ocean dipole on Zimbabwe droughts. Int. J. Climatol. 28, 2011–2029. https://doi.org/10.1002/joc.1695

Manatsa, D., Matarira, C.H., 2009. Changing dependence of Zimbabwean rainfall variability on ENSO and the Indian Ocean dipole/zonal mode. Theor. Appl. Climatol. 98, 375–396. https://doi.org/10.1007/s00704-009-0114-0

Manatsa, D., Mukwada, G., 2012. Rainfall Mechanisms for the Dominant Rainfall Mode over Zimbabwe Relative to ENSO and/or IODZM. Sci. World J. 2012, 1–15. https://doi.org/10.1100/2012/926310

Manatsa, D., Mukwada, G., Siziba, E., Chinyanganya, T., 2010a. Analysis of multidimensional aspects of agricultural droughts in Zimbabwe using the Standardized Precipitation Index (SPI). Theor. Appl. Climatol. 102, 287–305. https://doi.org/10.1007/s00704-010-0262-2

Manatsa, D., Mukwada, G., Siziba, E., Chinyanganya, T., 2010b. Analysis of multidimensional aspects of agricultural droughts in Zimbabwe using the Standardized Precipitation Index (SPI). Theor. Appl. Climatol. 102, 287–305. https://doi.org/10.1007/s00704-010-0262-2

Manatsa, D., Reason, C., 2017. ENSO-Kalahari Desert linkages on southern Africa summer surface air temperature variability: ENSO Kalahari Desert linkage on surface air temperature. Int. J. Climatol. 37, 1728–1745. https://doi.org/10.1002/joc.4806

Mander, Ü., Kull, A., Kuusemets, V., Tamm, T., 2000. Nutrient runoff dynamics in a rural catchment: influence of land-use changes, climatic fluctuations and ecotechnological measures. Ecol. Eng. 14, 405–417.

Marambanyika, T., Beckedahl, H., 2016. Wetland utilisation patterns in semi-arid communal areas of Zimbabwe between 1985 and 2013 and the associated benefits to livelihoods

of the surrounding communities. Trans. R. Soc. South Afr. 71, 175–186. https://doi.org/10.1080/0035919X.2016.1152520

Marambanyika, T., Beckedahl, H., Ngetar, N.S., Dube, T., 2016. Assessing the environmental sustainability of cultivation systems in wetlands using the WET-Health framework in Zimbabwe. Phys. Geogr. 1–21. https://doi.org/10.1080/02723646.2016.1251751

Marteau, R., Sultan, B., Moron, V., Alhassane, A., Baron, C., Traoré, S.B., 2011. The onset of the rainy season and farmers' sowing strategy for pearl millet cultivation in Southwest Niger. Agric. For. Meteorol. 151, 1356–1369. https://doi.org/10.1016/j.agrformet.2011.05.018

Martin, K.L., Hwang, T., Vose, J.M., Coulston, J.W., Wear, D.N., Miles, B., Band, L.E., 2017. Watershed impacts of climate and land use changes depend on magnitude and land use context. Ecohydrology 10, e1870. https://doi.org/10.1002/eco.1870

Masih, I., Maskey, S., Mussá, F.E.F., Trambauer, P., 2014. A review of droughts on the African continent: a geospatial and long-term perspective. Hydrol. Earth Syst. Sci. 18, 3635–3649. https://doi.org/10.5194/hess-18-3635-2014

Masters, G., Norgrove, L., others, 2010. Climate change and invasive alien species. UK CABI Work. Pap. 1.

Matiza, T., 1992. Wetlands in Zimbawe an overview, in: Wetlands Ecology and Priorities for Conservation in Zimbabwe: Proceedings of a Seminar on Wetlands Ecology. IUCN, Switzerland, pp. 3–10.

Mazandarani, G.A., Ahmadi, A.Z., Ramazani, Z., 2013. Investigation analysis of the agronomical characteristics of the daily rainfall in rain-fed agriculture (case study: Tehran). Int. J. Agric. Crop Sci. 5, 612.

Mazvimavi, D., 2010. Investigating changes over time of annual rainfall in Zimbabwe. Hydrol. Earth Syst. Sci. 14, 2671–2679. https://doi.org/10.5194/hess-14-2671-2010

McCartney, M., Cai, X., Smakhtin, V., 2013. Evaluating the flow regulating functions of natural ecosystems in the Zambezi Basin. International Water Management Institute (IWMI). https://doi.org/10.5337/2013.206

McCauley, L.A., Anteau, M.J., 2014. Generating Nested Wetland Catchments with Readily-Available Digital Elevation Data May Improve Evaluations of Land-Use Change on Wetlands. Wetlands 34, 1123–1132. https://doi.org/10.1007/s13157-014-0571-9

McCauley, L.A., Anteau, M.J., van der Burg, M.P., Wiltermuth, M.T., 2015. Land use and wetland drainage affect water levels and dynamics of remaining wetlands. Ecosphere 6, 1–22. https://doi.org/10.1890/ES14-00494.1

McKee, T.B., Doesken, N.J., Kleist, J., others, 1993. The relationship of drought frequency and duration to time scales, in: Proceedings of the 8th Conference on Applied Climatology. American Meteorological Society Boston, MA, pp. 179–183.

McKinney, M.L., 2008. Effects of urbanization on species richness: A review of plants and animals. Urban Ecosyst. 11, 161–176. https://doi.org/10.1007/s11252-007-0045-4

Meng, L., Roulet, N., Zhuang, Q., Christensen, T.R., Frolking, S., 2016. Focus on the impact of climate change on wetland ecosystems and carbon dynamics. Environ. Res. Lett. 11, 100201. https://doi.org/10.1088/1748-9326/11/10/100201

Mengistu, D., Bewket, W., Lal, R., 2014. Recent spatiotemporal temperature and rainfall variability and trends over the Upper Blue Nile River Basin, Ethiopia: Climate variability, trends, upper Blue Nile basin, Ethiopia. Int. J. Climatol. 34, 2278–2292. https://doi.org/10.1002/joc.3837

Meque, A., Abiodun, B.J., 2015. Simulating the link between ENSO and summer drought in Southern Africa using regional climate models. Clim. Dyn. 44, 1881–1900. https://doi.org/10.1007/s00382-014-2143-3

Mharapara, I.M., 1998. Zimbabwe Country Paper. Experiences on wetland characterisation, classification, management and utilisation for Agricultural development in Zimbabwe.

Mhlanga, B., Maruziva, R., Buka, L., 2014a. Mapping wetland characteristics for sustainable development in Harare: The case of Borrowdale West, Highlands, National Sport stadium and Mukuvisi Woodlands wetlands. Ethiop. J. Environ. Stud. Manag. 7, 488. https://doi.org/10.4314/ejesm.v7i5.3

Mhlanga, B., Maruziva, R., Buka, L., 2014b. Mapping wetland characteristics for sustainable development in Harare: The case of Borrowdale West, Highlands, National Sport stadium and Mukuvisi Woodlands wetlands. Ethiop. J. Environ. Stud. Manag. 7, 488. https://doi.org/10.4314/ejesm.v7i5.3

Millenium Ecological Assessment, 2005. Ecosystems and Human Well being synthesis.

Mirza, M.M.Q., 2003. Climate change and extreme weather events: can developing countries adapt? Clim. Policy 3, 233–248. https://doi.org/10.3763/cpol.2003.0330

Mitchell, A., 2013. wetland threats,pred.pdf.

Mitsch, W.J., Gosselink, J.G., 2007. Wetlands, Fourth. ed. John Wiley and Sons, Inc., Canada.

Mitsch, W.J., Gosselink, J.G., 2000. The value of wetlands: importance of scale and landscape setting. Ecol. Econ. 35, 25–33.

Moore, P., Garratt, R., 2006. Biomas of the earth-wetlands. Chelsea House, New York, USA.

Moser, S.C., 2010. Communicating climate change; history, challenges, processes and future directions. Willey Interdiscip. Rev. Change 1, 31–53.

Moyce, W., Mangeya, P., Owen, R., Love, D., 2006. Alluvial aquifers in the Mzingwane catchment: Their distribution, properties, current usage and potential expansion. Phys. Chem. Earth Parts ABC 31, 988–994. https://doi.org/10.1016/j.pce.2006.08.013

Moyo, M., Dorward, P., Craufurd, P., 2017. Characterizing Long Term Rainfall Data for Estimating Climate Risk in Semi-arid Zimbabwe, in: Leal Filho, W., Belay, S., Kalangu, J., Menas, W., Munishi, P., Musiyiwa, K. (Eds.), Climate Change Adaptation in Africa: Fostering Resilience and Capacity to Adapt. Springer International Publishing, Cham, pp. 661–675. https://doi.org/10.1007/978-3-319-49520-0_41

Msipa, M., 2009. Landuse changes between 1972 and 2008 and current water quality of wetlands in Harare, Zimbabwe (Unpublished Masters Thesis). University of Zimbabwe, Harare.

Muchuru, S., Botai, J.O., Botai, C.M., Landman, W.A., Adeola, A.M., 2016. Variability of rainfall over Lake Kariba catchment area in the Zambezi river basin, Zimbabwe. Theor. Appl. Climatol. 124, 325–338. https://doi.org/10.1007/s00704-015-1422-1

Mueller, K.E., Blumenthal, D.M., Pendall, E., Carrillo, Y., Dijkstra, F.A., Williams, D.G., Follett, R.F., Morgan, J.A., 2016. Impacts of warming and elevated CO_2 on a semi-arid grassland are non-additive, shift with precipitation, and reverse over time. Ecol. Lett. 19, 956–966. https://doi.org/10.1111/ele.12634

Mugandani, R., Wuta, M., Makarau, A., Chipindu, B., 2012. Re-classification of agro-ecological regions of Zimbabwe in conformity with climate variability and change. Afr. Crop Sci. J. 20, 361–369.

Muhire, I., Ahmed, F., 2015. Spatio-temporal trend analysis of precipitation data over Rwanda. South Afr. Geogr. J. 97, 50–68. https://doi.org/10.1080/03736245.2014.924869

Munyati, C., 2000. Wetland change detection on the Kafue Flats, Zambia, by classification of a multitemporal remote sensing image dataset. Int. J. Remote Sens. 21, 1787–1806. https://doi.org/10.1080/014311600209742

Mupangwa, W., Walker, S., Twomlow, S., 2011. Start, end and dry spells of the growing season in semi-arid southern Zimbabwe. J. Arid Environ. 75, 1097–1104. https://doi.org/10.1016/j.jaridenv.2011.05.011

Murungweni, M.F., 2013. Effects of Land-use change on quality of urban wetlands. A case of Monavale wetlands in Harare. Geoinformatics and Geostatistics 1, 1–13.

Murwira, A., Madamombe, E., Schmidt, M., 2004. The Role of Wetlands in Flood Mitigation: The Zambezi Wetlands Case Study. IUCN-World Conservation Union.

Mushore, T., Manatsa, D., Pedzisai, E., Muzenda-Mudavanhu, C., Mushore, W., Kudzotsa, I., 2017. Investigating the implications of meteorological indicators of seasonal rainfall performance on maize yield in a rain-fed agricultural system: case study of Mt. Darwin District in Zimbabwe. Theor. Appl. Climatol. 129, 1167–1173. https://doi.org/10.1007/s00704-016-1838-2

Mutanga, O., Adam, E., Cho, M.A., 2012. High density biomass estimation for wetland vegetation using WorldView-2 imagery and random forest regression algorithm. Int. J. Appl. Earth Obs. Geoinformation 18, 399–406. https://doi.org/10.1016/j.jag.2012.03.012

Mutayoba, E., Kashaigili, J.J., 2017. Evaluation for the Performance of the CORDEX Regional Climate Models in Simulating Rainfall Characteristics over Mbarali River Catchment in the Rufiji Basin, Tanzania. J. Geosci. Environ. Prot. 05, 139–151. https://doi.org/10.4236/gep.2017.54011

Mwita, E., Menz, G., Misana, S., Becker, M., Kisanga, D., Boehme, B., 2013. Mapping small wetlands of Kenya and Tanzania using remote sensing techniques. Int. J. Appl. Earth Obs. Geoinformation 21, 173–183. https://doi.org/10.1016/j.jag.2012.08.010

Mwita, E.J., 2013. Land cover and land use dynamics of semi-arid wetlands: A case of Rumuruti (Kenya) and Malinda (Tanzania). J. Geophys. Remote Sens. S1 1, 2169–0049.

Nan Liu, Han Wang, 2010. Ensemble Based Extreme Learning Machine. IEEE Signal Process. Lett. 17, 754–757. https://doi.org/10.1109/LSP.2010.2053356

Ndhlovu, N., 2009. A preliminary Assessment of teh Wetland biological integrity in relation to land-useAcase of the Intunjambili wetland, Matopo District Zimbabwe. (Unpublished Masters Thesis). University of Zimbabwe, Harare.

Ndiweni N. and Gwate O., 2014. Public Perceptions of Climate Variability Risks on Wetland Management : A Case of Ward 15 of Matobo North District, Zimbabwe. 3, 28–38.

New, M., Hewitson, B., Stephenson, D.B., Tsiga, A., Kruger, A., Manhique, A., Gomez, B., Coelho, C.A.S., Masisi, D.N., Kululanga, E., Mbambalala, E., Adesina, F., Saleh, H., Kanyanga, J., Adosi, J., Bulane, L., Fortunata, L., Mdoka, M.L., Lajoie, R., 2006. Evidence of trends in daily climate extremes over southern and west Africa. J. Geophys. Res. 111. https://doi.org/10.1029/2005JD006289

Ngongondo, C., Xu, C.-Y., Gottschalk, L., Alemaw, B., 2011. Evaluation of spatial and temporal characteristics of rainfall in Malawi: a case of data scarce region. Theor. Appl. Climatol. 106, 79–93. https://doi.org/10.1007/s00704-011-0413-0

Nikulin, G., Jones, C., Giorgi, F., Asrar, G., Büchner, M., Cerezo-Mota, R., Christensen, O.B., Déqué, M., Fernandez, J., Hänsler, A., van Meijgaard, E., Samuelsson, P., Sylla, M.B., Sushama, L., 2012. Precipitation Climatology in an Ensemble of CORDEX-

Africa Regional Climate Simulations. J. Clim. 25, 6057–6078. https://doi.org/10.1175/JCLI-D-11-00375.1

Nnaji, C.C., Mama, C.N., Ukpabi, O., 2016. Hierarchical analysis of rainfall variability across Nigeria. Theor. Appl. Climatol. 123, 171–184. https://doi.org/10.1007/s00704-014-1348-z

Nyamasyo, K., Kihima, O., 2014. Changing Land Use Patterns and Their Impacts on Wild Ungulates in Kimana Wetland Ecosystem, Kenya. Int. J. Biodivers. 2014, 1–10. https://doi.org/10.1155/2014/486727

Oliver, J.E., 1980. MONTHLY PRECIPITATION DISTRIBUTION: A COMPARATIVE INDEX. Prof. Geogr. 32, 300–309. https://doi.org/10.1111/j.0033-0124.1980.00300.x

Ollis, D., Ewart-Smith, J., Day, J., Job, N., Macfarlane, D., Snaddon, C., Sieben, E., Dini, J., Mbona, N., 2015. The development of a classification system for inland aquatic ecosystems in South Africa. Water SA 41, 727. https://doi.org/10.4314/wsa.v41i5.16

Osbahr, H., Twyman, C., Adger, W.N., Thomas, D.S., 2010. Evaluating successful livelihood adaptation to climate variability and change in southern Africa. Ecol. Soc. 15, 27.

Ozesmi, S.L., Bauer, M.E., 2014. Satellite remote sensing of wetlands. Wetl. Ecol. Manag. 10, 381–402. https://doi.org/10.1023/A:1020908432489

Pachauri, R.K., Mayer, L., Intergovernmental Panel on Climate Change (Eds.), 2015. Climate change 2014: synthesis report. Intergovernmental Panel on Climate Change, Geneva, Switzerland.

Pecl, G.T., Araújo, M.B., Bell, J.D., Blanchard, J., Bonebrake, T.C., Chen, I.-C., Clark, T.D., Colwell, R.K., Danielsen, F., Evengård, B., Falconi, L., Ferrier, S., Frusher, S., Garcia, R.A., Griffis, R.B., Hobday, A.J., Janion-Scheepers, C., Jarzyna, M.A., Jennings, S., Lenoir, J., Linnetved, H.I., Martin, V.Y., McCormack, P.C., McDonald, J., Mitchell, N.J., Mustonen, T., Pandolfi, J.M., Pettorelli, N., Popova, E., Robinson,

S.A., Scheffers, B.R., Shaw, J.D., Sorte, C.J.B., Strugnell, J.M., Sunday, J.M., Tuanmu, M.-N., Vergés, A., Villanueva, C., Wernberg, T., Wapstra, E., Williams, S.E., 2017. Biodiversity redistribution under climate change: Impacts on ecosystems and human well-being. Science 355, eaai9214. https://doi.org/10.1126/science.aai9214

Pilgrim, D.H., Cordery, I., Baron, B.C., 1982. Effects of catchment size on runoff relationships. J. Hydrol. 58, 205–221.

Pinto, I., Lennard, C., Tadross, M., Hewitson, B., Dosio, A., Nikulin, G., Panitz, H.-J., Shongwe, M.E., 2016. Evaluation and projections of extreme precipitation over southern Africa from two CORDEX models. Clim. Change 135, 655–668. https://doi.org/10.1007/s10584-015-1573-1

Poff, N.L., Allan, J.D., Bain, M.B., Karr, J.R., Prestegaard, K.L., Richter, B.D., Sparks, R.E., Stromberg, J.C., 1997. The Natural Flow Regime. BioScience 47, 769–784. https://doi.org/10.2307/1313099

Pohl, B., Macron, C., Monerie, P.-A., 2017. Fewer rainy days and more extreme rainfall by the end of the century in Southern Africa. Sci. Rep. 7, 46466. https://doi.org/10.1038/srep46466

Qu, M., Wan, J., Hao, X., 2014. Analysis of diurnal air temperature range change in the continental United States. Weather Clim. Extrem. 4, 86–95. https://doi.org/10.1016/j.wace.2014.05.002

Quinn, N.W.T., Epshtein, O., 2014. Seasonally-managed wetland footprint delineation using Landsat ETM+ satellite imagery. Environ. Model. Softw. 54, 9–23. https://doi.org/10.1016/j.envsoft.2013.12.012

Rahman, M.I., 2013. Climate Change: a Theoretical Review. Interdiscip. Descr. Complex Syst. 11, 1–13. https://doi.org/10.7906/indecs.11.1.1

Ramachandra, T.V., Meera, D.S., Alakananda, B., 2013. Influence of catchment land cover dynamics on the physical, chemical and biological integrity of wetlands. Environ. We-Int. J. Sci. Technol. 8, 37–54.

Ramirez-Villegas, J., Jarvis, A., 2010. Downscaling global circulation model outputs: the delta method decision and policy analysis Working Paper No. 1. Policy Anal. 1, 1–18.

Randriamahefasoa, T.S.M., Reason, C.J.C., 2017. Interannual variability of rainfall characteristics over southwestern Madagascar. Theor. Appl. Climatol. 128, 421–437. https://doi.org/10.1007/s00704-015-1719-0

Rapp, D., 2014. Assessing Climate change;Temperature, Solar radiation and Heat balance, Third. ed. Springer International publisher, Switzerland.

Rashford, B.S., Adams, R.M., Wu, J., Voldseth, R.A., Guntenspergen, G.R., Werner, B., Johnson, W.C., 2016. Impacts of climate change on land-use and wetland productivity in the Prairie Pothole Region of North America. Reg. Environ. Change 16, 515–526. https://doi.org/10.1007/s10113-015-0768-3

Reason, C.J.C., 2017. Variability in rainfall over tropical Australia during summer and relationships with the Bilybara High. Theor. Appl. Climatol. https://doi.org/10.1007/s00704-017-2085-x

Reason, C.J.C., Hachigonta, S., Phaladi, R.F., 2005. Interannual variability in rainy season characteristics over the Limpopo region of southern Africa. Int. J. Climatol. 25, 1835–1853. https://doi.org/10.1002/joc.1228

Reason, C.J.C., Jagadheesha, D., 2005. A model investigation of recent ENSO impacts over southern Africa. Meteorol. Atmospheric Phys. 89, 181–205. https://doi.org/10.1007/s00703-005-0128-9

Reason, C.J.C., Keibel, A., 2004. Tropical cyclone Eline and its unusual penetration and impacts over the southern African mainland. Weather Forecast. 19, 789–805.

Rebelo, L.-M., Finlayson, C.M., Nagabhatla, N., 2009. Remote sensing and GIS for wetland inventory, mapping and change analysis. J. Environ. Manage., The GlobWetland Symposium: Looking at wetlands from spaceThe GlobWetland Symposium 90, 2144–2153. https://doi.org/10.1016/j.jenvman.2007.06.027

Recha, C.W., Makokha, G.L., Traore, P.S., Shisanya, C., Lodoun, T., Sako, A., 2012. Determination of seasonal rainfall variability, onset and cessation in semi-arid Tharaka district, Kenya. Theor. Appl. Climatol. 108, 479–494. https://doi.org/10.1007/s00704-011-0544-3

Ricaurte, L.F., Olaya-Rodríguez, M.H., Cepeda-Valencia, J., Lara, D., Arroyave-Suárez, J., Max Finlayson, C., Palomo, I., 2017. Future impacts of drivers of change on wetland ecosystem services in Colombia. Glob. Environ. Change 44, 158–169. https://doi.org/10.1016/j.gloenvcha.2017.04.001

Richardson, C.J., 1994. Ecological functions and human values in wetlands: A framework for assessing forestry impacts. Wetlands 14, 1–9. https://doi.org/10.1007/BF03160616

Rodríguez, J.F., Saco, P.M., Sandi, S., Saintilan, N., Riccardi, G., 2017. Potential increase in coastal wetland vulnerability to sea-level rise suggested by considering hydrodynamic attenuation effects. Nat. Commun. 8, 16094. https://doi.org/10.1038/ncomms16094

Root, T.L., Schneider, S.H., 2002. Climate change: overview and implications for wildlife. Wildl. Responses Clim. Change North Am. Case Stud. 10, 765–766.

Rosso, P.H., Ustin, S.L., Hastings, A., 2005. Mapping marshland vegetation of San Francisco Bay, California, using hyperspectral data. Int. J. Remote Sens. 26, 5169–5191. https://doi.org/10.1080/01431160500218770

Rundquist, D.C., Narumalani, S., Narayanan, R.M., 2001. A review of wetlands remote sensing and defining new considerations. Remote Sens. Rev. 20, 207–226. https://doi.org/10.1080/02757250109532435

Russo, S., Marchese, A.F., Sillmann, J., Immé, G., 2016. When will unusual heat waves become normal in a warming Africa? Environ. Res. Lett. 11, 054016. https://doi.org/10.1088/1748-9326/11/5/054016

Sanchez-Moreno, J.F., Mannaerts, C.M., Jetten, V., 2014. Influence of topography on rainfall variability in Santiago Island, Cape Verde: Influence of topography on rainfall variability in Cape Verde. Int. J. Climatol. 34, 1081–1097. https://doi.org/10.1002/joc.3747

Sang, L., Zhang, C., Yang, J., Zhu, D., Yun, W., 2011. Simulation of land use spatial pattern of towns and villages based on CA–Markov model. Math. Comput. Model. 54, 938–943. https://doi.org/10.1016/j.mcm.2010.11.019

Sango, I., Godwell, N., 2015. Climate change trends and environmental impacts in the Makonde Communal Lands, Zimbabwe. South Afr. J. Sci. 111, 1–6.

Sanikhani, H., Kisi, O., Amirataee, B., 2017. Impact of climate change on runoff in Lake Urmia basin, Iran. Theor. Appl. Climatol. https://doi.org/10.1007/s00704-017-2091-z

Sanogo, S., Fink, A.H., Omotosho, J.A., Ba, A., Redl, R., Ermert, V., 2015. Spatio-temporal characteristics of the recent rainfall recovery in West Africa. Int. J. Climatol. 35, 4589–4605. https://doi.org/10.1002/joc.4309

Scharsich, V., Mtata, K., Hauhs, M., Lange, H., Bogner, C., 2017. Analysing land cover and land use change in the Matobo National Park and surroundings in Zimbabwe. Remote Sens. Environ. 194, 278–286. https://doi.org/10.1016/j.rse.2017.03.037

Schmidt, K.S., Skidmore, A.K., 2003. Spectral discrimination of vegetation types in a coastal wetland. Remote Sens. Environ. 85, 92–108. https://doi.org/10.1016/S0034-4257(02)00196-7

Schuijt, K., 2002a. Land and water use of wetlands in Africa: Economic values of African wetlands.

Schuijt, K., 2002b. Land and water use of wetlands in Africa: Economic values of African wetlands.

Sheffield, J., Andreadis, K.M., Wood, E.F., Lettenmaier, D.P., 2009. Global and Continental Drought in the Second Half of the Twentieth Century: Severity–Area–Duration Analysis and Temporal Variability of Large-Scale Events. J. Clim. 22, 1962–1981. https://doi.org/10.1175/2008JCLI2722.1

Sheffield, J., Wood, E.F., Chaney, N., Guan, K., Sadri, S., Yuan, X., Olang, L., Amani, A., Ali, A., Demuth, S., Ogallo, L., 2014. A Drought Monitoring and Forecasting System for Sub-Sahara African Water Resources and Food Security. Bull. Am. Meteorol. Soc. 95, 861–882. https://doi.org/10.1175/BAMS-D-12-00124.1

Shongwe, M.E., Lennard, C., Liebmann, B., Kalognomou, E.-A., Ntsangwane, L., Pinto, I., 2015. An evaluation of CORDEX regional climate models in simulating precipitation over Southern Africa: CORDEX simulation of rainfall over Southern Africa. Atmospheric Sci. Lett. 16, 199–207. https://doi.org/10.1002/asl2.538

Sibanda, S., Grab, S.W., Ahmed, F., 2017. Spatio-temporal temperature trends and extreme hydro-climatic events in southern Zimbabwe. South Afr. Geogr. J. 1–23. https://doi.org/10.1080/03736245.2017.1397541

Sica, Y.V., Quintana, R.D., Radeloff, V.C., Gavier-Pizarro, G.I., 2016. Wetland loss due to land use change in the Lower Paraná River Delta, Argentina. Sci. Total Environ. 568, 967–978. https://doi.org/10.1016/j.scitotenv.2016.04.200

Singh, S.K., Srivastava, P.K., Gupta, M., Thakur, J.K., Mukherjee, S., 2014. Appraisal of land use/land cover of mangrove forest ecosystem using support vector machine. Environ. Earth Sci. 71, 2245–2255. https://doi.org/10.1007/s12665-013-2628-0

Sithole, A., Murewi, C.T., 2009. Climate variability and change over southern Africa: impacts and challenges. Afr. J. Ecol. 47, 17–20.

Sithole, B., 1999. Use and access to Dambos in communal lands in Zimbabwe. “Institutional consideration” (Unpublished PhDThesis). University of Zimbabwe, Harare.

Spinoni, J., Naumann, G., Carrao, H., Barbosa, P., Vogt, J., 2014. World drought frequency, duration, and severity for 1951-2010: World drought climatologies for 1951-2010. Int. J. Climatol. 34, 2792–2804. https://doi.org/10.1002/joc.3875

Stahl, K., Moore, R.D., Floyer, J.A., Asplin, M.G., McKendry, I.G., 2006. Comparison of approaches for spatial interpolation of daily air temperature in a large region with complex topography and highly variable station density. Agric. For. Meteorol. 139, 224–236. https://doi.org/10.1016/j.agrformet.2006.07.004

Stepanek, P., Zahradnicek,R, Huth, R, 2011. Interpolation techniques used for data quality control and calculation of technical series: an example of a Central European daily timeseries.URL http://cat.inist.fr/?aModele=afficheN&cpsidt=24467030 (accessed 26.03.2017).

Subedi, P., Subedi, K., Thapa, B., 2013. Application of a Hybrid Cellular Automaton – Markov (CA-Markov) Model in Land-Use Change Prediction: A Case Study of Saddle Creek Drainage Basin, Florida. Appl. Ecol. Environ. Sci. 1, 126–132. https://doi.org/10.12691/aees-1-6-5

Sun, G., McNulty, S.G., Shepard, J.P., Amatya, D.M., Riekerk, H., Comerford, N.B., Skaggs, W., Swift, L., 2001. Effects of timber management on the hydrology of wetland forests in the southern United States. Spec. Issue Sci. Manag. For. SUSTAIN 143, 227–236. https://doi.org/10.1016/S0378-1127(00)00520-X

Szantoi, Z., Escobedo, F., Abd-Elrahman, A., Smith, S., Pearlstine, L., 2013. Analyzing fine-scale wetland composition using high resolution imagery and texture features. Int. J. Appl. Earth Obs. Geoinformation 23, 204–212. https://doi.org/10.1016/j.jag.03.01.2013

Tadross, M., Suarez, P., Lotsch, A., Hachigonta, S., Mdoka, M., Unganai, L., Lucio, F., Kamdonyo, D., Muchinda, M., 2009. Growing-season rainfall and scenarios of future change in southeast Africa: implications for cultivating maize. Clim. Res. 40, 147–161. https://doi.org/10.3354/cr00821

Tadross, M.A., Hewitson, B.C., Usman, M.T., 2005a. The interannual variability of the onset of the maize growing season over South Africa and Zimbabwe. J. Clim. 18, 3356–3372.

Tadross, M.A., Hewitson, B.C., Usman, M.T., 2005b. The interannual variability of the onset of the maize growing season over South Africa and Zimbabwe. J. Clim. 18, 3356–3372.

Teferi, E., Uhlenbrook, S., Bewket, W., Wenninger, J., Simane, B., 2010. The use of remote sensing to quantify wetland loss in the Choke Mountain range, Upper Blue Nile basin, Ethiopia. Hydrol. Earth Syst. Sci. 14, 2415–2428. https://doi.org/10.5194/hess-14-2415-2010

Therrell, M.D., Stahle, D.W., Ries, L.P., Shugart, H.H., 2006. Tree-ring reconstructed rainfall variability in Zimbabwe. Clim. Dyn. 26, 677–685. https://doi.org/10.1007/s00382-005-0108-2

Tolessa, T., Senbeta, F., Kidane, M., 2017. The impact of land use/land cover change on ecosystem services in the central highlands of Ethiopia. Ecosyst. Serv. 23, 47–54. https://doi.org/10.1016/j.ecoser.2016.11.010

Tshiala, M.F., Olwoch, J.M., Engelbrecht, F.A., 2011. Analysis of temperature trends over Limpopo province, South Africa. J. Geogr. Geol. 3, 13.

Unganai, L.S., 1996a. Historic and future climatic change in Zimbabwe. Clim. Res. 6, 137–145.

Unganai, L.S., 1996b. Historic and future climatic change in Zimbabwe. Clim. Res. 6, 137–145.

Unganai, L.S., Mason, S.J., 2002. Long-range predictability of Zimbabwe summer rainfall. Int. J. Climatol. 22, 1091–1103. https://doi.org/10.1002/joc.786

Usman, M.T., Reason, C.J.C., 2004. Dry spell frequencies and their variability over southern Africa. Clim. Res. 26, 199–211. https://doi.org/10.3354/cr026199

Valtanen, M., Sillanpää, N., Setälä, H., 2014. The Effects of Urbanization on Runoff Pollutant Concentrations, Loadings and Their Seasonal Patterns Under Cold Climate. Water. Air. Soil Pollut. 225. https://doi.org/10.1007/s11270-014-1977-y

van der Valk, A.G., Volin, J.C., Wetzel, P.R., 2015. Predicted Changes in Interannual Water-Level Fluctuations Due to Climate Change and Its Implications for the Vegetation of the Florida Everglades. Environ. Manage. 55, 799–806. https://doi.org/10.1007/s00267-014-0434-4

Vanderlinder, M.S., Neale, C.M.U., Rosenberg, D.E., Kettenring, K.M., 2014. Use of Remote Sensing to Assess Changes in Wetland Plant Communities Over An 18-Year Period: A Case Study from the Bear River Migratory Bird Refuge, Great Salt Lake, Utah. West. North Am. Nat. 74, 33–46. https://doi.org/10.3398/064.074.0104

Verhoeven, J., Arheimer, B., Yin, C., Hefting, M., 2006. Regional and global concerns over wetlands and water quality. Trends Ecol. Evol. 21, 96–103. https://doi.org/10.1016/j.tree.2005.11.015

Vicente-Serrano, S.M., Beguería, S., López-Moreno, J.I., 2010. A Multiscalar Drought Index Sensitive to Global Warming: The Standardized Precipitation Evapotranspiration Index. J. Clim. 23, 1696–1718. https://doi.org/10.1175/2009JCLI2909.1

Voldseth, R.A., Johnson, W.C., Gilmanov, T., Guntenspergen, G.R., Millett, B.V., 2007. MODEL ESTIMATION OF LAND-USE EFFECTS ON WATER LEVELS OF NORTHERN PRAIRIE WETLANDS. Ecol. Appl. 17, 527–540.

Wagener, T., Wheater, H., Gupta, H.V., 2004. Rainfall-runoff modelling in gauged and ungauged catchments. Imperial College Press ; Distributed by World Scientific, London : Singapore ; Hackensack, N.J.

Wagner, P.D., Kumar, S., Schneider, K., 2013. An assessment of land use change impacts on the water resources of the Mula and Mutha Rivers catchment upstream of Pune, India. Hydrol. Earth Syst. Sci. 17, 2233–2246. https://doi.org/10.5194/hess-17-2233-2013

Walters, D.J.J., Kotze, D.C., O'Connor, T.G., 2006. Impact of land use on vegetation composition, diversity, and selected soil properties of wetlands in the southern Drakensberg mountains, South Africa. Wetl. Ecol. Manag. 14, 329–348. https://doi.org/10.1007/s11273-005-4990-5

Wang, J., Feng, J., Yan, Z., Hu, Y., Jia, G., 2012. Nested high-resolution modeling of the impact of urbanization on regional climate in three vast urban agglomerations in China: CLIMATE IMPACT OF URBANIZATION IN CHINA. J. Geophys. Res. Atmospheres 117, n/a-n/a. https://doi.org/10.1029/2012JD018226

Wang, Q., Liao, J., 2009. Estimation of wetland vegetation biomass in the Poyang Lake area using Landsat TM and Envisat ASAR data. p. 78411D–78411D–10. https://doi.org/10.1117/12.873263

Welde, K., Gebremariam, B., 2017. Effect of land use land cover dynamics on hydrological response of watershed: Case study of Tekeze Dam watershed, northern Ethiopia. Int. Soil Water Conserv. Res. 5, 1–16. https://doi.org/10.1016/j.iswcr.2017.03.002

Weldon, D., Reason, C.J.C., 2014. Variability of rainfall characteristics over the South Coast region of South Africa. Theor. Appl. Climatol. 115, 177–185. https://doi.org/10.1007/s00704-013-0882-4

Wetland International, n.d. Wetland Internatuional Annual Review 2009.

WMO, 2017. WMO statement o the State of the Global Climate in 2016.

Wood, E.F., 1995. Scaling behaviour of hydrological fluxes and variables: empirical studies using a hydrological model and remote sensing data. *Hydrological Processes*, *9*(3-4), pp.331-346.

Wu, Q., Lane, C.R., 2017. Delineating wetland catchments and modeling hydrologic connectivity using LiDAR data and aerial imagery. Hydrol. Earth Syst. Sci. Discuss. 1–32. https://doi.org/10.5194/hess-2017-1

Yang, X., Zheng, X.-Q., Chen, R., 2014. A land use change model: Integrating landscape pattern indexes and Markov-CA. Ecol. Model. 283, 1–7. https://doi.org/10.1016/j.ecolmodel.2014.03.011

Zedler, J.B., Kercher, S., 2004. Causes and Consequences of Invasive Plants in Wetlands: Opportunities, Opportunists, and Outcomes. Crit. Rev. Plant Sci. 23, 431–452. https://doi.org/10.1080/07352680490514673

ZIMSTAT, Z., 2016. Zimbabwe Demographic and Health Survey 2015: Final Report.

APPENDIX 1

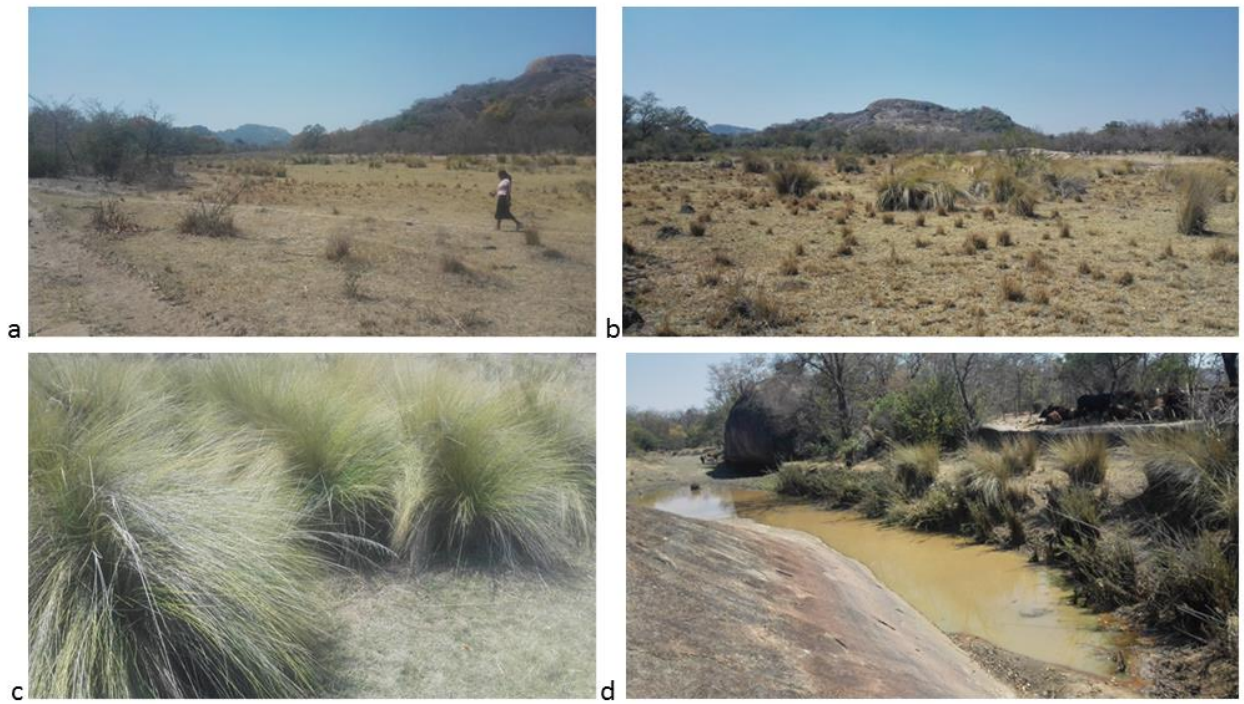

Plate 1: Wetland Photos (a-d) taken in different parts of Shashe sub-catchment during the winter season (May 2015)

Plate 2: Wetland Photos (a-d) taken in different parts of Shashe sub-catchment during the summer season (February 2015)